Université d'Ottawa · University of Ottawa

PETROGENESIS OF THE SUDBURY IGNEOUS COMPLEX: THE SHOCKING STORY

by

Ann Therriault

A thesis presented to the Faculty of Graduate and Postdoctoral Studies

in partial fulfilment of the requirements

for the degree of Ph.D. in Earth Sciences

OTTAWA-CARLETON GEOSCIENCE CENTRE

AND

UNIVERSITY OF OTTAWA

OTTAWA, CANADA

ABSTRACT

The Sudbury Structure, Ontario, is the remnant of a 1.85 Ga old impact crater, 200-250 km in diameter. Erosion and tectonism have affected the Sudbury Structure and resulted in considerable brittle and ductile deformation, and the removal of the surface expression of the crater structure and all exterior deposits typical of many terrestrial impact structures. However, substantial amounts of the interior deposits, including the craterfill products, have been preserved within the Sudbury Basin. Although most workers acknowledge an impact origin for the Sudbury Structure, the origin of the Sudbury Igneous Complex (SIC), located inside the Sudbury Structure, remains controversial. The objectives of this study are to elucidate the division of the SIC into lithologically separate phases and to understand their relation to impact and endogenic igneous processes by using physical, chemical and computer methods, and to model the genesis of the SIC.

The SIC is a 2.5-3.0 km thick, ~ 60 x 27 km elliptical igneous-rock body, consisting of four major lithologies (top to base): granophyre, quartz gabbro, norite, and the so-called contact sublayer. All these lithologies are continuous across the complex, except for the contact sublayer. Modal compositions reveal that the current nomenclature is improper. According to the IUGS classification, "quartz gabbro" samples should be classified as quartz monzogabbros and "norite" samples as quartz gabbros or quartz monzogabbros. In view of these observations, an updated terminology is proposed (top to base): upper unit, transition zone, middle unit, lower unit, and contact sublayer.

Gradational mineralogical and geochemical variations between the SIC lithological units

are evidence of a single melt system for the SIC. The occurrence of primary hydrous minerals, deuteric alteration, and abundant micrographic and granophyric intergrowths demonstrate that this melt was rich in H_2O. The intergrowths and other far-from-equilibrium textures are likely due to rapid crystallization as a result of a large undercooling caused by the exsolution of a volatile phase. The SIC differs from other known terrestrial impact melt sheets only by its great thickness and its chemical layering. It is concluded that the SIC is a differentiated impact melt sheet, the only one identified on Earth to date.

SOMMAIRE

La structure de Sudbury (SS), Ontario, est un astroblème vieux de 1,85 Ga avec un diamètre originel de 200 à 250 km. L'érosion et le tectonisme ont affecté la SS, résultant en une déformation considérable du cratère et l'effacement de l'expression morphologique de celui-ci et de ses dépôts extérieurs. Cependant, une quantité appréciable des dépôts intérieurs, incluant différentes brèches d'impact, ont été préservés. Malgré que la plupart des chercheurs reconnaissent une origine météoritique pour la SS, l'origine du complexe ignée de Sudbury (CIS), situé au centre de la SS, demeure controversée. La présente étude a pour buts de modeler la génèse du CIS, d'en élucider la division en phases lithologiques distinctes et de mieux comprendre leur relation avec les procédés d'impact et endogéniques.

Le CIS représente un corps rocheux igné elliptique d'environ 60 x 27 km, d'une épaisseur de 2,5 à 3,0 km, et composé de quatre lithologies principales (de haut en bas): granophyre, quartz gabbro, norite, et la dite sous-couche de contact. Ces lithologies sont continues sur l'étendue du complexe, exceptée la sous-couche de contact. Des analyses de composition modale révèlent que la nomenclature actuelle est erronée. Selon la classification IUSG, les échantillons de "quartz gabbro" sont des quartz monzogabbros tandis que certains des échantillons de "norite" sont des quartz gabbros alors que les autres sont des quartz monzogabbros. D'après ces observations, une nouvelle terminologie n'utilisant que des termes non-pétrogénétiques est proposée.

Les variations minéralogiques et géochimiques graduelles entre les différentes lithologies du CIS sont évidences que celui-ci se soit comporté comme un système à magma unique. La

présence de minéraux hydratés primaires, d'une altération deutérique et d'abondantes textures micrographiques et granophyriques démontrent que ce magma était riche en H_2O. L'abondance de ces textures et de textures loin-de-l'équilibre suggère que la cristallisation des roches du CIS fut rapide et le résultat d'une surfusion causée par l'exsolution d'une phase volatile. Le CIS ne diffère des autres couches d'impactites terrestres connues que par sa grande épaisseur et sa stratification chimique. Il est conclu que le CIS représente une couche d'impactite différenciée, la seule identifiée sur Terre à ce jour.

TABLE OF CONTENTS

LIST OF TABLES

LIST OF ILLUSTRATIONS

ACKNOWLEDGMENTS

Firstly, I must thank God for enabling me to finish this thesis and still have time for a family life and give birth to two children (Sandi in September 1997 and Sean in January 2000). Naturally, the great patience of my husband has also contributed to the success of this work and growth of our family. And thank God for my friend Jean Dougherty and my parents, without whom this thesis would not have been submitted. Will I ever be able to repay them?

This work was initiated by Dr. R.A.F. Grieve, whom has taught me a great deal. I hope to know as much as him one day... I am fortunate that Dr. A.D. Fowler accepted to take me on as his Ph.D. student. I am also fortunate to be an employee of Natural Resources Canada's Geological Survey of Canada. Many thanks to my Division Director and Supervisor for allowing me to pursue my doctoral studies and for providing financial and technical support.

Drill cores, field assistance, constructive discussions and permission to disclose data and results are greatly acknowledged and appreciated from INCO Ltd, Copper Cliff, Ontario, and in particular, from Gordon Morrison. I must also acknowledge the work of Markus Ostermann, who carried out his geochemical study for his Ph.D. using some of my samples, which I provided for him. This is the reason why his data has been incorporated into this study.

Many thanks to Katherine Venance who operated the CAMECA SX50 electron microprobe and carried out many of the analyses presented in this work. Also many thanks to Dr. K. Benn of the University of Ottawa for the use of his camera and microscope to take photomicrographs, some of which are illustrated in this thesis. Finally, thanks to my friends and family who put up with me during my studies and always offered help, a good ear and advice.

1. INTRODUCTION

The Sudbury Structure (N46°36',W81°11'), Ontario, is renowned for its very large ore deposits. Located at the boundary of two geological provinces (Superior and Southern Provinces) of the Canadian Shield, the Sudbury Structure encompasses an area > 15,000 km^2. It includes fractured and brecciated Archean and Huronian rocks cross-cut by the Offset dykes and multiple veins and lenses of Sudbury Breccia (*i.e.*, pseudotachylites), the so-called Footwall Breccia flooring the Sudbury Igneous Complex (SIC), the SIC, and the Sudbury Basin. The Sudbury Basin consists of the Onaping, Onwatin, and Chelmsford Formations (Figs. 1 and 2). In the last two decades, considerable advances have been made in understanding the character of large impact structures and impact processes. These have led to a generalized working hypothesis for the origin of the Sudbury Structure (*e.g.*, Grieve *et al.*, 1991; Stöffler *et al.*, 1994; Deutsch and Grieve, 1994; Deutsch *et al.*, 1995). While initially highly controversial, the impact origin of many geological features of Sudbury, as first suggested by Dietz (1964) and later confirmed by the work of Dietz and Butler (1964), Bray *et al.* (1966) and French (1969, 1970), is now broadly recognized. Based on these geological features, the Sudbury Structure is regarded as the eroded and tectonized remnant of an originally 200-250 km diameter impact basin (*e.g.*, Grieve *et al.*, 1991; Deutsch *et al.*, 1995; Spray and Thompson, 1995).

The SIC is elliptically shaped in map view, ~ 60 km by 27 km. It is 2.5-3.0 km thick, with an estimated preserved volume of ~ 8,000 to ~ 14,000 km^3 (Grieve, 1994). In previous work, the SIC was subdivided into norite, quartz gabbro and granophyre (*e.g.*, Dressler *et al.*, 1992; Fig. 2). The SIC may be divided into three regions: the South Range (the southern half

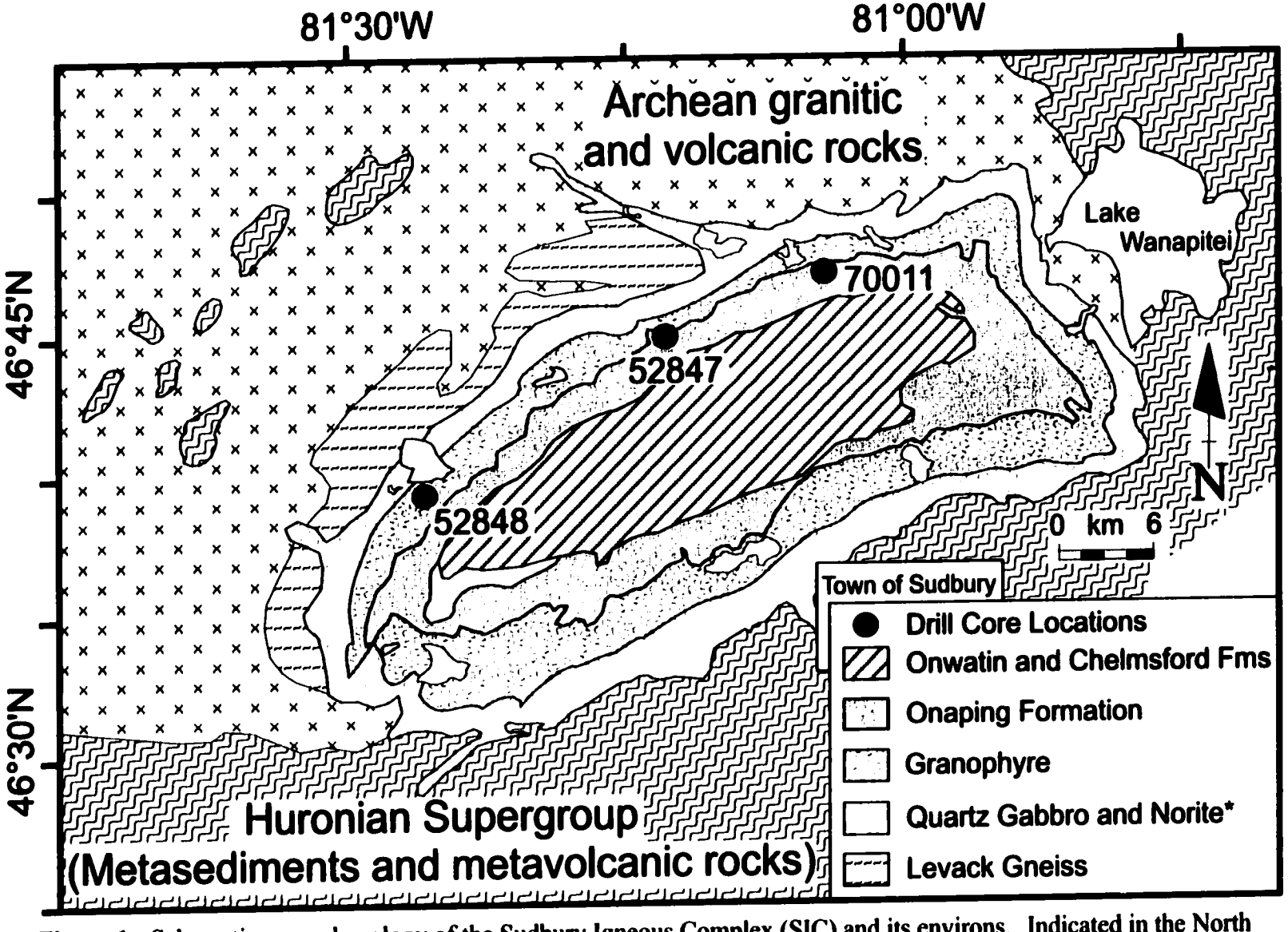

Figure 1. Schematic general geology of the Sudbury Igneous Complex (SIC) and its environs. Indicated in the North Range is the location of the drill cores mentioned in the text. *In this work, these two lithologies are reclassified as quartz monzogabbro and/or quartz gabbro, leading to a proposed updated terminology. See Section 3.1 in the text.

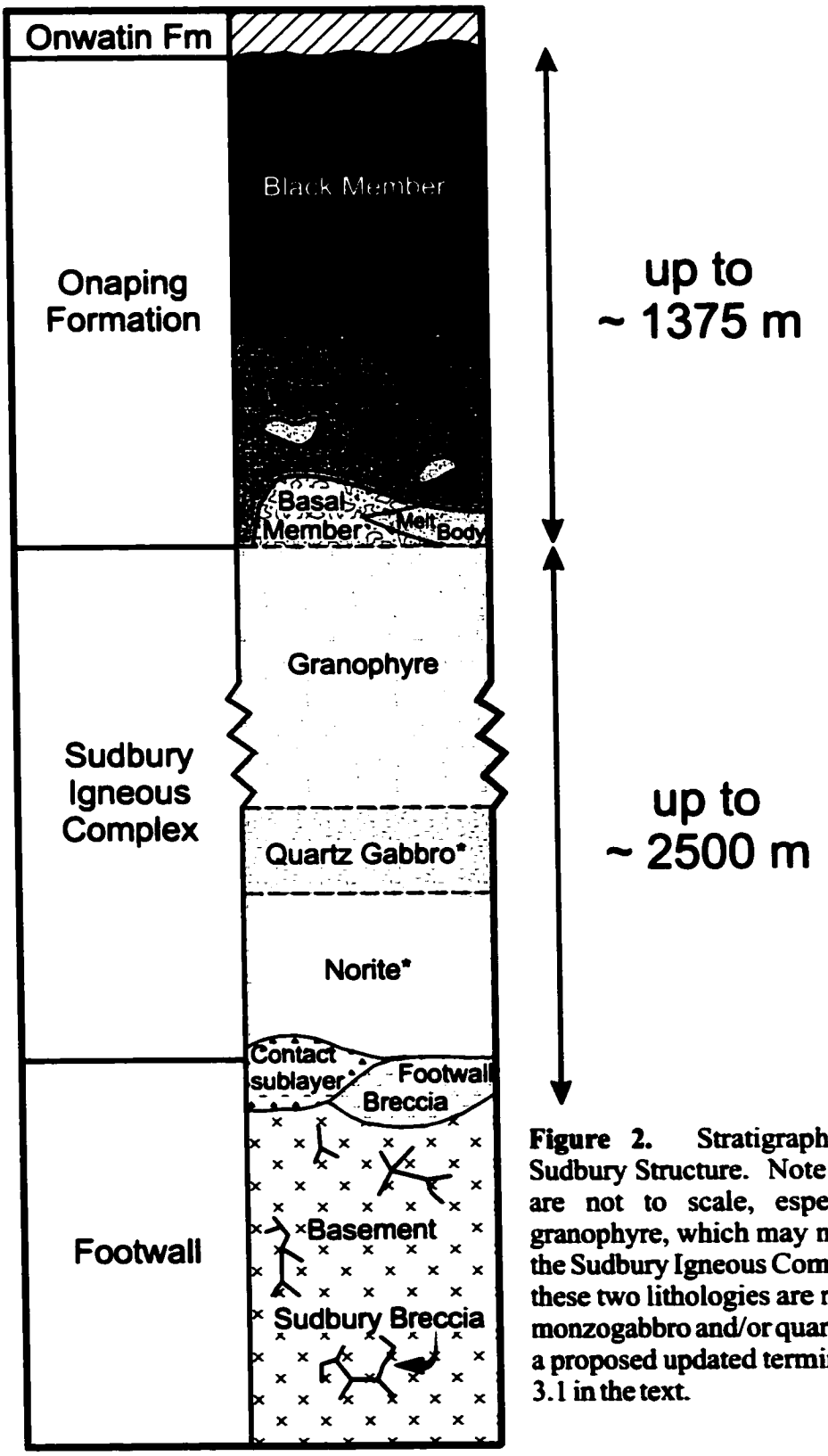

Figure 2. Stratigraphic column of the Sudbury Structure. Note that the thicknesses are not to scale, especially that of the granophyre, which may make up to ~ 60% of the Sudbury Igneous Complex. * In this work, these two lithologies are reclassified as quartz monzogabbro and/or quartz gabbro, leading to a proposed updated terminology. See Section 3.1 in the text.

of the SIC), which dips steeply northward or vertically, the East Range (the eastern section of the SIC running roughly north-south), which dips vertically, and the North Range (the northern half of the SIC), which dips about 30° to 50° to the south (Dressler, 1984). In addition, discontinuous bodies of contact sublayer occur at its base (Fig. 2).

Although the SIC has been known for over a century, considerable debate has been generated concerning its nature and origin. The work of French (1967, 1968) was crucial in the recognition of the impact origin of the Onaping Formation, which overlies the SIC and, until that time, had been regarded as a volcanic rock unit, thus providing evidence for an endogenic origin of the SIC and the Sudbury Structure itself. With few and imprecise data at the time, the origin of the SIC remained elusive. Dietz (1964) proposed that the SIC was the result of an impact-triggered intrusion, an hypothesis supported by Pattison (1979) and Dressler *et al.* (1987). French (1969, 1970) interpreted the SIC has due to the unroofing of a magma chamber by the impact event. Nowadays, he (*e.g.*, French, 1998) and others (*e.g.*, Grieve *et al.*, 1991; Stöffler *et al.*, 1994; Deutsch and Grieve, 1994; Deutsch *et al.*, 1995) recognize the Sudbury Structure as a large complex impact structure. They also postulate the SIC as the remains of a coherent impact melt sheet similar to those of other large terrestrial impact structures. Meanwhile, the previously favoured interpretation that the SIC was a crustally contaminated mantle magma (*e.g.*, Naldrett and Hewins, 1984; Naldrett *et al.*, 1986) has been revived by Norman (1994) and Rousell *et al.* (1997). Also, Dence (1972) suggested that the SIC was partly an impact melt and partly a mantle melt. An hypothesis shared by, most recently, Chai and Eckstrand (1993, 1994), Dressler *et al.* (1996) and Zhou *et al.* (1997). These authors suggest that the contact sublayer,

norite and quartz gabbro of the SIC represent a contaminated endogenic magma; whereas, the granophyre of the SIC represents the impact melt. Lightfoot *et al.* (1997a) concluded that the original impact melt could have been contaminated by a volumetrically small (< 20%) influx of mantle-derived picritic magma. More recently, Marsh and Zieg (1999) interpret the SIC to be the result of crystallization from silicate emulsion in an impact melt, which does not require or rule out the admixture of a mantle component. Naldrett (1999) now views the SIC as having been formed solely through impact melting. Using most current ideas and published data, Naldrett (1999) proposes a comprehensive model of the formation of the Sudbury Structure and the SIC, and points to many remaining questions about them. Naldrett (1999) suggests that a magma comprising cumulates represented by the South Range Norite + Felsic Norite + Quartz Gabbro corresponds to the initial composition of the impact melt. He further suggests that parts of the overlying impact breccias were melted and incorporated into the upper part of the impact melt, giving it a lower density than the lower part. This would have resulted in two-layer convection within the melt sheet.

Compared to other terrestrial impact melt sheets, the SIC differs in its chemical layering and its great thickness. The SIC also differs from terrestrial layered igneous intrusive complexes by its granodioritic (Collins, 1934) and not gabbroic bulk composition and its distinctive crustal isotopic signature (*e.g.*, Faggart *et al.*, 1985; Naldrett *et al.*, 1986; Deutsch, 1994). The ideas that the SIC is differentiated and that its various lithologies are genetically related are not a radical concept. It was a tenet of previous work, wherein the SIC was considered to have a mantle source (*e.g.*, Collins, 1934; Naldrett and Hewins, 1984).

1.1 Regional Geology

The area around the SIC consists of Archean metavolcanic, metasedimentary and granitic rocks, emplaced more than 2600 Ma ago, and Proterozoic metasedimentary and metavolcanic rocks of the Huronian Supergroup, deposited and folded between 2500-2219 Ma (Card *et al.*, 1977; Card, 1978). To the north of the SIC, the Cartier Batholith, which crystallized 2642 ± 1 Ma ago (U-Pb age of zircon; Meldrum *et al.*, 1997), and the Levack gneiss complex (Langford, 1960; Card, 1994) occur within the Archean granitic rocks. The Levack gneiss (Fig. 1) is a complex comprising an assortment of felsic, mafic, ultramafic and sedimentary rocks, locally metamorphosed to the granulite facies about 2647 ± 2 Ma (U-Pb age for zircon; Krogh *et al.*, 1984). After deposition and deformation of the Huronian Supergroup, four major magmatic events have occurred within the rocks of the area. The Nipissing diabase sills were emplaced at 2219.4 +3.6/-3.5 Ma ago (U-Pb age for baddeleyite and rutile in diabase; Corfu and Andrews, 1986). Granitoid plutons intruded at 1749 +12/-8 Ma (U-Pb age for igneous titanite in granodiorite; Davidson and van Breemen, 1994) and 1464 +2/-1 Ma (U-Pb age for zircon in granite; Davidson and van Breemen, 1994). Last, the Sudbury diabase dyke swarm was emplaced about 1235 +7/-3 Ma ago (U-Pb age for baddeleyite and zircon in diabase; Dudàs *et al.*, 1994; Krogh *et al.*, 1987). Since 2500 Ma ago and besides the 1850 ± 1 Ma Sudbury impact event (averaged U-Pb age for zircon and baddeleyite in norite and granophyre; Krogh *et al.*, 1984), the area has been affected on a regional scale by: (1) the Blezardian orogeny, dated at 2.4 to 2.3 Ga ago (Riller *et al.*, 1999), (2) the Penokean orogeny, which lasted from 1890 to 1830 Ma ago (van Schmus, 1980; Hoffman, 1989), although most significant deformation may have

ceased prior to the impact event (Zolnai *et al.*, 1984; Fueten and Redmond, 1997), (3) a NW-thrusting deformation event (Fueten and Redmond, 1997) between 1453 ± 6 Ma (U-Pb age for zircon in pegmatites; Krogh, 1994) and ~ 1445 Ma (monazite ages in a biotite-garnet schist and a quartzofeldspathic gneiss; Dudàs *et al.*, 1994), and (4) the Grenvillian orogeny *ca.* 1000 Ma ago, which destroyed the southeastern part of the Sudbury Structure, but otherwise had apparently only a minor effect on the area (*e.g.*, Brocoum and Dalziel, 1974). Hirt *et al.* (1993) and Roest and Pilkington (1994) have demonstrated that the Sudbury Structure was most likely originally circular. Erosion (~ 5 to 8 km of stratigraphy; *e.g.*, Dence, 1972; Golightly, 1994) and tectonism have affected the Sudbury Structure over 1.85 Ga. The result was considerable brittie and ductile deformation of the crater components and removal of the surface expression of the crater structure and all exterior deposits. However, substantial amounts of the interior crater deposits, including craterfill products (*i.e.*, the Onaping, Onwatin and Chelmsford Formations; *e.g.*, Grieve *et al.*, 1991; Deutsch *et al.*, 1995; Ames *et al.*, 1998), have been preserved.

The various lithological units of the SIC are described as follows. The contact sublayer is a fine- to medium-grained noritic rock that occurs discontinuously around much of the outer margin of the SIC in kilometre-sized radial depressions called "troughs" (Morrison, 1984). Much of the contact sublayer is characterized by abundant xenoliths and Cu-Ni mineralization. Some of the xenoliths are identifiable as locally derived country rocks, others constitute a suite of ultramafic and mafic rocks of unknown source, which may be genetically linked to the SIC (*e.g.*, Lightfoot *et al.*, 1997b). A gradational contact is observed between the contact sublayer and the overlying norite. The norite is medium- to coarse-grained, dark green to black, and

consists of cumulus plagioclase and enstatite with intercumulus quartz, augite, magnetite and ilmenite, and may contain amphibole and/or biotite (Naldrett and Hewins, 1984). In the North Range, the norite is up to 1000 m thick (Fig. 3). The norite has been further divided into a quartz-rich norite, a mafic norite, and a felsic norite (Fig. 4; Naldrett and Hewins, 1984). The quartz-rich norite is restricted to the South Range and the mafic norite is restricted to the North Range. The felsic norite is most abundance in the North Range, but is much more restricted in its development in the South Range, where it is referred to as South Range Norite (Naldrett and Hewins, 1984). A gradational contact is also observed between the norite and the quartz gabbro. The quartz gabbro is medium- to coarse-grained, exhibits a decrease in enstatite content at higher stratigraphic levels and an increase in quartz, augite, magnetite, ilmenite, apatite, titanite and granophyric intergrowths abundance. In the North Range, the quartz gabbro is up to 500 m thick (Fig. 3). Within the lower part of the quartz gabbro occurs a thin layer of leucocratic quartz gabbro (referred to as the "blue band" or "tonalite" by the personnel of INCO Ltd.). This lithology is slightly richer in chlorite, poorer in micrographic intergrowths, contains only trace amounts of titanite, and its pyroxene crystals are more uralitized compared to the quartz gabbro immediately above and below it. The contact between the quartz gabbro and the overlying granophyre is also gradational over a zone up to 200 m thick. In the present work, this latter boundary is referred to as the transition zone (Figs. 3 and 4). The granophyre is, in general, coarse-grained, altered, and consists of plagioclase, a granophyric intergrowth of quartz and alkali feldspar and minor amounts of biotite and opaque oxide minerals. In the North Range, the granophyre is up to 1500 m thick (Fig. 3). A plagioclase-rich facies is found within the top of

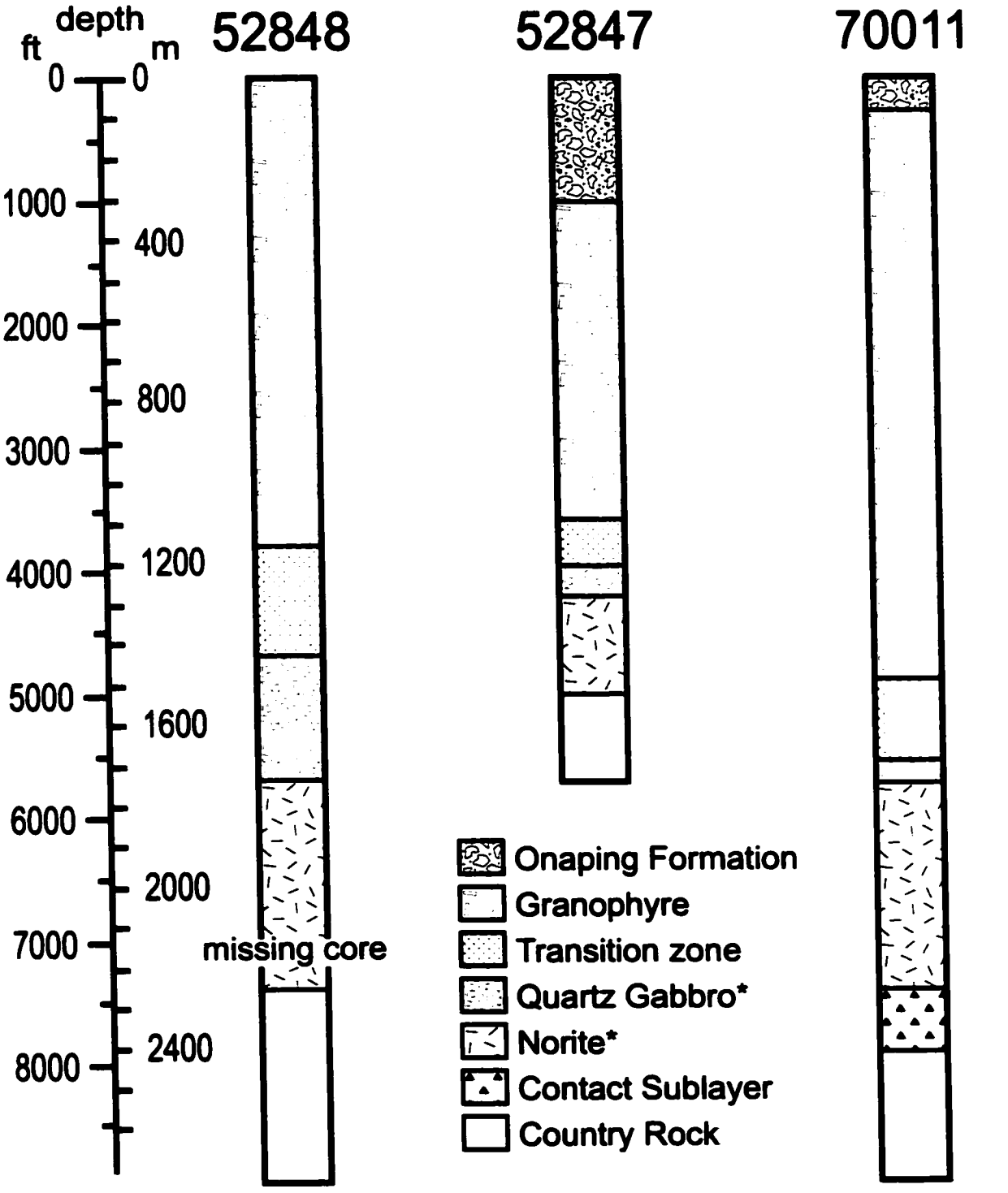

Figure 3. General description of the drill cores mentioned in the text. Note that all contacts are gradational, except the contact with the country rocks. * In this work, these two lithologies are reclassified as quartz monzogabbro and/or quartz gabbro, leading to a proposed updated terminology. See Section 3.1 in the text.

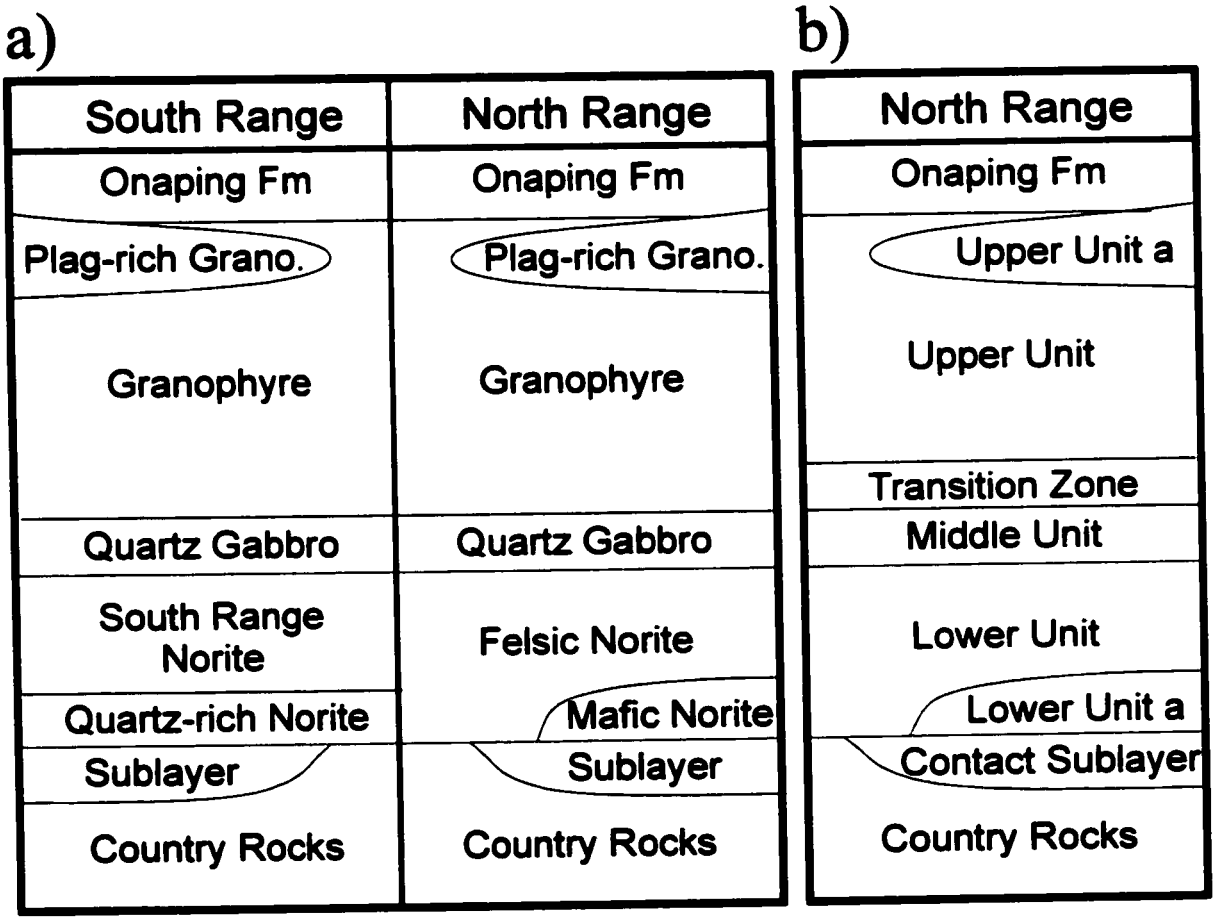

Figure 4. Units of the Sudbury Igneous Complex according to: **(a)** previous work, and **(b)** this work. Not to scale. See text for details.

the granophyre and, in places, at its upper limit with the basal member of the Onaping Formation (*e.g.*, Peredery and Naldrett, 1975). The Offsets are quartz diorite dykes (ten presently known, *e.g.*, Wood and Spray, 1998; Scott and Spray, 1999) are concentric or radial to the SIC and they contain abundant inclusions.

1.2 Previous Work

The first publications about the lithologies of the SIC date back to the early 1890's (*cf.*, Giblin, 1984). In the following 100 years, various terminologies were applied to this rock suite and several hypotheses of origin have been set forth and debated. The number of recognized phases, or lithologies, within the SIC have increased from just two, norite and micropegmatite (granophyre) in the 1890's, to norite - transition zone - micropegmatite in the 1930's (Collins, 1934), to norite - oxide-rich gabbro - micropegmatite in the 1970's, to norite - quartz gabbro - micropegmatite in the 1980's (Naldrett *et al.*, 1970) and, currently, norite - quartz gabbro - granophyre. Barlow (1904) was first to introduce the term, Nickel-Bearing Eruptive to describe the norite and the granophyre. In the 1960's, this term was replaced by the Sudbury Nickel Irruptive, which was simplified to Nickel Irruptive. Since the 1980's (perhaps a little earlier), the term Sudbury Igneous Complex, or SIC, has been in use.

Williams (1891) and von Foullon (1892) were the first to describe the norite. The norite and granophyre were thought to occur in two separate "ranges" (now called North Range and South Range). However, Walker (1897) then Coleman (1905, 1913) suggested that these two units actually formed a continuous basin at depth. Stevenson (1961, 1963) studied the

granophyre. He described an additional phase gradational with the top of the granophyre and in sharp contact with the overlying Onaping Formation. He called it pepper-and-salt micro-pegmatite, and interpreted it as the upper chilled contact of the granophyre. The pepper-and-salt micropegmatite is fine-grained, contains inclusions of quartzite and granite. In addition, Stevenson (1963) noted that his mineralogical and textural observations indicated a high intrusion temperature and rapid cooling of the granophyre. Stevenson and Colgrove (1968) recognized four phases within the norite (including the quartz gabbro) and three phases within the granophyre. Naldrett *et al.* (1970) documented variations between the rock suite of the North Range and South Range, observing phase layering and cryptic mineral variations. Peredery and Naldrett (1975) distinguished two phases of granophyre: (1) granophyric micropegmatite, the main component, and (2) plagioclase-rich micropegmatite (Stevenson's pepper-and-salt micropegmatite). They interpreted the plagioclase-rich granophyre as either a highly recrystallized matrix of the basal breccia (basal member of the Onaping Formation), or a melt rock believed to be related to meteoritic impact. In addition, they interpreted the plagioclase-rich phase as the upper part of the oxide-rich gabbro, which would have been split off by the intrusion of the granophyric micropegmatite. Finn (1993), after a detailed mapping program in an area of the North Range, recognized various phases of granophyre, including an heterogeneous granophyre, which is a continuous unit along the boundary with the overlying Onaping Formation, the plagioclase-rich phase, which occurs as dykes and in a discontinuous unit below the heterogeneous granophyre, a "typical" granophyre, and various phases of this "typical" granophyre based on variations in grain size and mineralogy.

Walker (1897), Barlow (1904) and Coleman (1905, 1913) described the norite-granophyre contact as gradational; whereas, Knight (1917, 1923) showed that chemically much of the change from norite to granophyre occurs across a relatively narrow transition zone. Despite these observations, Knight (1917, 1923) and Phemister (1926) suggested that the norite and granophyre were separate intrusions, with the norite being the oldest of the two. Coleman *et al.* (1929) reiterated that the norite-granophyre showed a gradational contact and interpreted the system as one magma differentiated *in situ*. Again, Collins (1934, 1937) supported the earlier observation of Barlow (1904) and Coleman (1913) that the norite-granophyre contact was transitional over a few tens of metres. Collins (1937), agreeing with Barlow (1904) and Coleman (1913), suggested that the norite - transition zone - granophyre system was emplaced as a sill, which subsequently differentiated in place. Subsequently, Thode *et al.* (1962), on the basis of sulfur isotope and other data, suggested that the SIC was emplaced as a single sheet-like body of magma, which differentiated by gravitational settling. Hawley (1962) observed crystal layering within the suite and interpreted this observation as an indication of crystal settling from one mass. Stevenson and Colgrove (1968) suggested that the SIC was a layered intrusion, which crystallized by *in situ* fractionation. Naldrett *et al.* (1970) and Gasparrini and Naldrett (1972) suggested that the system fractionated continuously by gravitational settling to form the norite, quartz gabbro and lower granophyre and, thus, originated as a layered intrusion. A rare earth element (REE) study of the SIC by Kuo and Crocket (1979) indicated that the phases are comagmatic and most likely formed by fractional crystallization processes. Most recently, a detailed study of the chemical composition of apatite crystals from the SIC by Warner *et al.*

(1998) and an isotopic study of sulfide ores and SIC lithologies by Dickin *et al.* (1999) support the view that the SIC evolved by fractional crystallization of a single melt, which was silica-rich and had a substantial crustal component if not wholly crustally derived. Dickin *et al.* (1999) performed least-squares mixing calculations using major element data, microprobe data from plagioclase cores, and calculated average pyroxene microprobe analyses from the South Range (data of Naldrett *et al.*, 1970). They successfully modelled the fractional crystallization of the lower unit ("norite"), middle unit ("quartz gabbro") and upper unit (granophyre) in close approximation to their observed proportions. Hypotheses favouring the SIC as an impact melt, in general, assume a one melt system.

Despite many observations supporting a one melt system, the idea of multiple melt injections has been revived on several occasions. First, Williams (1957) and again Thomson (1969) interpreted the norite and granophyre as successive injections. Naldrett and Kullerud (1967), based on their study of the norite, also suggested multiple injections. The hypothesis of these latter authors consists of an earlier magma differentiated from dunite to felsic norite and a subsequent intrusion of mafic norite followed by xenolithic norite. Ariskin *et al.* (1999) questioned the results of Dickin *et al.* (1999), based on their numerical simulations of convective-cumulative *in situ* differentiation of two initial liquids, which they believed to represent the original SIC melt composition. Their results indicate that the total amount of granophyre does not exceed 12 vol.% of the modelled SIC, under the assumption of a closed melt system.

Using the U-Pb dating method on zircon and baddeleyite crystals, Krogh *et al.* (1984)

reported a date of 1848.9 + 4.0/- 2.7 Ma for a North Range felsic norite, 1850.0 + 3.4/- 2.4 Ma for a North Range mafic norite, 1850.0 ± 1.3 Ma for a South Range norite, and 1850.5 ± 3 Ma for a granophyre. Corfu and Lightfoot (1996) reported dates of 1848.1 ± 1.8 to 1849.1 ± 1.1 Ma for contact sublayer samples. All of these dates are basically indistinguishable and point to a contemporaneous age for all lithologies of the SIC.

Faggart *et al.* (1985), using Sm-Nd isotopic data, were first to demonstrate that the SIC consists of remelted rocks of the surrounding Huronian Supergroup and Archean basement. Walker *et al.* (1991), using Re-Os isotope systematics, Dickin *et al.* (1996), using Pb isotope ratios, and Dickin *et al.* (1999), using Os isotope compositions, demonstrated that the ores of the SIC were also of crustal origin, *i.e.*, derived from remelted Archean basement plus Huronian material. Deutsch (1994) showed that lithologies of the SIC (norite, quartz gabbro, contact sublayer) have Nd and Sr isotopic compositions corresponding to those of the country rocks and, thus, do not require an additional component of material extracted from the mantle. Lightfoot *et al.* (1997a), based on trace and major element geochemical data, and Dickin *et al.* (1999), based on available isotopic and geochemical data, also demonstrated that all of the SIC lithologies shared a common source and that a mantle contribution was not necessary. According to Lightfoot *et al.* (1997a), compositional variations within the SIC (the apparent compositional break between the norite and the granophyre and the volume ratio of granophyre to norite) are not readily explained by simple *in situ* fractionation involving a single body of magma. Ariskin *et al.* (1999) also stressed the problem of the observed granophyre volume. Taylor (1967) demonstrated that a secondary reaction has changed the isotopic composition of

some of the granophyre minerals, and Gibbins and McNutt (1975) demonstrated that greenschist facies metamorphism generated open system conditions in the granophyre but not in the norite; warranting caution when interpreting geochemical variations within the SIC. Also, recently, Thompson *et al.* (1998) through a study of pseudotachylites north of the SIC suggest that, contrary to previous ideas, the North Range has indeed been affected by a protracted period of post-impact, low-grade thermal metamorphism.

1.3 Objectives

A major objective of this thesis is the examination of the SIC and its division into lithological units, and their relation to possible impact and/or endogenic igneous processes. As such, the objectives of this thesis can be broken down into the following series of scientific questions. Is there evidence of shock metamorphism within the SIC? Are there remnant inclusions of country rock within the SIC (other than the obvious ones in the contact sublayer, and at the base and top of the SIC)? Is the bulk composition of the SIC really granodioritic and, if so, why? What was the initial composition of the SIC melt? Did the contact sublayer, norite, quartz gabbro and granophyre result from the differentiation of a single melt system? Under what conditions did the SIC crystallize? Was the SIC superheated? Was it undercooled? Why does the SIC contain a large amount of granophyre in comparison to other layered igneous complexes? What is the relative timing of the crystallization of the SIC and its various lithologies? To answer these questions, a detailed petrography study, and physical, chemical and computer models were used.

2. SAMPLING, INSTRUMENTATION AND METHODOLOGY

From 1994 to 1999, several visits were made to Sudbury, which included sampling from the core repository of INCO Ltd, Copper Cliff, Ontario, and field work, including N-S traverses across the Sudbury Basin and in specific locations for more detailed work. This thesis mainly involves samples taken from three drill cores, drilled in the North Range of the Sudbury Basin (Fig. 1), and made available by INCO Ltd. Surface outcrop samples and field observations were used for completeness and to refine concepts and ideas on a larger scale than that available from the drill cores. Two of the drill cores (70011 and 52847) span a continuous section from the Onaping Formation, overlying the SIC, to the brecciated basement rocks, underlying the SIC (Fig. 3). The third drill core (52848) spans a section from within the top of the granophyre to the brecciated basement rocks. Samples were taken from these cores at specific depths and additional extensive sampling was carried out over the contacts. Polished thin sections were made of most samples (totalling over 200 thin sections).

Drill core 70011 is the least complex of those studied in terms of lithology and geochemistry, and thus detailed petrography, mineralogy and geochemistry of the SIC (contact sublayer to granophyre) was done mainly using samples from this drill core. Within drill cores 70011 and 52847, about mid-way through the lower unit ("norite") and above, microprobe analyses revealed that pyroxene crystals are replaced by relatively late-magmatic amphibole, indicating that these drill cores are, in fact, altered. In order to verify the mineralogy and petrology of these drill cores, samples from drill core 52848 were used, since they have been least affected by late-magmatic (or deuteric) alteration.

Petrographic studies were done using a Leitz binocular petrographic microscope. In general, the observations are very similar to previous petrographic studies made on different rock suites of the SIC (samples from drill cores or surface outcrops). In some instances, however, the results differ from those of previous workers, and new observations are reported. Photomicrographs were taken using a Hund 35mm camera mounted on a Leitz binocular microscope (at the Geological Survey of Canada, Ottawa), a 35mm camera mounted on a Wild Heerbrugg-Leitz binocular microscope and an Olympus 35mm camera mounted on an Olympus BH-2 binocular microscope (both of these latter instruments are located at the University of Ottawa in the Department of Earth Sciences).

Modal analyses were carried out on nineteen (19) polished thin sections, 2.5 cm by 4.5 cm, under a Leitz binocular petrographic microscope, to determine the modal bulk composition of each sample selected. More than 800 points were counted for halved core sections and more than 1000 points for full core sections. The points were spaced at 0.5 mm intervals across the width of the thin section and along traverses spaced at 1 mm intervals across the length of the thin section.

A suite of 33 samples was chosen for electron microprobe analyses. Mineral compositions (Appendix A) were obtained using wavelength-dispersive X-ray spectrometry (WDS) with either a CAMECA CAMEBAX or a CAMECA SX-50 electron microprobe located at the Geological Survey of Canada in Ottawa. Analyses obtained with the CAMEBAX were matrix-corrected using the PAP scheme; whereas, those obtained with the SX-50 were corrected using the ZAF scheme. Standards used are a mix of synthetic and natural metals and silicates.

The settings were 20 kV and 10 nA for all minerals when using the SX-50. On the CAMEBAX, the settings were 20 kV and 10 nA for feldspars, 15 kV and 25 nA for pyroxenes, and 15 kV and 10 nA for amphiboles, oxides and titanites. All analyses were done using a focussed beam, except for feldspar analyses for which a beam spot of ~ 10 μm was used with the SX-50. Results are considered accurate to within ± 2% for major and minor elements (Appendix A). Calculation of mineral formulae was done following the method described in Deer *et al.* (1985).

Measurements of planar deformation features (PDFs) were obtained using standard U-stage techniques. The poles to all sets of PDFs and the optic axes of each quartz grain were plotted on a stereonet (Wulff net projection). These data were then rotated to a c-axis vertical orientation, and using a template of all rational crystallographic orientations (with the c-axis in a vertical orientation), a best fit to rational crystallographic orientations of quartz was obtained (*e.g.*, Robertson *et al.*, 1968). Each rational crystallographic orientation on the template is represented by a 5° circle to allow for measurement error. The procedure involves overlaying the template onto the data for each quartz grain and then rotating the template, which is not fixed to allow for c-axis measurement error, until the best fit to the poles of the PDFs is obtained. This method, although time consuming, retains the angular relationship(s) among multiple sets of PDFs, as well as with the optic axis. Thus, unlike other methods, which consider only the inclinations of PDF poles relative to the optic axis, rigorous assignment is made of particular PDFs to specific crystallographic orientations in quartz.

Whole-rock major, trace, and rare earth element geochemistry was carried out on 106 samples used in this study. The geochemical analyses were performed at the laboratories of the

Geological Survey of Canada in Ottawa (Appendix B), using wavelength-dispersive X-ray fluorescence spectrometry (XRF) on fused disks for major element detection, and inductively coupled plasma-mass spectrometry (ICP-MS) for trace and rare earth element detection. Rapid chemical methods were used to detect FeO, H_2OT, CO_2T, S and LOI. The content of Fe_2O_3 was calculated using $Fe_2O_3 = Fe_2O_3T$ (through ICP-MS) - 1.11134 * FeO (volumetric). Precision estimates of data are given in Appendix B. Data used in diagrams were normalized to 100 wt% for all major elements, excluding H_2OT, CO_2T and S values (Appendix C). The normalized major elements together with trace elements were converted to molar proportions (Appendix C) for use in the Pearce Element Ratios (PER) calculations. Major element analyses were used to calculate the CIPW norms of samples using the program NEWPET. Results for individual samples from all three drill cores are given in Appendix D.

The relatively new software package MELTS (Ghiorso and Sack, 1995) was used to simulate the crystallization of the SIC. This software package models chemical mass transfer in magmatic systems. It is based upon algorithms for energy minimization described by Ghiorso *et al.* (1983), Ghiorso (1985), and Ghiorso and Kelemen (1987) and incorporates new procedures for determination of the saturation state and stability of strongly non-ideal solid solutions with respect to silicate melt (Ghiorso, 1994). The MELTS software package was obtained via anonymous FTP from internet node fondue.geology.washington.edu. It was run interactively on a "UNIX"-level workstation at the Geological Survey of Canada in Ottawa.

3. PETROGRAPHY AND MINERALOGY

3.1 Modal Compositions

Table I contains data of the modal composition of samples from drill core 70011. Compared to previously published modal composition data, the data presented in this study consist of a more comprehensive list of minerals and include alteration products. Many alteration minerals occur as micro-inclusions within plagioclase crystals and, thus, the modal content of plagioclase crystals was adjusted accordingly (see footnotes of Table I for details). In this study, the term "micrographic" is used for reasonably regular (cuneiform) and well defined microscopic intergrowths of quartz and alkali feldspar; whereas, the term "granophyric" is used for intergrowths of quartz and alkali feldspar that are more irregular and, especially, those that radiate from plagioclase crystals (for details, see section 3.5 "Textures"). It is most likely that this terminology reflects three-dimensional effects, the crystal orientation of the intergrowths and not necessariiy a different mode of crystallization for the intergrowths. Figure 5 shows the distribution of minerals in relative proportions observed in drill core 70011. In addition, throughout the cores, numerous thin veins of epidote, chlorite, calcite, quartz, or a combination of these minerals, are found cutting the long axis of the drill cores at angles of 45° to 90°.

As indicated in Table I, the contact sublayer samples are composed mainly of plagioclase and orthopyroxene, and, thus, they conform to the IUGS classification of norite (Streckeisen, 1976). However, the "norite" samples, as shown in Table I, contain primary amphibole crystals and all samples from the upper part of the "norite" contain clinopyroxene (augite) crystals but are free of orthopyroxene (enstatite) crystals. Thus, the "norite" samples do not conform to the

Table I: Modal compositions, in volume percent, from point counts in representative samples of the SIC lithologies in drill core 70011.

Lithology	**A**	**B**	**B**	**B**	**B**	**B**	**C**	**D**	**C**	**C**	**E**	**E**	**E**	**F**	**F**	**F**	**F**	**F**	**F**
Sample #	**97**	**69**	**94**	**153**	**131**	**61**	**60**	**129**	**150**	**59**	**89**	**180**	**55**	**54**	**5**	**4**	**3**	**2**	**85**
Depth (m)	**2305.8**	**2252.5**	**2011.7**	**1831.8**	**1828.8**	**1752.6**	**1735.8**	**1731.3**	**1723.6**	**1676.4**	**1630.7**	**1566.7**	**1493.5**	**1463**	**1310.6**	**1005.8**	**701.0**	**396.2**	**94.5**
points	**814**	**728**	**2362**	**2179**	**1017**	**1027**	**1005**	**1027**	**1014**	**1037**	**1026**	**1031**	**1007**	**1019**	**1022**	**1018**	**974**	**1021**	**1028**
plag	49.0	48.5	21.5 (48.6)[1]	19.5 (44.9)[1]	18.9 (42.9)[1]	24.1 (45.3)[1]	17.3 (43.6)[1]	17.2 (46.6)[1]	9.9 (36.6)[2]	12.3 (43.7)[2]	8.1 (40.5)[2]	14.3 (36.3)[3]	13.2 (23.3)[3]	15.2 (20.5)[4]	15.8 (21.5)[4]	27.0 (31.1)[4]	23.9 (23.9)[4]	28.2 (31.9)[4]	16.1 (19.9)[4]
cpx	8.2	2.6	1.9	1.5	8.2	15.2	15.2	11.8	9.6	2.0	tr	tr	tr	tr	-	-	-	-	-
opx	12.8	3.2	2.2	-	-	-	-	-	-	-	-	-	-	-	-	-	-	-	-
hbln	tr	3.2	3	2.1	6.7	5.1	2.6	5.9	12.5	11.3	8.0	3.5	2.3	tr	tr	tr	1.2	3.3	-
actinolite	tr	tr	tr	tr	-	-	-	-	-	tr	-	-	-	-	-	-	-	-	-
biotite	1.5	4.7	-	-	-	-	-	-	10.6	11.1	20.0	16.6	13.5	12.3	13.6	5.5	3.1	3.8	4.3
quartz	2.1	15.3	6.1	4.1	2.7	1.7	2.8	2.9	3.0	3.2	3.4	3.6	4.8	2.8	2.7	3.1	6.3	4.0	3.7
K-feldspar	tr	4.9	5.6	7.3	4.5*	2.2*	2.5	1.8	1.3	tr	2.0	2.7	5.3	2.4	1.2	2.2	2.3	3.3	tr
graphic	-	-	7.2	16.1	12.9	13.5	13.5	8.4	11.6	4.8	5.3	17.1	40.8	48.6	52.1	46.9	43.4	35.9	60.7
granophy.	-	-	8.8	4.1	5.5	6.8	6.3	5.1	5.1	8.0	12.2	8.9	7.4	7.6	3.8	2.0	1.2	6.0	3.1
apatite	tr	tr	tr	tr	tr	tr	tr	tr	tr	tr	tr	tr	tr	tr	tr	tr	tr	tr	tr
oxides	3.9	tr	1.0	tr	1.3	tr	tr	tr	tr	2.4	tr	2.4	1.1	tr	tr	tr	1.6	3.8	tr
titanite	-	tr	tr	tr	tr	tr	1.1	tr	2.7	2.7	4.2	tr	tr	tr	tr	tr	tr	tr	tr
chlorite	2.3	3.0	6.6	8.8	4.6	2.9	3.9	6.3	4.2	8.7	8.4	1.5	tr	-	tr	5.8	13.6	6.5	4.7
epidote	tr	tr	11.1	14.7	16.6	12.7	15.7	18.6	16.0	20.0	15.2	21.5	8.1	8.4	8.6	5.3	3.2	4.8	5.9
sec. biotite	2.0	4.9	1.8	2.5	3.6	1.1	1.5	2.2	6.0	6.7	5.2	5.5	2.5	tr	tr	-	-	-	-
clinozoisite	1.1	4.3	15.0	9.3	8.3	9.9	12.2	11.7	5.3	5.4	6.3	tr	tr	tr	tr	-	-	-	-
uralite	15.6	4.0	6.3	8.4	5.8	3.7	4.3	6.8	1.1	tr	tr	-	-	-	-	-	-	-	-
calcite	-	-	tr	tr	tr	-	-	-	-	-	-	-	-	-	-	-	tr	-	-

Lithology: A = contact sublayer; B = lower unit ("norite"); C = middle unit ("quartz gabbro"); D = "blue-band"; E = transition zone; F = upper unit (granophyre)

Abbreviations: plag = plagioclase; cpx = clinopyroxene; opx = orthopyroxene; hbln = hornblende; graphic = micrographic intergrowths; granophy. = granophyric intergrowths; sec. biotite = secondary biotite

Added due to alteration: [1] = clinozoisite + 1/2 chlorite + 3/4 epidote + 1/4 biotite; [2] = clinozoisite + 1/4 chlorite + 3/4 epidote + 1/2 biotite; [3] = clinozoisite + 1/4 chlorite + 3/4 epidote + 1/4 biotite; [4] = 1/5 chlorite + 1/3 epidote + 1/5 biotite

* = 60% as overgrowth

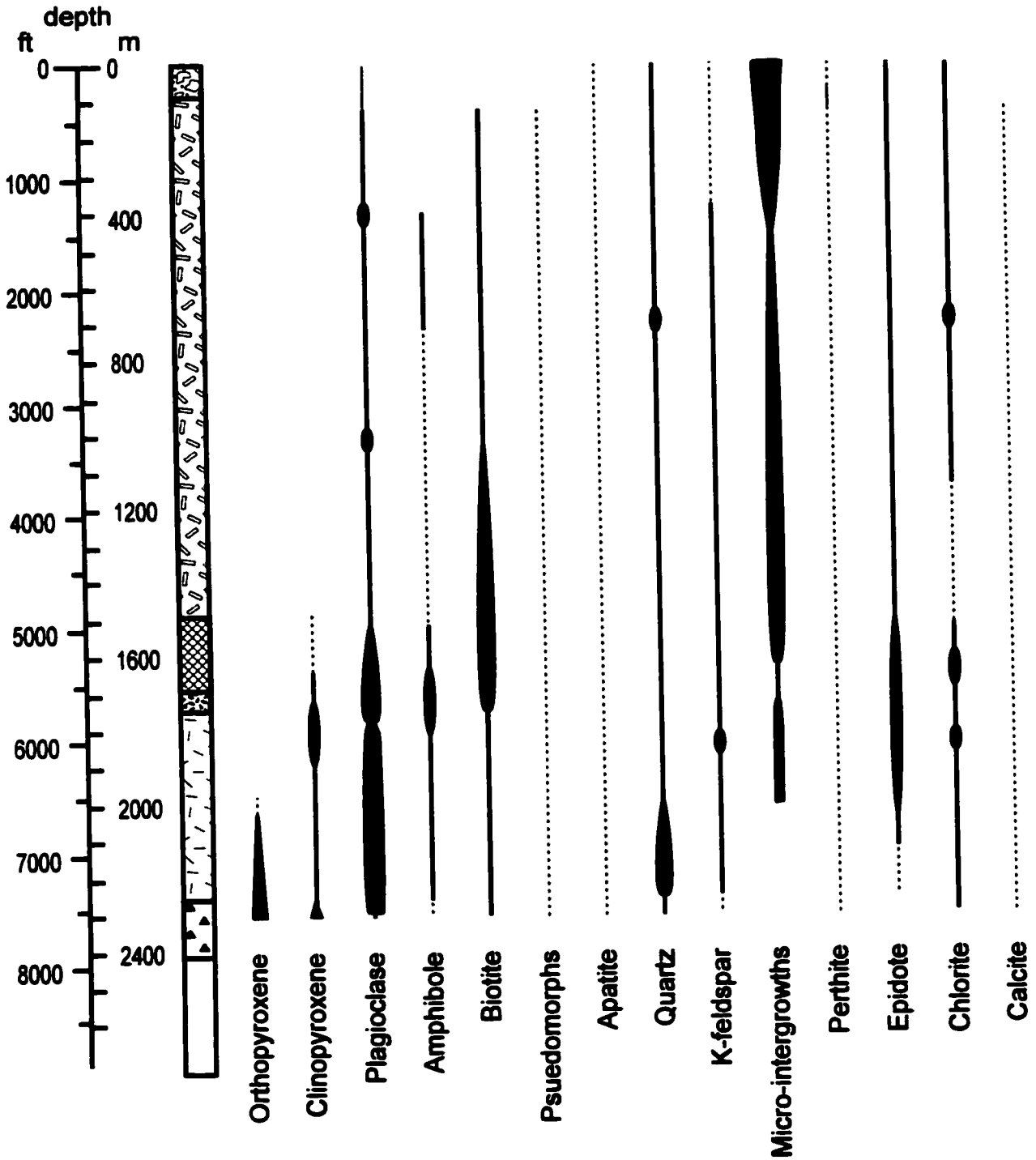

Figure 5. Occurrence of mineral species with stratigraphy in drill core 70011. Lithology patterns as in Figure 3. The thickness of the lines corresponds to the relative abundance of the mineral. A dashed line is an abundance in trace amounts. Micro-intergrowths = micrographic and granophyric intergrowths.

IUGS definition of norite (Streckeisen, 1976). Moreover, on a Streckeisen (quartz (Q) - alkali feldspar (A) - plagioclase (P)) diagram, the modal analysis of the "norite" samples plot within the quartz monzogabbro field and one sample (at the base of this unit) plots within the quartz gabbro field (Fig. 6). Although the "quartz gabbro" samples consist mainly of labradorite and augite, their modal abundance of micrographic and granophyric intergrowths (and, thus, alkali feldspar) is relatively too high to conform to the IUGS definition (Streckeisen, 1976). On a Streckeisen diagram, the modal analysis of "quartz gabbro" samples plot within the quartz monzogabbro field (Fig. 6). As for the other SIC samples listed in Table I, the contact sublayer sample plots within the norite field, the granophyre samples plot within the granite field, and transition zone samples straddle the granite, granodiorite and quartz monzogabbro fields (Fig. 6). The trend observed in Figure 6 is directly related to the modal abundance of plagioclase and quartz crystals. Note that similar results are obtained when using the modal data of North Range samples presented in Naldrett *et al.* (1970) (Fig. 6). As the SIC has often been compared to layered mafic igneous intrusions and the current nomenclature of SIC lithologies has genetic implications, new terms are proposed to alleviate the use of misleading compositional names. However, since the terminology is entrenched in the literature, "norite", "quartz gabbro" and "granophyre" will be used in the remainder of this thesis, together with the new terms. Here, the "norite" will be referred to as the lower unit, the "quartz gabbro" as the middle unit, and the granophyre as the upper unit; the terms contact sublayer and transition zone are, respectively, kept and introduced (Fig. 4).

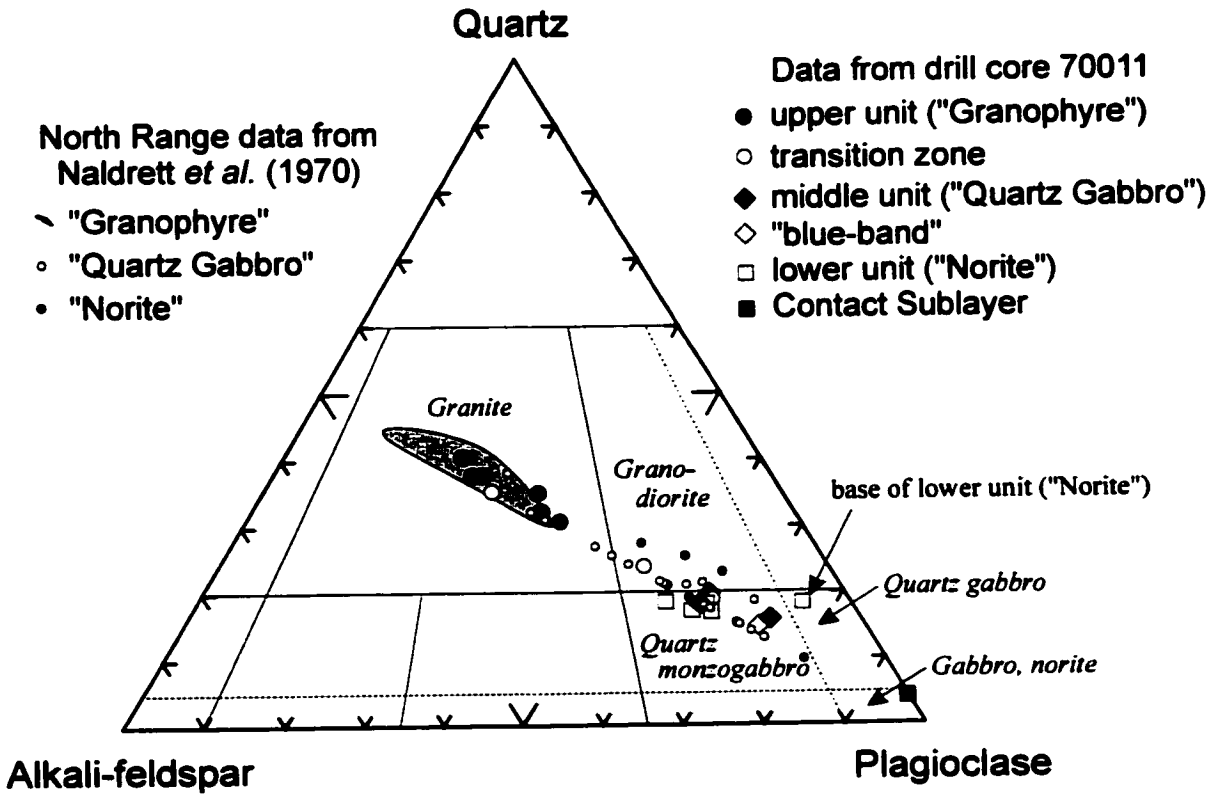

Figure 6. Streckeisen (QAP) diagram for the SIC rock samples used for the modal analyses given in Table I and for published data from Naldrett *et al.* (1970). See text for details.

3.2 Description of Lithologies

3.2.1 Contact sublayer

In the drill cores studied, the contact sublayer is observed only in drill core 70011, as a layer up to 150 m thick (Fig. 3). A comprehensive petrological description of the contact sublayer may be found in Pattison (1979) and Lightfoot *et al.* (1997b). The contact sublayer is a medium- to coarse-grained heterogeneous rock, dark gray, inclusion-rich, with a hypidiomorphic texture, interstitial quartz and K-feldspar, and very rare granophyric intergrowths. These granophyric intergrowths consist mainly of quartz and oligoclase (An_{10-15}). The quartz component of these intergrowths is virtually free of micro-inclusion; whereas, the feldspar component contains some epidote micro-inclusions, an observation consistently made throughout the SIC and not to be repeated for each lithology, hereafter.

Major mineral phases consist of slightly sericitized labradorite-andesine crystals (An_{67} to An_{32}, 35-45 vol.%; Fig. 7a), altered small (up to 2 mm in diameter) and equant enstatite crystals (10-15 vol.%), and altered diopside crystals (5-10 vol.%). Diopside crystals have augite exsolution lamellae, which have an etched pattern or parting commonly lined by Fe-Ti oxides. In a specific phase of the contact sublayer, not observed in the drill cores studied, olivine occurs as rare cumulus crystals (Pattison, 1979). Most plagioclase crystals are slender, less than 8 mm in length and normally zoned, having rim compositions as low as An_{32} (Fig. 7a). The clinopyroxene crystals are anhedral to subhedral and may reach up to 8 mm in length. Minor mineral phases consist of amphibole, biotite, chlorite and abundant disseminated sulfides (> 3 vol.%). The amphibole and biotite crystals are anhedral to subhedral, up to 2 mm in diameter,

Figure 7. Ab-Or-An diagrams of all microprobe analyses of feldspar crystals, including matrix components and overgrowth, rim and core of xenocrysts and phenocrysts in samples from drill core 70011: (a) contact sublayer; (b) lower unit ("norite"); (c) middle unit ("quartz gabbro"); (d) transition zone; and (e) upper unit (granophyre). See Appendix A for complete analyses.

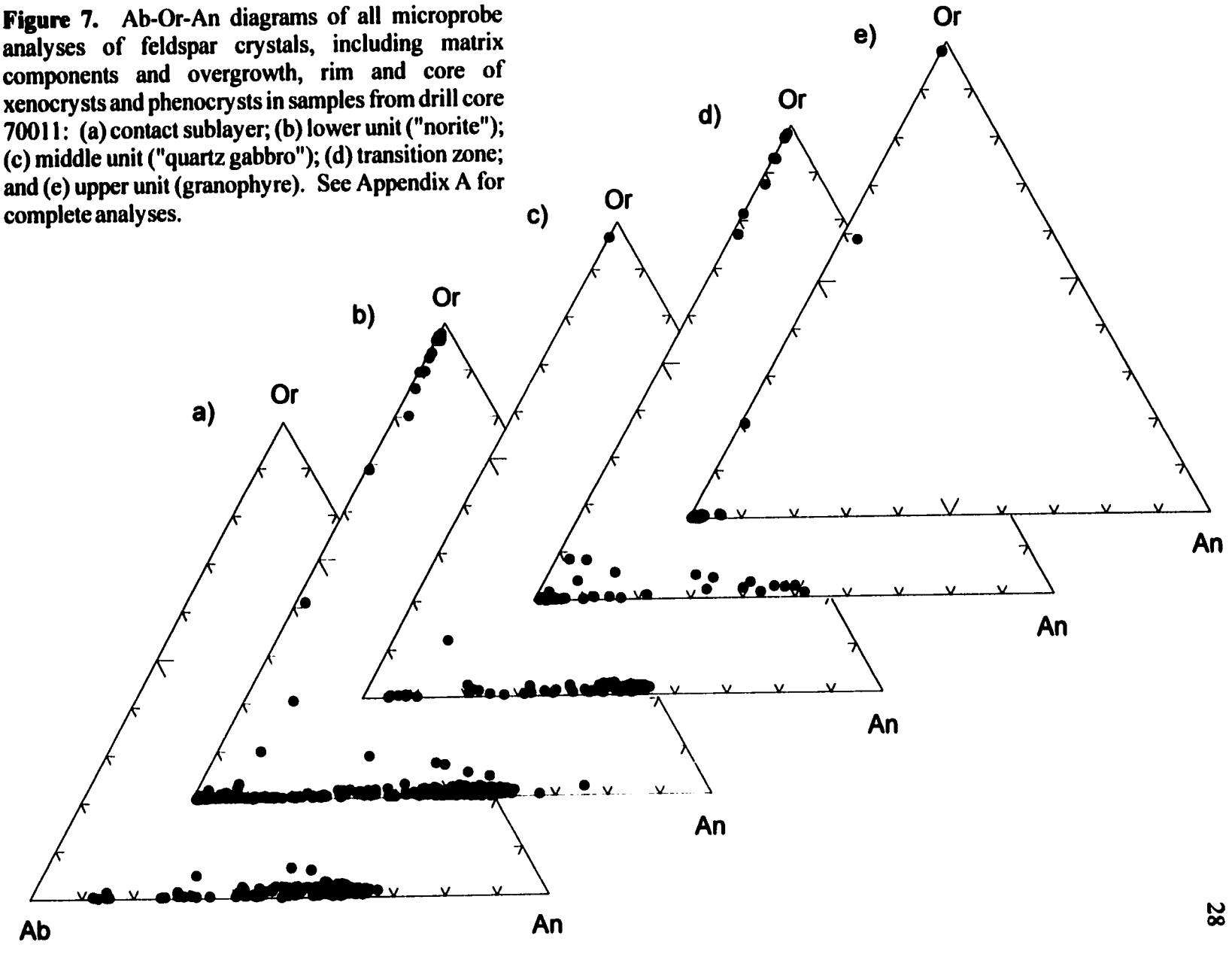

and are most likely primary, as they enclose small plagioclase (Fig. 8a), ilmenite and/or quartz crystals. Biotite and chlorite crystals may have multiple kink-bands. Sulfide (mainly pyrrhotite, pentlandite and chalcopyrite, and minor pyrite) crystals occur as aggregates up to 2 mm in diameter, which may commonly have a halo of finely disseminated sulfide (mainly pyrrhotite, chalcopyrite and pyrite) (Fig. 8b). Inclusions are also abundant in and characteristic of the contact sublayer. Monomineralic inclusions consist mainly of quartz and plagioclase xenocrysts (Fig. 8c). Lithological inclusions consist of country rocks (such as diabase, melanorite, olivine melanorite and metamorphosed melanorite; Fig. 8c) and ultramafic rocks (such as wehrlite and dunite) of unknown origin, but which are believed to be genetically linked to the SIC (*e.g.*, Lightfoot *et al.*, 1997b). These inclusions range in size from a few millimeters to a few meters. The xenocrysts of plagioclase are up to 4 mm in length and wider than the primary plagioclase crystals (Fig. 8c). They show faint to well-developed oscillatory extinction patterns (Fig. 8d) or reverse zoning and commonly corroded or abraded rims.

3.2.2 Lower unit ("norite")

The lower unit is approximately 500 m thick in drill core 70011. It is medium-grained, gray and contains cumulus plagioclase and clinopyroxene. This unit may be further subdivided into a lower part, about 300 m thick, the base of which is marked by a sharp increase in quartz content (5-20 vol.%), and an upper part, about 200 m thick, which is free of enstatite crystals. Quartz crystals are up to 1.0 mm in diameter and most are interpreted as xenocrysts, because of their rounded or irregular edges. In the lower part of the lower unit ("norite"), plagioclase

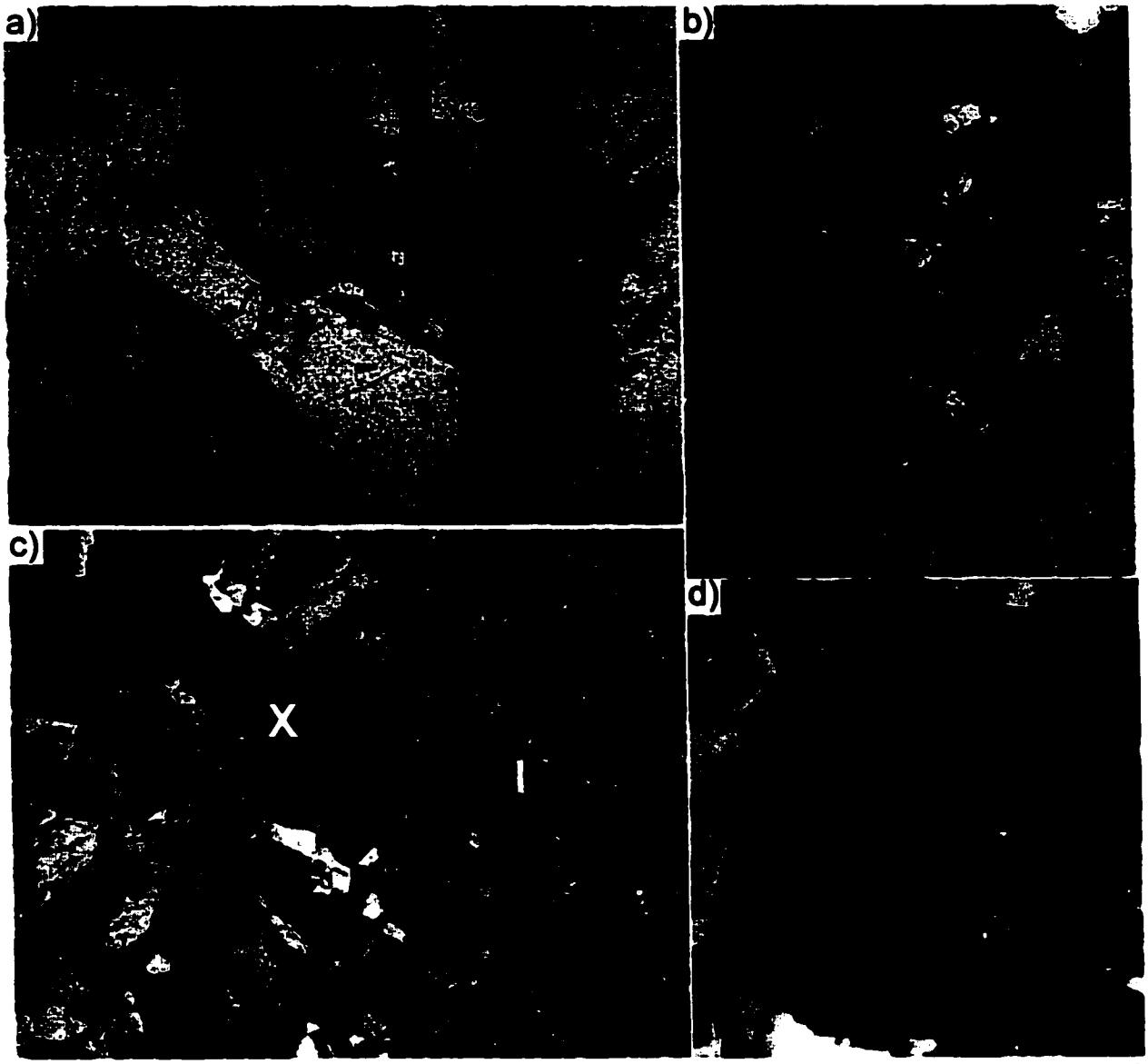

Figure 8. Photomicrographs of the contact sublayer: **(a)** primary biotite (brown) and amphibole (green) oikocrysts enclosing plagioclase laths (sample SUD-71-1994, plane light, field-of-view = 6 mm); **(b)** pyrrhotite-pyrite (reds and yellows) and chalcopyrite (greenish) bleb surrounded by a halo of fine pyrrhotite, pyrite and chalcopyrite (sample SUD-71-1994, reflected light, field-of-view = 2 mm); **(c)** The right-hand side of the picture consists of a melanorite inclusion (I); whereas, the left-hand side is the enclosing matrix in which occurs a plagioclase xenocryst (X) wider than the other plagioclase crystals (sample SUD-155-1995, cross-polarized light, field-of-view = 14.5 mm); and **(d)** close-up view of this xenocryst showing twins, running WNW-ESE across the faint oscillatory zoning pattern, and two overgrowths, one at extinction (black) and a second thinner and less regular overgrowth (gray). Fractures filled by chlorite cut across the xenocryst (cross-polarized light, field-of-view = 2.5 mm).

crystals are abundant (40-50 vol.%) and up to 4.0 mm in length. Cumulus enstatite and inverted pigeonite crystals are less abundant (4-8 vol.%) and up to 2.5 mm in length, both being more abundant than augite (2-5 vol.%), which occurs as crystals up to 4 mm in length. Cumulus and secondary amphibole and biotite crystals occur in minor amounts (≤5 vol.%), and are all up to 1 mm in diameter (Fig. 9a). The upper part of the lower unit ("norite") is similar to the lower part, differing only in amounts of quartz crystals (≤5 vol.%), augite crystals (8 to 20 vol.%), which are up to 2.5 mm in diameter, primary amphibole (up to 10 vol.%), and no cumulus enstatite.

Plagioclase, throughout the lower unit, occurs as subhedral prisms or laths with a strongly zoned rim (andesine, An_{20-55}) around an unzoned core (labradorite, An_{55-62}) and with a thin overgrowth of albite-oligoclase (An_{1-25}; Fig. 7b). In the lower part of the lower unit, plagioclase laths have a second thin overgrowth of orthoclase, which branches into the matrix (Fig. 9b). Most plagioclase crystals are heterogeneously altered by any combination of the following: sericite, epidote/clinozoisite, biotite and chlorite. Their overgrowth is free of alteration (Fig. 9b). Plagioclase crystals with faint (remnant) oscillatory extinction pattern (Fig. 9c) and/or showing reverse zoning (An_{1-16}) are interpreted as xenocrysts (see section 3.3.1 Plagioclase, below). Very small albite (An_{0-10}) inclusions occur within larger orthoclase crystals. Orthopyroxene occurs as enstatite intergrowths in augite, or as crystals in clusters with augite crystals. Poikilitic augite, enclosing plagioclase crystals, occurs as subhedral crystals with a thin diopside overgrowth (Fig. 9d). Some augite crystals have a sharp and finely spaced parting and/or show exsolution lamellae (Fig. 9d; poorer in Ca and richer in Fe than their host), both of which may be lined by

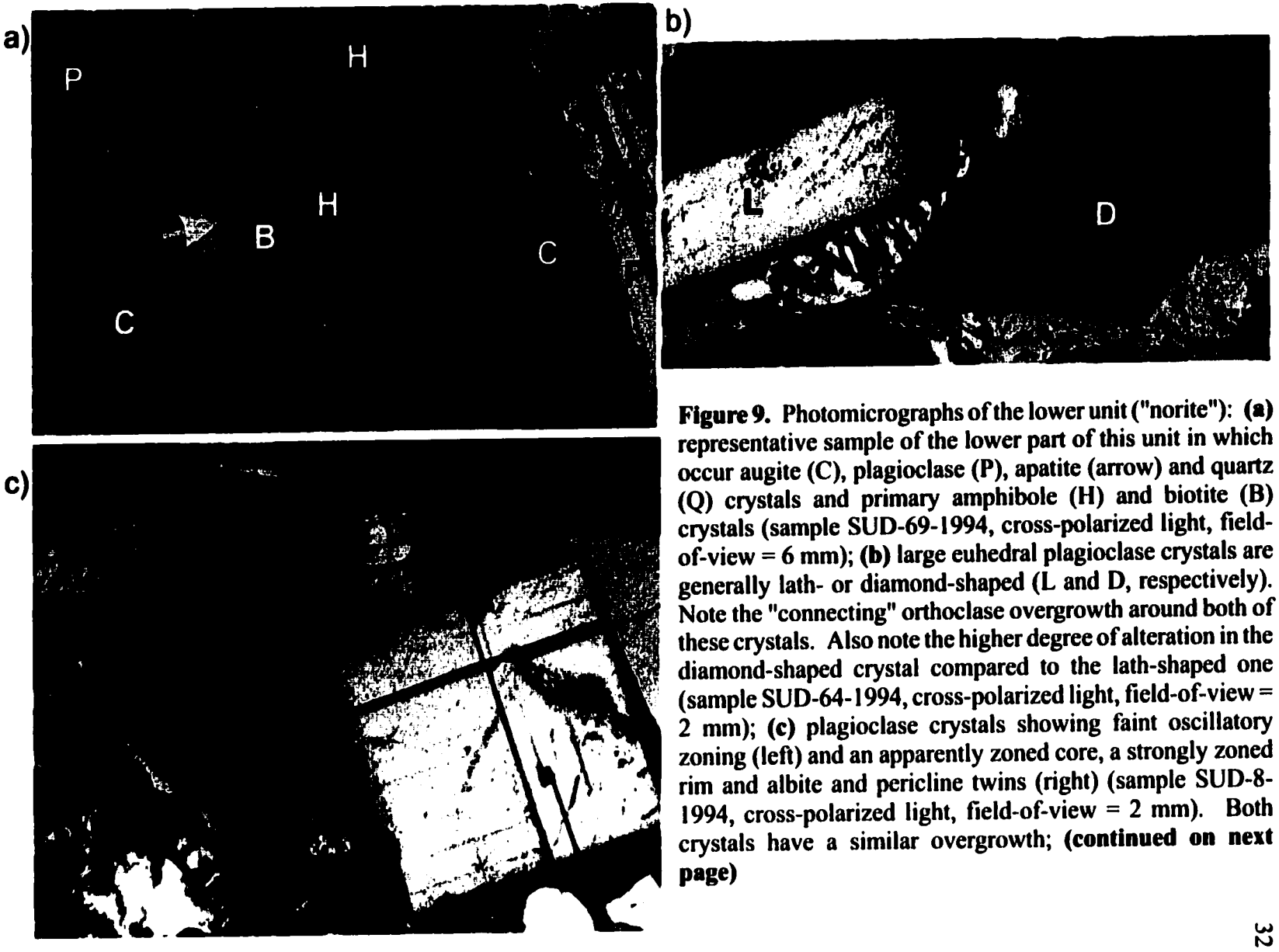

Figure 9. Photomicrographs of the lower unit ("norite"): **(a)** representative sample of the lower part of this unit in which occur augite (C), plagioclase (P), apatite (arrow) and quartz (Q) crystals and primary amphibole (H) and biotite (B) crystals (sample SUD-69-1994, cross-polarized light, field-of-view = 6 mm); **(b)** large euhedral plagioclase crystals are generally lath- or diamond-shaped (L and D, respectively). Note the "connecting" orthoclase overgrowth around both of these crystals. Also note the higher degree of alteration in the diamond-shaped crystal compared to the lath-shaped one (sample SUD-64-1994, cross-polarized light, field-of-view = 2 mm); **(c)** plagioclase crystals showing faint oscillatory zoning (left) and an apparently zoned core, a strongly zoned rim and albite and pericline twins (right) (sample SUD-8-1994, cross-polarized light, field-of-view = 2 mm). Both crystals have a similar overgrowth; **(continued on next page)**

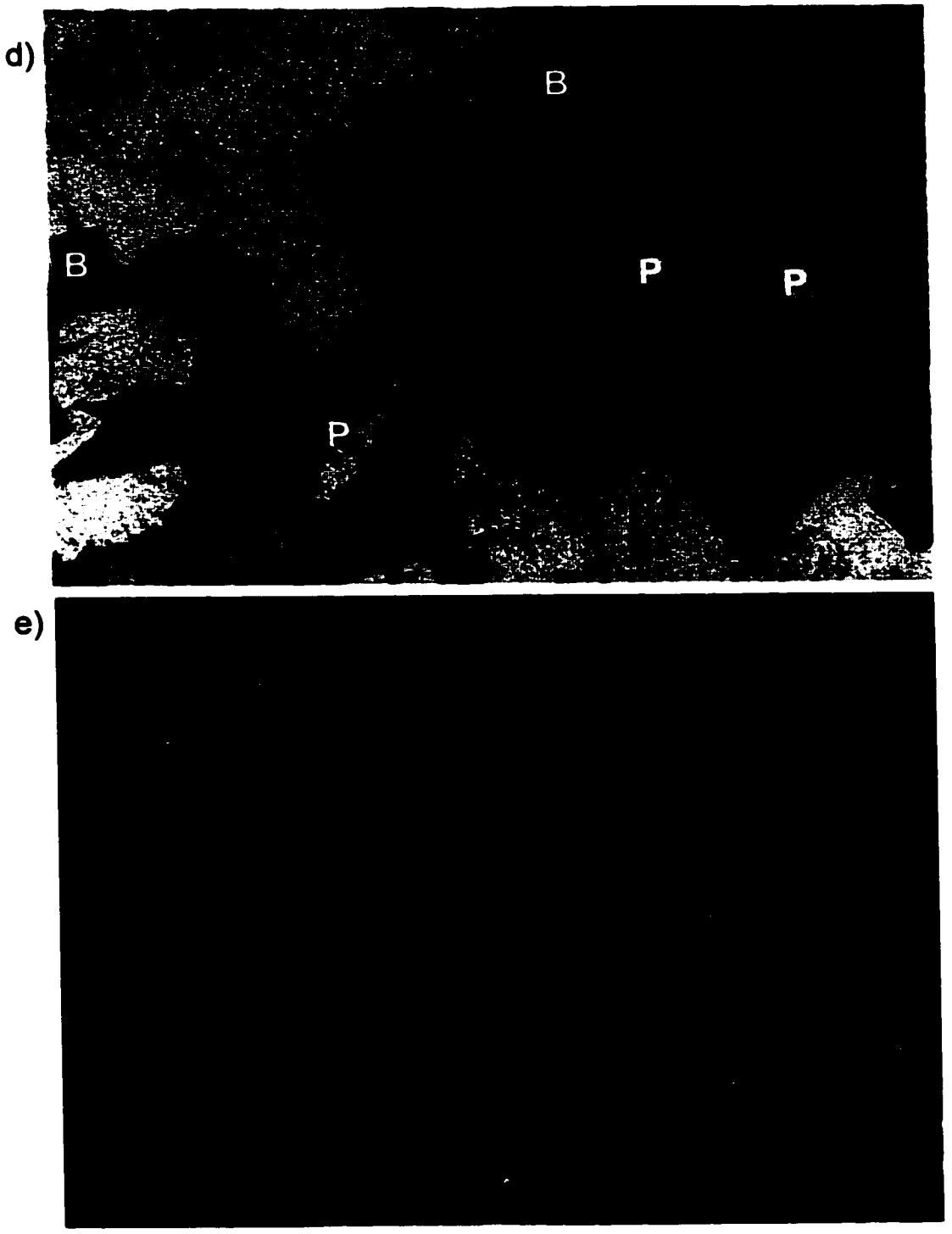

Figure 9 (continued). **(d)** partially altered pyroxene oikocryst with exsolution lamellae (running NNW-SSE) and enclosing plagioclase laths (P) (sample SUD-8-1994, plane light, field-of-view = 2 mm). Note the amphibole mantle (greenish) around the oikocryst and biotite crystals (B); and **(e)** primary amphibole crystal with 60-120° cleavage (close-up view of (a), cross-polarized light, field-of-view = 1 mm).

magnetite. Most pyroxene crystals, especially along parting/cleavage planes, are partly replaced by chlorite, amphibole, and/or biotite (Fig. 9d), and needles of actinolite and ferro-actinolite may occur in the margins of the crystals. Almost all pyroxene crystals are mantled by amphibole, which is free of alteration and may very well be primary (Fig. 9d). Amphibole crystals with a classic crystal form (Fig. 9e), which demonstrates that they grew in an environment where space was not constrained by other crystals, or was only partially constrained, are interpreted as primary (see also section 3.3.3 Amphiboles). Accessory minerals in the lower unit ("norite") consist of apatite (Fig. 9a), pyrite, titanite, ilmenite, magnetite and titaniferous magnetite. Micrographic and granophyric intergrowths (totalling up to ~20 vol.%) are the most common interstitial phases, except at the base of the lower unit ("norite") where none were observed. The micrographic and granophyric fields, contrary to the contact sublayer, contain no plagioclase and consist mainly of quartz intergrown with alkali feldspar (orthoclase and minor albite).

An additional rock type of the lower unit ("norite"), a mafic quartz gabbro ("mafic norite" in previous work), observed in drill core 52848, is also part of the North Range of the SIC and has been described by previous workers (*e.g.*, Stevenson and Colgrove, 1968; Hewins, 1970, 1971). It is a discontinuous layer up to 100 m thick at the base of the lower unit ("norite"). This mafic quartz gabbro ("mafic norite") consists mainly of small white "anorthosite" inclusions, which may be very abundant, coarse plagioclase oikocrysts enclosing euhedral orthopyroxene crystals in excess of clinopyroxene crystals, and quartz intergrown with perthite (Hewins, 1974). Other minerals, in minor amounts, include biotite, magnetite and ilmenite.

3.2.3 Middle unit ("quartz gabbro")

Approximately 100 m thick in drill core 70011, the middle unit ("quartz gabbro") is slightly coarser-grained than the lower unit ("norite"). It is dark gray, and contains cumulus plagioclase (35-45 vol.%), clinopyroxene (2-10 vol.%), amphibole (10-15 vol.%), biotite (15-20 vol.%) and titanite + magnetite (2-5 vol.%) (Fig. 10a). The base of the middle unit ("quartz gabbro") is marked by a sharp increase in the abundance of amphibole crystals, some of which are primary, and the reappearance of primary biotite crystals.

Plagioclase occurs as subhedral to euhedral prismatic and lath-shaped crystals 0.5-3.0 mm in length (Fig. 10a). Towards the top of the middle unit ("quartz gabbro"), crystals may be boxy-cellular in form. Plagioclase crystals are normally zoned labradorite-andesine (An_{45-56}, core; An_{31-48}, rim), with a noticeable albite-oligoclase (An_{5-25}) overgrowth (Fig. 7c), which is about one tenth of the crystal width. Highly altered, diamond-shaped, albite crystals (An_{0-5}; Fig. 7b), with no apparent overgrowth are also observed (Fig. 10a). Clinopyroxene occurs as subhedral to anhedral prismatic and lath-shaped augite crystals, 0.1-3.0 mm in length (Fig. 10a). In general, needles of actinolite and ferro-actinolite are disseminated heterogeneously within the crystals (Fig. 10b). Exsolution lamellae, too fine to be analysed with the microprobe, are observed in some augite crystals. Amphibole occurs as anhedral to subhedral prismatic and lath-shaped crystals up to 1.5 mm in length (Fig. 10a); whereas, the amphibole pseudomorphs after clinopyroxene are singly-twinned (Fig. 10c). Rare primary amphibole occurs as subhedral to euhedral crystals, <2 mm in diameter, with well-developed cleavage (Fig. 10d). Primary biotite crystals, subhedral to euhedral and < 1.0 mm in diameter, are common (Fig. 10d). These are

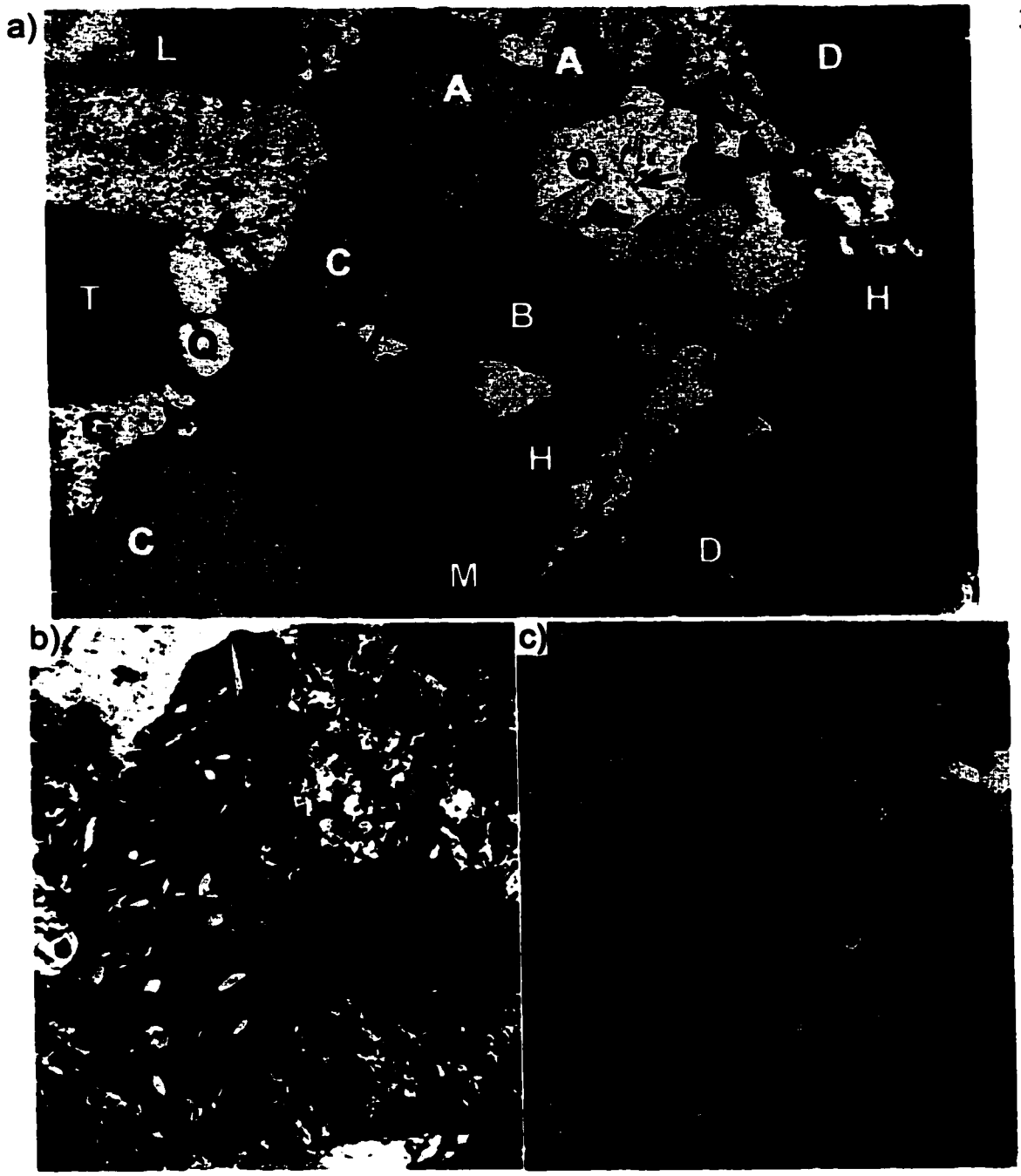

Figure 10. Photomicrographs of the middle unit ("quartz gabbro"): **(a)** representative sample showing lath-shaped (L) versus diamond-shaped (D) plagioclase crystals, clinopyroxene (C), hornblende (H), biotite (B), quartz (Q, enclosing an apatite needle (arrow)), apatite (A), titanite (T) and magnetite (M) crystals and granophyric fields (G) (sample SUD-151-1995, plane light, field-of-view = 6 mm); **(b)** actinolite and ferro-actinolite needles in an augite crystal (left) and singly twinned amphibole crystal (right) (sample SUD-60-1994, cross-polarized light, field-of-view = 1 mm); **(c)** singly twinned amphibole crystals (blues and yellows) and plagioclase laths (sample SUD-60-1994, cross-polarized light, field-of-view = 10 mm); **(continued next page)**

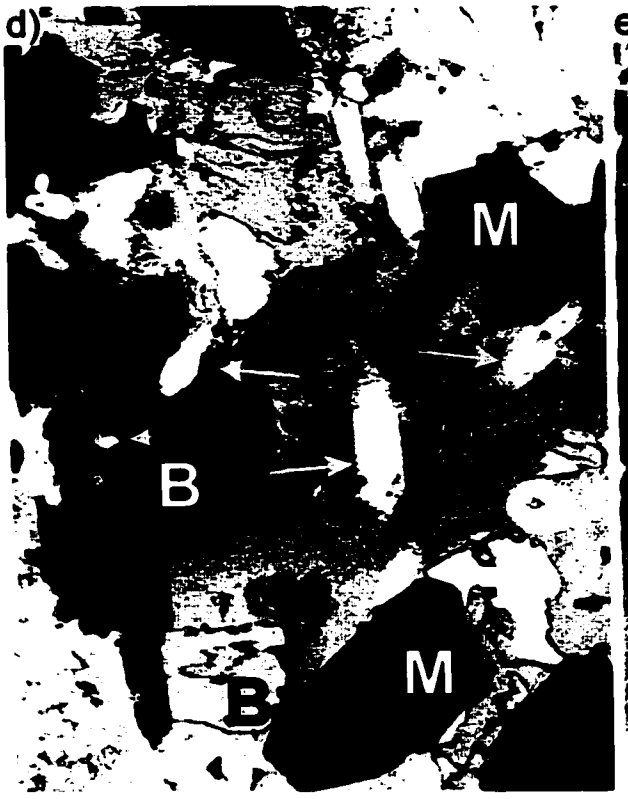

Figure 10 (continued). **(d)** primary amphibole (right, H) and primary biotite (left, B) oikocrysts enclosing apatite (arrows) crystals (sample SUD-142-1995, plane light, field-of-view = 1.5 mm). Note also the subhedral equidimensional crystals of magnetite (M); **(e)** titanite pseudomorph with rods of ilmenite running parallel to its long axis (bottom) and skeletal magnetite (top) crystals (sample SUD-151-1995, plane light, field-of-view = 1 mm); and **(f)** skeletal apatite crystal (sample SUD-150-1995, plane light; field-of-view = 300 μm).

both interpreted to be primary based upon the relationship of their crystal faces to those of adjacent minerals and on the basis that they poikitilically enclose apatite and Fe-Ti oxide cumulus crystals (Fig. 10d).

Subhedral equidimensional magnetite crystals are 0.1-1.0 mm in diameter (Fig. 10d). Skeletal magnetite crystals are rare (Fig. 10e). Ilmenite occurs as elongate crystals up to 2 mm in length forming an octahedrally oriented network within pseudomorphs of titanite after magnetite (Fig. 10e). Near the top of the middle unit ("quartz gabbro"), ilmenite may occur as discrete crystals up to 1.5 mm long. Apatite occurs as an accessory mineral (Fig. 10a). Some apatite crystals are skeletal, *i.e.*, have a central cavity parallel to their c-axis, which may extend over much of the crystal length, or show intricate growth patterns (*e.g.*, Fig. 10f). Micrographic and granophyric intergrowths (totalling up to ~ 20 vol.%) are the most common interstitial phases (Fig. 10a). These consist mainly of quartz intergrown with orthoclase and minor albite, as in the lower unit ("norite"). All minerals in the middle unit ("quartz gabbro") are highly altered except for amphibole; plagioclase is altered to sericite and epidote (Fig. 10a), and augite is altered to uralitic amphibole and partly replaced by biotite, amphibole and epidote (Fig. 10a). In drill core 52848, the alteration of mafic minerals is less severe.

A few bands of leucocratic quartz monzogabbro (Fig. 6) or plagioclase "cumulate" (termed "blue-band" or "tonalite" by the personnel of INCO Ltd.), up to 10 m thick in drill core 70011, occur near the base of the middle unit ("quartz gabbro"), a few tens of meters above the lower unit ("norite"). In comparison with the bulk of the middle unit ("quartz gabbro"), these bands contain only rare titanite crystals, less than 1 mm in diameter, and are slightly

impoverished in micrographic intergrowths (and, thus, poorer in interstitial material). They are enriched in plagioclase, stubby or slender crystals up to 6 mm in length, and in alteration products, especially chlorite, epidote and uralitic amphibole, which give the rocks their blue color.

3.2.4 Transition zone

As stated in the introduction, this work, for the first time, recognizes an extended gradational contact between the middle unit ("quartz gabbro") and the upper unit (granophyre), and warrants its independent description as the "transition zone". Approximately 150 m thick in drill core 70011, the transition zone is medium-grained, pink, and contains cumulus plagioclase (23-41 vol.%), amphibole (2-8 vol.%), minor amounts of magnetite (1-3 vol.%) and titanite (0.5-4 vol.%), and trace amounts of apatite (Figs. 11a and 11b). The base of the transition zone is defined by a sharp increase in biotite content and the first appearance of very large cumulus apatite (Fig. 11b).

Subhedral albite-oligoclase laths (An_{0-15}), up to 5 mm in length, poikilitically enclose augite crystals and coexist with rare laths with andesine-labradorite core (An_{35-52}) - oligoclase rims (An_{14-30}; Fig. 7d). Overgrowths on these plagioclase crystals consist of coarse microperthite (Fig. 11d), which is continuous with the interstitial micrographic and granophyric intergrowths. Amphibole crystals are subhedral and up to 2 mm in length (Fig. 11a). Cumulus magnetite crystals, which decrease abruptly in abundance with higher stratigraphic levels, are euhedral and 1 mm in diameter (Fig. 11a). Ilmenite crystals are elongate and up to 3 mm in length (Fig. 11c).

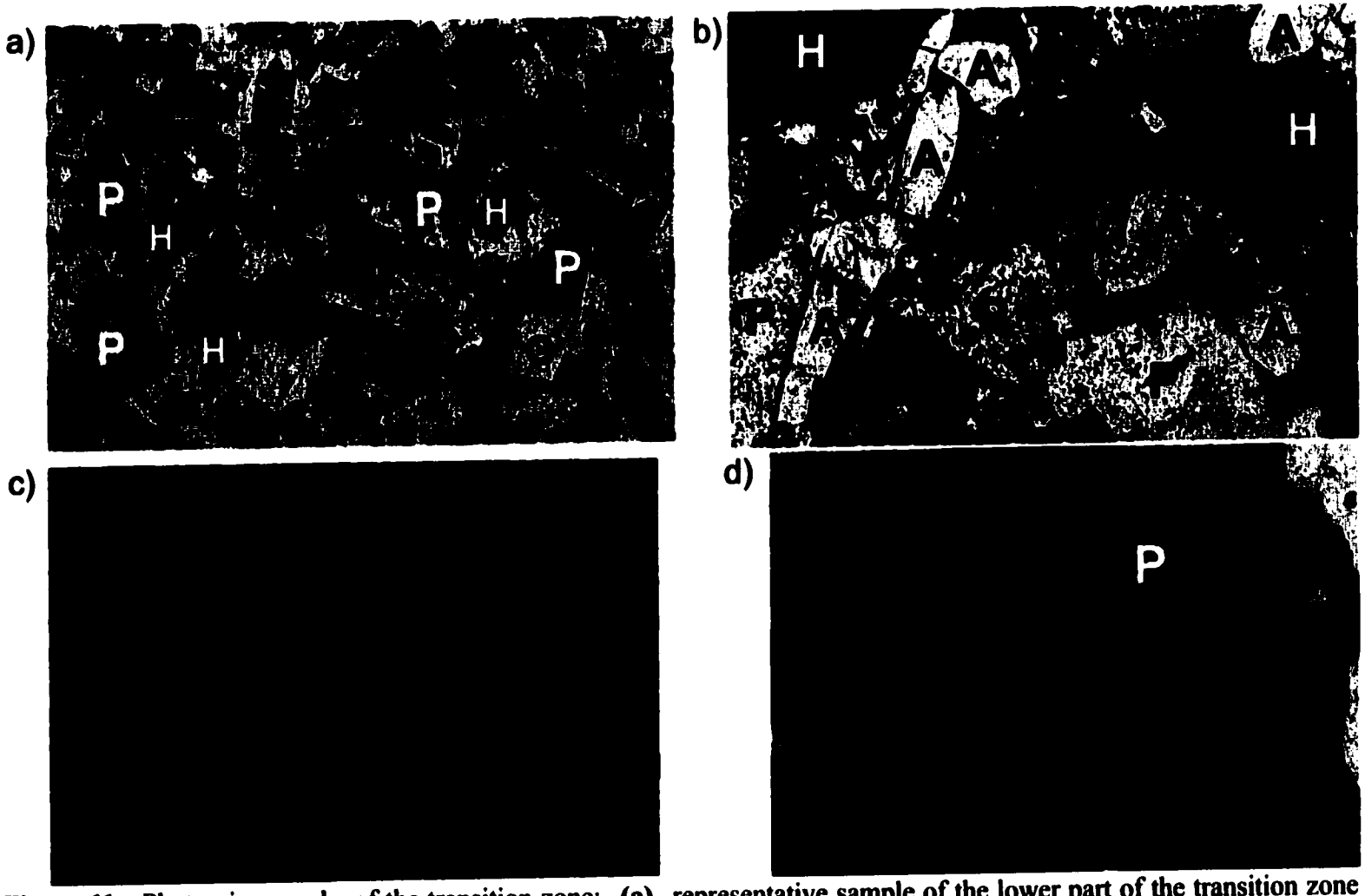

Figure 11. Photomicrographs of the transition zone: **(a)** representative sample of the lower part of the transition zone showing plagioclase (gray, P), amphibole (yellow to green, H), and magnetite (black) crystals in a matrix of micrographic and granophyric intergrowths (white, G) (sample SUD-89-1994, plane light, field-of-view = 14.5 mm); **(b)** representative sample of the upper part of the transition zone (sample SUD-88-1994, plane light, field-of-view = 6 mm). Note the large apatite crystals (A). Other minerals as in (a); **(c)** needles of ilmenite surrounded by micrographic and granophyric intergrowths in the upper part of the transition zone (sample SUD-125-1995, plane light, field-of-view = 2 mm); and **(d)** perthite overgrowth around a plagioclase lath (P) (sample SUD-125-1995, cross-polarized light, field-of-view = 2 mm).

The abundance of titanite crystals, all up to 1 mm in diameter, increases from less than 1 % to about 5 % with higher stratigraphic levels. Most titanite crystals have a rounded irregular shape, somewhat suggestive of a rhombohedral cross-section. A few crystals have an octahedral cross-section, suggesting that they are pseudomorphs after magnetite. Apatite occurs as stubby or long euhedral crystals up to 3 mm in length, which may be corroded by the matrix (Fig. 11b). Epidote crystals are subhedral to euhedral and up to 4 mm in diameter.

Micrographic and granophyric intergrowths, consisting of quartz and perthite or microcline, are very large in interstitial areas and their abundance increases with higher stratigraphic levels, from 15 to 50 vol.%. Within the top of the transition zone, the decrease in the abundance of alteration products and mafic minerals (easily altered) results in a sharp decrease of the intensity of alteration. Even the plagioclase crystals become noticeably less altered with higher stratigraphic levels (compare Figs. 11a and 11b), especially albite crystals compared to coexisting oligoclase-andesine crystals. A slight preferential alignment of most of the plagioclase crystals is observed throughout the transition zone. Stevenson and Colgrove (1968) observed a strong lineated fabric, imparted by aligned plagioclase.

3.2.5 Upper Unit (granophyre)

Approximately 1400 m thick in drill core 70011, the upper unit (granophyre) is coarse-grained, heterogeneous and apparently unlayered. It is composed mainly of micrographic and granophyric intergrowths (same composition as in the transition zone, *i.e.*, quartz and perthite or microcline). Also present in varying volumetric amounts are albite laths ($An_{<5}$; Fig. 7e) up

to 5 mm in length, large anhedral quartz crystals up to 4 mm in length, and crystals of perthite, epidote, biotite and amphibole. Minor and accessory minerals include apatite, calcite, and chlorite. The upper unit (granophyre) may be subdivided into a lower part, a middle part, and an upper part.

The lower part of the upper unit (granophyre) is up to 400 m thick, light pink and contains abundant micrographic and granophyric intergrowths (55-60 vol.%), albite laths (20-25 vol.%), quartz crystals (2-5 vol.%) and minor amounts of perthite (Fig. 12a). Fields of intergrowths may be up to 8 mm. A greater abundance of epidote (5-10 vol.%) and primary biotite (10-15 vol.%) crystals characterize the lower part of the granophyre. Epidote crystals are subhedral to euhedral and up to 5 mm in diameter, some of which are zoned (Fig. 12b). Biotite occurs as large subhedral to euhedral crystals, up to 0.5 mm in diameter, and as disseminated needles and plates within the matrix (Fig. 12a). The lower part of the upper unit (granophyre), with its sligthly coarser grain-size, has more of a cumulate texture (Fig. 12a) than the other parts of the upper unit (granophyre) (Figs. 12c and 12d).

The middle part of the upper unit (granophyre) is about 400 m thick, gray and characterized by an increase in chlorite content (10-15 vol.%), primary amphibole (1-3 vol.%) and oxides (1-3 vol.%). It also contains abundant micrographic and granophyric intergrowths (40-45 vol.%), albite laths (20-25 vol.%), quartz crystals (4-8 vol.%) and less perthite, epidote, and primary biotite (Fig. 12c), than in the lower part of the upper unit (granophyre). Perthite laths are rarely skeletal and up to 1.0 mm in length. Brown biotite needles and plates are slightly longer than in the lower part of the upper unit (granophyre). Green biotite crystals may be up

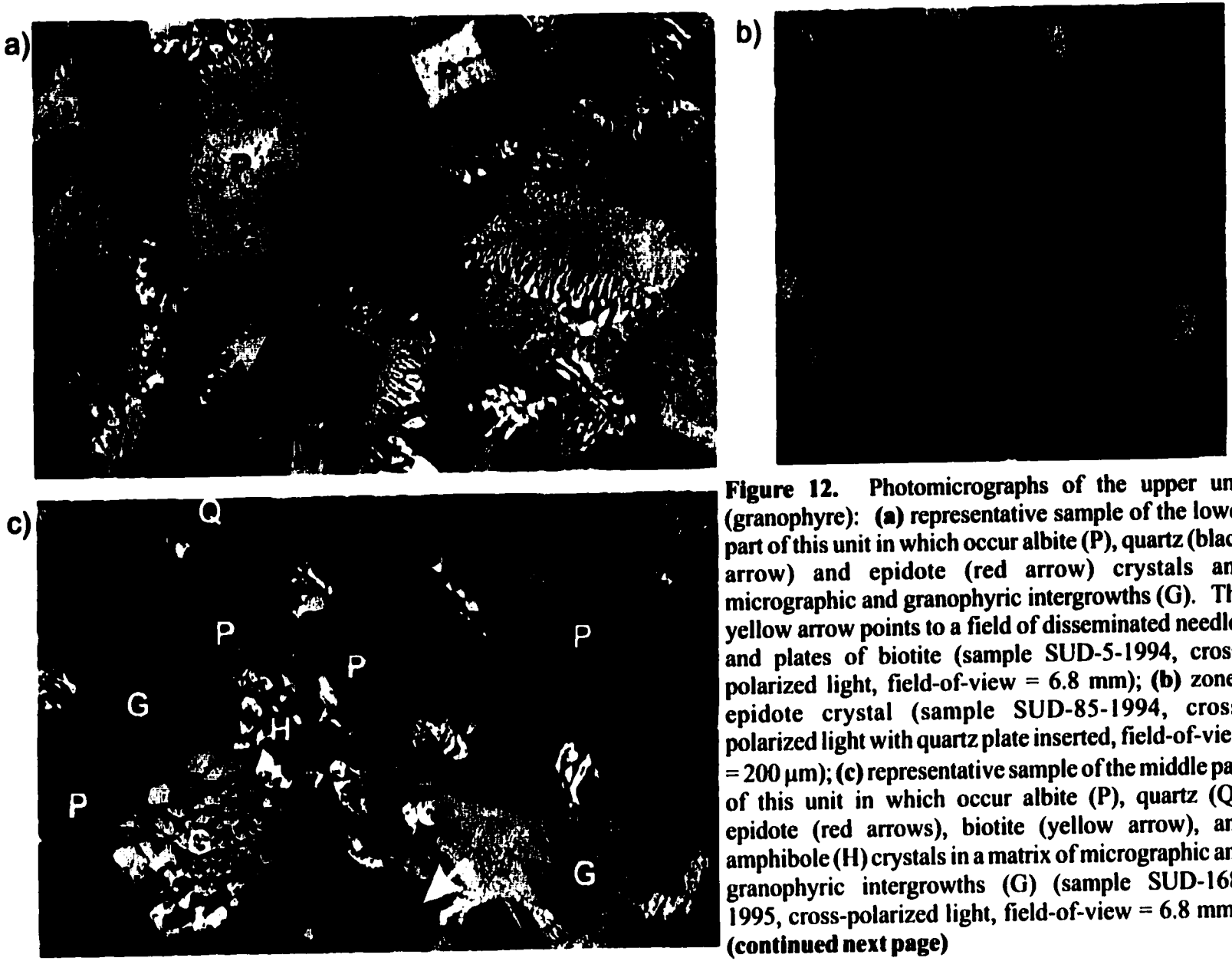

Figure 12. Photomicrographs of the upper unit (granophyre): **(a)** representative sample of the lower part of this unit in which occur albite (P), quartz (black arrow) and epidote (red arrow) crystals and micrographic and granophyric intergrowths (G). The yellow arrow points to a field of disseminated needles and plates of biotite (sample SUD-5-1994, cross-polarized light, field-of-view = 6.8 mm); **(b)** zoned epidote crystal (sample SUD-85-1994, cross-polarized light with quartz plate inserted, field-of-view = 200 μm); **(c)** representative sample of the middle part of this unit in which occur albite (P), quartz (Q), epidote (red arrows), biotite (yellow arrow), and amphibole (H) crystals in a matrix of micrographic and granophyric intergrowths (G) (sample SUD-168-1995, cross-polarized light, field-of-view = 6.8 mm); **(continued next page)**

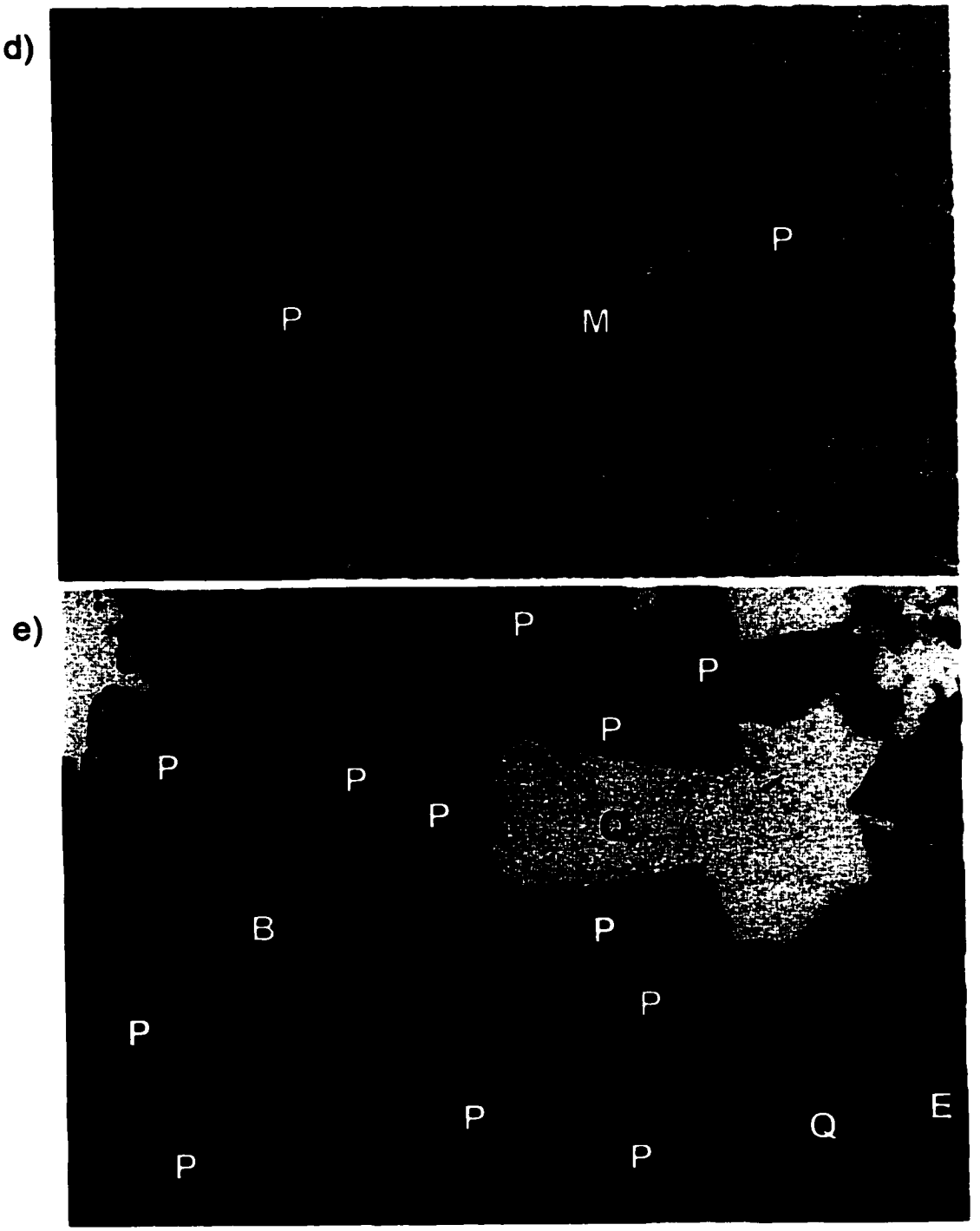

Figure 12 (continued). **(d)** representative sample of the upper part of this unit with a boxy-cellular plagioclase crystal (extinct, P) surrounded by granophyric intertrowths, magnetite crystal (M) and biotite needles (yellowish-brown) (sample SUD-85-1994, cross-polarized light, field-of-view = 14.5 mm); and **(e)** individual crystals of perthite (P) together with quartz (Q) and epidote (E) crystals and a field of Fe-Ti oxides and biotite crystals (B) in the upper part of this unit (sample SUD-144-1995, cross-polarized light, field-of-view = 1.5 mm).

to 0.5 mm in diameter. Acicular amphibole crystals, up to 8 mm, are common but few, and usually amphibole occurs as single crystals up to 0.5 mm in length (Fig. 12c) or as aggregates up to 1.0 mm in diameter. Epidote and chlorite occur as aggregates of crystals up to 2 mm in diameter (Fig. 12c). Titanite pseudomorphs after ulvöspinel-magnetite are less than 1 mm in diameter and calcite crystals filling interstices are less than 0.5 mm in diameter. Fields of intergrowths may be up to 5 mm.

The upper part of the upper unit (granophyre) is up to 300 m thick, medium-grained and pink (due to traces of hematite). It contains very abundant micrographic and granophyric intergrowths (60-65 vol.%), albite laths (15-25 vol.%), quartz crystals (2-5 vol.%), minor perthite, and abundant monomineralic and lithic inclusions, up to 3.0 mm in diameter. Albite crystals are typically acicular or boxy-cellular and serve as nuclei for micrographic and granophyric intergrowths (Fig. 12d). Perthitic crystals may be boxy-cellular and, with a length of up to 1.5 mm (Fig. 12e), are larger than in the other parts of the upper unit (granophyre). Fields of intergrowths may be up to 5 mm.

A dark gray inclusion-rich and plagioclase-rich (30-35 vol.%) discontinuous layer of medium- to fine-grained granophyre, which decreases in grain-size with higher stratigraphic levels, occurs within the top of the upper unit (granophyre) and may be as thick as 200 m in drill core 70011. The inclusions are a few millimeters to a few tens of centimeters, heterogeneously distributed and monomineralic (mainly quartz and feldspar) or consist of rock fragments (mainly quartzite and granite). Plagioclase crystals are more acicular in this layer than the rest of the granophyre and may be up to 5 mm in length. Initially called "pepper-and-salt micropegmatite"

by Stevenson (1961, 1963), it was renamed "plagioclase-rich micropegmatite" by Peredery and Naldrett (1975), and has since evolved into "plagioclase-rich granophyre" in the Sudbury related literature. The intergrowths in the matrix of this discontinuous layer are well defined and occur principally in a reasonably regular and cuneiform fashion, rather than in a radiating fashion and are, thus, deemed as micrographic, rather than granophyric intergrowths. Other major constituents are anhedral quartz crystals and orthoclase crystals, both up to 2 mm in length. Also present are minor acicular amphibole, most likely pseudomorphic after augite, up to 5 mm in length and biotite flakes and needles less than 2 mm in length. The top of the upper unit (granophyre) is not so easily defined but the base of the overlying basal member of the Onaping Formation is marked by the appearance of quartz inclusions with planar deformation features (for a definition see section 3.3.5 Quartz, below).

In hand specimen, the change from one part of the upper unit (granophyre) to the other is marked mainly by a change in color and the appearance of acicular amphibole (most likely pseudomorphic after augite) in the middle part of the upper unit (granophyre) and in the plagioclase-rich granophyre. Apatite, zircon, and titanite are common interstitial phases occurring in minor amounts throughout the upper unit (granophyre). Apatite occurs as needles less than 0.5 mm in length. Alteration minerals include calcite, chlorite, epidote, green biotite and amphibole.

3.3 Mineralogy

3.3.1 Plagioclase

Representative plagioclase microprobe analyses are given in Table II. The Ab-An-Or data of all plagioclase crystals analysed are plotted in Figure 7, and the variation in An content with depth is shown in Figure 13. A progressive decrease in An content, from An_{67} to An_{33}, is observed from the base of the contact sublayer to the top of the transition zone (Fig. 13b) and is accompanied by a general decrease in FeO content of the plagioclase crystals (Table II). From within the upper part of the lower unit ("norite") to the top of the transition zone, albite-oligoclase crystals (An_{2-15}; Fig. 13a) may be present together with the Ca-rich plagioclases, and, in fact, become more abundant than the latter with higher stratigraphic levels. An abrupt change to only albite (An_1-An_5) occurs from the transition zone to the upper unit (granophyre) (Fig. 13), and, throughout the upper unit (granophyre), the An content of plagioclase crystals remains constant (Fig. 13a). Most plagioclase crystals have a thin overgrowth of albite-oligoclase (An_{0-25}; Fig. 13b), but with higher stratigraphic levels, starting in the upper part of the lower unit ("norite"), an increasing number of plagioclase crystals have a thin to wide microcline or microperthite overgrowth.

Electron microprobe analyses and petrography throughout the SIC indicate that some plagioclase crystals have a reversed zoning (Fig. 13) and exhibit complex twinning or extinction patterns upon microscope stage rotation. Combination of patterns observed include dark and light bands running about 45° from the long axis of crystals (Fig. 14a) and, upon microscope stage rotation, oscillatory-like dark and light zones without a trace of the former bands (Fig.

Table II: Selected microprobe analysis of plagioclase crystals in drill core 70011.

Lithology	A	A	B	B	B	B	B	B	B	C	C
Sample #	71-1994	71-1994	7-1994	7-1994	174-1995	174-1995	174-1995	174-1995	174-1995	60-1994	60-1994
Depth (m)	2291.2	2291.2	1981.2	1981.2	1810.5	1810.5	1810.5	1810.5	1810.5	1735.8	1735.8
point	Pl3 core	Pl3 rim	Pl5 core	Pl5 rim	Pl8 core	Pl4 rim	Pl2 core	Pl2 rim	Pl2 over	Pl7 core	Pl7 rim
SiO_2	51.65	57.85	52.82	54.36	63.63	65.24	53.40	55.97	58.54	53.53	55.30
Al_2O_3	30.80	26.71	29.86	28.60	21.85	21.22	28.16	27.02	24.70	28.00	27.28
FeO	0.60	0.43	0.51	0.35	0.31	0.02	0.71	0.55	0.48	0.59	0.60
CaO	13.56	9.04	12.04	10.55	2.47	1.70	10.85	8.98	6.46	10.94	9.62
Na_2O	3.66	6.33	4.72	5.84	10.40	10.32	5.27	6.24	7.77	5.35	5.89
K_2O	0.24	0.35	0.25	0.10	0.05	0.08	0.30	0.19	0.20	0.35	0.30
BaO	0.00	0.19	0.38	0.19	0.22	0.03	0.06	0.00	0.06	0.00	0.00
SrO	0.11	0.11	0.17	0.00	0.04	0.12	0.00	0.17	0.15	0.04	0.16
Total	100.61	101.02	100.75	100.00	98.97	98.75	98.75	99.12	98.36	98.81	99.15
Ab	32.36	54.82	40.89	49.78	88.16	91.22	45.98	55.06	67.73	46.03	51.64
Or	1.37	1.97	1.45	0.57	0.29	0.48	1.74	1.10	1.14	1.99	1.71
An	66.27	43.22	57.66	49.65	11.55	8.31	52.27	43.83	31.14	51.98	46.64
An/(Ab+An)	67.19	44.08	58.51	49.94	11.58	8.35	53.20	44.32	31.50	53.04	47.46

Lithology	E	E	E	E	E	E	E	F	F	F	F
Sample #	89-1994	89-1994	89-1994	89-1994	179-1995	179-1995	173-1995	5-1994	5-1994	85-1994	85-1994
Depth (m)	1630.7	1630.7	1630.7	1630.7	1562.1	1562.1	1503.6	1310.6	1310.6	94.5	94.5
point	Pl5 core	Pl5 rim	Pl8 core	Pl8 rim	Pl1 core	Pl1 rim	Pl4 rim	Pl6 core	Pl6 rim	lath core	lath rim
SiO_2	53.72	54.80	58.87	62.96	66.03	66.25	62.92	66.26	66.60	66.41	65.64
Al_2O_3	28.59	27.27	25.17	22.64	20.49	20.50	22.39	20.00	20.02	20.54	19.66
FeO	0.57	0.54	0.34	0.21	0.09	0.38	0.08	0.00	0.00	0.06	0.46
CaO	10.72	9.70	6.67	3.55	0.88	0.79	2.90	0.52	0.47	0.52	1.14
Na_2O	5.51	5.82	7.27	9.91	11.01	11.13	9.67	11.31	11.27	10.79	11.13
K_2O	0.18	0.38	0.75	0.05	0.05	0.04	0.11	0.10	0.03	0.08	0.16
BaO	0.17	0.06	0.08	0.11	0.00	0.00	0.47	0.08	0.00	0.22	0.00
SrO	0.25	0.17	0.02	0.00	0.08	0.00	0.04	0.14	0.21	0.04	0.00
Total	99.71	98.74	99.17	99.43	98.64	99.09	98.57	98.41	98.60	98.66	98.19
Ab	47.69	50.90	63.51	83.22	95.50	95.99	85.28	96.99	97.55	96.96	93.79
Or	1.01	2.19	4.30	0.30	0.27	0.24	0.61	0.56	0.19	0.48	0.88
An	51.30	46.91	32.19	16.48	4.23	3.77	14.11	2.46	2.27	2.46	5.33
An/(Ab+An)	51.83	47.96	33.64	16.53	4.24	3.78	14.20	2.47	2.27	2.57	5.37

Lithology: A = contact sublayer; B = lower unit ("norite"); C = middle unit ("quartz gabbro"); E = transition zone; F = upper unit (granophyre)

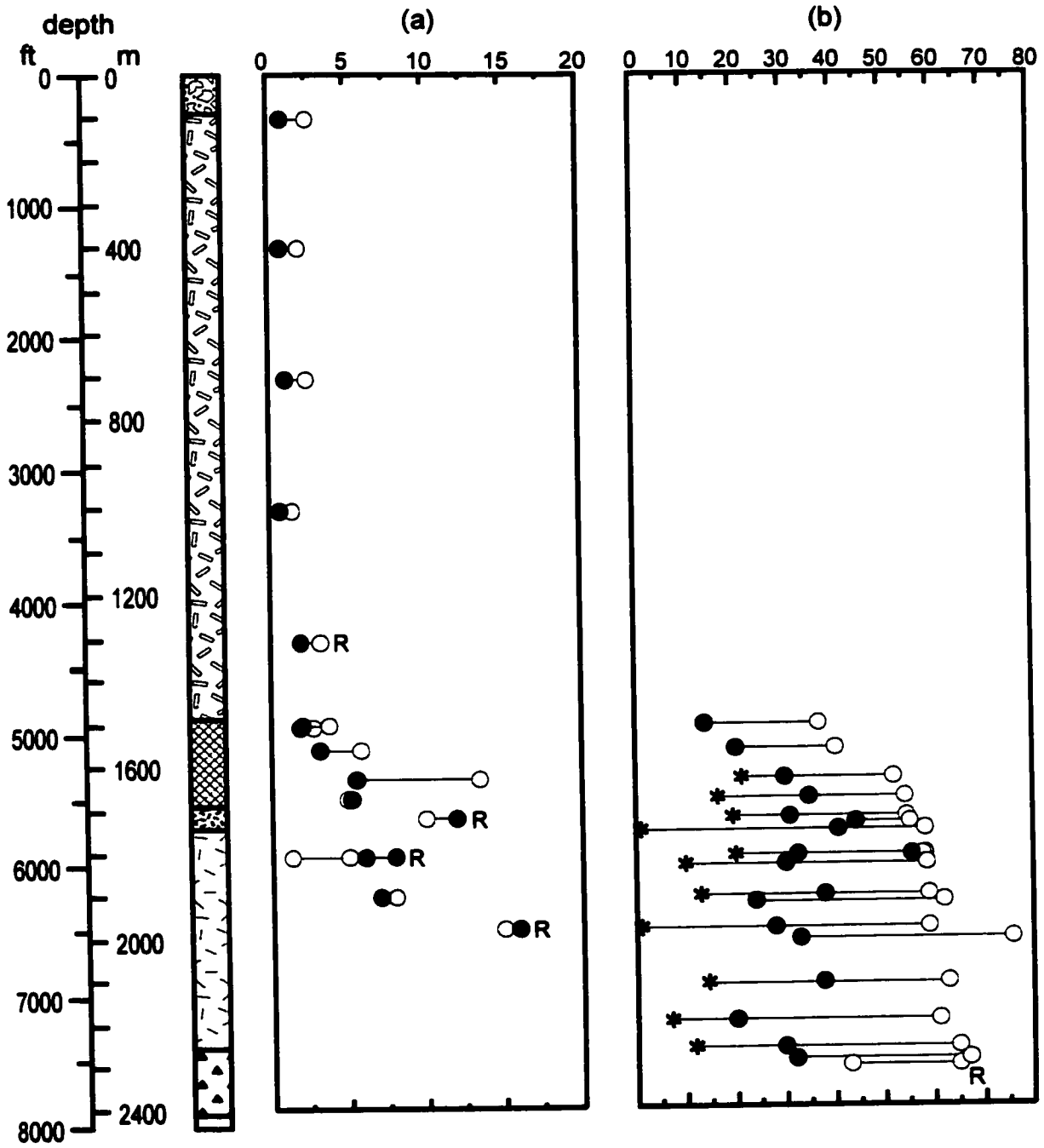

Figure 13. Anorthite molar percentage content in plagioclase from samples in drill core 70011: (a) Na-rich crystals and (b) Ca-rich crystals. Open circles are cores, filled circles are rims, asterisks are overgrowths (minimum value) and R indicates crystals with reverse zoning. Lithology patterns as in Figure 3. Note change in scale from (a) to (b). See text for details.

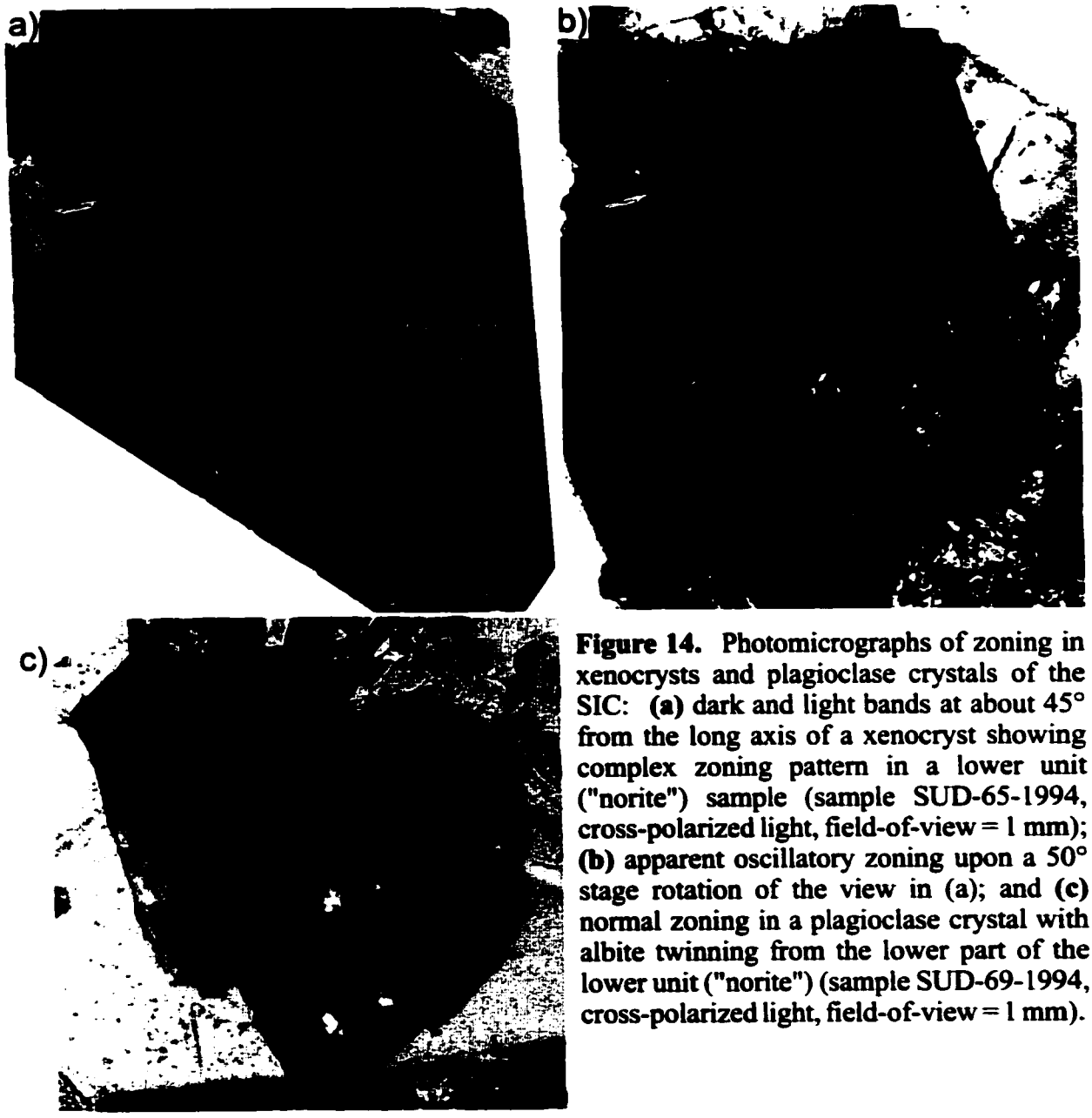

Figure 14. Photomicrographs of zoning in xenocrysts and plagioclase crystals of the SIC: **(a)** dark and light bands at about 45° from the long axis of a xenocryst showing complex zoning pattern in a lower unit ("norite") sample (sample SUD-65-1994, cross-polarized light, field-of-view = 1 mm); **(b)** apparent oscillatory zoning upon a 50° stage rotation of the view in (a); and **(c)** normal zoning in a plagioclase crystal with albite twinning from the lower part of the lower unit ("norite") (sample SUD-69-1994, cross-polarized light, field-of-view = 1 mm).

14b). Adjacent plagioclase crystals with normal zoning have regular albite twinning. Often both coexisting reversed and normally zoned crystals are mantled by a thin < 0.3 mm optically continuous layer of albite-oligoclase (An_{5-25}). Clearly, the diverse chemical trends of these coexisting plagioclases do not represent a magmatic growth trend for either near to, or far from equilibrium growth, and consequently the reversed zoned crystals, and possibly some normally zoned crystals, are interpreted as xenocrysts.

Most plagioclase crystals have either Carlsbad or albite twins, or both (Fig. 15a), and have undulose extinction, due to compositional zoning. Within the lower unit ("norite"), plagioclase crystals may also have pericline twins (Fig. 15a). A finely spaced exsolution lamellae pattern, presumably Bøggild intergrowths given the chemistry of the crystals, locally occurs (Fig. 15b) in samples from the base of the lower unit ("norite") up to within the upper part of the lower unit ("norite"). The host crystal is usually strained, *i.e.*, has undulatory extinction, and the lamellae are usually too fine to be chemically distinguished. In the middle unit ("quartz gabbro"), plagioclase crystals commonly have albite twinning, rarely have oscillatory extinction pattern and may be rimmed by biotite. Oscillatory extinction pattern is most prominent at the base of the lower unit ("norite") and disappears in higher stratigraphic levels to the point that, in the middle unit ("quartz gabbro"), plagioclase crystals have an unzoned core with a thin strongly zoned rim. The plagioclase crystals with an "interesting remnant" oscillatory extinction pattern (sometimes only one of the Carlsbad twins has this oscillatory pattern, Fig. 15c) are interpreted as xenocrysts, as no compositional zoning or change could be attributed to the pattern components. Some of these crystals have a "corroded" outline. Only some plagioclase crystals

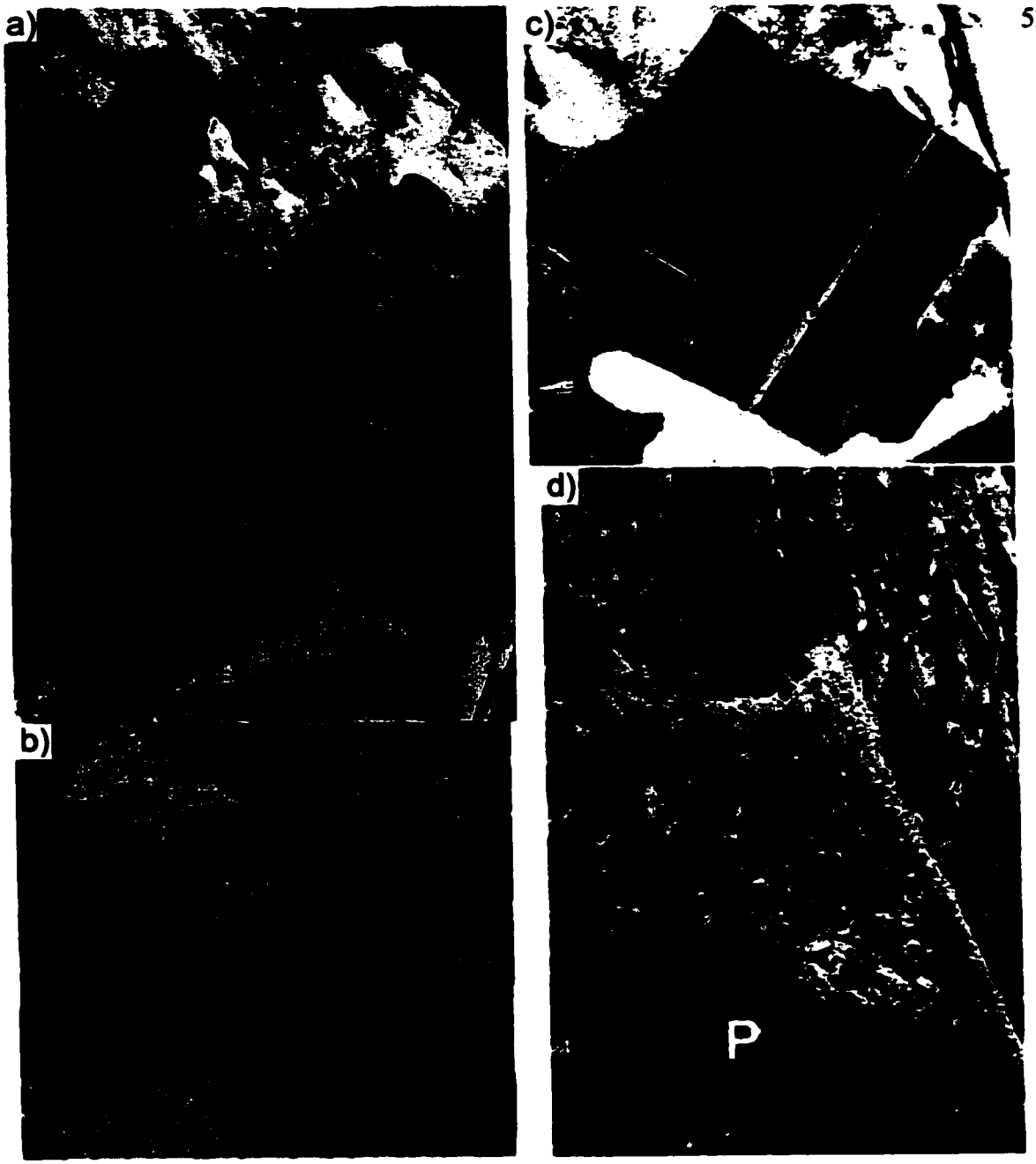

Figure 15. Photomicrographs of plagioclases in the SIC: **(a)** Carlsbad (right edge) or albite twins (lower edge and top right corner) versus pericline and albite twins (left crystal) in the lower unit ("norite") (sample SUD-154-1995, cross-polarized light, field-of-view = 2 mm); **(b)** crystal with presumably Bøggild intergrowths (fine lamellae perpendicular to albite twins) in the lower unit ("norite") (sample SUD-7-1994, cross-polarized light, field-of-view = 200 μm); **(c)** Carlsbad twin (top side) with apparent oscillatory zoning; whereas, the other is normally zoned in the lower part of the lower unit ("norite") (sample SUD-8-1994, cross-polarized light, field-of-view = 2 mm); and **(d)** altered lath (P) with fluid inclusions at its edges in the quartz gabbro (sample SUD-151-1995, cross-polarized plane light (lower half), field-of-view = 500 μm).

are boxy-cellular or skeletal, *i.e.*, euhedral crystals with highly irregular growth, in the upper part of the lower unit ("norite") and within the middle unit ("quartz gabbro"); whereas, they are very abundant within the transition zone and the upper unit (granophyre) (Fig. 12d). In the upper unit (granophyre), albite crystals have no apparent overgrowth.

Plagioclase crystals are commonly fractured. In the contact sublayer and at the base of the lower unit ("norite"), these fractures are filled by alteration products, mainly chlorite (Figs. 8d and 9c). The abundance of chessboard albite and disseminated crystallites of epidote within plagioclase crystals indicates that extensive albitization has occurred within the SIC and that the plagioclase host to the epidote flakes was originally more calcic. However, microprobe analyses suggest that alteration of plagioclase crystals appears to only slightly lower their An content, as adjacent altered and unaltered crystals have very similar chemistry. There is no apparent correlation between the intensity of alteration and the size or shape of plagioclase crystals. Patches of unaltered plagioclase crystals are observed within the thin sections. In addition, throughout the SIC, some plagioclase crystals contain a relatively large amount of fluid micro-inclusions at their edges (Fig. 15d); whereas, their core may be free of alteration.

3.3.2 Pyroxenes

Microprobe analyses of pyroxene crystals are shown in Figure 16. A selected number of representative analyses are given in Table III and the complete data set is given in Appendix A. The data reveal that, above the depth of 1905 m, which corresponds roughly to the base of the upper part of the lower unit ("norite"), all augite crystals in drill core 70011 are

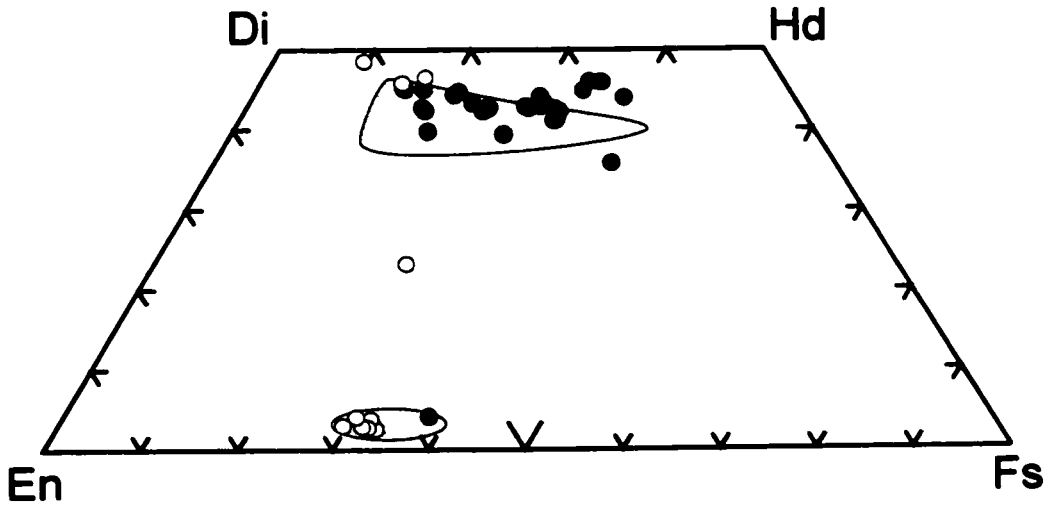

Figure 16. Pyroxene quadrilateral plot of microprobe analysis in pyroxene crystals from the SIC. White circles = contact sublayer samples and one lower unit ("norite") sample from drill core 70011; black circles = lower unit ("norite") to transition zone samples from drill core 52848; gray fields = contact sublayer to upper unit (granophyre) data from Naldrett *et al.*, 1970.

Table III: Selected microprobe analyses of pyroxene crystals and amphibole pseudomorph after pyroxene crystals in drill cores 70011 and 52848. See text for details.

Lithology	A	A	A	B*	B*	C*	E*
Sample #	97-1994	97-1994	97-1994	48-1994	48-1994	140-1995	43-1994
Depth (m)	2305.8	2305.8	2305.8	2106.2	2106.2	1432.6	1288.4
Pyroxene	px1 main	px1 main	px6 core	px4 rim	px7 core	core6	core2
SiO_2	51.57	51.11	53.22	51.18	49.55	49.64	50.38
TiO_2	0.67	0.50	0.18	0.38	0.70	0.71	0.15
Al_2O_3	2.30	1.63	1.58	0.86	1.56	1.77	0.49
FeO	9.29	16.31	18.72	23.51	12.86	13.23	18.03
MgO	13.67	17.61	23.91	20.00	11.55	0.35	8.13
MnO	0.21	0.33	0.27	0.58	0.35	12.72	0.57
CaO	22.00	11.26	1.47	1.92	21.15	19.54	20.54
Na_2O	0.38	0.23	0.02	0.00	0.29	0.31	0.18
K_2O	0.00	0.02	0.00	0.02	0.04	0.00	0.01
Cr_2O_3	0.19	0.18	0.30	0.03	0.06	0.00	0.07
NiO	0.02	0.04	0.02	-	-	0.00	0.00
Total	100.28	99.22	99.68	98.48	98.10	98.27	98.55
Wo	45.58	23.23	2.98	3.99	44.76	42.95	43.98
En	39.40	50.52	67.41	57.85	34.00	27.97	17.42
Fs	15.02	26.25	29.61	38.16	21.24	29.08	38.60

Lithology	A	B	B	C	C/E*	E	F
Sample #	71-1994	66-1994	63-1994	59-1994	166-1995	87-1994	3-1994
Depth (m)	2291.2	2199.1	1905.0	1676.4	1421.3	1508.8	701.0
Amphibole	core2	main1	core	core6	main18	main	core
SiO_2	52.89	53.74	53.13	50.11	51.70	50.69	51.68
TiO_2	0.12	0.04	0.25	0.08	0.04	0.26	0.04
Al_2O_3	2.94	0.41	1.04	3.87	2.31	0.72	1.06
FeO	12.63	10.81	18.51	20.10	20.48	29.73	21.35
MgO	15.98	12.29	12.28	10.27	10.51	4.73	9.91
MnO	0.44	0.33	0.90	0.33	0.15	0.52	0.37
CaO	12.05	21.11	12.37	12.06	12.39	12.08	13.05
Na_2O	0.30	0.13	0.10	0.44	0.29	0.12	0.17
K_2O	0.03	0.03	0.07	0.25	0.13	0.08	0.07
Cr_2O_3	0.10	0.03	0.04	0.07	0.05	0.04	0.03
NiO	-	0.03	0.03	0.00	0.02	0.00	0.03
Total	97.49	98.94	98.72	97.58	98.07	98.97	97.76
Name[1]	actinolite	cannilloite	actinolite	ferro-actinolite	ferro-actinolite	ferro-actinolite	ferro-actinolite

Lithology: A = contact sublayer; B = lower unit ("norite"); C = middle unit ("quartz gabbro"); E = transition zone; F = upper unit (granophyre); * = drill core 52848

Note: [1] = nomenclature according to Leake *et al.* (1997)

pseudomorphed by amphibole (actinolite, ferro-actinolite, and minor cannilloite and hornblende; Table III and Appendix A). In drill core 52847, a similar observation is made. For this reason, analyses of pyroxene crystals from drill core 52848 are used in Table III and Figure 16 to show the primary chemical variation of pyroxene across the SIC. As in the Skaergaard Intrusion, augite is generally enriched in Al_2O_3 relative to coexisting pigeonite (Table III). No significant amount of Cr_2O_3 nor NiO is detected in the SIC pyroxenes. The amphibole pseudomorphs have a chemical composition very close to that of the pristine pyroxene crystals, varying only in their contents of Na_2O, K_2O and Al_2O_3, which are, in general, slightly higher, and in their CaO and TiO2 contents and element totals, which are, in general, slightly lower than in the pristine pyroxene crystals.

Throughout the SIC, the pleochroic color of pyroxene crystals becomes deeper/darker with higher stratigraphic levels (*i.e.*, the Fe content of crystals increases; Fig. 16). Enstatite and pigeonite occur only in the contact sublayer and in the lower part of the lower unit ("norite") (Fig. 16). A kink-band or unusual twin was observed in one of these orthopyroxene crystals (Fig. 17a). From the contact sublayer into the upper unit (granophyre), augite crystals increase in Fe content, with only a slight variation in Ca content (Fig. 16). In the contact sublayer, clinopyroxene (mainly augite and salite) crystals have thin exsolution lamellae detectable optically (Fig. 17b), but not resolvable with the microprobe. In the lower part of the lower unit ("norite"), clinopyroxene (mainly augite) crystals have polysynthetic twins, contain abundant micro-inclusions and have a patchy and undulose extinction, suggesting compositional zoning. Some acicular crystals are also observed. A large overgrowth, or mantle, of ferrohornblende,

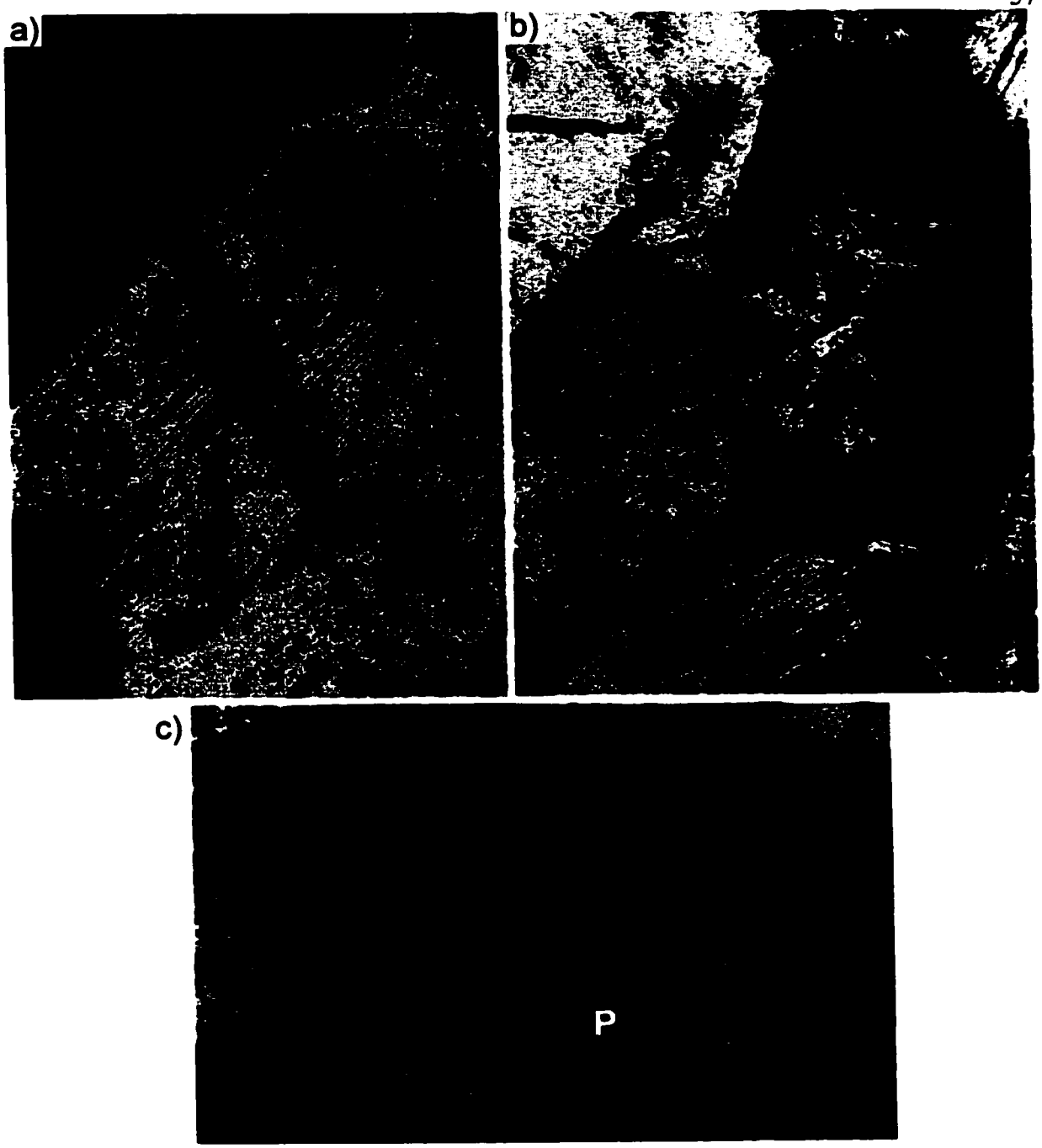

Figure 17. Photomicrographs of pyroxene crystals in the SIC: **(a)** kink-band or twin in an ortho-pyroxene (hypersthene) crystal in a sample of the contact sublayer (sample SUD-155-1995, cross-polarized light, field-of-view = 1 mm); **(b)** augite crystal showing exsolution lamellae in the contact sublayer (sample SUD-9-1994, cross-polarized light, field-of-view = 2 mm); and **(c)** augite crystal enclosing a plagioclase crystal (P) and showing exsolution lamellae at a high angle from the twinning plane in the lower part of the lower unit ("norite") (sample SUD-8-1994, cross-polarized light, field-of-view = 1.5 mm).

magnesio-hornblende, edenite or ferro-edenite, which may be altered to chlorite, is very common on most pyroxene crystals (Figs. 9a and 9d). No mantles of amphibole are observed on clinopyroxene crystals of the contact sublayer (Fig. 17b). In the lower unit ("norite") and the middle unit ("quartz gabbro"), clinopyroxene (mainly augite) crystals are commonly twinned and some have thin exsolution lamellae running at a high angle to the twinning plane (Fig. 17c). In the middle unit ("quartz gabbro"), augite crystals usually have an overgrowth of biotite and amphibole, and crystals are partly to completely altered to uralitic amphibole (Fig. 10a). In the transition zone, none of the augite crystals have exsolution lamellae. Very rare, small augite crystals, occurring within larger crystals of amphiboie (ferro-actinolite, -hornblende and -edenite) or biotite, are observed in the lower part of the upper unit (granophyre); whereas, no pyroxene crystals are observed in the upper part of the upper unit (granophyre). Throughout the SIC, the pyroxene crystals may have been altered to uralitic amphibole, and very small magnetite crystals may line their exsolution lamellae or parting planes (Fig. 17a). Needles of actinolite and ferro-actinolite are oberved within pyroxene crystals of the lower unit ("norite") and middle unit ("quartz gabbro") (Fig. 10b).

3.3.3 Amphiboles

Microprobe analyses of selected amphibole crystals are shown in Table IV and complete analyses are given in Appendix A. Compositionally, primary amphiboles have, in general, higher Al_2O_3 (> 3.6%), TiO2 (>0.4%), Na_2O (> 0.6%), K_2O (> 0.4%) and Cl (> 0.11%) contents than secondary amphiboles. The former are classified as edenite, ferro-edenite, ferro- and

Table IV: Selected microprobe analyses of amphiboles in drill cores 70011 and 52848.

Lithology	cont. sub.[1,2]	lower unit ("norite")[2]		middle unit		(quartz gabbro)[2]	transition zone[3]
Sample #	71-1994	153-1995		60-1994			43-1994
Depth (m)	2291.2	1831.8		1735.8			1288.4
point	Act3	Act alt2	ferroHbl core3	Act core1	Act lam	magnesioHbl8	edenite man
SiO_2	54.71	52.08	46.03	53.45	52.00	46.64	48.34
Al_2O_3	1.41	2.93	5.72	2.05	3.22	5.08	5.88
TiO_2	0.03	0.12	1.25	0.09	0.38	1.26	0.48
FeO	11.75	16.10	21.91	16.53	17.31	21.08	18.35
MgO	17.26	14.03	9.64	13.38	12.75	11.23	12.41
MnO	0.24	0.29	0.36	0.31	0.35	0.22	0.32
CaO	12.07	11.96	10.15	11.98	11.91	9.94	10.57
Na_2O	0.01	0.25	0.93	0.16	0.23	0.98	1.59
K_2O	0.06	0.12	0.76	0.13	0.17	0.69	0.60
Cr_2O_3	0.19	0.02	0.00	0.10	0.04	0.00	0.00
NiO	0.00	0.07	0.02	0.00	0.01	0.00	0.08
F	0.00	0.00	0.00	0.00	0.00	0.00	0.00
Cl	0.08	0.05	0.40	0.04	0.10	0.26	0.10
P_2O_5	0.00	0.00	0.03	0.00	0.07	0.00	0.03
BaO	0.00	0.00	0.00	0.21	0.19	0.00	0.08
SO_2	0.08	0.00	0.00	0.00	0.00	0.00	0.00
SrO	0.00	0.00	0.00	0.00	0.00	0.00	0.06
ZnO	0.06	0.01	0.13	0.02	0.07	0.06	0.00
V_2O_3	0.07	0.06	0.13	0.03	0.13	0.11	0.06
Total	98.02	98.10	97.47	98.48	98.92	97.55	98.94
Si	7.80	7.60	7.04	7.78	7.58	7.09	7.15
Al	0.24	0.50	1.03	0.35	0.55	0.91	1.02
Ti	0.00	0.01	0.14	0.01	0.04	0.14	0.05
Fe^{2+}	1.40	1.97	2.80	2.01	2.11	2.68	2.27
Mg	3.67	3.05	2.20	2.90	2.77	2.54	2.74
Mn	0.03	0.04	0.05	0.04	0.04	0.03	0.04
Ca	1.84	1.87	1.67	1.87	1.86	1.62	1.67
Na	0.00	0.07	0.28	0.05	0.06	0.29	0.46
K	0.01	0.02	0.15	0.02	0.03	0.13	0.11
Cr	0.02	0.00	0.00	0.01	0.01	0.00	0.00
Ni	0.00	0.01	0.00	0.00	0.00	0.00	0.01
F	0.00	0.00	0.00	0.00	0.00	0.00	0.00
Cl	0.02	0.01	0.10	0.01	0.03	0.07	0.03
P	0.00	0.00	0.00	0.00	0.01	0.00	0.00
Ba	0.00	0.00	0.00	0.01	0.01	0.00	0.00
S	0.01	0.00	0.00	0.00	0.00	0.00	0.00
Sr	0.00	0.00	0.00	0.00	0.00	0.00	0.01
Zn	0.01	0.00	0.01	0.00	0.01	0.01	0.00
V	0.01	0.01	0.02	0.00	0.01	0.01	0.01
Total	15.07	15.17	15.50	15.06	15.12	15.52	15.56

Abbreviations: Act = actinolite; alt = alteration; lam = lamellae; Hbl = hornblende; man = mantle

Notes: Stoichiometry based on 23 oxygens. [1] = contact sublayer. [2] = Drill core 70011. [3] = Drill core 52848.

magnesio-hornblende and the latter as actinolite and ferro-actinolite (nomenclature of Leake *et al*, 1997). As discussed in the previous section, amphibole pseudomorphs after primary pyroxene are generally the rule in drill cores 70011 (above the top of the lower part of the lower unit ("norite")) and 52847 (throughout). As for pyroxene, amphibole crystals become enriched in Fe with higher stratigraphic levels (Table IV).

Primary and secondary amphiboles can easily be distinguished from each other using a transmitted-light microscope. Primary amphiboles have a dark brown-green pleochroism and occur as euhedral crystals (Fig. 18a) and mantles (Figs. 9a and 9d), both with a non-fibrous nature. Single euhedral crystals with well-defined 60-120° cleavages are observed, though rarely. Secondary amphiboles have a blue-green pleochroism and a non-fibrous nature, and occur as singly-twinned prismatic crystals within the matrix (up to 5 mm in length; Fig. 18b), or as tiny needles within pyroxene crystals (Fig. 18b). A finer-grained fibrous species of actinolite and ferro-actinolite (uralitic) is common at the rims of, or disseminated throughout, clinopyroxene and orthopyroxene crystals (Fig. 18c).

Amphibole forms an important intercumulus phase in the contact sublayer and lower unit ("norite"), mainly occurring as patchy replacements of, and as mantles around, clinopyroxene. It is a cumulus phase in the middle unit ("quartz gabbro") and the transition zone. Crystals of amphibole in the middle unit ("quartz gabbro") are up to 2 mm in length and are usually less altered than other mineral phases. Pleochroic haloes, presumably from zircon, are observed within some amphibole crystals of the middle unit ("quartz gabbro"). In the upper unit (granophyre), amphibole occurs as dendritic and bladed ferro-actinolite, ferrohornblende and

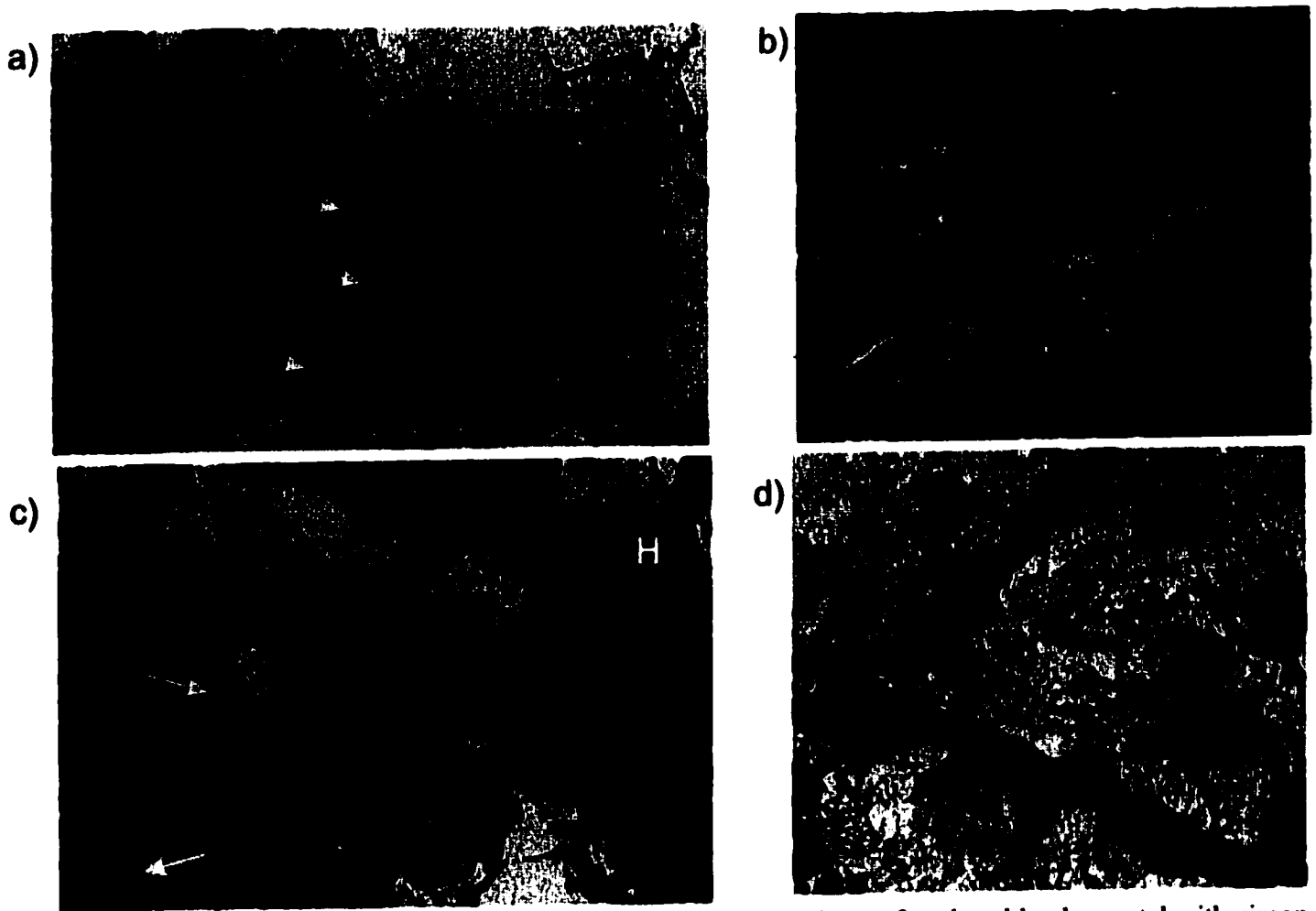

Figure 18. Photomicrographs of amphibole crystals in the SIC: **(a)** primary ferrohornblende crystal with zircon pleochroic haloes (arrows) in the lower unit ("norite") (sample SUD-153-1995, plane light, field-of-view = 1 mm); **(b)** singly-twinned secondary actinolite (top) and needles of actinolite and ferro-actinolite in an augite crystal (bottom) of the middle unit ("quartz gabbro") (sample SUD-60-1994, cross-polarized light, field-of-view = 1.5 mm); **(c)** uralitic fibrous amphibole (arrows) in an augite crystal of the lower unit ("norite") (sample SUD-69-1994, plane light, field-of-view = 6 mm). Note the primary euhedral amphibole (greenish brown) in the center of the picture and the clear ferrohornblende mantle (H) around a highly altered pyroxene crystal; and **(d)** acicular actinolite crystals lined by Fe-Ti oxide crystals in the middle part of the upper unit (granophyre) (sample SUD-2-1994, plane light, field-of-view = 7.5 mm).

ferro-edenite crystals (Fig. 18d), which are most likely pseudomorphs after augite.

3.3.4 Biotite

In the contact sublayer and at the base of the lower unit ("norite"), brown biotite crystals may poikilitically enclose crystals of plagioclase (Fig. 8a), ilmenite and/or quartz and are most likely primary. In the lower part of the lower unit ("norite"), crystals are subhedral, rarely strained or kinked, may fill interstices, and may contain abundant rutile needles (Fig. 19a). Pleochroic haloes, presumably of zircon, may be present in the biotite crystals of the lower unit ("norite"). No primary biotite is observed in the upper part of the lower unit ("norite") but is observed again at the base of the middle unit ("quartz gabbro") and above. In the middle unit ("quartz gabbro"), biotite crystals usually occur as needles (< 0.1 mm) or subhedral plates and scales (< 0.5 mm) (Fig. 10a). Most biotite crystals have a slight undulatory extinction. In the transition zone and the upper unit (granophyre), biotite occurs as abundant needles disseminated within the matrix, often forming fibrous spherulitic-like aggregates (Fig. 19b). Above the contact sublayer, biotite crystals are often partially altered to chlorite or to green biotite, which also occurs as an alteration product of primary amphibole. Crystals of green biotite are subhedral, up to 2 mm in length, and form aggregates.

3.3.5 Quartz

In the lower unit ("norite"), most quartz crystals filling interstices are < 1 mm in diameter, anhedral with an usually undulose extinction and sutured crystal boundaries. Many

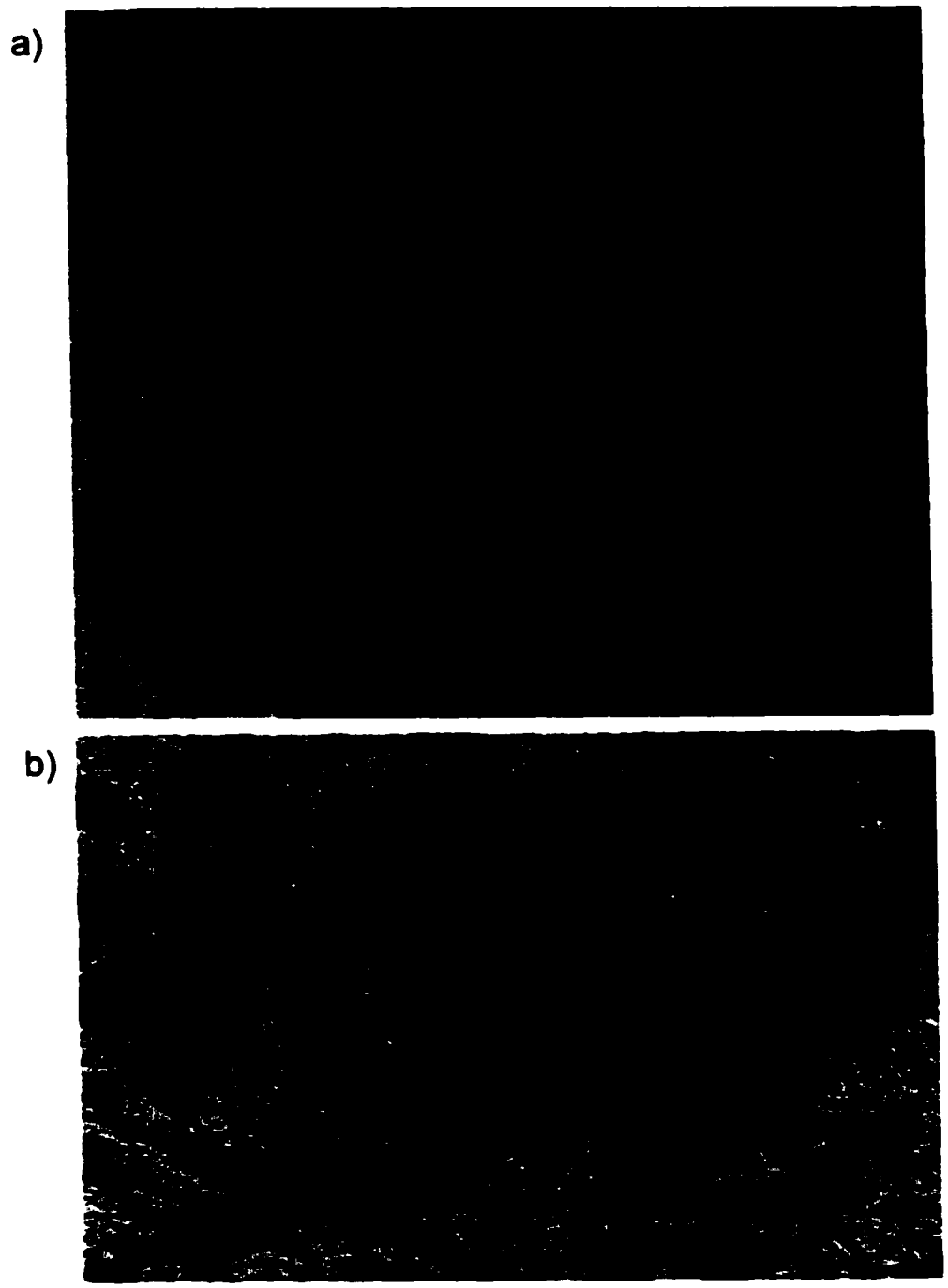

Figure 19. Photomicrographs of biotite crystals in the SIC: **(a)** subhedral crystal enclosing abundant needles of rutile in a lower unit ("norite") sample (sample SUD-7-1994, plane light, field-of-view = 200 μm); and **(b)** abundant biotite needles, disseminated or forming sheaf-like aggregates, in the matrix of the upper unit (granophyre) (sample SUD-53-1994, plane light, field-of-view = 200 μm).

are fractured and some may be skeletal (Fig. 20a). Most of these quartz crystals are interpreted as xenocrysts, or remnants thereof. Crystals intricately linked to the micrographic and granophyric intergrowths are ≤ 1 mm and locally euhedral and skeletal (Fig. 20b). In the middle unit ("quartz gabbro"), quartz crystals reach up to 0.4 mm in diameter, contain abundant micro-inclusions, and show undulatory extinction. In the transition zone and the upper unit (granophyre), quartz crystals are subhedral to euhedral, reaching up to 3 mm in diameter, and commonly show undulatory extinction.

Extremely rare subhedral quartz xenocrysts in the lower unit ("norite") and bottom of the transition zone have remnant planar deformation features (PDFs) as shown in Figure 21. Perhaps the most common diagnostic and unequivocal indicator of shock pressures greater than 10 GPa are PDFs in quartz. When fresh, most PDFs are amorphous lamellae (non-decorated PDFs) occurring as multiple sets of parallel, planar optical discontinuities across a single grain and are oriented parallel to rational crystallographic planes of low Miller indices (Stöffler and Langenhorst, 1994; Grieve *et al.*, 1996). Decorated PDFs consist of planes of tiny vugs, which are secondary features formed by thermal annealing of non-decorated PDFs, and are the most common type of PDFs in the floors and in annealed breccias of terrestrial impact craters (*e.g.*, Robertson *et al.*, 1968).

Five sets of PDFs were measured in three quartz xenocrysts from the SIC (Fig. 22 and Table V). One set in sample SUD-8-1994 from the lower unit ("norite"), one set in sample SUD-94-1994 from the lower unit ("norite") and three sets in sample SUD-89-1994 from the transition zone (Figs. 21a and 21b). The best fit to the poles of the PDFs of each quartz xenocryst yields

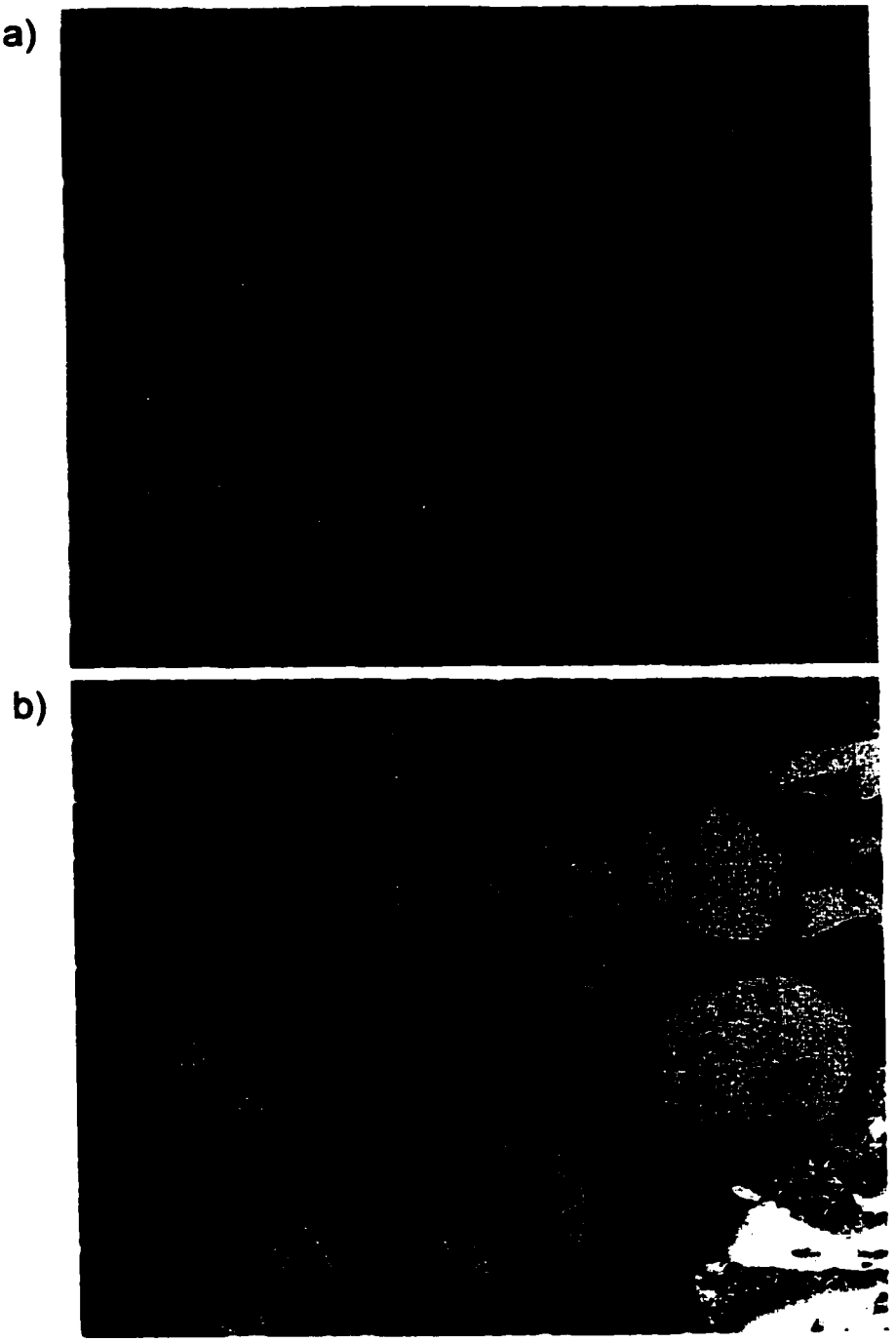

Figure 20. Photomicrographs of quartz crystals in the SIC: **(a)** skeletal quartz crystal (Q) and plagioclase (P), biotite (B) and apatite (A) crystals in the lower unit ("norite") (sample SUD-66-1994, plane light, field-of-view = 4 mm); and **(b)** skeletal quartz in micrographic intergrowths in the transition zone (sample SUD-185-1995, cross-polarized light, field-of-view = 1.5 mm).

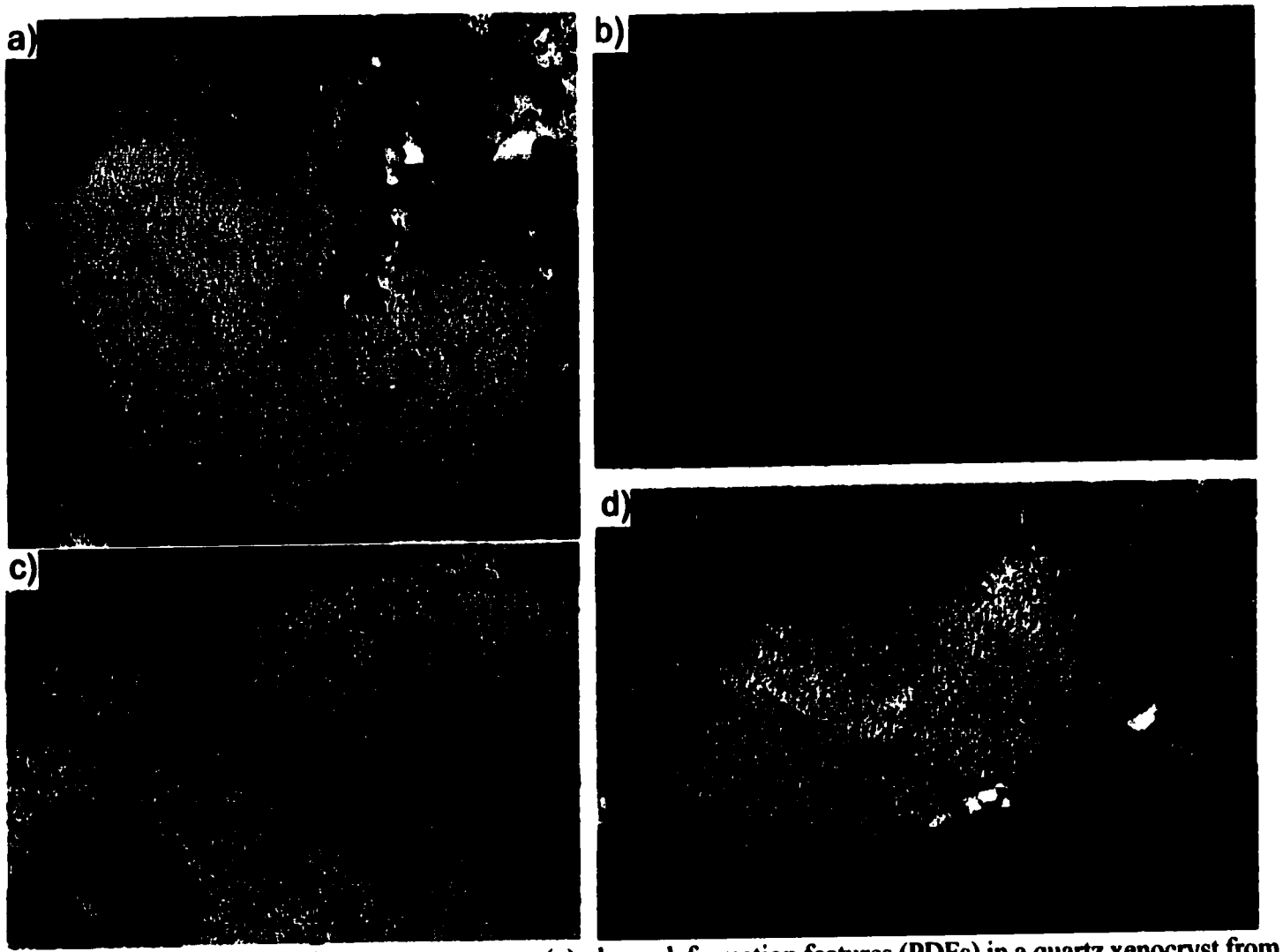

Figure 21. Photomicrographs of quartz xenocrysts: **(a)** planar deformation features (PDFs) in a quartz xenocryst from the transition zone of the SIC (sample SUD-89-1994, cross-polarized light, field-of-view = 1 mm); **(b)** close-up view of the lower portion of the xenocryst shown in (a) (plane light, field-of-view = 500 μm); **(c)** PDFs in a quartz inclusion from the basal member of the Onaping Formation (sample SUD-83-1994, cross-polarized light, field-of-view = 2 mm); and **(d)** another quartz inclusion having PDFs within the basal member (as in (c)).

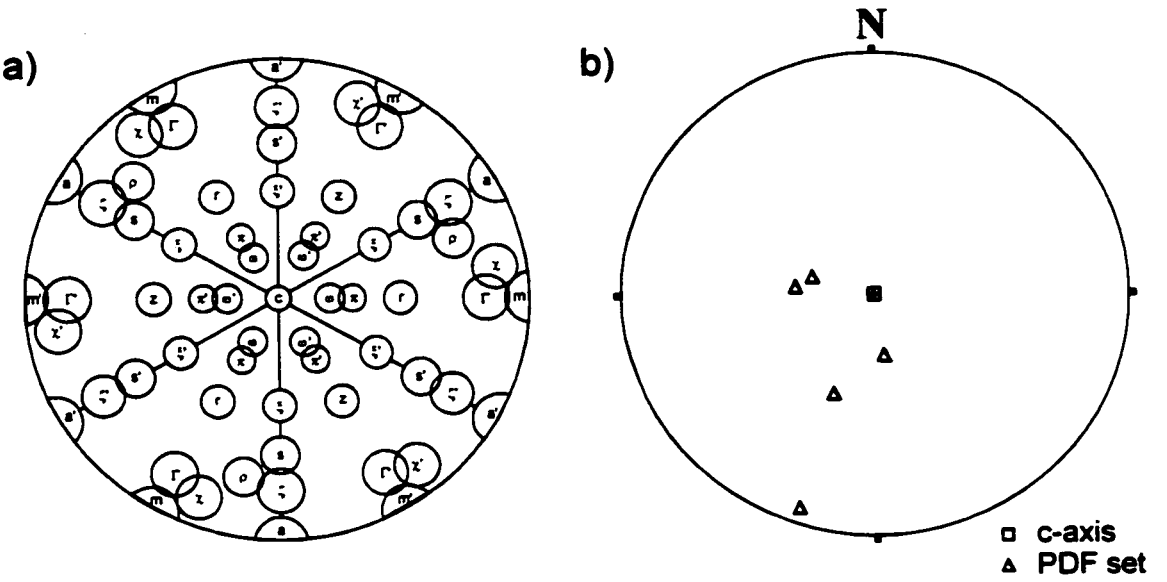

Figure 22. **(a)** Quartz crystallography as shown on a Wulff net projection. **(b)** Wulff net projection of rotated planar deformation features (PDFs) measurements in quartz xenocrysts from the transition and lower unit ("norite") of the SIC. This c-axis vertical projection is used with a template of crystallographic indices of quartz (a) to determine the PDFs orientations.

Table V: Planar deformation features (PDFs) in quartz xenocrysts *vs.* crystallographic indices in quartz, for samples SUD-89-1994, SUD-8-1994 and SUD-94-1994 of the SIC, as obtained from stereonet plots.

Plane	Miller-Bravais index	Polar angle with c-axis	Number of PDF sets
c	(0001)	0°	-
ω	$\{10\bar{1}3\}$	22°56'	-
π	$\{10\bar{1}2\}$	32°25'	3
ξ	$\{11\bar{2}2\}$	47°43'	1
r,z	$\{10\bar{1}1\},\{01\bar{1}1\}$	51°47'	-
s	$\{11\bar{2}1\}$	65°33'	-
ρ	$\{21\bar{3}1\}$	73°25'	-
ζ	$\{22\bar{4}1\}$	77°12'	-
τ	$\{40\bar{4}1\}$	78°52'	-
χ	$\{50\bar{6}1\}$	82°04'	-
m,a	$\{10\bar{1}0\},\{11\bar{2}0\}$	90°	1
total			5

crystallographic orientations of 32° (*i.e.*, parallel to the π {10$\bar{1}$2}), 48° (*i.e.*, parallel to ξ {11$\bar{2}$2}) and 90° (*i.e.*, parallel to the m {10$\bar{1}$0} or a {11$\bar{2}$0}). Quartz xenocrysts in the Onaping Formation commonly contain multiple sets of PDFs (French, 1967, 1968). In the basal member two sets in one grain were measured to be parallel to the crystallographic orientation of 23° (*i.e.*, ω {10$\bar{1}$3}; Figs. 21c and 21d), which agrees with the data of French (1967, 1968). Unlike PDFs observed in shocked target rocks from other impact structures and from the overlying Onaping Formation, the PDFs observed in the lower unit ("norite") and the transition zone of the SIC are very faint.

3.3.6 Alkali feldspars

The Ab-An-Or data of all alkali feldspar crystlas are plotted in Figure 7 and complete microprobe analyses are given in Appendix A. At the base of the lower unit ("norite"), alkali feldspar crystals are < 2 mm in diameter, anhedral and altered, have sutured crystal boundaries and undulose extinction, and fill gaps/interstices. Some crystals are clearly microcline, having a well defined cross-hatched pattern; others commonly have microperthite exsolutions, *i.e.*, contain exsolution lamellae of albite. Alteration of alkali feldspars by sericite usually follows cleavage planes. In the middle unit ("quartz gabbro"), most alkali feldspar crystals, 0.5 to 1.0 mm wide, have microperthite exsolutions as described above for the lower unit ("norite"). In the upper unit (granophyre), only rare individual orthoclase or microcline crystals are observed (besides the perthite and microcline component of the micro-intergrowths); whereas, in the upper part of the upper unit (granophyre), perthite is abundant and, besides occurring as a component

of micro-intergrowths, may occur as discrete crystals (Fig. 23a). From the top of the middle unit ("quartz gabbro") through the base of the Onaping Formation, plagioclase crystals are mantled by a coarse microperthite overgrowth, which is continuous with the micrographic and granophyric intergrowths surrounding the plagioclase crystal (Fig. 23b).

3.3.7 Apatite

In the SIC, at the base of the lower unit ("norite"), apatite crystals occur as intercumulus crystals that are prismatic, up to 0.4 mm in length, or rod-shaped, up to 1.5 mm in length. In the lower unit ("norite") and the middle unit ("quartz gabbro"), apatite occurs as cumulus prismatic crystals up to 0.3 mm and rods and needles up to 2.0 mm in length. These apatite crystals may commonly be skeletal (Fig. 10f), or may occur as needles in quartz crystals (Fig. 10a). In the transition zone of drill core 70011, apatite occurs as large cumulus lath-shaped crystals up to 2.0 mm in length. Some crystals may be skeletal (Fig. 11b). In the upper unit (granophyre), apatite occurs as intergranular crystals up to 0.5 mm. In drill core 52848, but less so in drill cores 52847 and 70011, apatite is commonly poikilitically enclosed in augite, amphibole and biotite crystals.

These observations concur with those of Warner *et al.* (1998), who made a detailed study of apatite crystals and their textural and compositional variations in three traverses (NW, NE, and SW) across the SIC. Warner *et al.* (1998) present chemical data for apatite from the SIC. These data show that the apatite has a low Cl/F ratio, similarly to layered igneous complexes, but it is enriched in light rare earth elements (LREE) and, near the base of the SIC, is also enriched in Si and REEs compared to other layered igneous complexes.

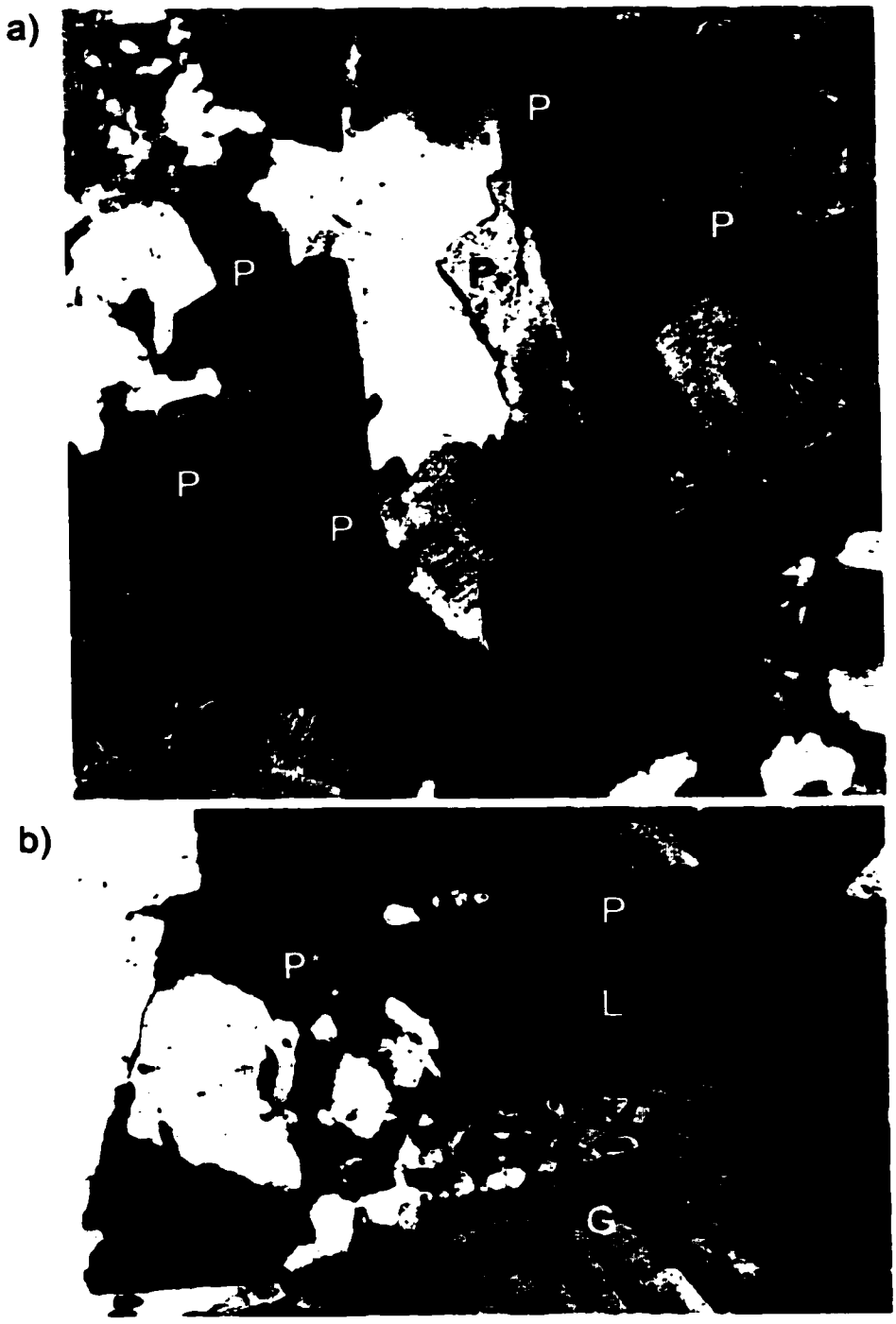

Figure 23. Photomicrographs of perthite within the upper part of the upper unit (granophyre): **(a)** individual perthite crystals (P) (sample SUD-144-1995, cross-polarized light, field-of-view = 2 mm); and **(b)** albite lath (L) with perthite overgrowth (P), which is continuous with the perthite component (P*) of micrographic intergrowths (G) (sample SUD-144-1995, cross-polarized light, field-of-view = 2 mm).

3.3.8 Fe-Ti Oxides and Titanite

In the SIC, Fe-Ti oxide minerals consist mostly of ilmenite, magnetite, and titaniferous magnetite (Figs. 24a and 24b). Secondary hematite is most common in the upper unit (granophyre) (Fig. 24c). Microprobe analyses given in Appendix A indicate that in the lower unit ("norite") titaniferous-magnetite crystals are enriched in V_2O_3 and depleted in MnO contents in relation to co-existing ilmenite crystals. There are two modes of occurrence of magnetite. One contains abundant lamellae of ulvöspinel and is intimately associated with ilmenite in lamellar form. The other does not contain microscopically visible Ti-bearing phases and occurs as separate crystals (Figs. 24a and 24b). Ilmenite occurs in two distinct forms: as trellis networks of lamellar and skeletal intergrowths in magnetite, and as individual subhedral crystals. Gradation between textural varieties are observed with stratigraphic level changes.

In the lower unit ("norite"), magnetite and titaniferous-magnetite occur as granular masses, rods, or have an octahedral cross-section, and may have a chlorite or titanite corona (Fig. 24d). All crystals are up to 2 mm. In the middle unit ("quartz gabbro"), Fe-Ti oxides consist mainly of magnetite crystals up to 1 mm in size and some crystals may be skeletal (Fig. 10c). The cumulus Fe-Ti oxide in the transition zone and upper unit (granophyre) is magnetite, containing lamellae of ilmenite and is accompanied by rare intercumulus ilmenite. These observations concur with those of Gasparrini and Naldrett (1972), who made a detailed study of magnetite and ilmenite crystals in drill cores and traverses across the SIC.

Titanite crystals are ubiquitous throughout drill cores 70011 and 52847. In drill core 52848, titanite crystals are only observed in the transition zone and upper unit (granophyre).

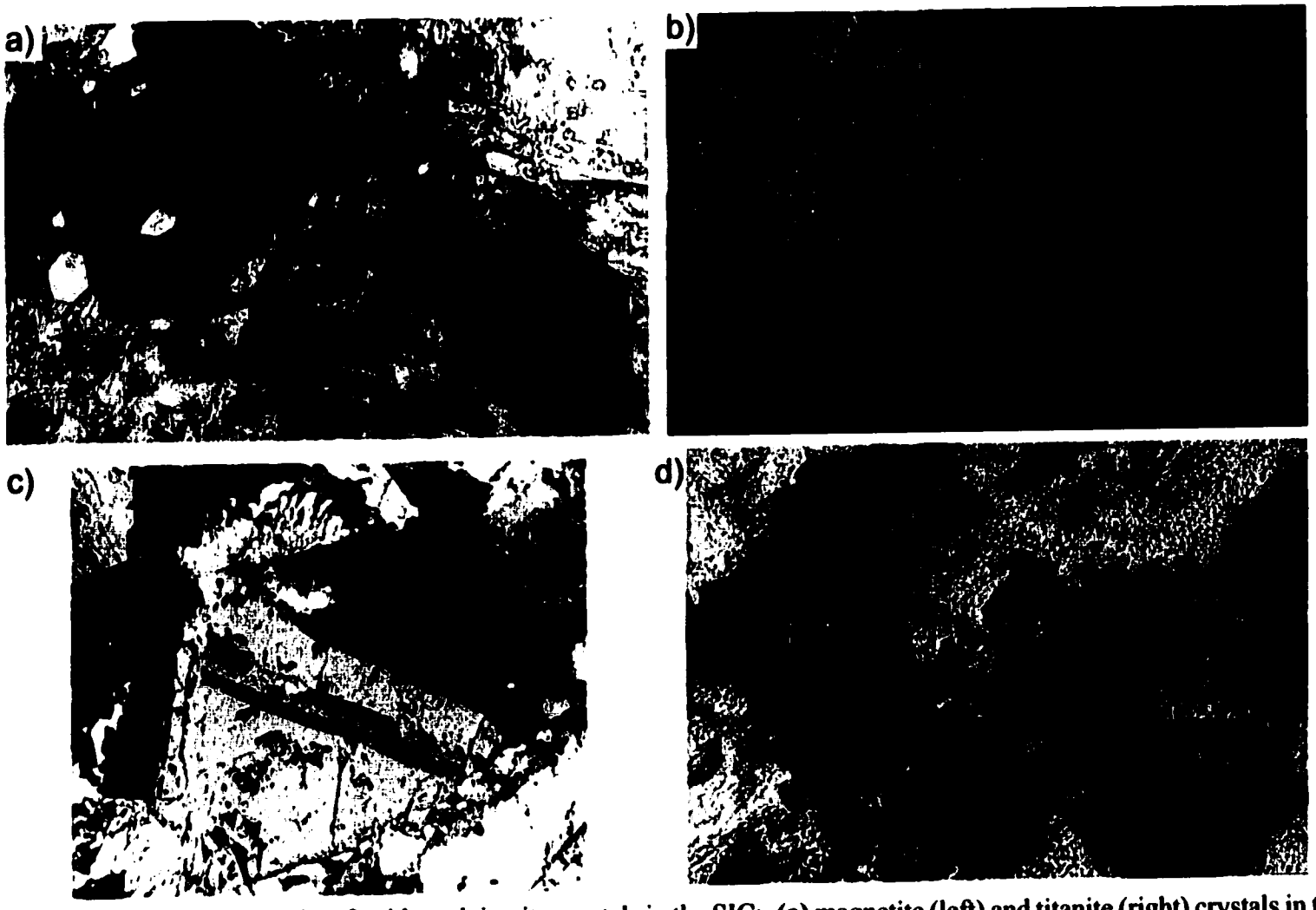

Figure 24. Photomicrographs of oxide and titanite crystals in the SIC: **(a)** magnetite (left) and titanite (right) crystals in the middle unit ("quartz gabbro") (sample SUD-59-1994, plane light, field-of-view = 2 mm); **(b)** as in (a) but in reflected light and showing the thin corona of titanite (dark gray) around the magnetite crystal (light gray) and ilmenite rods within the titanite crystal; **(c)** hematite rods in an albite crystal from the upper part of the upper unit (granophyre) (sample SUD-167-1995, cross-polarized light, field-of-view = 4 mm); and **(d)** titanite corona around magnetite crystals in the lower unit ("norite") (sample SUD-90-1994, plane light, field-of-view = 2 mm).

Titanite occurs as rounded individual anhedral crystals, up to 2 mm in diameter, as a thin corona around magnetite crystals, rare subhedral to euhedral crystals up to 2 mm in diameter (Figs. 24a and 24b), or rare granular masses < 0.1 mm in diameter. In the transition zone and upper unit (granophyre), titanite crystals are less than 0.5 mm in diameter. Single titanite crystals may be interlocked with augite crystals. Microprobe analyses given in Appendix A indicate that the titanite crystals decrease in TiO_2 content and increase in Al_2O_3 content from the contact sublayer to the upper unit (granophyre).

3.4 Alteration and Secondary Minerals

In drill cores 70011 and 52847, early crystallized minerals (plagioclase and pyroxene) are greatly affected by alteration; whereas, later crystallized minerals (*e.g.*, amphibole mantles and micrographic and granophyric intergrowths) are virtually unaltered. This observation suggests that the alteration of the SIC is mainly deuteric in nature. The amount and intensity of alteration decreases with depth in all the cores. At a depth exceeding about 500 m below the boundary of the upper unit (granophyre) - transition zone in drill core 70011, alteration is reduced to a slight sericitization and saussuritization of plagioclase crystals and a slight uralitization of pyroxene crystals. Drill core 52847 is altered throughout. The alteration in drill core 52848 consist mainly of a slight sericitization and saussuritization of plagioclase crystals and uralitization of pyroxene crystals, with more intense alteration occurring heterogeneously throughout the drill core.

The distribution of alteration products is heterogeneous on the scale of the drill core, rock

unit, sample, thin section, and crystal. For example, in a thin section, a crystal of a given mineral phase is unaltered; whereas the adjacent crystal is altered. An explanation for the variation in degree of alteration between individual crystals of a given mineral phase in one thin section may be related to the section view of the given crystals. A section close to the crystal surface is more altered; whereas, a section cut deeper within the crystal is unaltered. Throughout the SIC, the principal alteration products are clinozoisite and epidote (after feldspars), uralitic amphibole (after pyroxene), biotite (after plagioclase, pyroxene, and amphibole), and chlorite (after plagioclase, pyroxene, amphibole, and biotite). Products filling vugs and gaps within crystals consist of silicate (unknown), oxide, chlorite, quartz, and calcite, in various combinations. In sample SUD-152-1995 (depth of 1826.7 m in drill core 70011, *i.e.*, within the lower unit ("norite")), all mafic minerals, which make up less than 5 vol.% of the rock, are highly altered and the most abundant minerals are calcite, plagioclase, epidote and Fe-Ti oxides.

3.4.1 Pseudomorphs after ulvöspinel-magnetite and after amphibole

Pseudomorphs of biotite + titanite + ilmenite ± sulfide (mainly pyrite and pyrrhotite) ± chlorite after ulvöspinel-magnetite crystals (Fig. 25a), up to 3 mm in diameter, and of biotite + titanite ± amphibole after primary amphibole crystals (Fig. 25b), up to 2 mm in diameter, are observed throughout the drill cores 70011 and 52847. The abundance of pseudomorph aggregates per thin section increases with higher stratigraphic levels reaching a maximum within the middle unit ("quartz gabbro") and, then, decreases until no pseudomorph aggregates are observed within the top of the upper unit (granophyre), just below the upper limit with the

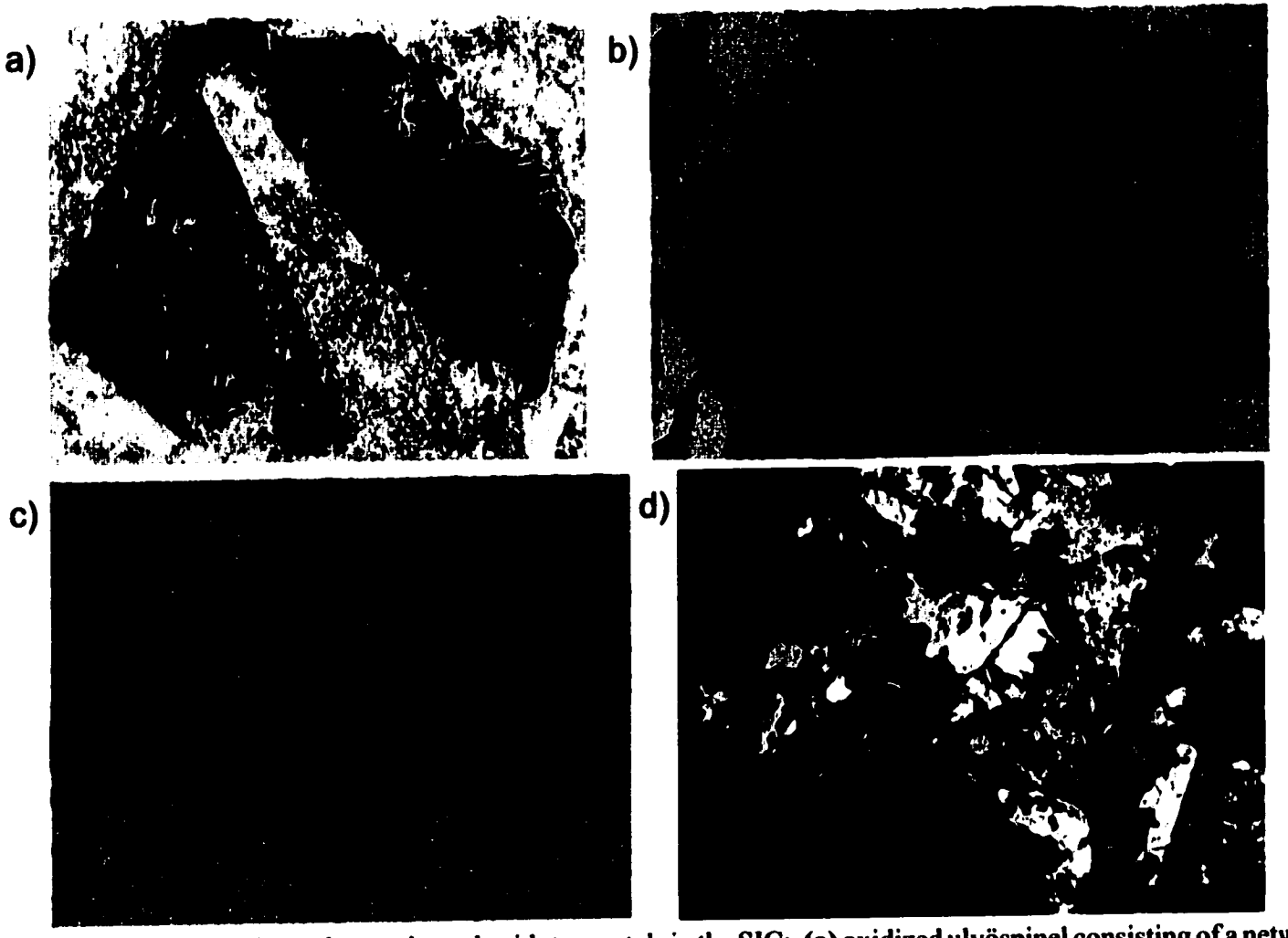

Figure 25. Photomicrographs of pseudomorphs and epidote crystals in the SIC: **(a)** oxidized ulvöspinel consisting of a network of ilmenite needles and rods within titanite and biotite from the lower unit ("norite") (sample SUD-6-1994, plane light, field-of-view = 4 mm; P = altered plagioclase lath); **(b)** pseudomorph aggregate of amphibole and biotite with a network of ilmenite and titanite needles and rods after a primary amphibole crystal and which is lined by ilmenite and biotite crystals in the lower unit ("norite") (sample SUD-7-1994, cross-polarized light, field-of-view = 2 mm); **(c)** epidote crystals (yellowish) within the upper part of the upper unit (granophyre) (sample SUD-50-1994, plane light, field-of-view = 2.5 mm); and **(d)** as in (c) but cross-polarized light showing the composite character of the crystals.

Onaping Formation. In drill core 52848, these same pseudomorphs are only observed in highly altered samples of the transition zone.

Well-preserved trellis networks of titanite and ilmenite rods after {111} ilmenite have partly or totally replaced the original ulvöspinel-magnetite crystals, or occur along cleavage planes of the original amphibole crystals (Figs. 25a and 25b). The rims of these pseudomorphs are commonly lined by ilmenite (Figs. 25a and 25b) and, in the contact sublayer and at the base of the lower unit ("norite"), they are often mantled by, or associated with, biotite (Fig. 25b). However, with higher stratigraphic levels, the biotite "mantles" disappear and the amount of replacement by titanite over the other replacing minerals increases. Secondary titanite is formed through the metasomatic introduction of CaO and SiO_2 from plagioclase decomposition and the interaction with deuteric fluids. The removal of FeO from ulvöspinel generates the chlorite and/or amphibole and/or ilmenite and/or sulfide observed within the pseudomorphs.

3.4.2 Epidote

Throughout the SIC, epidote occurs mainly as small flakes, as large as a few tens of microns, in plagioclase crystals, suggesting that they were originally more calcic. The abundance of this secondary epidote directly reflects the intensity of alteration of the sample. As drill cores 52847 and 70011 are more altered than drill core 52848, these former drill cores have a higher content of epidote than the latter. In the contact sublayer and lower part of the lower unit ("norite") of drill core 70011, this secondary epidote constitutes less than 5% of the modal composition. It increases from 10 vol.% at the base of the upper part of the lower unit ("norite")

to more than 20 vol.% in the transition zone and then decreases to about 5 vol.% in the upper unit (granophyre) (Table I). A similar variation in mode is observed in drill core 52847.

Small amounts of coarse-grained (larger than 0.5 mm) epidote crystals are observed disseminated within the matrix of samples throughout drill core 70011 and within the upper unit (granophyre) samples of all three drill cores studied. Some of these epidote crystals may be primary, as suggested by their crystal form and sutured boundaries (Figs. 25c and 25d). In general, these coarser-grained epidote crystals are color-zoned and have pleochroic pale yellowish-green cores and almost colorless rims. They also become less colourful in higher stratigraphic levels. In the lower part of the lower unit ("norite"), epidote occurs as anhedral individual grains up to 0.5 mm; whereas, it forms aggregate masses in the upper part of the lower unit ("norite") and in the middle unit ("quartz gabbro"). In the transition zone and the upper unit (granophyre), epidote occurs as crystal aggregates, up to 2 mm in diameter (Figs. 25c and 25d), together with biotite crystals, which may be acicular, and sometimes with apatite needles. Throughout the SIC, epidote crystals, or aggregates thereof, generally form wormy or interfingering contacts with plagioclase and quartz crystals and against microgranophyric intergrowths; whereas, they have a euhedral shape with amphibole and biotite crystals.

3.4.3 Uralitic amphiboles

In the SIC, actinolite and ferro-actinolite occur as a colorless to pale green fibrous amphibole from the uralitization of pyroxene crystals. In the upper part of the lower unit ("norite"), complete zones of actinolite are observed within the pyroxene crystals. Uralitization

of enstatite takes place first, through simple hydration, then, with increasing alteration an interchange of calcium, magnesium, and iron between orthopyroxene and clinopyroxene may occur. As alteration increases, actinolite is replaced by darker green, more pleochroic ferro-actinolite.

3.4.4 Chlorite

In the lower unit ("norite"), chlorite may be abundant (up to 10%), occurring as anhedral plates and scales, up to 1 mm in diameter, usually replacing pyroxenes, amphiboles and, more rarely, biotite. Chlorite crystals have an undulatory extinction and may be fractured. In the middle unit ("quartz gabbro"), chlorite forms interstitial anhedral crystals between plagioclase and augite crystals. From the middle unit ("quartz gabbro") to the top of the upper unit (granophyre), chlorite also occurs as scattered grains in plagioclase and is abundant as fine-grained aggregates, up to 2 mm in diameter, along grain boundaries and in interstices.

3.4.5 Calcite

Calcite crystals occur mainly as veinlets, interstitial material, or fill voids throughout the SIC. Grain size ranges up to 0.5 mm. Calcite is most abundant in the lower part of the lower unit ("norite") and upper part of the upper unit (granophyre) and is generally associated with chlorite, biotite, Fe-Ti oxides, and sometimes uralitic amphibole. Its relationships with other minerals and well-formed crystals suggest that calcite is the result of hydrothermal deposition.

3.5 Textures

Rapid crystallization or far-from-equilibrium textures are pervasive throughout the rocks of the SIC. These include boxy-cellular and skeletal crystals of plagioclase, skeletal apatite and quartz crystals, acicular crystals of apatite, albite and augite, clinopyroxene (augite) and biotite, spherulitic biotite, micrographic and granophyric intergrowths, dendritic or skeletal quartz crystals within these intergrowths, and spherulitic-like texture of quartz and alkali feldspar intergrowths.

Plagioclase crystals may be boxy-cellular or skeletal above the top of the middle unit ("quartz gabbro"). The outline of these latter crystals may be either squarish with a hollow center, in a complex "U-shape" (Fig. 12d), or very complex altogether. Quartz crystals in the lower unit ("norite") may be skeletal (*i.e.*, having a hollow center) and are usually closely associated with micrographic intergrowths. Skeletal crystals of apatite are characterized by an axial cavity parallel to their c-axis and are observed above the middle of the lower unit ("norite"). Similar elongated cavities have been documented in tourmaline and attributed to rapid crystal growth (Manning, 1982). Acicular apatite crystals are observed in the lower unit ("norite") and middle unit ("quartz gabbro"). Acicular albite crystals, up to 3 mm in length and acting as nuclei for micrographic and granophyric intergrowths, occur in the upper part of the upper unit (granophyre). Acicular crystals of augite are observed in the lower unit ("norite") and acicular amphibole in the upper unit (granophyre). Given the alteration effects in the SIC, these acicular amphibole crystals are most likely pseudomorphs after acicular augite. In the upper unit (granophyre), acicular crystals of biotite are observed, some clustered into spherulitic aggregates.

Fields of micrographic and granophyric intergrowths (Fig. 26a) have extinction in "domains" (Fig. 26b), the quartz component having a straight extinction and the K-feldspar component having undulose extinction. Micrographic and granophyric intergrowths developed towards the base of the lower unit ("norite") are usually not well defined. The area of these fields increases with higher stratigraphic levels from less than 2 mm at the base of the lower unit ("norite") to about 1 cm within the upper unit (granophyre). At the base of the lower unit ("norite"), the size of the micrographic intergrowths themselves is relatively coarse and then becomes finer until the top of the middle unit ("quartz gabbro"), where it starts to increase to reach a maximum within the upper unit (granophyre). At the top of the upper unit (granophyre), within the plagioclase-rich granophyre, the intergrowths are the finest. The granophyric intergrowths become finer but longer and more numerous/denser with higher stratigraphic levels. Barker (1970) stated that the size of granophyric intergrowths is affected by the rate of crystallization for a given composition. With more rapid cooling, their size decreases. This would indicate that the upper unit (granophyre) has undergone more rapid cooling than the other lithologies of the SIC. In the lower unit ("norite") and the upper unit (granophyre), the quartz component of these fields may be dendritic (Fig. 26c), and/or in the middle unit ("quartz gabbro") and upper unit (granophyre) the quartz component may be skeletal (Fig. 20b). The micro-intergrowth fields may develop into spherulitic-like textures in the upper unit (granophyre) (Fig. 26d). Swanson and Fenn (1986) demonstrated, through dynamic crystallization experiments, that high ΔT and rapid undercooling are required to form textures such as dendritic and spherulitic quartz. Intergrowths immediately surrounding plagioclase crystals are usually

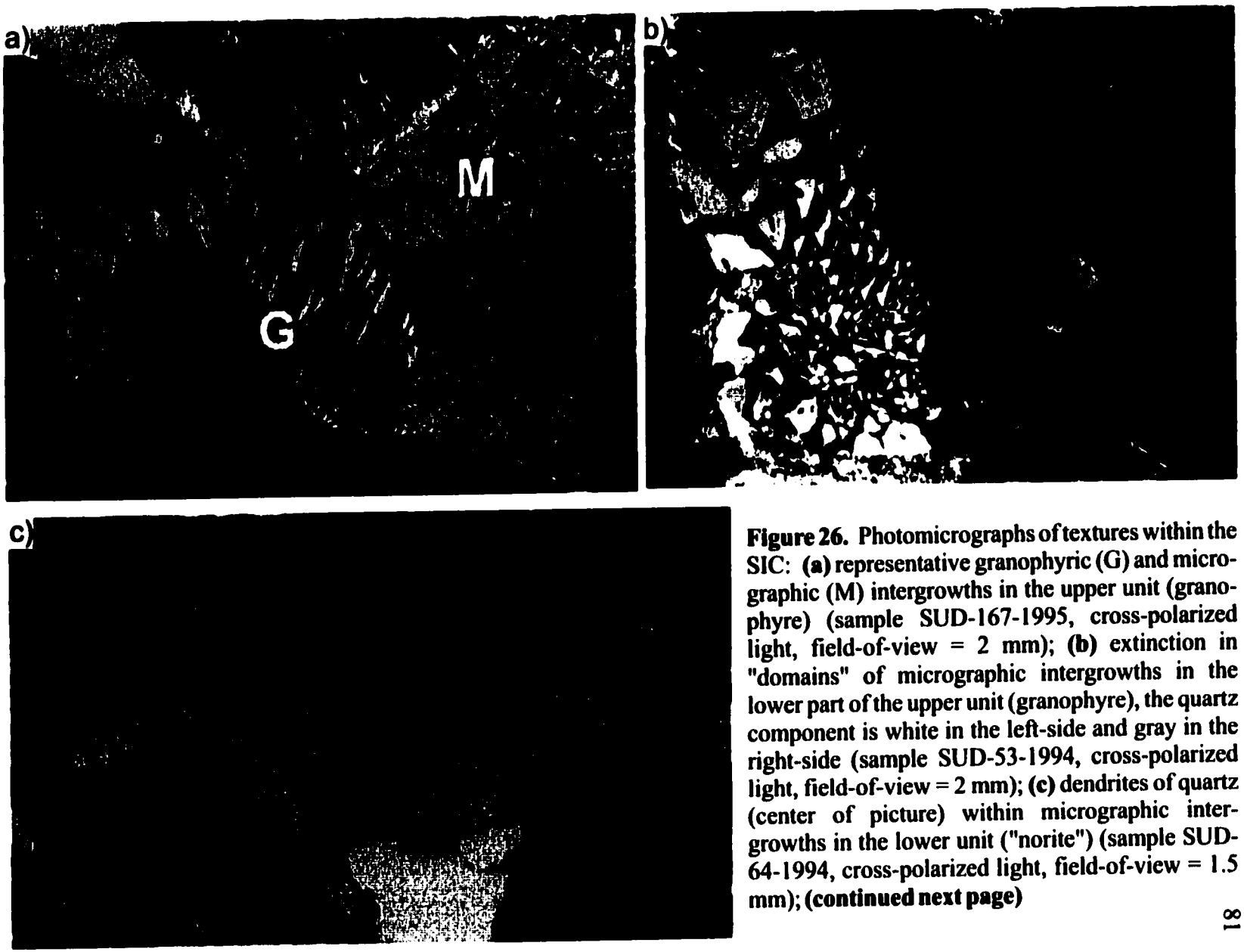

Figure 26. Photomicrographs of textures within the SIC: **(a)** representative granophyric (G) and micrographic (M) intergrowths in the upper unit (granophyre) (sample SUD-167-1995, cross-polarized light, field-of-view = 2 mm); **(b)** extinction in "domains" of micrographic intergrowths in the lower part of the upper unit (granophyre), the quartz component is white in the left-side and gray in the right-side (sample SUD-53-1994, cross-polarized light, field-of-view = 2 mm); **(c)** dendrites of quartz (center of picture) within micrographic intergrowths in the lower unit ("norite") (sample SUD-64-1994, cross-polarized light, field-of-view = 1.5 mm); **(continued next page)**

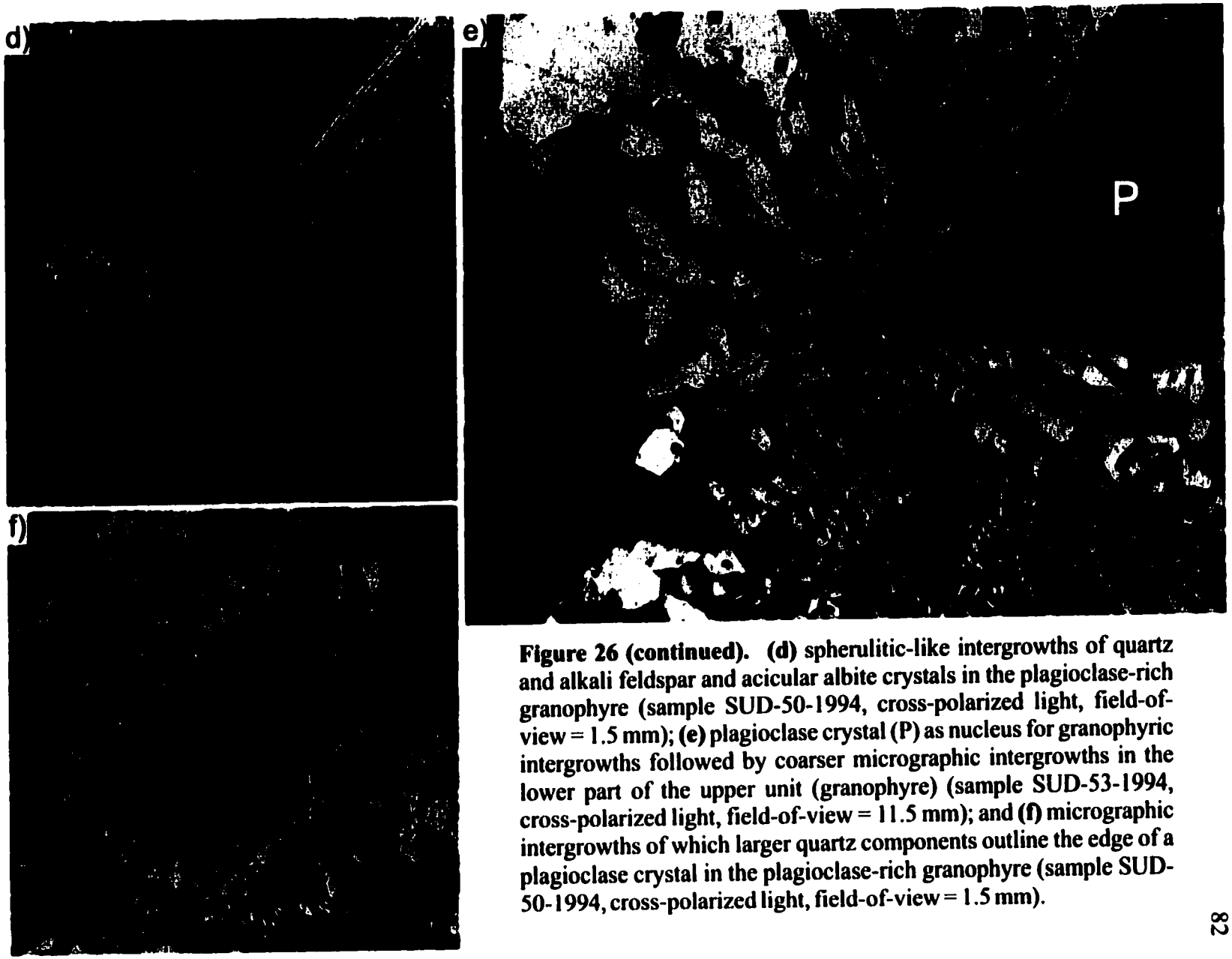

Figure 26 (continued). **(d)** spherulitic-like intergrowths of quartz and alkali feldspar and acicular albite crystals in the plagioclase-rich granophyre (sample SUD-50-1994, cross-polarized light, field-of-view = 1.5 mm); **(e)** plagioclase crystal (P) as nucleus for granophyric intergrowths followed by coarser micrographic intergrowths in the lower part of the upper unit (granophyre) (sample SUD-53-1994, cross-polarized light, field-of-view = 11.5 mm); and **(f)** micrographic intergrowths of which larger quartz components outline the edge of a plagioclase crystal in the plagioclase-rich granophyre (sample SUD-50-1994, cross-polarized light, field-of-view = 1.5 mm).

finer-grained than those a few millimeters away from these nuclei (Fig. 26e). However, at the edges of the plagioclase crystals, the quartz component of the intergrowth is usually coarse-grained (Fig. 26f).

3.6 Summary and Interpretation

The SIC is a succession of genetically related layers, lying conformably one above the other, and showing no evidence of chilling between them. In fact, no contacts *per se* are observed between the various lithologies within the SIC. The "contacts" are best described as gradational zones up to a few tens of meters thick, except for a relatively thick one (up to 200 m), the transition zone, which occurs between the middle unit ("quartz gabbro") and the upper unit (granophyre) (Fig. 3). Moreover, detailed mapping and a careful microscopic and geochemical study are required in order to define the SIC layers and their extent. Neither rhythmic (*i.e.*, repetition of rock types in higher stratigraphic levels) nor finer, cm-scale layering is observed within the North Range of the SIC. Phase layering (*i.e.*, appearance and disappearance of minerals) and cryptic layering (*i.e.*, chemical variation in mineral composition, such as Fe- or Na-enrichment with increasing stratigraphic levels) are observed on a large scale (Fig. 5).

The relationship between plagioclase and pyroxene in the lower unit ("norite") suggests that they nucleated together, probably *in situ*, with pyroxene forming fewer nuclei than plagioclase. As the minerals grew, pyroxene encased the plagioclase, arresting further growth. These well-formed laths of plagioclase included in larger pyroxene crystals suggest a somewhat

earlier start to plagioclase nucleation and crystallization. In support of this interpretation, augite and amphibole crystals, but not plagioclase crystals, poikilitically enclose apatite crystals. The relationship between pyroxene and plagioclase crystals in the middle unit ("quartz gabbro") may be explained by a relatively high nucleation rate of pyroxene, which concentrated many smaller crystals between tabular plagioclase in a granular ("intergranular") texture.

Only rare cumulus crystals of olivine are present in the SIC, in a specific phase of the contact sublayer (Pattison, 1979; Lightfoot *et al.*, 1997b) and in some mafic and ultramafic inclusions (Lightfoot *et al.*, 1997b). The inner core of discrete cumulus plagioclase crystals is essentially unzoned, with an abrupt change to normal zoning close to their rims, which are fairly Na-rich. Finely spaced exsolution lamellae, presumably Bøggild intergrowths given the chemistry of their host, within the lower unit ("norite") are evidence of slow cooling and unmixing from high temperatures. The SIC pyroxenes are continuously enriched in Fe in higher stratigraphic levels, following the "Skaergaard trend" (Fig. 16). Primary amphibole and biotite crystals occur throughout the SIC, from the lower part of the lower unit ("norite") through the upper unit (granophyre), and are indicative of the presence of a hydrous phase early in the crystallization history of the SIC. The occurrence of microcline in the lower unit ("norite") also indicates that this lithology crystallized in the presence of a hydrous phase. According to Warner *et al.* (1998), apatite crystals of the SIC have an anomalous chemical composition suggestive of rapid crystallization and degassing of the melt.

Many rapid and non-equilibrium crystallization textures are observed throughout the rocks of the SIC. Of these textures, the micrographic and granophyric intergrowths are the most

voluminous and impressive, comprising less than 20 vol.% of the lower unit ("norite") but increasing to 70 vol.% of the upper unit (granophyre). Micrographic intergrowths of K-rich and Na-rich feldspar with quartz are usually the product of subsolvus crystallization at higher water pressures and their formation is connected to the presence of abundant fluids (Lentz and Fowler, 1992).

One of the first mineralogical changes to occur in the SIC, in the lower unit ("norite") for some parts of the SIC (*e.g.*, drill cores 70011 and 52847) and in the middle unit ("quartz gabbro") for other parts of the SIC (*e.g.*, drill core 52848), was the formation of ilmenite trellis networks in magnetite crystals by oxidation during cooling (*cf.*, Buddington and Lindsley, 1964; Taylor, 1964). This transformation was either accompanied by or preceded by replacement of the clinopyroxene by actinolite and ferro-actinolite. Alteration of plagioclase to albite and epidote followed. The leaching of magnetite and primary amphibole occurred only in some parts of the SIC (*e.g.*, drill cores 70011 and 52847), with skeletal ilmenite trellis networks in an assemblage of titanite, biotite, and/or amphibole being all that remain of the original grains. Widespread heterogeneous alteration of all the SIC lithologies in some parts of the SIC (*e.g.*, drill cores 70011 and 52847), or alteration of only the middle unit ("quartz gabbro") and transition zone throughout the rest of the SIC, indicates movement of a large volume of a fluid phase. Uralitization of pyroxene crystals and saussuritization of plagioclase crystals are characteristics of deuteric alteration. This observation, together with the occurrence of primary hydrous minerals, indicates that the alteration fluid was "magmatic water", *i.e.*, exsolved from the crystallizing melt. Moreover, this fluid was capable of dissolving and removing iron. These

interpretations are in agreement with previous work describing the alteration of the SIC upper unit (granophyre) by a highly saline aqueous fluid (*e.g.*, Taylor, 1967; Schandl *et al.*, 1986; Li and Naldrett, 1993) and more recent work by Molnár *et al.* (1997) and Marshall *et al.* (1999) indicating that the Sudbury Structure was affected by five separate fluids: an exsolved fluid from the SIC, a regional groundwater/metamorphic fluid, a regional fluid heated by the SIC during the waning stages of its emplacement, a CO_2-bearing Penokean fluid, and neotectonic brines.

4. WHOLE-ROCK GEOCHEMISTRY

4.1 Major Elements

The average composition (major elements only) and CIPW norms of the SIC and its five major lithologies (including the transition zone as defined in this work) are given in Table VI. All of the SIC lithologies and the basal member of the Onaping Formation have the same normative minerals, *i.e.*, quartz, orthoclase, albite, anorthite, hypersthene, magnetite, ilmenite, apatite, and calcite, although in varying amounts. The Onaping Formation, upper unit (granophyre) and lower unit ("norite") samples have either normative corundum or diopside; whereas, the transition zone, middle unit ("quartz gabbro") and contact sublayer have only normative diopside. Samples with normative corundum indicate that they are slightly oversaturated in alumina, compared to the other samples. Normative hematite appears in the calculated CIPW norm of only one Onaping Formation sample, in drill core 70011, and two samples of the middle unit ("quartz gabbro"), in drill core 52848 (Appendix D).

To illustrate the variation in CIPW norms and their use in distinguishing between the different lithologies, Or-Q-An and An-Q-Hy ternary diagrams were constructed (Fig. 27). The upper unit (granophyre) and transition zone are marked by high values of normative quartz, orthoclase and albite, and low values of normative anorthite, diopside and hypersthene, relative to the middle unit ("quartz gabbro"), lower unit ("norite") and contact sublayer (Table VI; Fig. 27). The middle unit ("quartz gabbro") is marked by relatively high values of normative diopside, magnetite and ilmenite, and low values of normative calcite; whereas, the lower unit ("norite") is marked by a high value of normative hypersthene and a low value of normative

Table VI: Average bulk rock composition and CIPW norms of the SIC and its lithologies from normalized data of: a) drill core 70011. The average SIC composition calculated by Collins (1934) is shown for comparison.

	Upper unit (granophyre) 62.4%		Transition zone 5.8%		Middle unit ("quartz gabbro") 4.7%		Lower unit ("norite") 22.5%		Contact sublayer 4.6%		SIC average 100.0%	SIC from Collins
	23 samples	std.dev.	4 samples	std.dev.	5 samples	std.dev.	12 samples	std.dev.	2 samples	std.dev.	46 samples	(1934)
SiO_2	68.71	1.29	61.52	3.67	55.25	1.38	58.82	0.62	52.33	0.25	64.57	63.14
TiO_2	0.81	0.11	1.43	0.31	1.45	0.39	0.57	0.07	0.54	0.00	0.81	0.74
Al_2O_3	12.80	0.31	13.52	0.11	14.32	0.85	16.17	0.54	15.36	0.51	13.79	14.65
Fe_2O_3	1.74	0.43	2.47	0.39	3.53	1.02	1.33	0.20	2.20	0.99	1.80	1.52
FeO	4.02	0.67	6.70	1.14	7.86	0.83	5.43	0.38	7.50	0.57	4.84	5.17
MnO	0.07	0.01	0.14	0.02	0.14	0.02	0.11	0.01	0.14	0.01	0.09	0.08
MgO	0.88	0.29	1.39	0.69	3.57	0.09	4.15	0.47	8.28	0.76	2.12	2.85
CaO	2.19	0.53	4.48	1.13	7.36	0.29	6.47	0.71	7.67	0.52	3.79	4.03
Na_2O	3.49	0.38	3.55	0.30	2.95	0.20	3.45	0.75	2.40	0.14	3.41	3.20
K_2O	3.60	0.45	2.46	0.28	1.70	0.23	1.53	0.42	1.33	0.36	2.87	2.91
P_2O_5	0.17	0.04	0.39	0.13	0.29	0.26	0.13	0.03	0.09	0.00	0.18	0.16
H_2OT	1.33	0.18	1.82	0.17	1.88	0.09	1.66	0.28	2.00	0.00	1.49	1.24
CO_2T	0.18	0.16	0.32	0.22	0.08	0.04	0.25	0.22	0.20	0.00	0.20	0.23
S	0.04	0.03	0.05	0.05	0.10	0.03	0.05	0.03	0.20	0.10	0.05	0.08
Lol	0.49	0.83	2.56	-	0.84	1.15	0.68	1.07	2.42	-	0.76	-
Total	100.52		102.80		101.32		100.80		102.66		100.77	100.00
Q	27.69	2.47	18.90	5.90	10.14	0.64	11.39	2.11	2.09	1.30		
C	0.40	0.65	0.00	0.00	0.00	0.00	0.02	0.06	0.00	0.00		
Or	21.26	2.68	14.57	1.67	10.02	1.33	9.07	2.46	7.83	2.14		
Ab	29.52	3.24	30.02	2.52	24.98	1.66	29.19	6.37	20.31	1.20		
An	7.56	2.03	13.68	1.77	20.82	2.22	24.02	3.32	27.23	0.96		
Di	0.86	0.99	3.34	4.64	11.01	1.46	4.60	4.41	7.29	1.39		
Hy	6.50	1.39	9.94	1.50	12.80	0.91	16.23	3.48	28.42	0.70		
Mt	2.53	0.63	3.58	0.57	5.12	1.48	1.93	0.28	3.19	1.44		
Il	1.53	0.20	2.72	0.60	2.74	0.75	1.08	0.13	1.03	0.00		
Ap	0.41	0.09	0.93	0.31	0.69	0.61	0.32	0.06	0.21	0.00		
Cc	0.42	0.36	0.74	0.50	0.18	0.10	0.57	0.49	0.45	0.00		
Total	98.68		98.42		98.50				98.05			

Table VI: b) drill core

	Upper unit (granophyre) 61.7%	Transition zone 7.4%		Middle unit ("quartz gabbro") 7.0%		Lower unit ("norite") 23.9%	SIC average 100.0%
	1 sample	5 samples	std.dev.	3 samples	std.dev.	1 sample	10 samples
SiO_2	67.74	62.57	0.78	60.17	0.69	59.90	64.95
TiO_2	0.95	0.84	0.26	0.62	0.04	0.54	0.82
Al_2O_3	12.73	14.18	0.53	15.74	0.27	17.10	14.09
Fe_2O_3	1.50	1.94	0.51	1.43	0.15	1.80	1.60
FeO	4.71	5.41	0.24	5.52	0.21	4.00	4.65
MnO	0.08	0.11	0.01	0.12	0.01	0.10	0.09
MgO	0.85	2.30	0.42	3.51	0.30	3.58	1.80
CaO	2.46	5.05	0.39	5.84	0.18	6.35	3.82
Na_2O	3.31	3.40	0.15	2.99	0.10	3.70	3.39
K_2O	3.62	2.38	0.16	1.92	0.13	1.58	2.92
P_2O_5	0.20	0.26	0.11	0.14	0.03	0.10	0.18
H_2OT	1.40	1.60	0.16	2.06	0.21	2.00	1.61
CO_2T	0.50	0.08	0.04	0.10	0.00	0.10	0.35
S	0.03	0.04	0.03	0.03	0.01	0.01	0.03
Lol	2.13	0.00	0.00	1.47	1.28	0.00	1.42
Total	102.21	100.15		101.67		100.86	101.70
Q	27.29	18.52	1.38	15.40	0.66	12.64	
C	0.53	0.00	0.00	0.00	0.00	0.00	
Or	21.40	14.06	0.98	11.33	0.80	9.34	
Ab	28.01	28.80	1.30	25.33	0.80	31.31	
An	7.74	16.38	1.92	23.86	1.54	25.39	
Di	0.00	5.41	1.07	2.94	0.71	3.93	
Hy	8.11	10.16	1.59	15.45	1.34	12.16	
Mt	2.17	2.82	0.74	2.08	0.22	2.61	
Il	1.80	1.60	0.49	1.18	0.07	1.03	
Ap	0.47	0.61	0.26	0.33	0.06	0.24	
Cc	1.14	0.18	0.10	0.23	0.00	0.23	
Total	98.66	98.54		98.11		98.88	

Table VI: c) drill core

	Upper unit (granophyre) 44.4%		Transition zone 18.9%		Middle unit ("quartz gabbro") 13.2%		Lower unit ("norite") 12.4%		Lower unit (" mafic norite") 11.1%		SIC average 100.0%
	3 samples	std.dev.	4 samples	std.dev.	6 samples	std.dev.	3 samples	std.dev.	2 samples	std.dev.	18 samples
SiO_2	69.30	0.71	59.50	1.93	52.70	1.20	51.98	0.64	45.78	1.10	60.51
TiO_2	0.74	0.08	2.20	0.25	2.92	0.48	2.59	0.61	3.76	0.57	1.87
Al_2O_3	12.80	0.14	12.91	0.43	13.55	0.44	14.86	1.14	13.95	0.36	13.31
Fe_2O_3	2.20	0.28	3.71	0.32	3.83	0.84	2.84	1.80	5.48	0.46	3.14
FeO	3.20	0.57	5.71	0.49	8.44	0.85	7.15	2.47	9.54	0.79	5.56
MnO	0.09	0.01	0.15	0.01	0.18	0.02	0.15	0.02	0.17	0.01	0.13
MgO	0.58	0.10	2.23	0.32	3.73	0.16	3.97	0.31	5.32	0.19	2.25
CaO	2.42	1.04	4.79	0.75	7.24	0.48	8.47	0.42	10.30	0.06	5.12
Na_2O	3.35	0.07	3.88	0.38	3.01	0.18	2.94	0.15	2.62	0.17	3.27
K_2O	4.10	0.28	2.26	0.28	1.45	0.16	1.16	0.14	0.56	0.03	2.64
P_2O_5	0.15	0.02	0.73	0.22	1.21	0.19	1.09	0.51	1.60	0.10	0.68
H_2OT	1.20	0.14	-	-	1.70	0.22	1.23	0.15	0.70	-	0.99
CO_2T	0.05	0.07	-	-	0.12	0.04	0.10	0.00	0.10	-	0.31
S	0.03	0.03	-	-	0.13	0.02	0.12	0.02	0.16	-	0.06
Loi	0.00	0.00	1.33	1.01	0.48	1.18	1.09	0.51	0.11	0.16	0.46
Total	100.19		99.40		100.70		99.73		100.16		100.30
Q	27.33	0.85	15.49	1.70	10.35	1.31	7.86	1.00	3.17	0.01	
C	0.00	0.00	0.00	0.00	0.00	0.00	0.00	0.00	0.00	0.00	
Or	23.47	1.79	13.33	1.64	8.59	0.93	6.50	0.31	3.31	0.17	
Ab	30.46	2.24	32.81	3.08	25.51	1.50	24.96	1.52	22.17	1.44	
An	7.04	0.49	11.17	2.16	19.16	0.89	25.28	2.93	24.66	0.12	
Di	0.96	0.82	6.46	0.56	6.81	1.88	8.73	1.60	12.73	10.30	
Hy	5.16	0.62	8.93	1.56	13.89	2.48	13.42	1.52	14.23	1.10	
Mt	2.80	0.17	3.91	0.15	5.38	1.32	5.45	0.24	7.96	0.64	
Il	1.37	0.09	4.18	0.48	5.55	0.91	4.53	1.07	7.14	1.07	
Ap	0.33	0.03	1.76	0.53	2.87	0.46	2.39	1.41	3.79	0.24	
Cc	0.23	0.00	0.00	0.00	0.19	0.09	0.15	0.13	0.12	0.16	
Total	99.16		98.03		98.31		99.29		99.26		

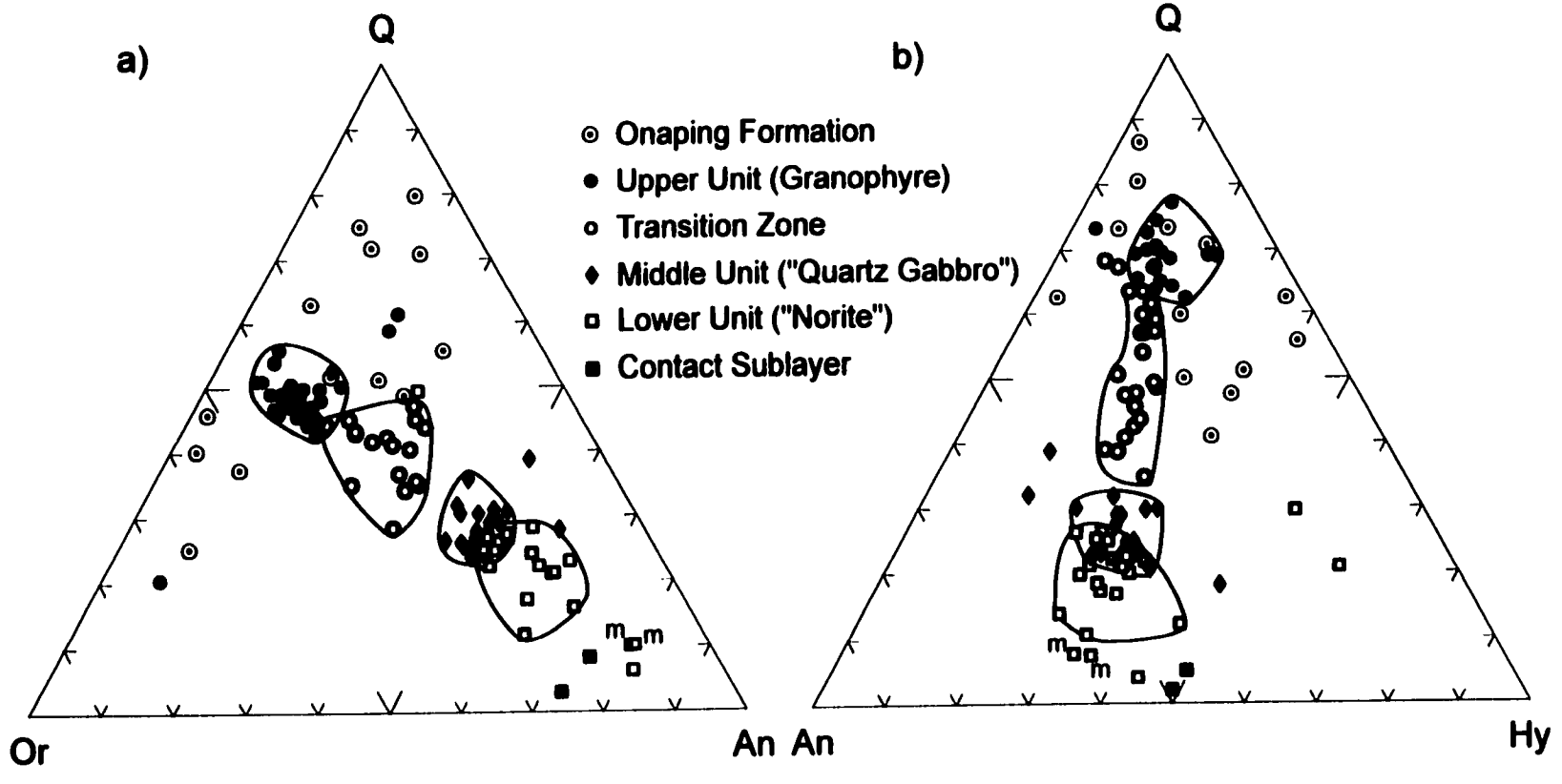

Figure 27. Ternary diagrams of CIPW normative data for samples from all three drill cores studied: (a) orthoclase (Or) - quartz (Q) - anorthite (An); and (b) anorthite (An) - quartz (Q) - hypersthene (Hy). m = lower unit ("mafic norite") in drill core 52848. Data points outside their respective groupings are either highly altered or fine-grained more aplitic-like samples. See text for details.

ilmenite. Mafic quartz gabbro ("mafic norite") samples of the lower unit ("norite") are intermediate to the norite field and contact sublayer samples and are characterized by very low values of normative orthoclase (Fig. 27). Finally, the contact sublayer is characterized by the highest values of normative hypersthene and lowest values of normative albite and quartz. Samples from the Onaping Formation have a great variation/range in their normative values (most likely an effect of inclusions) compared to all SIC lithologies. Data points outside their respective groupings are either highly altered or fine-grained more aplitic-like samples.

All whole-rock geochemical analyses of major oxides are given in Appendix B. For brevity and simplicity, only the data for drill core 70011 are illustrated, with respect to sample depth, in Figure 28. Similar trends are observed for drill cores 52847 and 52848, and, unless stated otherwise, observations within the remainder of this section pertain to all three drill cores. Of all the SIC lithologies, only the contact sublayer samples show a heterogeneous distribution. Variation in inclusion content is believed to be the cause of the variation between contact sublayer samples, as it is impossible to obtain samples that are entirely free of inclusions. Minimal geochemical variations are observed in the upper unit (granophyre) and lower unit ("norite") samples. The greatest geochemical variations, although gradational, are observed within the middle unit ("quartz gabbro") and the transition zone, and at the boundary of the upper unit (granophyre) with the overlying Onaping Formation (Fig. 28).

With higher stratigraphic levels, the SiO_2 content increases from lowest in the contact sublayer to highest at the upper unit (granophyre) - Onaping Formation boundary. The sharp variation in SiO_2 content at this latter boundary reflects the presence of numerous quartz and

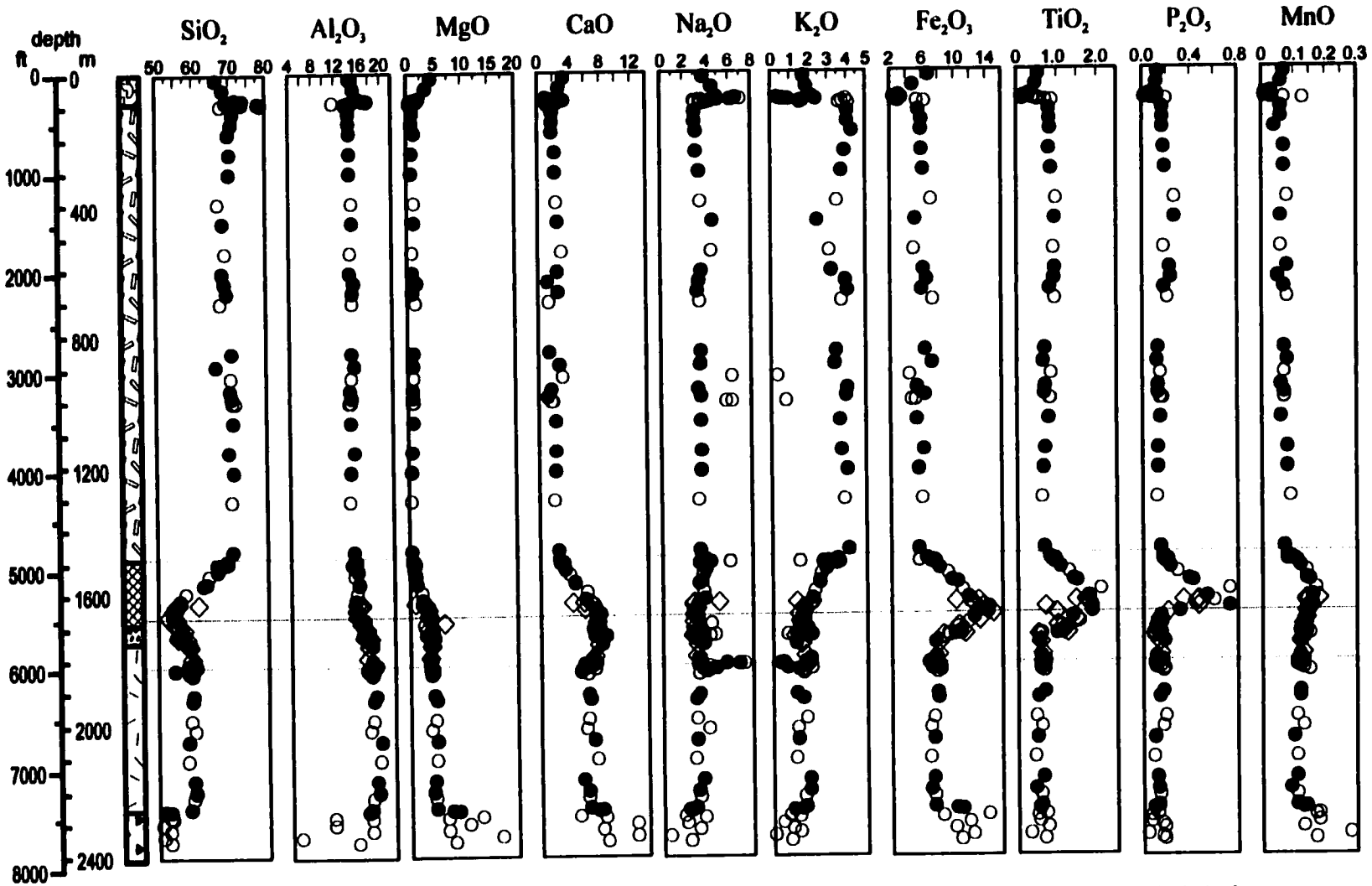

Figure 28. Major elements distribution with stratigraphy in drill core 70011. All data are in wt%. Filled circles are normalized data from this work; open circles are normalized data from Ostermann (1996); diamonds are data from McPherson Coombes (1996). Lithology patterns as in Figure 3. See text for details.

feldspar xenocrysts, which were impossible to remove from the samples. Another reason for these "anomalous" values is the higher modal abundance of cumulate albite, as reflected in a sharp increase in Na_2O at this boundary (Fig. 28). The increase in SiO_2 content is characterized by a small "sharp" jump from the sublayer to the lower unit ("norite"), then a slight and gradational decrease within the upper part of the lower unit ("norite") through the top of the middle unit ("quartz gabbro") followed by a gradational, but steep, increase from the top of the middle unit ("quartz gabbro") to the lower part of the upper unit (granophyre) (Fig. 28). An overall decrease with higher stratigraphic levels is seen for the contents of Al_2O_3, MgO and CaO; whereas, an overall increase with higher stratigraphic levels, together with a sharp decrease at the upper unit (granophyre)-Onaping Formation boundary, is seen for the K_2O content (Fig. 28). In drill core 70011, a sharp peak (high increase) in Na_2O (coupled with a sharp decrease in K_2O) occurs within the upper part of the lower unit ("norite") (at ~ 1820 m) and, as mentioned earlier, at the upper unit (granophyre)-Onaping Formation boundary (Fig. 28). The former corresponds to alteration, while the latter is due to a modal increase in cumulus albite, as mentioned earlier. In fact, the intensity and extent of the alteration within drill cores 52847 and 70011 limit any elaboration of the conclusions made here. A significant increase in K_2O is observed from the middle unit ("quartz gabbro") into the upper unit (granophyre). This K_2O increase is reflected by the sharp increase in modal content of granophyric and micrographic intergrowths (Fig. 5). Overall the Fe_2O_3 content decreases with higher stratigraphic levels, but a large peak is observed at the top of the middle unit ("quartz gabbro") (Fig. 28). At, or just above, this stratigraphic level, a large peak is also observed for TiO_2 and P_2O_5, and a smaller broad "peak" is observed for

MnO. Overall, the TiO_2 content increases with higher stratigraphic levels from the base to the top of the SIC; whereas, the MnO content decreases (Fig. 28). The values of Fe_2O_3, TiO_2 and P_2O_5 are higher throughout the lower unit ("norite") of drill core 52848 compared to drill cores 52847 and 70011. The peaks are, thus, subtler in drill core 52848, although reaching a higher maximum value. The Fe_2O_3, TiO_2 and MnO peaks are related to a higher abundance of titaniferous-magnetite crystals, which become a cumulus phase above the upper part of the lower unit ("norite") in all three drill cores. The lower maximum values of TiO_2 and P_2O_5 in drill cores 52847 and 70011 may result from the transformation of the cumulus titaniferous-magnetite into biotite + titanite + ilmenite pseudomorphs (see previous chapter). The P_2O_5 peak corresponds to an apatite-rich layer at the base of the transition zone. In general, apatite becomes a cumulus phase within the lower unit ("norite"), but occurs as an abundant mineral only above the middle unit ("quartz gabbro"). Higher P_2O_5 contents in drill core 52848 are explained by the presence of more abundant and larger apatite crystals throughout the drill core. The contents in CaO, Fe_2O_3 and MnO decrease significantly from the base to the top of the transition zone; whereas, the SiO_2 and K_2O contents increase.

On an AFM diagram, the SIC samples form tight groupings according to lithology and plot above, or straddle, the tholeiitic and calc-alkaline fields (Fig. 29a; similar trends are observed for the other two drill cores). These groups are even tighter on a Jensen diagram, indicating that alteration affected the Na_2O and K_2O contents of the samples (Fig. 29b). With higher stratigraphic levels, the data points are, first, enriched in alkali components (contact sublayer to lower unit ("norite") samples), then enriched in iron (lower unit ("norite") to middle

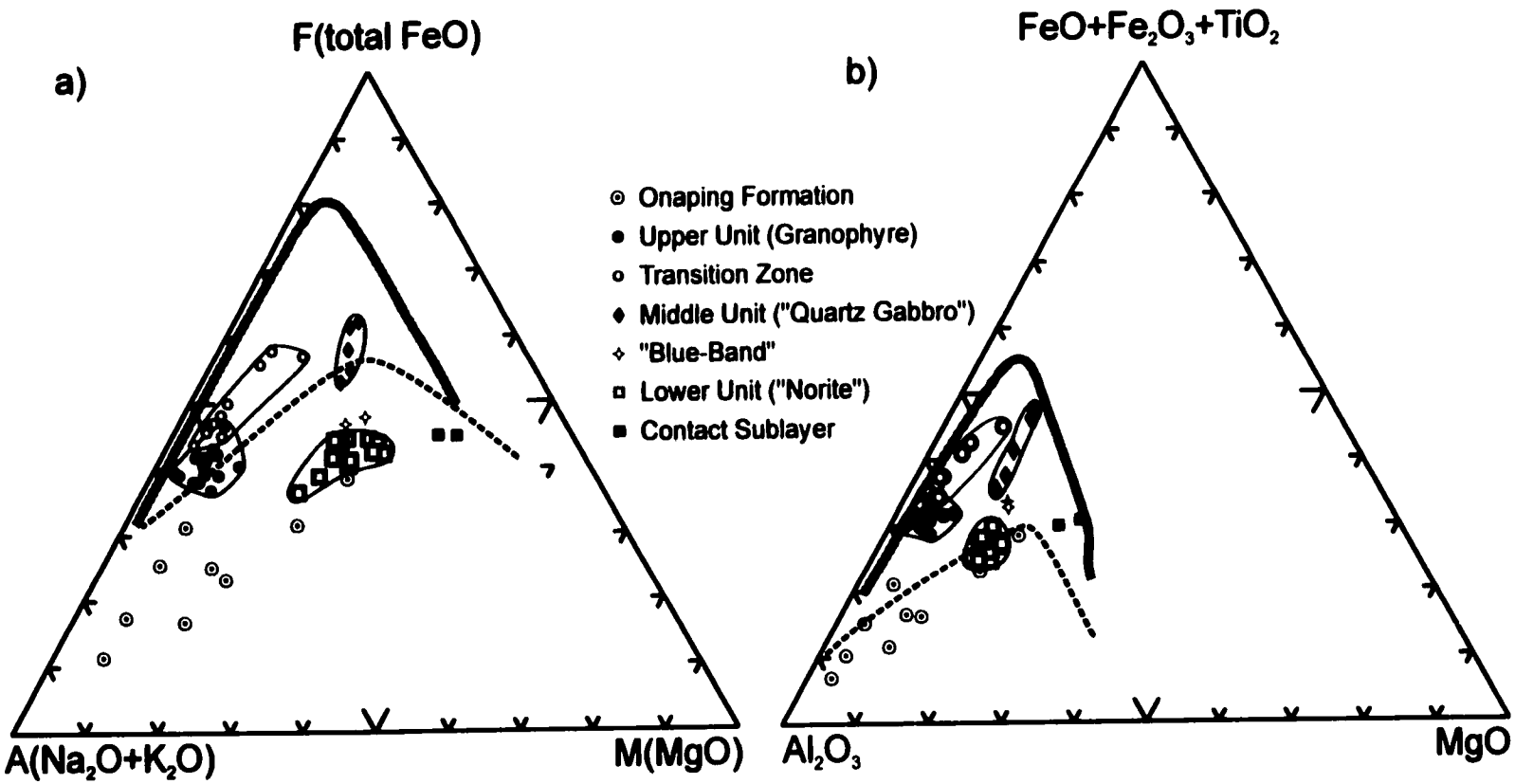

Figure 29. (a) AFM and (b) Jensen diagrams for samples of drill core 70011. Calculations done with normalized wt% data. Thick gray line = Skaergaard trend. Dashed line = division between the tholeiitic (above) and calc-alkaline (below) fields.

unit ("quartz gabbro") samples) and, finally, enriched in alkali components (middle unit ("quartz gabbro") to the top of the upper unit (granophyre)). Since the analyses are not free of a certain "contamination" by the inclusions, the contact sublayer and Onaping Formation samples may be disregarded from this series. The remaining lower unit ("norite"), middle unit ("quartz gabbro"), transition zone and upper unit (granophyre) samples of the SIC parallel the typical trend of layered igneous intrusions, such as Skaergaard, although fitting more or less inside this trend, but with less Fe enrichment (Fig. 29). This difference in the SIC is a direct effect of its bulk composition, which is more granodioritic than gabbroic (Table VI) compared to layered igneous complexes.

4.2 Trace Elements and Rare Earth Elements

Whole-rock geochemical analyses of trace elements for drill core 70011 are shown according to sample depth in Figure 30 and given in Appendix B. As for the major elements, observations are similar for all three drill cores and, thus, only drill core 70011 will be illustrated and discussed in detail. A large peak in V content is observed at the top of the middle unit ("quartz gabbro") (Fig. 30), just below the Fe_2O_3 peak discussed in the previous section. It is at this stratigraphic level that magnetite becomes an abundant cumulus phase. Within the upper part of the lower unit ("norite") through the transition zone, a broad Sc peak is observed (Fig. 30) and relates to the higher modal abundance of amphibole pseudomorphs after augite crystals (qualitative microprobe energy dispersive (EDS) analyses indicated that they contain Sc). The contact sublayer is greatly enriched in Cr, Ni, Zn, Co, S and Pb, compared to the rest of the SIC

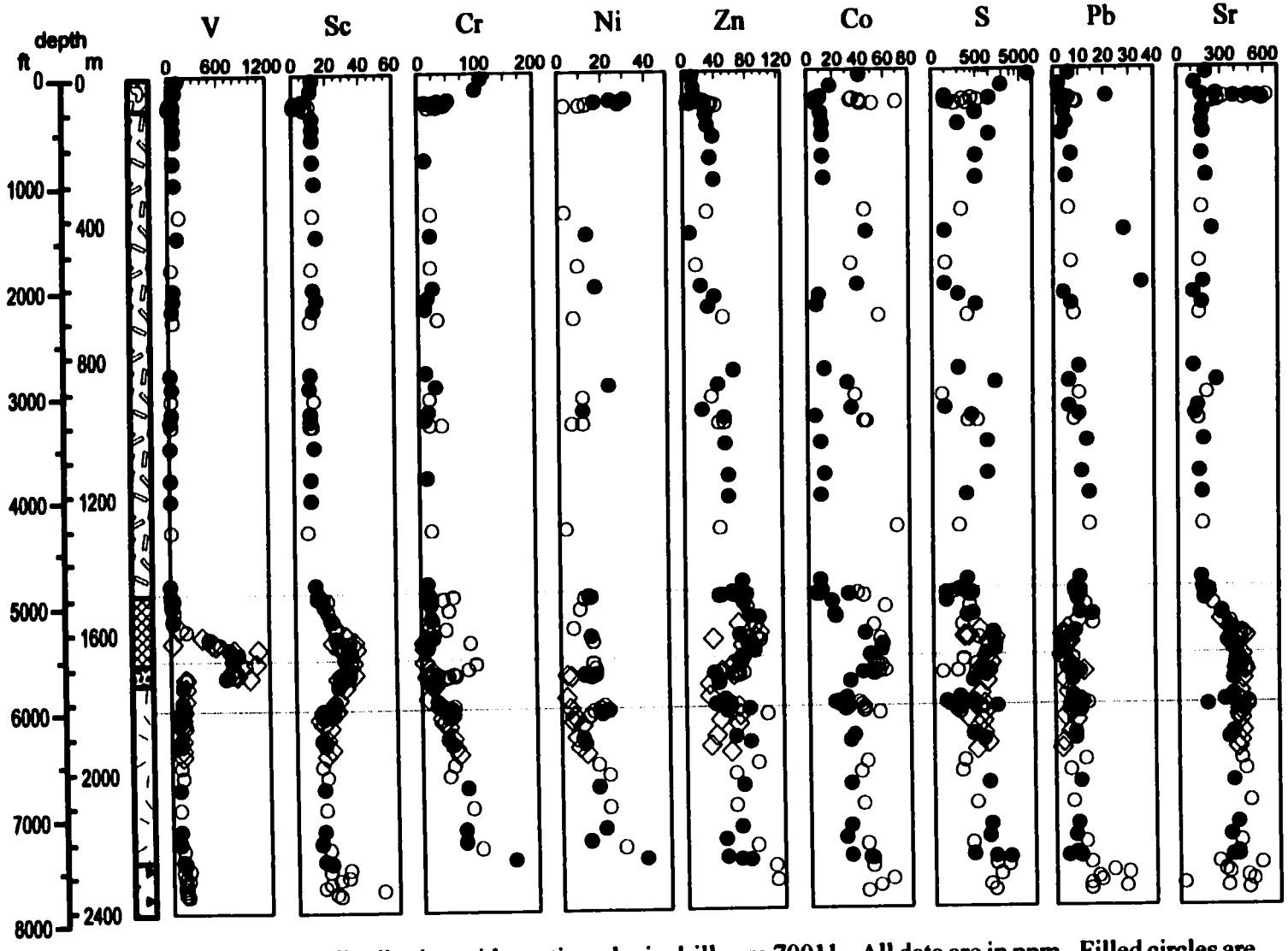

Figure 30. Trace elements distribution with stratigraphy in drill core 70011. All data are in ppm. Filled circles are normalized data from this work; open circles are normalized data from Ostermann (1996); diamonds are data from McPherson Coombes (1996). Lithology patterns as in Figure 3. See text for details.

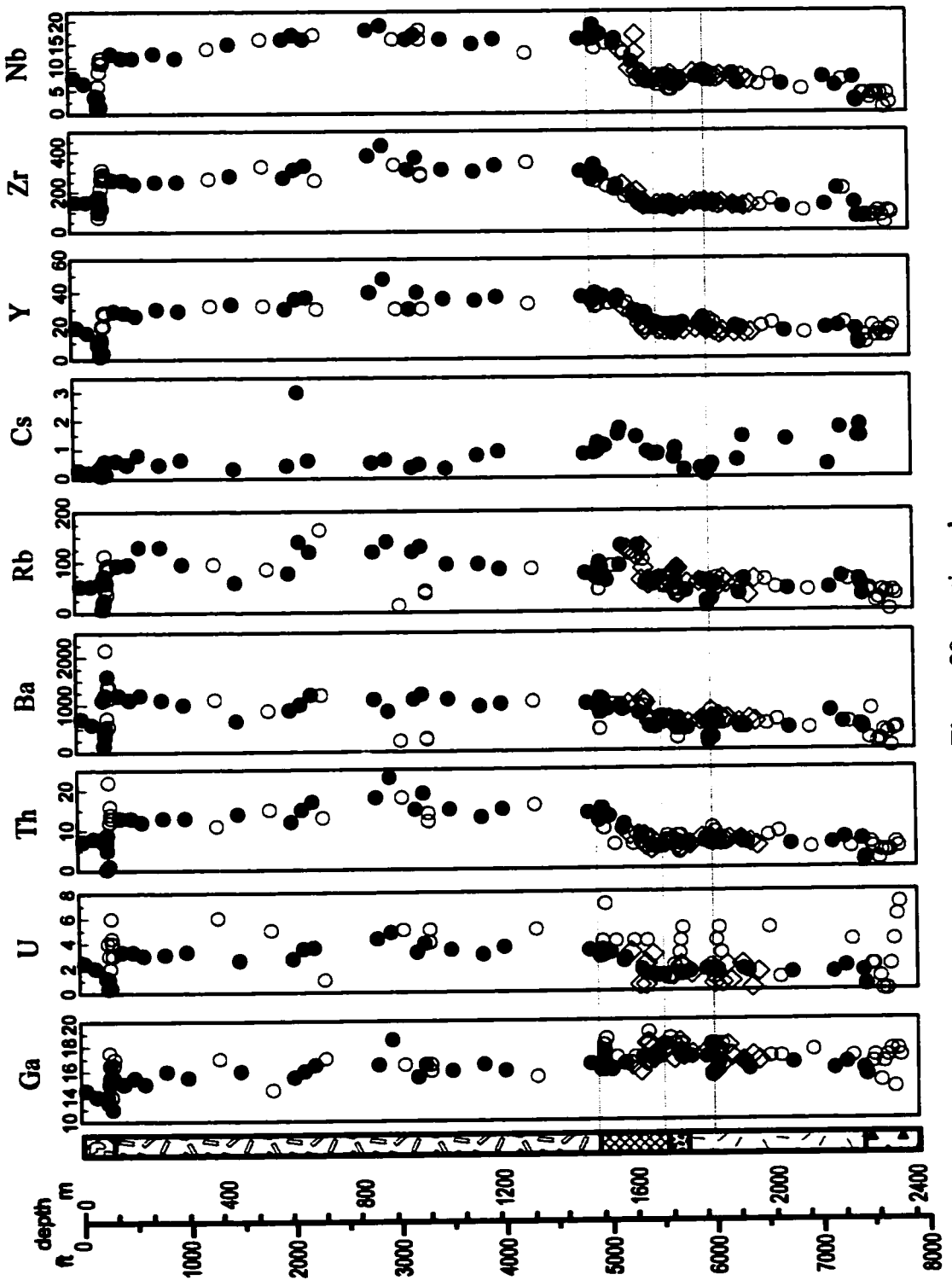

Figure 30. continued.

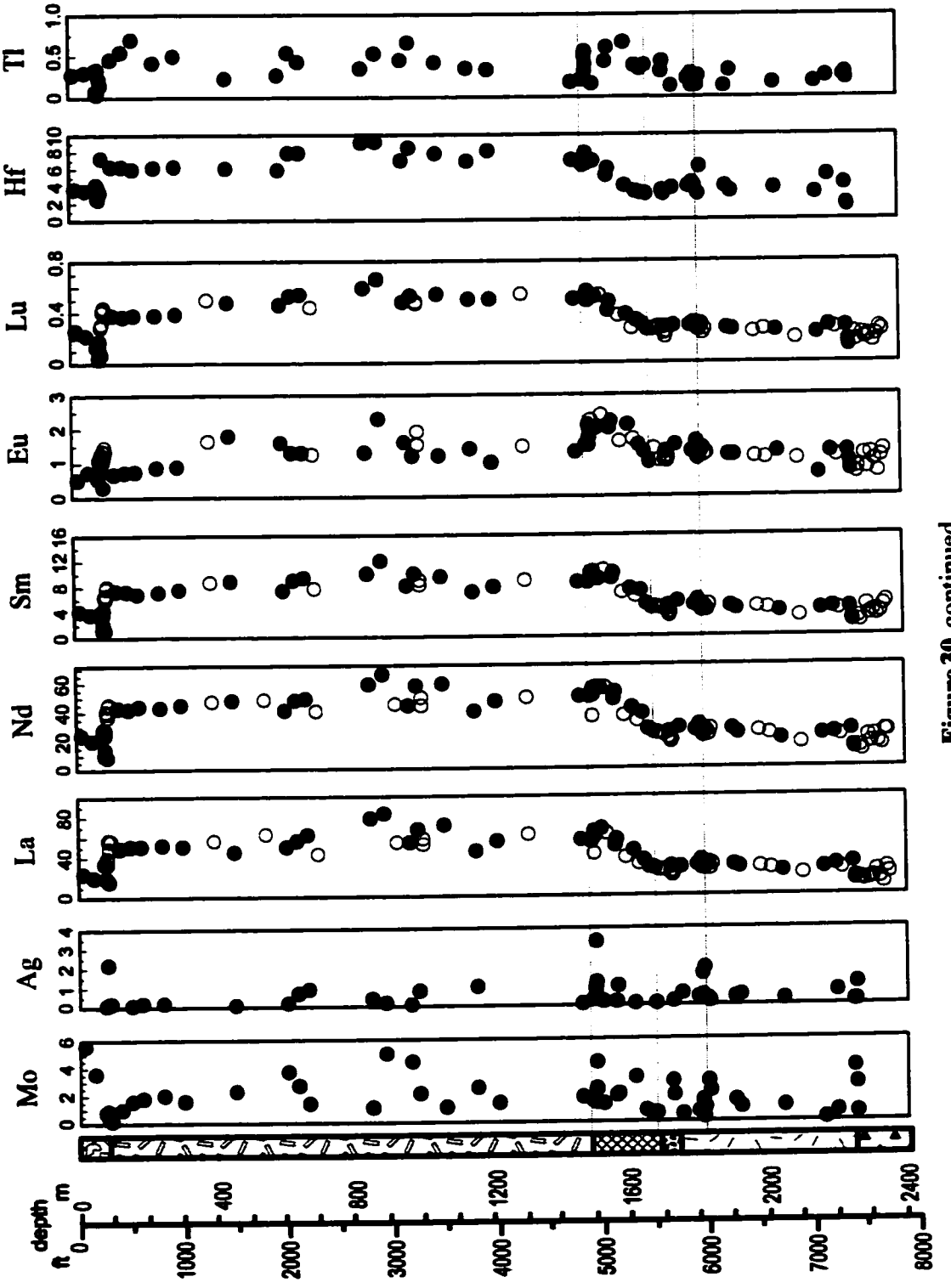

Figure 30. continued.

(Fig. 30), and this enrichment correlates with the high content of various sulfides and Cu-Ni ores within the contact sublayer.

Because of this enrichment, the variations from the base of the lower unit ("norite") to the top of the upper unit (granophyre) are subdued. In order to better illustrate these variations, the scales of Cr, Ni, Zn, Co, S and Pb were adjusted in Figure 30, thus removing some or all of the data points for the contact sublayer. The Cr and Ni contents generally decrease from the base to the top of the SIC. In the upper unit (granophyre), the contents of Zn and Co are depleted relative to the transition zone, middle unit ("quartz gabbro") and contact sublayer. The distribution of S is heterogeneous in drill cores 52847 and 70011, but more regular in drill core 52848. The highest S values are recorded for the lower unit ("norite") and middle unit ("quartz gabbro") samples, and they show little variation with changes in stratigraphic levels (Fig. 30). A gradual, but sharp, decrease in S values is observed from the base of the transition zone to the upper unit (granophyre) (Fig. 30). The lowest S values are recorded in the upper unit (granophyre) samples, and they show little variation with changes in stratigraphic levels (Fig. 30). There appears to be little variation in the Pb content throughout the SIC, excluding the contact sublayer and a few samples in the upper unit (granophyre) or altered samples.

An overall decrease with higher stratigraphic levels is observed for Sr with a more rapid decrease within the transition zone and a sharp and abrupt variation at the upper unit (granophyre) - Onaping Formation boundary. No specific or simple variation is observed for Ga and U throughout the SIC. The lower unit ("norite") and middle unit ("quartz gabbro") have more or less constant contents of Th, Ba, Rb, Y, Zr, Nb, and Hf. A sharp increase, with or

without a peak, in the content of these seven trace elements is observed with higher stratigraphic levels through the transition zone, and a sharp decrease is observed at the upper unit (granophyre) - Onaping Formation boundary. A peak is observed at the base of the transition zone for Rb, Cs and Tl. Overall, from the base to the top of the upper unit (granophyre), Th, Cs, Y, Zr, Nb, and Hf slightly decrease in content; whereas Ba, Rb, and Tl show a slight increase (Fig. 30). The Rb and Tl contents are actually quite variable from the upper part of the lower unit ("norite") and above, contrary to other trace elements (Fig. 30); an indication of their mobility during metamorphism.

No specific variation is observed for the Cu, Mo, Ag, Sn, Ta and Bi contents throughout the drill cores (as exemplified by Mo and Ag in Fig. 30), except that the Cu content is high in both the contact sublayer and Onaping Formation. The distribution of REEs (as exemplified by La, Nd, Sm, Lu, and except for Eu) in the SIC closely parallel one another. The lowest values occur in the contact sublayer and at the base of the Onaping Formation; whereas, the highest values occur in the upper unit (granophyre) (Fig. 30). In the lower unit ("norite") and middle unit ("quartz gabbro"), the REE content remains approximately constant with higher stratigraphic levels. A sudden jump in REE content occurs at the transition zone (Fig. 30) and is related to an apatite-rich layer occurring at this level; whereas, the high value of REEs content in the upper unit (granophyre) results from extreme fractionation of the SIC melt. In general, samples from drill core 52848 have higher REE contents. This is related to their greater abundance of apatite crystals, which are usually larger than in the other cores and in which REEs are highly compatible. At the top of the transition zone, a relatively broad and small "peak" is observed for

La, Ce, Pr, Nd, Sm, Eu, Gd and Tb (Fig. 30). A slight overall decrease in trace elements with higher stratigraphic levels occurs from the base to the top of the upper unit (granophyre).

Spider diagrams, as exemplified by samples of drill core 70011 (Fig. 31), show the remarkable similarity of REE patterns for samples of a given SIC lithology and also great similarities between upper unit (granophyre) and transition zone samples and middle unit ("quartz gabbro") and lower unit ("norite") samples. Note that some of the Onaping Formation samples straddle the upper unit (granophyre) data, but their REE ratio is highly variable, unlike the SIC lithologies. Chondritic ratios of REEs are basically the same for all three drill cores, except that the middle unit ("quartz gabbro") samples of drill core 52848 have slightly higher ratios (comparable to the transition zone values) than in the other two drill cores.

With higher stratigraphic levels, the REE content of the different lithologies increases (disregarding the Onaping Formation), keeping an overall pattern of enriched LREE and depleted HREE (Fig. 31). Moreover, the Eu anomaly also increases with higher stratigraphic levels. These increases are, however, not consistent at the scale of individual samples, *i.e.*, the REE content does not necessarily increase with each overlying sample. For example, the greatest Eu anomaly is observed in the plagioclase-rich granophyre (towards the top of the upper unit (granophyre), between the depths of 120 and 350 m in drill core 70011), but it is overlain by samples with smaller Eu anomalies before an increasing anomaly is again observed, within the Onaping Formation. In drill core 70011, the highest values of REEs are recorded in a sample from the middle part of the upper unit (granophyre) (at a depth of 893 m). Positive Eu anomalies are only rarely observed and occur mainly in the contact sublayer. These same observations are

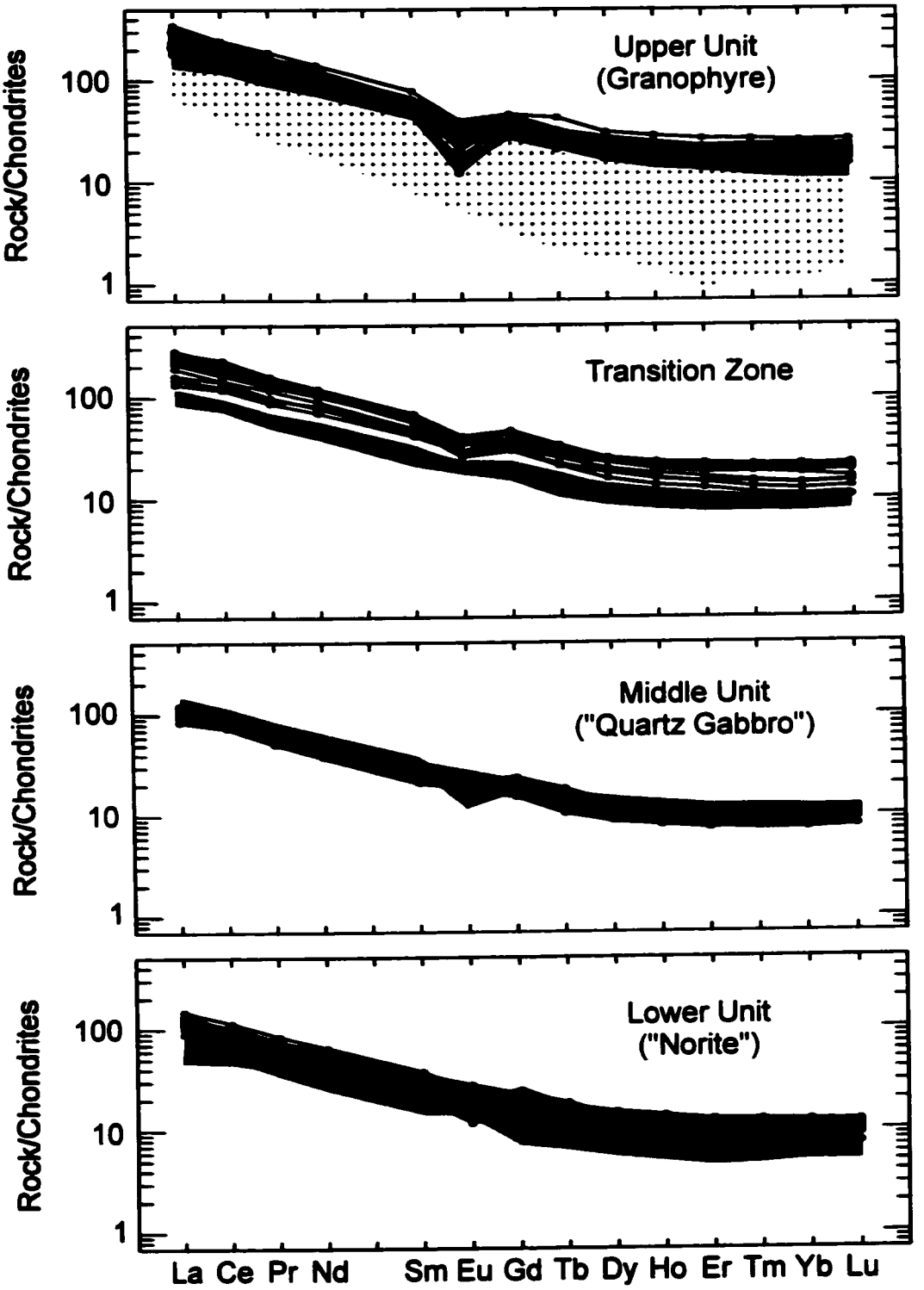

Figure 31. Spider diagrams of REEs versus ratio of rock samples normalized to chondrite (Sun and McDonough, 1989) for the SIC lithologies in drill core 70011. Shaded areas = underlying lithology (*cf.*, Fig. 3); dotted area = base of the Onaping Fm.

made in drill cores 52847 and 52848. Small and mixed positive and negative Eu anomalies are observed in the lower unit ("norite") and middle unit ("quartz gabbro") samples. This mixture of Eu anomalies may be due to alteration or an inheritance from the parent material, *i.e.*, the country rocks. Fowler and Doig (1983) have interpreted negative Eu anomalies as due to albitization of plagioclase or hydrothermal alteration. Only a few of the negative Eu anomalies occur in SIC samples that are unequivocally altered. The alternative explanation of the observed Eu anomalies is the inheritance from the country rocks. A strong positive Eu anomaly is recorded for Archean migmatite samples, a small Eu anomaly is recorded for Archean granite, Levack gneiss and Nipissing diabase samples, and a small to strong negative Eu anomaly is recorded for Huronian metasediments, metavolcanics and granite samples (according to the data of Chai and Eckstrand, 1994). Kuo and Crocket (1979) interpreted the overall decrease in total REE contents and increase in negative Eu anomaly within the upper unit (granophyre) as an increasing contribution of REEs from country rocks, through assimilation.

4.3 Pearce Element Ratios (PER)

Pearce element ratio (PER) diagrams were designed to overcome the closure problems or constant sum of geochemical analyses (*cf.*, Harker diagrams; Chayes, 1960; Pearce, 1968). Combinations of Pearce element ratios depend on knowledge of the stoichiometry of the mineral species inferred to be involved in the crystallization and fractionation of the magma (Russell and Stanley, 1990a,b). By plotting ratios of interest for a sample suite and determining the equation for the line of best fit by regression analysis, hypotheses may be tested regarding the

differentiation process(es) responsible for the chemical variation. The slope of the regression line is used to test suspected differentiation mechanisms. In the case of the SIC, based on the petrographical observations, the sample suites were tested for plagioclase, clinopyroxene, orthopyroxene, magnetite, ilmenite and apatite fractionation, respectively. Note that PER diagrams, in which the regression line passes through the origin, are considered invalid, since this may be an indication that the denominator element is not conserved. Thus, the intercept must differ from zero, given the propagated analytical uncertainty associated with the intercept (Pearce, 1987).

Pearce element ratios present data in comparison to a compositional variable that can be considered constant in the system under consideration. In order to do so, a conserved element, *i.e.*, one present in a constant amount through the evolution of the system, is used as the denominator in the ratio (Stanley, 1993). Bradshaw (1992) argues that Zr is the preferred choice for this denominator, as Zr remains incompatible in magmatic systems up to ≈68 wt% SiO_2. As the SiO_2 content of the SIC samples range, in general, from 51 to 70 wt% (Appendix B), Zr was used as the denominator in the PER. Compositional comparison is made in terms of material added or removed during crystallization, and the PER approach provides a method of monitoring the proportions of material added or removed.

Here, PER are first used to test whether the chemical data studied indicate that the samples are cogenetic. If the elements used in the ratios are conserved and the rocks are cogenetic, the ratios will be identical. Then, PER are used to identify the process responsible for the chemical variation. Elements used in the calculations of the PER are given in Table VII and

Table VI: Minerals, their compositions, and elements used in constructing Pearce Element ratios (PER) shown in Figure 32.

Mineral	Abbreviation	Stoichiometric composition	Elements used in Figure 32
Plagioclase Anorthite Albite	Pl An Ab	$CaAl_2Si_2O_8$ $NaAlSi_3O_8$	molar plagioclase = $\Delta Pl = \frac{\Delta Al_T}{2} + \frac{\Delta Na_T}{2} - \frac{\Delta K_T}{2}$ molar Si in plagioclase = $\Delta Si_{Pl} = \Delta Si_T - \Delta Si_{Or} - \Delta Si_{Au} - \Delta Si_{Hy} = \Delta Si_T - 2\Delta K_T + \Delta Al_T - 0.5\Delta Na_T - \Delta Mg_T - \Delta Fe_T^{+2} + \Delta Fe_T^{+3} + \Delta Ti_T$
Alkali feldspar	Or	$KAlSi_3O_8$	
Augite Diopside Hedenbergite	Au cpx (di) cpx (hd)	$CaMgSi_2O_6$ $CaFeSi_2O_6$	molar clinopyroxene = $\Delta Au = \Delta Ca_T - \Delta Ca_{An} = \Delta Ca_T - \Delta An = \Delta Ca_T - \frac{\Delta Al_T}{2} + \frac{\Delta Na_T}{2} - \frac{\Delta K_T}{2}$ molar Si in clinopyroxene = $\Delta Si_{cpx} = \Delta Si_T - \Delta Si_{Pl} - \Delta Si_{Or} - \Delta Si_{Hy} = \Delta Si_T - \Delta Na_T - \Delta K_T - \Delta Mg_T + \Delta Ca_T - \Delta Fe_T^{+2} + 0.5\Delta Fe_T^{+3} + \Delta Ti_T$
Hypersthene Enstatite Ferrosilite	Hy opx (en) opx (fs)	$MgSiO_3$ $FeSiO_3$	
Fe-Ti oxides Magnetite Ilmenite	 mt ilm	 $Fe^{+2}Fe_2^{+3}O_4$ $Fe^{+2}TiO_3$	
Apatite	ap	$Ca_5(PO_4)_3(F,OH,Cl)$	

$\Delta Si_T = \Delta Si_{An} + \Delta Si_{Ab} + \Delta Si_{Or} + \Delta Si_{Au} + \Delta Si_{Hy}$

$\Delta Al_T = \Delta Al_{An} + \Delta Al_{Ab} + \Delta Al_{Or} = \Delta Al_{An} + \Delta Na_T + \Delta K_T$

$\Delta Ca_T = \Delta Ca_{An} + \Delta Ca_{cpx} + \Delta Ca_{ap}$

$\Delta Na_T = \Delta Na_{Ab} = \Delta Ab$

$\Delta K_T = \Delta K_{Or} = \Delta Or$

$\Delta Mg_T = \Delta Mg_{cpx} + \Delta Mg_{opx} = \Delta Au + \Delta Hy$

$\Delta Fe_T^{+2} = \Delta Fe_{cpx}^{+2} + \Delta Fe_{opx}^{+2} + \Delta Fe_{mt}^{+2} + \Delta Fe_{ilm}^{+2}$

$\Delta Fe_T^{+3} = 0.5\Delta Fe_{mt}^{+3} = \Delta mt$

$\Delta Ti_T = \Delta Ti_{ilm}$

results are shown in Figure 32 for samples from all three drill cores studied.

When using ratios with conserved elements in a PER diagram, as in Figure 32a, all samples of the SIC (except altered ones and some contact sublayer samples) plot as a cluster within the error limits. Note that most of the Onaping Formation samples do not conform to this trend. Figure 32a indicates that the SIC samples are cogenetic. Figures 32b and 32c show PER diagrams constructed (so that the slope = 1) to test plagioclase and clinopyroxene fractionation, respectively. The slopes of the regression lines are close to 1 and suggest that the trend observed is due to plagioclase and clinopyroxene fractionation. No evidence of the effects of orthopyroxene, magnetite, ilmenite or apatite fractionation were observed. Figure 32d was constructed to test the relative influence between plagioclase and clinopyroxene fractionation on the SIC trend. Since the regression line has a slope less than 1, it indicates a more important role for clinopyroxene in the crystallization of the SIC, as compared to plagioclase. A cluster of eight lower unit ("norite") samples from drill core 70011 (enclosed in a dashed-line, Fig. 32d) plots just above this trend and these have a slope close to 1, suggesting that in these plagioclase- and augite-rich rocks, both minerals played an equally important role in their crystallization.

4.4 Simulations Using MELTS

The software package MELTS (Ghiorso and Sack, 1995) was used to estimate the initial crystallization temperatures of various liquid compositions tested as the SIC starting composition. The mineral composition, modal proportions, and fractional crystallization paths of these liquid compositions were simulated using MELTS at given temperatures, pressures and

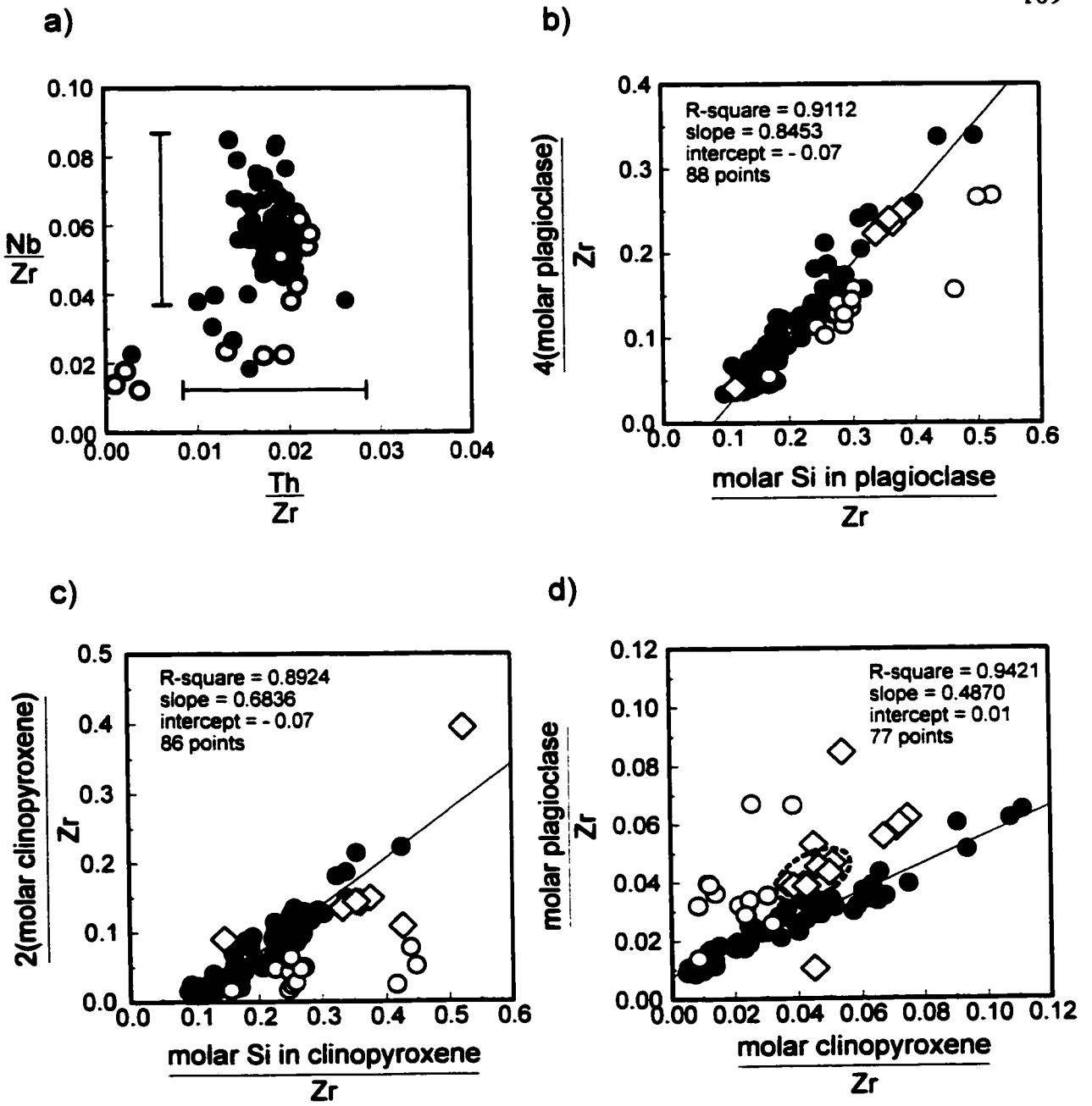

Figure 32. PER diagrams for samples from the three drill cores studied and testing: **(a)** cogenesis, **(b)** plagioclase fractionation, **(c)** clinopyroxene fractionation, and **(d)** the combination of plagioclase (y-axis) and clinopyroxene (x-axis) fractionations. In (a), the error brackets are calculated by propagation of error and demonstrate that the variation within the suite is less than the analytical error. Therefore Nb, Th and Zr may be considered as conserved elements. Open circles = Onaping Fm; filled circles = SIC lithologies; diamonds = samples disregarded from the best fit line, because they are highly altered. See Table VI for definition of denominators in (b), (c) and (d), and text for details.

over a range of oxygen fugacities.

A series of simulations, using the average composition calculated from drill core 70011 (Table VIII), were run from 1300 °C to as low as 700 °C, at various pressures and under various oxygen buffer conditions, in order to reproduce the trend observed on the AFM diagram (Fig. 29a) and/or the main mineralogical crystallization sequence observed for the SIC. The results yield no perfect match of the actual AFM trend for the fractional crystallization simulations. The closest match is obtained under conditions of the quartz-fayalite-magnetite (QFM) buffer at 0.12 Gpa, although the portion of the lower unit ("norite") sample suite was not reproduced (Fig. 33). Good matches to the mineralogical crystallization sequence were obtained under these same conditions, but the An content observed in the SIC plagioclase crystals of the contact sublayer and the lower unit ("norite") were not reproduced (Table IX). Also, quartz crystallizes before apatite in the simulated sequence; whereas, in the crystallization sequence observed in the SIC, apatite crystallizes before quartz (Table IX) as apatite is a cumulus mineral in the lower unit ("norite") and middle unit ("quartz gabbro").

To test the hypothesis of Lightfoot *et al.* (1997a), that a small volume (< 20 vol.%) of mantle-derived picritic magma was assimilated by the original impact melt, another series of simulations were carried out. In these simulations, a mafic liquid (Table VIII), at a temperature of 1300°C, was first assimilated by the average SIC composition of drill core 70011, at a temperature of 1400°C. Then, fractional crystallization of the mixture was simulated from 1300°C to 700°C, under various pressures and oxygen buffer conditions. Three volumes of mafic liquid were tested: 5, 10 and 20 vol.%. The mixture of 10 vol.% of the mafic liquid

Table VIII: Starting liquid compositions used in MELTS simulations under the QFM buffer conditions and at 0.12 GPa.

	SIC average from drill core 70011*	Mafic liquid	SIC + 10 vol.% assimilated mafic liquid	SIC + 20 vol.% assimilated mafic liquid	Manicouagan average composition[1]	Average lower unit ("norite")[2]
SiO_2	64.73	40.0	62.02	61.13	58.15	58.94
TiO_2	0.81	-	0.72	0.69	0.77	0.57
Al_2O_3	13.82	3.0	12.63	12.45	16.62	16.20
Fe_2O_3	0.99	-	0.98	0.93	0.97	1.02
FeO	5.58	7.0	5.69	5.40	5.04	5.72
MnO	0.09	-	0.08	0.08	0.11	0.11
MgO	2.13	48.0	7.23	8.84	3.52	4.16
CaO	3.80	2.0	3.60	3.67	5.96	6.48
Na_2O	3.42	-	3.04	2.92	3.84	3.46
K_2O	2.88	-	2.56	2.46	3.05	1.53
P_2O_5	0.18	-	0.16	0.15	0.22	0.13
H_2O	1.49	-	1.33	1.27	1.75	1.66
Total	99.92	100.0	100.04	99.99	100.00	99.98
Liquidus	1054.10°C	-	~ 1280°C	~ 1330°C	1108.40°C	1116.21°C
Viscosity @ liquidus	4.71 log 10 poise	-	2.70 log 10 poise	2.29 log 10 poise	3.53 log 10 poise	3.55 log 10 poise

Notes: All data in wt%.
* = using the average composition calculated in Table VIa.
[1] = using the average of 27 analyses from Floran *et al.*, 1978.
[2] = using the average lower unit composition calculated in Table VIa. + 5 % contact sublayer of Table VIa.

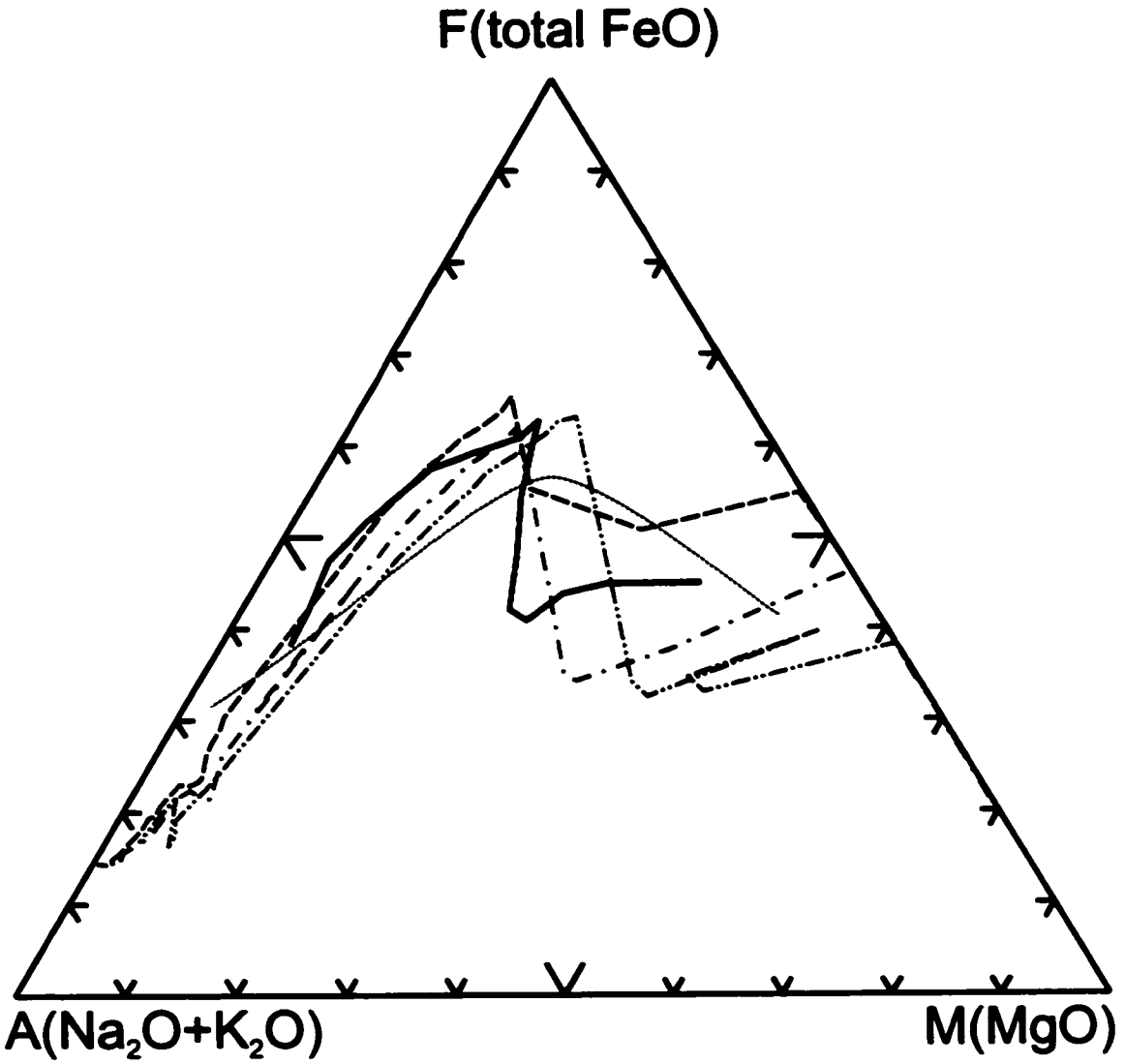

Figure 33. AFM diagram showing the observed trend for drill core 70011 of the SIC (gray line; see also Fig. 29a) and the calculated trend from MELTS using various starting liquid compositions (Table VIII) under fractional crystallization and QFM buffer conditions at a pressure of 0.12 GPa. The pink dashed line is for the average composition of drill core 70011. The orange single dot dashed line is for the average composition of drill core 70011 mixed with 10 vol.% of a mafic liquid. The blue double dots dashed line is for the average composition of the Manicouagan impact melt sheet. The boundary between tholeiitic (above) and calc-alkaline (below) fields is shown for reference (thin dashed line). See text for details.

Table IX: Mineral assemblages from MELTS simulations under QFM buffer conditions and at 0.12 GPa compared to that observed in the SIC.

SIC 70011 observed	MELTS average Manicouagan melt	MELTS SIC 70011	MELTS SIC + 20% mafic liq.	MELTS "norite"
- ol (Fo_{86-72})*	- ol (Fo_{76})	- ol (Fo_{61})	- ol (Fo_{88})	
- ol (Fo_{86-72}) ± opx ± plag (An_{60-80}) ± cpx*	- ol (Fo_{72}) + plag (An_{66})		- ol (Fo_{88}) + opx	
		- opx	- opx	- opx
- opx + plag (An_{60-70})	- cpx + plag (An_{60})	- cpx + plag (An_{47})	- opx + plag (An_{54})	- opx + plag (An_{68})
- cpx + opx + plag (An_{50-60})	- cpx + opx + plag (An_{56})			- cpx + opx + plag (An_{67})
				- 2 cpx + plag (An_{64})
				- 2 cpx + plag (An_{56}) + mt-ulv
- cpx + plag (An_{40-50}) + mt-ulv	- cpx + opx + plag (An_{54}) + mt-ulv	- cpx + plag (An_{45}) + mt-ulv	- opx + plag (An_{48}) + ulv-mt	- cpx + opx + plag (An_{50}) + mt-ulv
- cpx + plag (An_{30-40}) + mt-ulv + ap + water	- cpx + plag (An_{33}) + Kspar (Ab_{33}) + mt-ulv	- opx + plag (An_{42}) + mt-ulv	- opx + cpx + plag (An_{32}) + ulv-mt	- opx + plag (An_{30}) + mt-ulv + water
- cpx + plag (An_{20-30}) + mt-ulv + Kspar (Ab_{30-35}) + ap + H_2O	- cpx + opx + plag (An_{30}) + Kspar (Ab_{33}) + mt-ulv + water	- opx + plag (An_{28}) + Kspar (Ab_{35}) + mt-ulv	- cpx + plag (An_{30}) + Kspar (Ab_{34}) + ulv-mt + ilm	- opx + cpx + plag (An_{26}) + mt-ulv + water
- cpx + plag (An_{20-30}) + Kspar (Ab_{30-35}) + mt-ulv + ilm + ap + water	- cpx + opx + plag (An_{28}) + Kspar (Ab_{34}) + mt-ulv + ilm + water	- opx + cpx + plag (An_{28}) + Kspar (Ab_{32}) + mt-ulv + ilm	- cpx + opx + plag (An_{30}) + Kspar (Ab_{34}) + ulv-mt + ilm	- opx + cpx + plag (An_{25}) + Kspar (Ab_{34}) + mt-ulv + water
		- cpx + plag (An_{28}) + Kspar (Ab_{32}) + mt-ulv + ilm	- cpx + opx + plag (An_{27}) + Kspar (Ab_{32}) + mt-ulv + ilm + water	- cpx + plag (An_{22}) + Kspar (Ab_{34}) + mt-ulv + water
- cpx + plag (An_{20-30}) + mt-ulv + ilm + ap + qtz + san + water		- cpx + plag (An_{26}) + Kspar (Ab_{29}) + qtz + ilm	- cpx + plag (An_{22}) + Kspar (Ab_{31}) + qtz + mt-ulv + ilm + water	- cpx + plag (An_{19}) + Kspar (Ab_{34}) + qtz + mt-ulv + ilm + water
	- cpx + plag (An_{16}) + Kspar (Ab_{35}) + mt-ulv + ilm + ap + water	- cpx + plag (An_{27}) + Kspar (Ab_{28}) + qtz + ilm + ap + water	- cpx + plag (An_{20}) + Kspar (Ab_{32}) + qtz + ilm + ap + water + L	- cpx + plag (An_{17}) + Kspar (Ab_{34}) + qtz + ilm + water + L
	- cpx + plag (An_{15}) + Kspar (Ab_{36}) + qtz + mt-ulv + ilm + ap + water + L	- titanite + cpx + plag (An_{26}) + Kspar (Ab_{28}) + qtz + ap + water + L		

Notes: * = In inclusions of the contact sublayer
ol = olivine; opx = orthopyroxene; plag = plagioclase; cpx = clinopyroxene; Kspar = alkali feldspar; mt-ulv = magnetite-ulvospinel; ilm = ilmenite; ap = apatite; ulv-mt = ulvospinel-magnetite; qtz = quartz; san = sanidine; L = liquid.

assimilated within the SIC average bulk composition (Table VIII) gives the best match to the AFM trend under QFM buffer conditions at 0.12 GPa. In this case, the portion of the AFM trend represented by the lower unit is somewhat reproduced, but the overall simulated AFM trend slightly departs to the right of the actual SIC trend (Fig. 33). The mixture of 20 vol.% of the mafic liquid assimilated within the SIC average bulk composition (Table VIII) gives the best matches to the observed mineralogical crystallization sequence of the SIC. In this case, the An content observed in the SIC plagioclase crystals of the contact sublayer and lower unit ("norite") is not reproduced, and quartz crystallizes prior to apatite; whereas, in the SIC rock suite, apatite is observed to crystallize before quartz (Table IX).

The fact that the QFM buffer has to be used to reproduce the overall AFM trend and mineralogical sequence of the SIC is in general agreement with the data of Frost and Lindsley (1991), who indicate that the lower unit ("norite") and middle unit ("quartz gabbro") crystallized under fO_2 conditions of the QFM to QFM+2 buffers. The fact that simulation runs performed at a pressure of 0.12 GPa, which corresponds to a depth of 4 km, best approximate the observations is in agreement with an initial burial depth of ~ 2 km to the top of the SIC added to ~ 2 km to reach the top of the lower unit ("norite"). The fact that the portion of the AFM trend represented by the lower unit ("norite") of drill core 70011 is only (somewhat) reproduced, when the SIC average bulk composition is mixed with a mafic liquid, suggests that the granodioritic SIC average bulk composition used in the simulations does not correspond to the starting composition of the SIC.

Respective proportions of each SIC lithology vary between North and South Ranges (*cf.* Lightfoot *et al.*, 1997a; Naldrett and Hewins, 1984). The upper unit (granophyre) represents up to ~ 60% of the North Range; whereas, it represents only ~ 30% of the South Range. The transition zone represents about 10% of the North Range and may represent a greater proportion in the South Range. The middle unit ("quartz gabbro") represents less than 10% of the North Range, but represents up to 15% of the South Range. Finally, the lower unit ("norite") represents about 25% of the North Range and may represent up to 60% of the South Range. The South Range is, thus, more mafic than the North Range. Consequently, a calculated average composition of the SIC, using solely North Range data, will not necessarily reflect the overall starting composition of the SIC. It is concluded from the previous simulations that the starting composition of the SIC was more likely andesitic. Thus, other series of simulations were run under similar conditions as specified above using the average andesitic composition of the lower unit ("norite") from drill core 70011, the Offset dykes (Lightfoot *et al.*, 1997a) or the Manicouagan impact melt sheet (Table VIII). The choice of the Manicouagan impact melt sheet, although it is not differentiated, is based on the facts that it has an andesitic average bulk composition and the target rocks of the Manicouagan impact structure (*e.g.*, Grieve and Floran, 1978) are similar to those at Sudbury.

The simulation runs using the average composition of the lower unit ("norite") do not yield a closer AFM trend than for other simulations, but the mineralogical crystallization sequences obtained are good (Table IX). This starting liquid composition under QFM buffer conditions at a pressure of 0.12 GPa reproduce the An content of plagioclase crystals in the SIC

and permits water to exsolve relatively early in the crystallization sequence, but it does not crystallize apatite or olivine.

The simulation runs using a starting liquid composition equivalent to the most mafic Offset Dyke (Creighton Mine Offset; Lightfoot *et al.*, 1997a) and even the most felsic Offset Dyke (Manchester Offset; Lightfoot *et al.*, 1997a) do not yield particularly good or better matches to the observed AFM trend or mineralogical crystallization sequence of the SIC.

The simulation run using the average Manicouagan composition as a starting liquid under QFM buffer conditions at 0.12 GPa is in good agreement with the observations at Sudbury, both for the AFM trend and mineralogical crystallization sequence. This simulation yields a mineralogical crystallization sequence in perfect agreement with the observed crystallization sequence of the Manicouagan impact melt sheet (*cf.*, Floran *et al.*, 1978). In addition, this simulation yields apatite on the solidus prior to quartz and exsolves water relatively early compared to simulation runs using the SIC and SIC + mafic liquid compositions (Table IX).

The trends generated by the simulations on an AFM diagram show an early and late crystallization stages, which are not really observed in the SIC rock suite studied (Fig. 33). Some of the Onaping Formation samples match this late crystallization stage (compare Fig. 29a and Fig. 33), suggesting that the residual melt of the SIC mixed with the overlying breccia matrix. Some of the contact sublayer inclusions could correspond to the early crystallization stage.

The results from the MELTS software program suggest that the initial liquid composition of the SIC was andesitic, *i.e.*, less siliceous with silica content between 58 and 62 wt% and slightly more aluminous, calcic and phosphatic than the calculated average bulk composition

from the North Range alone (Table VIa). Moreover, the results from MELTS suggest that crystallization occurred under conditions close to the QFM buffer and at a pressure ranging from 0.08 to 0.12 GPa.

4.5 Summary

In the North Range, the SIC has an average bulk composition that is granodioritic (Table V). All SIC lithologies have quartz, orthoclase, albite, anorthite, hypersthene, magnetite, ilmenite and apatite in their CIPW norm calculations. The normative corundum occurring in samples of the upper unit (granophyre) and lower unit ("norite") is indicative of an aluminous crustal signature. Specific combinations of CIPW norm minerals can be used to distinguish between the different lithologies of the SIC (*cf.*, Table VI; Fig. 27).

All major and trace elements and REEs vary gradually through the lithologies of the SIC. Minor discrepancies in their distributions are observed at the upper unit (granophyre) - Onaping Formation boundary (caused by abundant inclusions and primary albite crystals), through the transition zone and middle unit ("quartz gabbro") (caused mainly by Fe-Ti oxides and apatite crystallization), and at specific depths (caused by alteration). A striking feature of the upper unit (granophyre) is the overall decrease in REE content and increase in the Eu anomaly observed with higher stratigraphic levels from its middle to its upper part.

The lower unit ("norite"), middle unit ("quartz gabbro"), transition zone and upper unit (granophyre) samples of the SIC on a Jensen diagram parallel the Skaergaard trend of FeO + Fe_2O_3 + TiO_2 enrichment, followed by an Al_2O_3 enrichment with higher stratigraphic levels.

Spider diagrams show the constant and gradual increasing ratio of REE patterns between SIC lithologies, with an overall pattern of enriched LREE and depleted HREE. Construction of PER diagrams indicate that the crystallization of the SIC is related to the fractionation of both plagioclase and clinopyroxene. Pearce element ratio diagrams and chemical trends demonstrate that the SIC lithologies are cogenetic and continuous, and that the Onaping Formation samples have a distinctly different trend.

Avermann and Brockmeyer (1992), who carried out a detailed petrographical and geochemical study of samples from the Onaping Formation, composed of impact breccias, and top of the upper unit (granophyre), concluded that the basal member of the Onaping Formation was in fact part of the SIC. However, the samples of the base of the Onaping Formation (*i.e.*, the basal member) from this study are geochemically distinct from the SIC lithologies, and on various diagrams these samples plot away from those of the SIC. It is, thus, concluded that the basal member of the Onaping Formation is not part of the SIC.

No perfect match of the AFM trend and mineralogical crystallization sequence of the SIC were obtained in the simulation runs tested using the software package MELTS. Of all the simulation runs, that using the average bulk composition of the Manicouagan impact melt sheet as the starting liquid gave the best results. It is concluded that the original bulk composition of the SIC was more likely andesitic and that this liquid crystallized at pressures ranging between 0.08 and 0.12 GPa and under conditions close to the QFM buffer.

5. DISCUSSION

5.1 Petrography and Mineralogy

Since the work of Naldrett *et al.* (1970), few detailed petrographical and mineralogical studies of the complete rock suite of the SIC have been published. The present study represents a modern investigation of the petrography and mineralogy of the SIC using samples from continuous drill cores and up to date laboratory techniques and instrumentation. As shown in Figure 13, the anorthite content of SIC plagioclase decreases with higher stratigraphic levels, from about An_{70} in the contact sublayer to about An_{30} in the transition zone. Naldrett *et al.* (1970) recorded a similar cryptic variation for their study of SIC plagioclase, with the exception that they did not record the presence of Na-rich plagioclase crystals within the lower unit ("norite") and middle unit ("quartz gabbro"). The observations and data presented in this study indicate that some of these Na-rich plagioclase crystals are xenocrysts; whereas, others are due to albitization of Ca-rich plagioclases. These xenocrysts have complex twinning and zoning patterns, which are similar to those observed in relic crystals found in impact melt rocks. Heterogeneous plagioclases with reverse zoning and complex twinning have been described from the Manicouagan impact melt rocks by Floran *et al.* (1978), who interpreted them as relic crystals. Reimold *et al.* (1999) published a photomicrograph from the Morokweng impact melt rocks (their Fig. 6A) in which they point to melting in central parts of plagioclase laths. These plagioclase laths appear similar to some of the plagioclases from the SIC, which are interpreted here as relic crystals. Although no relic augite crystals were observed in the upper unit (granophyre), as analysed by Naldrett *et al.* (1970) and Peredery and Naldrett (1975), the

pyroxene mineralogical data for all other SIC lithologies presented in this study agree with that of Hewins (1974) and Naldrett *et al.* (1970).

Observations presented here of pseudomorphs after magnetite indicate that oxidation and dissolution of magnetite did occur, possibly through autometamorphism, and, thus, that the SIC oxides were not so resistant to alteration, as implied by Gasparrini and Naldrett (1972). Taylor (1967), using oxygen isotopic data, showed that quartz and alkali feldspar in the SIC upper unit (granophyre) did not form together in equilibrium. His explanation for these data is that the upper unit (granophyre) interacted with abundant alkali-bearing aqueous fluids at a late (which he suspected to be deuteric) stage in its crystallization history, enriching the feldspar in ^{18}O; whereas, the coexisting quartz was practically unaffected. The extensive alteration of primary minerals (such as plagioclase to albite, epidote and sericite-clinozoisite, and pyroxene to uralitic amphibole, biotite and chlorite) is also indicative of deuteric alteration. Additional evidence of the effects of alteration within the Sudbury Structure have been most recently documented by Ames *et al.* (1998), Marshall *et al.* (1999) and Molnár *et al.* (1999).

5.2 Geochemistry

Compared to the data of Kuo and Crocket (1979), Chai and Eckstrand (1993, 1994) and Lightfoot *et al.* (1997a,c), the geochemical data presented in this study have the same overall patterns but include additional elements and samples. Chai and Eckstrand (1993, 1994) used Harker diagrams to show a large SiO_2 gap between the upper unit (granophyre) and other SIC lithologies. Lightfoot *et al.* (1997a), using a different and more extensive suite of samples,

including surface samples and drill core, could not rule out Chai and Eckstrand's "gap". Contrary to these previously published data sets, those of the present study were based on finer-scale sampling, as close as every 1 or 2 meters over lithological changes (or boundaries), and conclusively demonstrate that no gap in the distribution of major and trace elements exists, even using Harker diagrams (Fig. 34).

The transition zone, as defined in this study, bridges the "gap" between the top of the middle unit ("quartz gabbro") and the base of the upper unit (granophyre) (Fig. 34). Chai and Eckstrand's gap is, thus, due to undersampling, particularly of this transition zone, as they collected 37 samples from discontinuous outcrops in two traverses across the North and South Ranges, with a spacing of at least a few meters to tens of meters between samples. Lightfoot *et al.* (1997a) also appear to have undersampled the transition zone, although looking at their data plotted with depth (presented in Lightfoot *et al.*, 1997c), a gradation is observed between their "transition zone quartz gabbro" and "granophyre" samples.

The SiO_2 content variation, expressed as a depletion towards the top of the middle unit ("quartz gabbro") (Fig. 28), which has been used to postulate the "gap" mentioned above, may be explained as an effect of the iron enrichment of the liquid, as differentiation proceeded. In fact, a silica depletion and iron enrichment are modelled for mafic and ultramafic igneous intrusions (such as Skaergaard, Morse, 1990). During crystallization, the magma is enriched in iron at a late stage. However, with a high Po_2, probably as a result of an elevated water content dissolved in the magma, iron is oxidized and is, thereby, continuously removed as magnetite

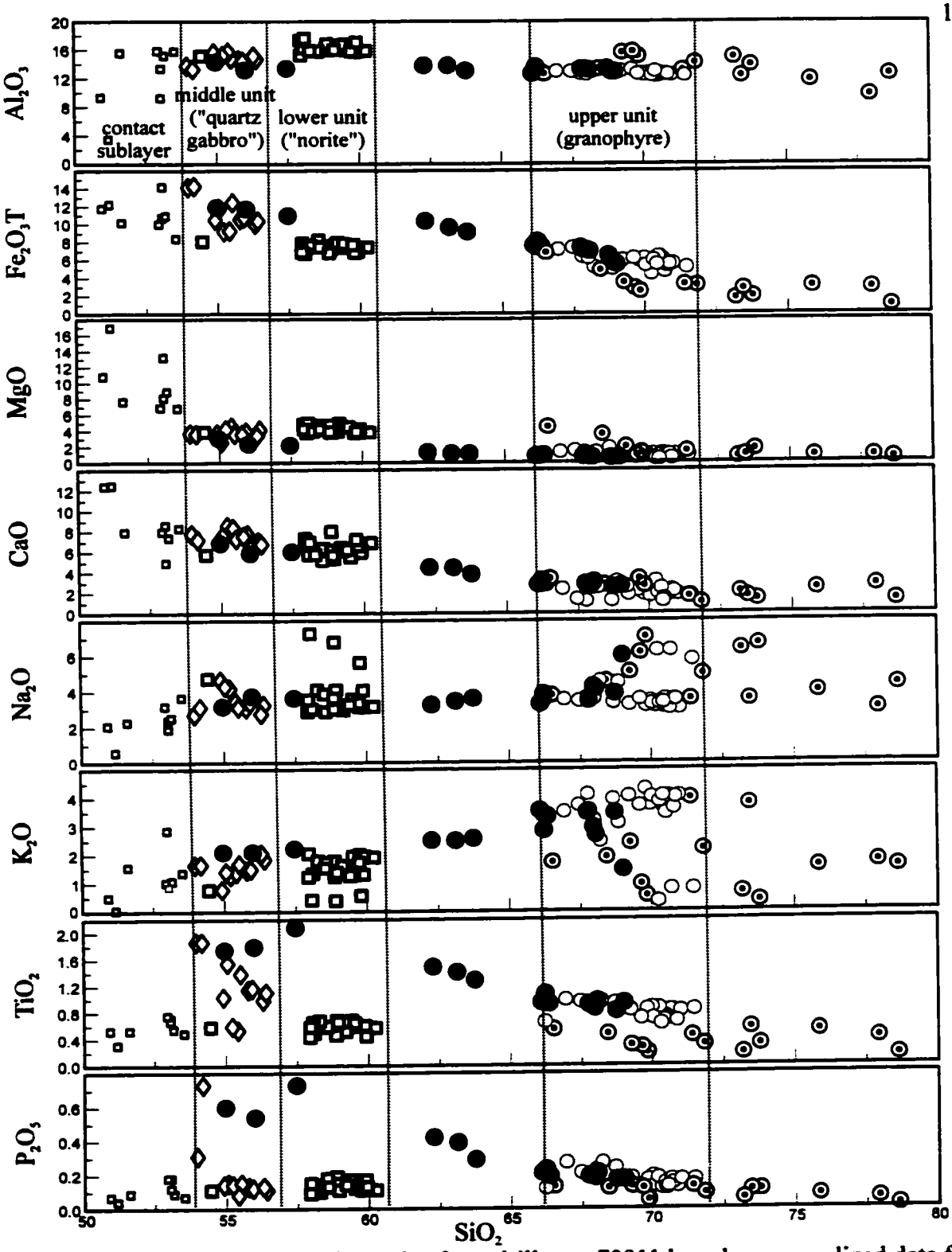

Figure 34. Harker diagrams of samples from drill core 70011 based on normalized data from this work and Ostermann (1996). Black circles = transition zone; dotted circles = Onaping Fm.

during crystallization of the magma. This precipitation of magnetite removes iron from the magma, forcing the remaining liquids toward silica-rich compositions. Thus, after major precipitation of Fe-Ti oxides in the middle unit (quartz gabbro), the silica content increases as observed in Figure 28. In tholeiitic systems, after Fe-Ti oxides saturate, the Fe/Mg ratio of the melt typically continues to increase; whereas, the absolute Fe content of the melt and its density decrease (Jaupart and Tait, 1995). These observations are consistent with those of the SIC (Fig. 35).

There is significant light REE enrichment in all the SIC rocks. At the top of the lower unit ("norite") a slight increase in REE content is observed, contrary to Chai and Eckstrand's slight decrease. Kuo and Crocket (1979) noticed the absence of a positive Eu anomaly in the contact sublayer and the presence of an invariably positive Eu anomaly in the lower unit ("norite"). In this study, positive Eu anomalies were observed in two samples of the contact sublayer (the others showing a negative Eu anomaly possibly due to inclusion contamination) and a negative Eu anomaly was observed in some lower unit ("norite") and many middle unit ("quartz gabbro") samples. In the previous chapter (section 4.2 "Trace Elements and Rare Earth Elements"), the variation in Eu anomalies was explained as either a reflection of parent material signatures or due to alteration. Contrary to Kuo and Crocket (1979) and Chai and Eckstrand (1994), it is demonstrated here that the magnitude of the negative Eu anomalies generally increases throughout the SIC. As Kuo and Crocket (1979) and Chai and Eckstrand (1994) remarked, towards the top of the upper unit (granophyre), the REE contents decrease with higher stratigraphic levels. However, contrary to Chai and Eckstrand (1994), the data presented here

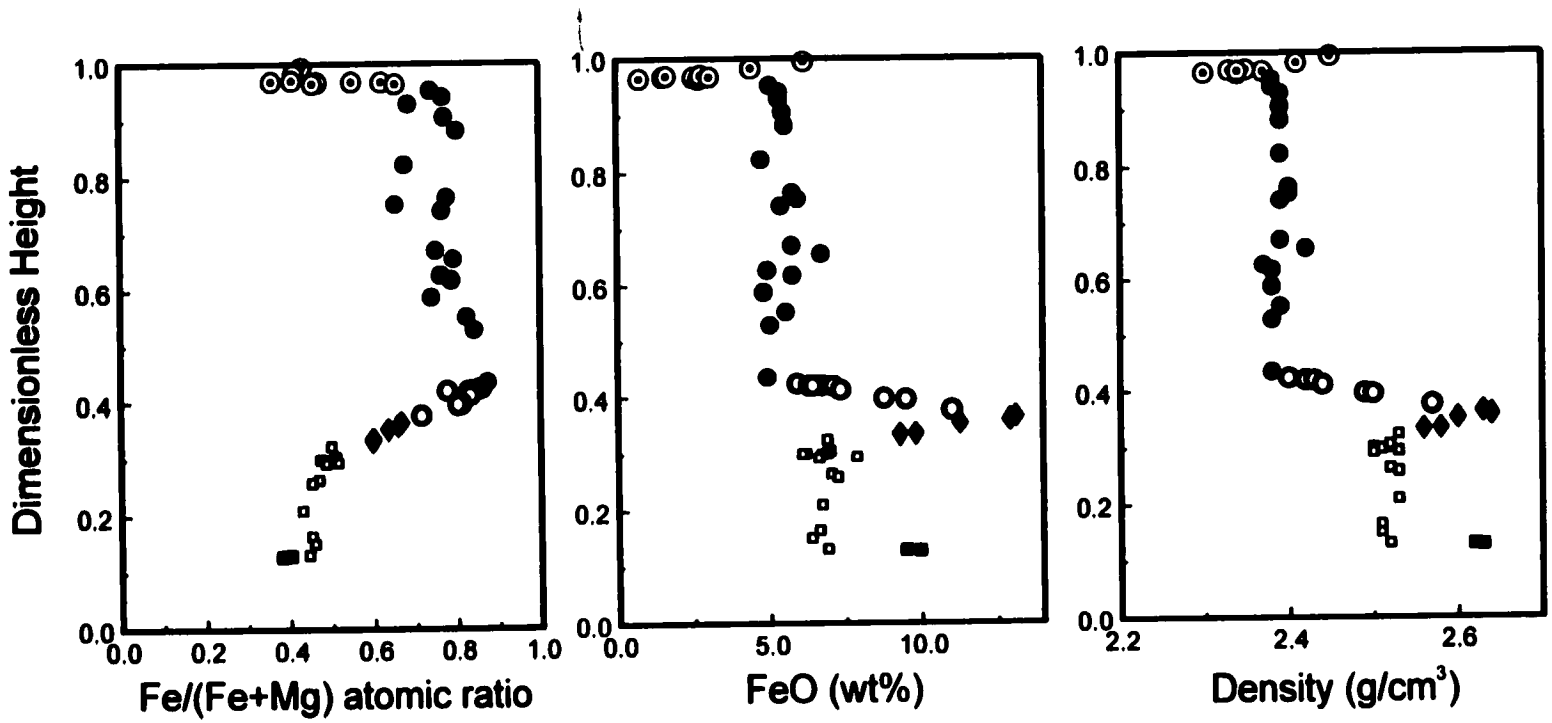

Figure 35. Distribution of the Fe atomic ratio, FeO (wt%) content and density variation within drill core 70011. Based on normalized data from this work and Ostermann (1996). Symbols as in Figure 34. Density calculations are according to the treatment of Hess (1989), using molar volume values at 1200°C.

show a significant and gradual decrease in REE contents from the top of the upper unit (granophyre) into the Onaping Formation (Fig. 30).

Thus, geochemical data indicate that the SIC behaved as a single melt system and that standard igneous differentiation processes occurred during its crystallization history.

5.3 Nature of Boundaries Between SIC Lithologies

In this work, the upper and lower limits of each unit (shown in Figure 3) have been defined using all data (modal, petrographical and geochemical) and the CIPW norms. The spacing between samples and available data are the main reasons for the precision in pin-pointing the position of these limits. For example, the position of the upper and lower limits of lithological units for drill core 70011 according to different data sets is given in Table X. The boundary between the Onaping Formation and the upper unit (granophyre) is well defined at 93.7 ± 0.8 m, although gradational over a few tens of meters. This is also true of the boundary between the lower unit ("norite") and contact sublayer, at 2254.0 ± 1.5 m. In this latter case, what has been assigned as contact sublayer may have been classified as "inclusion-rich norite" in previous work. The gradational character of the transition zone is emphasized by the ambiguity in determining the exact location of its top and base. The top of the transition zone is arbitrarily chosen at 1485.9 ± 22.9 m (*i.e.*, the mid-point between 1463.0 and 1508.8 m depth, Table X); whereas, the base of the transition zone is arbitrarily chosen at 1646.0 ± 15.3 m (*i.e.*, the mid-point between 1630.7 and 1661.2 m depth, Table X). As for the variation in the location of the middle unit ("quartz gabbro") - lower unit ("norite") boundary, it is mainly due to the

Table X: Position of lower and upper limits of lithological units in drill core 70011, based on data from closest samples.

Method	Onaping Fm / upper unit (granophyre)	upper unit (granophyre) / transition zone	transition zone / middle unit ("quartz gabbro")	"blue-band"	middle unit ("quartz gabbro") / lower unit ("norite")	lower unit ("norite") / contact sublayer
Modal composition (Table I) and petrography	93.0-94.5 93.7 ± 0.8 m	1463.0-1493.5 1478.3 ± 15.2 m	1630.7-1676.4 1653.6 ± 22.9 m	1728.2-1731.3 m	1735.8-1752.6 1744.2 ± 8.4 m	2252.5-2255.5 2254.0 ± 1.5 m
Geochemical profile (Figs. 28 & 30)			1630.7-1646.0 1637.9 ± 7.2 m	-	1731.3-1752.6 1741.9 ± 10.7 m	2249.4-2255.5 2252.5 ± 3.0 m
Harker diagrams (Fig. 34)				-		
AFM and Jensen diagrams (Fig. 29)[1]			1615.4-1646.0 1630.7 ± 15.3 m	1728.2-1731.3 m	1726.7-1752.6 1739.7 ± 13.0 m	
PER diagrams (Fig. 32)[1]				-		
Density distribution (Fig. 35)[1]		1478.3 ± 15.2 m	1630.7 ± 15.3 m	-		
CIPW norm (Table VI)		1504.2-1508.8 1506.5 ± 2.3 m	1630.7-1646.0 1637.9 ± 7.2 m	1728.2-1731.3 m		
Spider diagrams (Fig. 31)	93.0-94.5 93.7 ± 0.8 m	1493.5-1501.7 1497.6 ± 4.1 m	1646.0-1661.2 1653.5 ± 7.6 m	-	1726.7-1752.6 1739.7 ± 13.0 m	2249.4-2255.5 2252.5 ± 3.0 m
Best boundary position	93.7 ± 0.8 m	1485.9 ± 22.9 m	1646.0 ± 15.3 m	-	1744.2 ± 8.4 m	2254.0 ± 1.5 m

Note: [1] = limited data set

presence of a leucocratic quartz monzogabbro or plagioclase "cumulate" ("blue-band") within the bottom of the middle unit ("quartz gabbro"), between 1728.2 and 1731.3 m depth, and the lack of geochemical data for sample SUD-60-1994 at a 1735.8 m depth. Samples from leucocratic quartz monzogabbro bands may be singled-out using their petrographic character, CIPW norm (geochemical data from Ostermann, 1996) and position in AFM and Jensen diagrams (geochemical data from Ostermann, 1996). The modal and petrographic data set indicate that the middle unit ("quartz gabbro") - lower unit ("norite") boundary occurs at 1744.2 ± 8.4 m. This study demonstrate that all boundaries are gradational, especially those involving the transition zone, and pin-pointing their exact position will remain arbitrary and possibly best achieved using the geochemical data, especially the REE data.

5.4 Differentiation of the SIC

Intrusive bodies thicker than a few hundred meters, if not too siliceous or viscous, will differentiate (*e.g.*, Jaupart and Tait, 1995). With a thickness of ~2.5 km, the SIC was more than thick enough to do so. By having an initial composition that was more likely andesitic, as discussed in the previous chapter, the SIC was geochemically appropriate for differentiation to occur. The AFM and Jensen diagrams (Fig. 29) indicate that the SIC rocks represent a sequence of compositions consistent with an evolution by crystal fractionation. Similarly, the chemical variation of various mineral phases (plagioclase, pyroxene, and apatite) and the consistently greater abundance, with higher stratigraphic levels, of incompatible elements are evidence that progressive crystal fractionation was effective in the SIC.

The alternative hypothesis to fractional crystallization would be to suggest that the sequence of rock compositions observed was the result of mixing a felsic melt (from melting light crustal material) with a mafic melt (from melting dense crustal material or injection of a mantle magma), and, thus, contamination models have been proposed. Of these contamination models, the most recent ones include: > 90% crustal contamination of a magma (Walker *et al.*, 1991), ~ 50% crustal contamination of only the lower unit ("norite") and middle unit ("quartz gabbro") in addition to a "granophyre" impact melt (Chai and Eckstrand, 1994), and < 20% primitive picritic magma incorporated into a crustal impact melt (Lightfoot *et al.*, 1997a).

At 50% contamination of only the lower unit ("norite") and middle unit ("quartz gabbro"), the excess energy required for assimilation is ~ 10^{22} J, assuming a specific heat of 1.3 $Jg^{-1}K^{-1}$ and latent heat of fusion of 2.6 x 10^2 Jg^{-1} for granitic rocks (Grieve and Cintala, 1992). This is an unrealistic amount of energy for any intrusive body. Reiners *et al.* (1995) demonstrated that a magma can only assimilate crustal material in a proportion of 20% or less of its volume. Thus, the only viable contamination model would be that proposed by Lightfoot *et al.* (1997a). However, the geochemical data presented here and isotopic data previously published (*e.g.*, Dickin and Crocket, 1998; Dickin *et al.*, 1999) do not indicate the admixture of a mantle magma to a crustal melt (impact melt). If some mantle magma was injected into the impact melt, both melts would have to, first, convect or turbulently mix as one single system in order to homogenize and hide all trace of a mantle signature.

5.5 Hypothesis of Mantle Melt Involvement Within the SIC

If the SIC is a crustally contaminated mantle magma, it would be most akin to a layered igneous complex. Some petrographical and mineralogical features of the SIC are similar to and some are unlike those of typical layered igneous complexes (*cf.*, Morse, 1990; Maaløe, 1985; Hall, 1996). Note that the characteristics of igneous intrusions vary systematically, as a function of magma chamber thickness (*e.g.*, Jaupart and Tait, 1995). Compared to layered igneous complexes with a similar thickness, the SIC is much longer and wider. These proportions would have impaired wholesale convection of the system as one large cell and may have resulted in a series of relatively small convective cells.

Igneous complexes and the SIC show evidence of differentiation, phase layering, cryptic layering, a similar mineralogy (except for some xenocrysts) and similar alteration processes (*cf.*, Davidson and Wyllie, 1968; Elsdon, 1972; Harrigan and MacLean, 1976). Uncommon in layered igneous complexes are the presence of primary amphibole and biotite and the anomalous chemical composition of the SIC apatite crystals (Warner *et al.*, 1998). The SIC also differs from layered igneous complexes by containing, in general, markedly higher amounts of SiO_2, Na_2O and K_2O, and lower amounts of Al_2O_3, and its average bulk composition is andesitic to granodioritic rather than gabbroic. The total REE content of the SIC increases with higher stratigraphic levels (Fig. 30), as is in common layered igneous complexes. However, the REE content of the SIC is higher than in other complexes and significantly enriched in the LREE, which are characteristics of a crustal signature of the parental melt. The distinctive crustal isotopic signature of the SIC is another characteristic unlike layered igneous complexes (*e.g.*,

Faggart *et al.*, 1985; Naldrett *et al.*, 1986; Deutsch, 1994). These differences in geochemistry between the SIC and typical layered igneous complexes are consistent with the differences in mineralogy.

A striking difference with layered complexes is the large volume of granophyre occurring in the SIC. The filling of voids by granophyric and micrographic intergrowths of quartz and alkali feldspar is common to all layered complexes, but in the SIC the volume of these intergrowths is extreme. In layered igneous complexes, granophyres represent usually less than 5 vol.% of the system; whereas, the SIC upper unit (granophyre) represents up to 60 vol.% of the entire SIC. Nonetheless, the SIC upper unit (granophyre) has a bulk composition (containing in average 67-69 wt% SiO_2 and 3.6-4.1 wt% K_2O, Table V) within the range of the composition of granophyres, characterized by a SiO_2 content of 57-74 wt% and a K_2O content of 1.9-5.0 wt%, occurring as a relatively voluminous unit within igneous bodies.

Thus, the SIC has fundamental differences with typical layered igneous complexes. Most importantly, it does not contain evidence of a geochemical mantle signature. Simulation runs using the software package MELTS demonstrate that the SIC could have been "contaminated" by a primitive picritic magma, in a proportion of up to 20 vol.%, as suggested by Lightfoot *et al.* (1997a). However, evidence of such contamination remains elusive. If a fluid was injected through the crater floor, the impact melt would have had to adjust its volume by raising the roof against the lithostatic pressure or by "erupting". The influx of magma may only be confirmed by finding its feeder system and/or evidence of this volume adjustment after injection. In contrast to bowl-shaped or funnel-shaped layered igneous complexes of similar thickness, the

SIC was most likely originally disc-shaped and, thus, more akin to a thick sill. This geometry was obtained by the impact melt filling the crater depression, which in a large complex impact structure is flat rather than bowl-shaped (*cf.*, Grieve, 1987).

5.6 Hypothesis of an Impact Melt for a Component of or the Whole SIC

The observed SIC granophyre volume is in contradiction to the volume expected from standard igneous differentiation processes. For this main reason, many workers suggest that the bulk of the granophyre originated as an impact melt (*e.g.*, Dence, 1972; Chai and Eckstrand, 1993, 1994; Dressler *et al.*, 1996; Zhou *et al.*, 1997; Ariskin *et al.*, 1999). On the other hand, many workers favour the hypothesis that the whole SIC is an impact melt (*e.g.*, Grieve *et al.*, 1991; Stöffler *et al.*, 1994; Deutsch and Grieve, 1994; Deutsch *et al.*, 1995; French, 1998).

In terrestrial impact melt rocks, the most abundant minerals are plagioclase, orthopyroxene, quartz, clinopyroxene, and alkali feldspars. Only rare olivine crystals have been observed in the impact melt rocks of the Manicouagan structure, olivine crystals being generally unknown from other terrestrial impact melt rocks (even in those of the Morokweng structure, South Africa, referred to as "quartz norite" (Andreoli *et al.*, 1999)). In the SIC, only rare olivine crystals are observed within the contact sublayer and inclusions therein. Primary amphibole (mainly edenite, ferro-edenite and ferrohornblende), as mantles around pyroxene and as prismatic crystals, observed in the SIC, are common in some impact melt rocks (*e.g.*, Janisjärvi, Russia; Sazonova, 1983). In some instances, the concentrations of siderophile and other trace elements in impact melt rocks are in excess of their concentrations in the target rocks and indicate

contamination by various types of meteoritic impacting bodies (*e.g.*, Palme, 1980). Such enrichments cannot be differentiated in the SIC, because of the presence and effect of the Ni-Cu ores as discrete bodies within the SIC.

Recently, Re-Os isotopic studies have been used to show the meteoritic component of some terrestrial melt rocks and prove the impact origin of structures (*e.g.*, Koeberl *et al.*, 1994a,b). Koeberl *et al.* (1996) found that, in the Vredefort Structure, the higher Os content and lower $^{186}Os/^{187}Os$ ratio of most melt rocks (Vredefort Granophyre) compared to the country rocks indicated a meteoritic contamination of the melt rocks, and, thus, their impact origin. Norman (1994) stated that the Os isotopic compositions of the Sudbury ores used in mixing calculations favored an endogeneous origin for the SIC. Similar to what is observed in the Vredefort Structure, the data of Walker *et al.* (1991) indicate that the $^{186}Os/^{187}Os$ ratio of most of the contact sublayer ores is lower than that of the country rocks; whereas, their absolute Os content is higher. Thus, a meteoritic contamination, of at least the Sudbury ores, cannot be excluded, but as noted by Dickin *et al.* (1999), the present osmium isotope data for sulfide ores of the contact sublayer do not provide convincing evidence for significant meteoritic contamination. Additional Re-Os isotopic studies, especially of the other lithological components of the SIC, are required in order to make a definitive statement in this regard.

An important textural property of impact melt rocks is the presence of mineral and rock inclusions, which have undergone shock metamorphism to different degrees, have been variously reworked by the melt, and are set in a crystalline, or glassy, matrix. The sizes of such inclusions range from millimeters to several tens of meters, and variations in inclusion content with

stratigraphic level are observed in thick melt sheets, varying from one to several tens of percent (*e.g.*, Engelhardt, 1984). In the SIC, mineral and rock inclusions, up to a few meters, are observed in all lithologies and especially in the contact sublayer and lower unit ("norite"), and at the top of the upper unit (granophyre). Inclusion populations of terrestrial impact melt rocks are dominated by the most refractory material of the target, *i.e.*, quartz, plagioclase and alkali feldspar, and, thus, mafic inclusions appear to be preferentially digested. Most SIC lithologies of the North Range contain numerous inclusions, which include the shocked quartz and plagioclase xenocrysts reported here for the first time.

The amount of melt generated in an impact event is a function of the impact velocity, physical properties of the impact body and target, and, most importantly, the size of the impact body (for details see Grieve and Cintala, 1992). The SIC volume is estimated at ~ 8,000 to ~ 14,000 km^3 (Grieve, 1994) and is in general agreement with the empirical relation between melt volume and crater diameter for other terrestrial impact structures in crystalline targets and the estimated original size of the Sudbury Structure (Grieve and Cintala, 1992; Grieve, 1994; Stöffler *et al.*, 1994). Its stratigraphic location corresponds to that of melt sheets observed at large complex impact structures, *i.e.*, immediately above breccias and/or brecciated basement rocks and overlain by breccias (Grieve *et al.*, 1991). Also, the average bulk composition of the SIC can be modelled as a mixture of the lithologies of the target area (Grieve *et al.*, 1991).

Of the large terrestrial impact structures known, which occur in crystalline target rocks, two are comparable in size to the Sudbury Structure: Vredefort and Chicxulub. The Vredefort Structure, South Africa, has an original diameter of ~ 300 km (Therriault *et al.*, 1997) and is also

comparable in age (~ 2.0 Ga; Allsopp *et al.*,1991; Kamo *et al.*, 1995; Spray *et al.*, 1995) to the Sudbury Structure. It has been eroded below its original crater floor and only remnants of its melt sheet are observed in the form of dykes (the Vredefort Granophyre; *e.g.*, Therriault *et al.*, 1996). The Chicxulub structure, Mexico, has an original diameter of ~ 180 km (*e.g.*, Pilkington *et al.*, 1994) and is buried under ~ 1 km of post-impact sediments and no drill core, to date, samples the entire melt sheet. The two thickest coherent terrestrial impact melt sheets exposed at surface are that of the Manicouagan impact structure, Quebec, with a pre-erosional estimated thickness of 300-400 m (Floran *et al.*, 1978), and that of the Popigai impact structure, Russia, with a pre-erosional estimated thickness of ~ 600 m (*e.g*, Masaitis, 1994). A ~ 250 m thick section remains at Manicouagan, and the entire impact melt sheet has been sampled by drilling at Popigai. Differentiation is not a characteristic of these relatively thick coherent impact melt sheets. For example, no apparent variation in An content of plagioclase crystals with stratigraphic level have been observed. Geochemical homogeneity over horizontal distances of kilometers is the striking characteristic of terrestrial impact melt sheet.

The SIC has very few characteristics unlike that of terrestrial impact melt sheets. Given all data and observations, the SIC is best interpreted as a differentiated impact melt sheet.

5.7 A Water-rich Single Melt System

The unusual proportion of upper unit (granophyre) to lower unit ("norite") - middle unit ("quartz gabbro") has been used to suggest that two melts are at the origin of the SIC (*e.g.*, Dence, 1972; Chai and Eckstrand, 1993, 1994; Dressler *et al.*, 1996; Zhou *et al.*, 1997; Ariskin

et al., 1999). However, the continuity in chemical trends, without abrupt changes, from well below to well above the lower limit of the upper unit (granophyre) (Figs. 28 and 30), can be used as an argument against a separate origin for the upper unit (granophyre), whether by separate intrusion or by contamination, as in the case of the Dufek intrusion (Ford, 1970). The geochemical profiles of the SIC support the genetic linkage and crystallization of all SIC lithologies from a single melt system. This is perhaps best shown by the systematic increase in abundance of REEs and the substantial uniformity in REE patterns (excluding Eu anomalies) between the SIC lithologies, with no real change in light to heavy REE ratios (Fig. 31). Also, Pearce elements ratios (PER) support the cogenetic relationship of the SIC units (Fig. 32a).

Based on the extensive deuteric alteration of primary minerals, the dissolution of magnetite, the extensive development of micrographic and granophyric intergrowths and the presence of primary hydrous minerals (such as amphibole and biotite), this single melt system crystallized in a water-rich environment. In addition, the presence of cumulus magnetite indicate that the crystallization environment had a high Fe^{3+}:Fe^{2+} ratio. One of the most striking characteristic of the SIC is its water content. Harris *et al.* (1970) show that granitic bodies, which result from igneous processes and have high water pressures, intersect their solidi at pressures of 0.1-0.2 GPa, corresponding to a depth of 3-6 km in the crust. Thus, these granitic bodies are usually completely crystalline (under equilibrium conditions) by the time the pressure falls to 0.1 GPa. It is speculated that the SIC was a large water-rich body of essentially granitic composition, that was liquid at shallow depth, making it very unusual in relation to the work of Harris *et al.* (1970). One process that could generate such a water-rich "granitic" body at shallow

depth is impact melting.

5.8 Crystallization History of the SIC

An impact melt is formed (at shock pressures > 50-60 GPa and temperatures > 2000 °C) by shock decompression near the point of impact and ensuing melting and vaporization of the target material, followed by mixing with rock and mineral inclusions as it is driven into the expanding crater cavity (Grieve *et al.*, 1977; Melosh, 1989). Such a melt is superheated and turbulently well-mixed with relatively cold inclusions (*e.g.*, Onorato *et al.*, 1978). Inclusions act as a heat sink and, thereby, rapidly cool the melt in their vicinity, which may lead to far-from-equilibrium textures (*e.g.*, Manicouagan; Floran *et al.*, 1978), until thermal equilibrium between melt and inclusions is reached (*e.g.*, Onorato *et al.*, 1978). For example, this takes 6,000 to 10,000 seconds in the case of Manicouagan (Onorato *et al.*, 1978).

As an impact melt, the SIC would have been initially superheated, contained inclusions and turbulently mixed. Once thermal equilibrium between melt and inclusions was reached, cooling of this initially homogenized melt slowed down, enabling it to differentiate, as it is thick enough to do so, was enclosed in a relatively "warm crust" (> 850 K up to 1.2 km away from the SIC-country rock contact, Ivanov and Deutsch, 1999) and covered by ~ 1.4 km of overlying impact breccias (Onaping Formation, Fig. 1; initially 300-850 K, Ivanov and Deutsch, 1999), which acted as a thermal insulator.

At this stage, the temperature difference between the SIC and underlying crust would have been ~ 600 K; whereas, that between the SIC and the overlying Onaping Formation would

have been ~ 1000-1500 K. Thus, a larger degree of cooling would have occurred at the top of the SIC compared to its base, as the petrographical observations show. The occurrence of euhedral and blocky plagioclase laths throughout much of the SIC serving as nuclei for micrographic and granophyric intergrowths, together with inverted pigeonite crystals and very fine exsolution lamellae, presumably Bøggild intergrowths, within plagioclase crystals of the lower unit ("norite"), are evidence that early crystallizing conditions in the SIC were near to equilibrium, *i.e.*, similar to standard plutonic conditions. The build up of fluid micro-inclusions in the margins of some of these crystals (Fig. 15d) indicates increasing water pressure conditions during the growth of the granophyre textures. The change from euhedral morphology of the granophyre core plagioclase to the outer skeletal, dendritic and stellate habits represents a severe change in environment. Such textures are indicative of far-from-equilibrium conditions and are typically seen in rocks that have undergone abrupt undercooling, *i.e.*, volcanic rocks. Given the vertical extent (~ 2 km) of the non-equilibrium features in the SIC and at least ~ 1.4 km of overlying breccias (Onaping Formation; Fig. 2), it is highly unlikely that the undercooling could arise from rapid cooling by heat transfer through the thick SIC.

In the Alid volcanic center, Eritrea, northeast Africa, Lowenstern *et al.* (1997) describe older granophyric blocks within pumice deposits erupted ~ 23.5 ka ago. These granophyric blocks, containing 50-70 vol% of granophyric intergrowths and high SiO_2 (~ 74 wt%) and K_2O (~ 5 wt%) contents, are interpreted to be comagmatic with the pumice and would represent parts of the crystalline carapace (walls or roof) of the pyroxene rhyolite intrusion (Lowenstern *et al.*, 1997). Lowenstern *et al.* (1997) related the development of the granophyre to previous eruptions

of the Alid volcanic center. Volatile exsolution provided the thrust for the eruption and simultaneously the conditions causing the development of the micrographic and granophyric intergrowths. The eruption at ~ 23.5 ka transported the previously formed granophyres to the surface as cognate xenoliths. This is in contrast with granophyres occurring as volumetrically insignificant veins within the Banded series of the Stillwater Complex, Montana. These are characterized by very low K_2O content and near-constant high SiO_2 and they are interpreted to have evolved during the latest stages of consolidation, in equilibrium with a high-temperature aqueous chloride solution (Czamanske *et al.*, 1991).

Given the evidence for high fluid pressure within the SIC (*e.g.*, primary hydrous minerals, extensive deuteric alteration, dissolution of magnetite, and the geochemistry of apatite crystals), it is possible that the SIC granophyre formed in response to a sudden loss of water pressure in the system. Such a drop in water pressure has the effect of increasing the liquidus and solidus temperatures or effectively undercooling the melt. Hence, it is envisaged that the skeletal and dendritic quartz and feldspar grew epitaxially on the existing euhedral and blocky plagioclase phenocrysts due to a rapid exsolution of the hydrous phase.

Other evidence of volatiles loss is provided by the SIC apatite crystals. In the SIC, the chemical variation of apatite with higher stratigraphic levels is explained, by Warner *et al.* (1998), as being due to rapid crystallization and indicates that degassing of the melt occurred prior to the top of the middle unit ("quartz gabbro") (*i.e.*, at the peak of saturation in iron, vapor, etc.). As in the case of the Skaergaard Intrusion, the lithological change to granophyre coincides with the increase in F/Cl ratios of apatites in the SIC (data from Warner *et al.*, 1998). Sonnenthal

(1990) determined that this change, in the Skaergaard Intrusion, indicates the saturation in volatiles of the melt and the exsolution of a hydrous phase. It is most likely this hydrous phase, which is the cause of the deuteric alteration discussed above. Thus, it is proposed that the exsolution of a volatile phase rapidly undercooled (and possibly supercooled) the residual melt of the SIC, causing its crystallization as granophyre. At the same time, residual liquid in the base of the lower unit ("norite") most likely also crystallized relatively rapidly, as granophyric textures are also observed in these rocks.

While non-equilibrium conditions prevailed in the upper unit (granophyre), the lower unit ("norite") and middle unit ("quartz gabbro") were most likely largely crystallized, resulting in a crystalline mush. During the differentiation of the SIC, as Fe was consumed, alkalis and alumina were enriched in the liquid. Then, undercooling of this residual liquid through the exsolution of a volatile phase produced the granophyric matrix of the middle unit ("quartz gabbro"), transition zone and upper unit (granophyre) and that of the interstices of the lower unit ("norite"). Complete solidification of the SIC would have taken thousands of years (*e.g.*, Ariskin *et al.*, 1999) and possibly more than 100 thousand years (Ivanov and Deutsch, 1999) enabling the grain-size to become medium to coarse. Throughout, and subsequent to, its crystallization history, the SIC underwent hydrothermal alteration as indicated by the data. Molnár *et al.* (1997) and Marshall *et al.* (1999) demonstrated that hydrothermal processes were involved in the redeposition of some of the ores in the Sudbury Structure.

6. CONCLUSION

The overall objective of this study was to determine the origin of the SIC. It is concluded that the SIC represents the only known differentiated terrestrial impact melt sheet. No other complete and differentiated impact melt sheet is currently known on Earth. The crystallization history of the SIC may be summarized as follows: (1) formation of an impact melt that behaved as a single melt system, (2) differentiation into the observable lithological units, (3) effective undercooling due to the exsolution of a volatile phase of the SIC in order to produce the micrographic and granophyric textures, and (4) development of a hydrothermal system, which redeposited some of the Sudbury sulphide ores.

It has been shown that the SIC possesses many affinities with terrestrial impact melt sheets and layered igneous complexes. However, the SIC differs less from other impact melt sheets than it does from layered igneous complexes. It differs from known terrestrial impact melt sheets in two respects: (1) its great thickness and (2) its chemical layering. By the same token, it differs from most layered igneous complexes in four respects: (1) its hydrous nature, (2) its initial composition was intermediate not mafic, (3) its crustal geochemical and isotopic signature, and (4) its large volume of granophyre.

The fact that the silicate liquid, which was to become the SIC, was generated by impact rather than endogenic igneous processes does not change the basic processes of silicate crystallization and fractionation. In order to differentiate into a series of distinct lithologies in the terrestrial environment, intrusive bodies must be at least a few 100s m thick and of appropriate composition (*e.g.*, Jaupart and Tait, 1995). The geochemical homogeneity and lack

of differentiation at terrestrial impact craters ≤100 km in diameter is due to the fact that the impact melt sheets produced were not thick enough (less than 600 m thick), probably too viscous, and crystallized too quickly for differentiation to occur.

The overall SiO_2-rich composition and hydrous nature of the SIC (for its Mg number) compared to common mantle magmas resulted in some second-order differences with differentiated basaltic magmas in the mineralogy, relative amounts, textures and extent of the "mafic" (contact sublayer, lower unit ("norite") and middle unit ("quartz gabbro")) and "felsic" (transition zone and upper unit (granophyre)) components in the SIC. Fractional crystallization simulation runs using the MELTS software program demonstrate that an andesitic rather than a granodioritic starting composition is required to reproduce the geochemical and mineralogical observations made for the SIC. The concept that the SIC was formed from a primitive mantle magma contaminated by country rocks is precluded by its crustal isotopic signature. Moreover, the energy needed for the required amount of contamination is unrealistic.

Problems remaining to be clarified and/or resolved are the exact starting composition of the SIC, the reasons for the observed volume of granophyre, the early crystallization of olivine from the original SIC melt, and the origin and emplacement of the contact sublayer. Naldrett *et al.* (1970) state that in the system diopside-forsterite-silica, a liquid crystallizing hypersthene + augite + quartz in the proportions observed for the lower part of the lower unit ("norite") would not be capable of crystallizing olivine and, thus, is not the parent melt for the mafic and ultramafic inclusions occurring within the contact sublayer. Even considering that many of the quartz crystals observed in the lower part of the lower unit ("norite") are xenocrystic in origin,

one expects that there would have been too much SiO_2 in the melt in order to be able to crystallize olivine. Results of Prevec (2000), using two different geochemical modelling programs (COMAGMAT and PELE) under 0.1 GPa and QFM buffer conditions, show that the average bulk composition (granodioritic in his simulations) of the SIC cannot crystallize olivine but that more andesitic melt compositions can. However, MELTS simulations ran in this study, under similar conditions as Prevec (2000) and using a similar granodioritic SIC average bulk composition as a starting liquid, did predict the early crystallization of olivine (Table IX). Moreover, the best match to the geochemical and mineralogical data was obtained using the andesitic average composition of the Manicouagan impact melt sheet. The contact sublayer has many mineralogical and geochemical affinities with the lower unit ("norite") and middle unit ("quartz gabbro") of the SIC and appears to be part of its differentiation trend as indicated by the chemical variation in mineral phases, major and trace elements and REEs and by the AFM, Jensen and Spider diagrams.

7. STATEMENT OF ORIGINAL CONTRIBUTION

Extensive, detailed sampling and an intensive petrographical and geochemical study of the complete rock suite of the SIC has been done for the first time. Modal composition analyses reveal that some of the SIC lithologies have been misnamed, leading to potential misconception of the origin and crystallization history of the SIC. The "norite" rock samples are classified here as quartz gabbro or quartz monzogabbro according to the IUGS classification; whereas, the "quartz gabbro" rock samples are classified as quartz monzogabbro (Fig. 6). An updated terminology using names free of a "genetic" connotation is, thus, proposed: contact sublayer, lower unit, middle unit, transition zone, and upper unit (Fig. 4). Reported here for the first time are the occurrence and measurements of planar deformation features (PDFs) in quartz xenocrysts from the lower unit ("norite") and transition zone, confirming the presence of shock metamorphic effects within the SIC. Also reported here for the first time is the occurrence of Na-rich plagioclase xenocrysts within the contact sublayer, lower unit ("norite") and middle unit ("quartz gabbro") providing the evidence that remnant inclusions of country rock are present throughout the SIC. Petrological and geochemical observations and results indicate that the initial composition of the SIC melt was most likely "andesitic" and water-rich. The "rediscovery" and importance of primary hydrous minerals in demonstrating the water-rich character of the SIC melt is made here for the first time. All observations, results and modelling demonstrate that the contact sublayer, lower unit ("norite"), middle unit ("quartz gabbro") and upper unit (granophyre) result from fractional crystallization of an originally single melt system, which was undercooled through the exsolution of a volatile phase. The exsolution accounts for

the widespread development of granophyre. Modeling results suggest that dunites, peridotites, and pyroxenites (representing some of the ultramafic inclusions observed in the contact sublayer) could, in fact, have crystallized from a relatively siliceous melt.

This study also introduces the idea that the total volume, and especially the thickness, of melt formed in an impact are among the most obvious factors in determining the potential for differentiation processes to occur within the impact melt sheet. When thick enough (more than several hundred meters) and of the right composition (not too siliceous), impact melt sheets on Earth will undergo significant igneous differentiation. This may have implications for crustal evolution of the early Earth, such as the generation of the first continental crust, and for the Moon, such as the differentiation of lunar impact melt sheets. This may warrant reconsideration of impact-generated magmatism versus endogeneous-derived magmatism on the Moon.

REFERENCES

Allsopp H.L., Fitch F.J., Miller J.A. and Reimold W.U. (1991) $^{40}Ar/^{39}Ar$ stepheating age determinations relevant to the formation of the Vredefort Dome. *S. Afr. J. Sci.* **87**, 431-442.

Ames D.E., Watkinson D.H. and Parrish R.R. (1998) Dating of a regional hydrothermal system induced by the 1850 Ma Sudbury impact event. *Geology* **26**, 447-450.

Andreoli M.A.G., Ashwal L.D., Hart R.J. and Huizaga J.M. (1999) A Ni- and PGE-enriched quartz norite impact melt complex in the Late Jurassic Morokweng impact structure, South Africa. *In* Large Meteorite Impacts and Planetary Evolution II (Dressler B.O. and Sharpton V.L., eds.), Boulder, Colorado, *Geol. Soc. Amer. Sp. Pap.* **339**, 91-108.

Ariskin A.A., Deutsch A. and Ostermann M. (1999) Sudbury Igneous Complex: Simulating phase equilibria and in situ differentiation for two proposed parental magmas. *In* Large Meteorite Impacts and Planetary Evolution II (Dressler B.O. and Sharpton V.L., eds.), Boulder, Colorado, *Geol. Soc. Amer. Sp. Pap.* **339**, 373-387.

Avermann M. and Brockmeyer P. (1992) The Onaping Formation of the Sudbury Structure (Canada); an example of allochthonous impact breccias. *Tectonophys.* **216**, 227-234.

Barker D.S. (1970) Compositions of Granophyre, Myrmekite, and Graphic Granite. *GSA Bull.* **81**, 3339-3350.

Barlow A.E. (1904) Report on the Origin, Geological Relations and Composition of the Nickel and Copper Deposits in the Sudbury Mining District, Ontario, Canada. *Geol. Surv. Can. Ann. Rep.* **873**, 236p.

Bradshaw T.K. (1992) The adaptation of Pearce element ratio diagrams to complex high silica systems. *Contr. Min. Pet.* **104**, 450-458.

Bray J.G. and Geological Staff (1966) Shatter cones at Sudbury. *J. Geol.* **74**, 243-245.

Brocoum S.T. and Dalziel I.W.D. (1974) The Sudbury Basin, the Southern Province, the Grenville Front and the Penokean Orogeny. *Geol. Soc. Amer. Bull.* **85**, 1571-1580.

Buddington A.F. and Lindsley D.H. (1964) Iron-titanium oxide minerals and synthetic equivalents. *J. Petrol.* **5**, 310-357.

Card K.D. (1978) Geology of the Sudbury-Manitoulin area, districts of Sudbury and Manitoulin. *Ont. Geol. Surv. Rep.* **166**, 238p.

Card K.D. (1994) Geology of Levack Gneiss Complex, the northern footwall of the Sudbury Structure, Ontario. *Geol. Surv. Can. Current Research* **1994-C**, 269-278.

Card K.D., Innes D.G. and Deblicki R.L. (1977) Stratigraphy, sedimentology and petrology of the Huronian supergroup in the Sudbury-Espanola area. *Ont. Div. Mines Geosc. Study* **16**, 99p.

Chai G. and Eckstrand O.R. (1993) Origin of the Sudbury Igneous Complex, Ontario - differentiate of two separate magmas. *In* Current Research, Part E, *Geol. Surv. Can. Paper* **93-1E**, 219-230.

Chai G. and Eckstrand O.R. (1994) Rare-earth element characteristics and origin of the Sudbury Igneous Complex, Ontario, Canada. *Chem. Geol.* **113**, 221-244.

Chayes F. (1960) On correlation between variables of constant sum. *J. Geophys. Res.* **65**, 4185-4193.

Coleman A.P. (1905) The Sudbury Nickel Region. *Rep. Ont. Bur. Mines, 1904* **14**, Part 3, 183p.

Coleman A.P. (1913) The Nickel Industry, with Special Reference to the Sudbury Region, Ontario. *Can. Dept. Mines, Mines Branch*, **170**, 206p.

Coleman A.P., Moore E.S. and Walker T.L. (1929) The Sudbury Nickel Irruptive. *Contr. Can. Mineral.* 1929, 54p.

Collins W.H. (1934) Life History of the Sudbury Nickel Irruptive. I. Petrogenesis. *Royal Society of Canada, Transactions, Third Series* **28**, 123-177.

Collins W.H. (1937) The Life History of the Sudbury Nickel Irrupive. IV. Mineralization. *Royal Soc. Can., Transactions, Third Series* **31**, 15-43.

Corfu F. and Andrews A.J. (1986) A U-Pb age for mineralized Nipissing Diabase, Gowganda, Ontario. *Can. J. Earth Sci.* **23**, 107-109.

Corfu F. and Lightfoot P.C. (1996) U-Pb Geochronology of the Sublayer Environment, Sudbury Igneous Complex, Ontario. *Econ. Geol.* **91**, 1263-1269.

Crossey L.J. and McCarville (1994) Post-impact hydrothermal systems: Manson impact structure. *Proceedings, International Symposium on the Observation of the Continental Crust Through Drilling* **7th**, Santa Fe, 211-214.

Czamanske G.K., Zientek M.L. and Manning C.E. (1991) Low-K granophyre of the Stillwater Complex, Montana. *Am. Mineral.* **76**, 1646-1661.

Davidson A. and van Breemen O. (1994) U-Pb ages of granites near the Grenville Front, Ontario. *In* Radiogenic age and isotopic studies, Report 8, *Geol. Surv. Can. Current Research* **1994-F**, 107-114.

Davidson A. and Wyllie P.J. (1968) Opaque oxide minerals of some diabase and granophyre associations in Pennsylvania. *Econ. Geol.* **63**, 950-960.

Deer W.A., Howie R.A., and Zussman J. (1985) *An Introduction to the Rock-forming Minerals.* Longman Group Limited, England, 528pp.

Dence M.R. (1972) Meteorite Impact Craters and the Structure of the Sudbury Basin. *In* New Developments in Sudbury Geology (Guy-Bray J.V., ed.), *Geol. Ass. Can. Sp. Pap.* **10**, 7-18.

Deutsch A. (1994) Isotope systematics support the impact origin of the Sudbury Structure (Ontario, Canada). *Geol. Soc. Amer. Sp. Pap.* **293**, 289-302.

Deutsch A. and Grieve R.A.F. (1994) The Sudbury Structure: Constraints on its genesis from Lithoprobe results. *Geophys. Res. Lett.* **21**, 963-966.

Deutsch A., Grieve R.A.F., Avermann M., Bischoff L., Brockmeyer P., Buhl D., Lakomy R., Müller-Mohr V., Ostermann M. and Stöffler D. (1995) The Sudbury Structure (Ontario, Canada): A tectonically deformed multi-ring impact basin. *Geol. Rundsch.* **84**, 697-709.

Dickin A.P. and Crocket J.H. (1998) Reply to the Comment by B.O. Dressler and V.L. Sharpton on AIsotopic evidence for distinct crustal sources of North and South Range ores, Sudbury Igneous Complex. *Geochim. Cosmochim. Acta* **62**, 319-322.

Dickin A.P., Artan M.A. and Crocket J.H. (1996) Isotopic evidence for distinct crustal sources of North and South Range ores, Sudbury Igneous Complex. *Geochim. Cosmochim. Acta* **60**, 1605-1613.

Dickin A.P., Nguyen T. and Crocket J.H. (1999) Isotopic evidence for a single impact melting origin of the Sudbury Igneous Complex. *In* Large Meteorite Impacts and Planetary Evolution II (Dressler B.O. and Sharpton V.L., eds.), Boulder, Colorado, *Geol. Soc. Amer. Sp. Pap.* **339**, 361-371.

Dietz R.S. (1964) Sudbury Structure as an Astrobleme. *J. Geol.* **72**, 412-434.

Dietz R.S. and Butler L.W. (1964) Shatter-cones orientation at Sudbury, Canada. *Nature* **204**, 280-281.

Dressler B.O. (1984) The effects of the Sudbury event and the intrusion of the Sudbury Igneous Complex on the footwall rocks of the Sudbury Structure. *In* The Geology and Ore Deposits of the Sudbury Structure (Pye E.G., Naldrett A.J. and Giblin P.E., eds.), *Ont. Geol. Surv. Sp. Vol.* **1**, 593-625.

Dressler B.O., Morrison G.G., Peredery W.V. and Rao B.V. (1987) The Sudbury Structure Ontario, Canada - A review. *In* Research in Terrestrial Impact Structures (Pohl, J., ed.), 39-68.

Dressler B.O., Peredery W.V. and Muir T.L. (1992) Geology and Mineral Deposits of the Sudbury Structure. *Ont. Geol. Surv. Guidebook* **8**, 38p.

Dressler B.O., Weiser T. and Brockmeyer P. (1996) Recrystallized impact glasses of the Onaping Formation and the Sudbury Igneous Complex, Sudbury Structure, Ontario, Canada. *Geochim. Cosmochim. Acta* **60**, 2019-2036.

Dudàs F.Ö., Davidson A. and Bethune K.M. (1994) Age of the Sudbury diabase dikes and their metamorphism in the Grenville Province, Ontario. *In* Radiogenic age and isotopic studies, Report 8, *Geol. Surv. Can. Current Research* **1994-F**, 97-106.

Elsdon R. (1972) Iron-titanium oxides minerals in the upper layered series, Kap Edvard Holm, East Greenland. *Mineral. Mag.* **38**, 946-956.

Engelhardt W.v. (1984) Melt products from terrestrial impact structures. *Proc. 27th Intern. Geol. Congr.* **19**, 149-163.

Faggart B.E., Basu A.R. and Tatsumoto M. (1985) Origin of the Sudbury Complex by meteoritic impact: Neodynium isotopic evidence. *Science* **230**, 436-439.

Finn G.C. (1993) Field relationships within the granophyre phase, North Range, Sudbury Igneous Complex (abstract). *Progr. with Abstr. - Geol. Ass. Can.; Mineral. Ass. Can.; Can. Gcophys. Union, Joint Ann. Meeting* **18**, A-30.

Floran R.J., Grieve R.A.F., Phinney W.C., Warner J.L., Simonds C.H., Blanchard D.P. and Dence M.R. (1978) Manicouagan impact melt, Quebec. 1. Stratigraphy, petrology, and chemistry. *J. Geophys. Res.* **83**, 2737-2759.

Ford A.B. (1970) Development of the layered series and caping granophyre of the Dufek intrusion of Antartica. *Geol. Soc. S. Afr. Sp. Publ.* **1**, 492-510.

Fowler A.D. and Doig R. (1983) The significance of europium anomalies in the REE spectra of granites and pegmatites, Mont Laurier, Quebec. *Geochim. Cosmochim. Acta* **47**, 1131-1137.

French B.M. (1967) Sudbury structure, Ontario: some petrographic evidence for origin by meteorite impact. *Science* **156**, 1094-1098.

French B.M. (1968) Sudbury structure, Ontario: some petrographic evidence for an origin by meteorite impact. *In* Shock Metamorphism of Natural Materials (French B.M. and Short N.M., eds.), Mono Book Corp., Baltimore, 383-412.

French B.M. (1969) Possible relations between meteorite impact and igneous petrogenesis as indicated by the Sudbury Structure, Ontario, Canada. *NASA, Goddard Space Flight Center,* **Publ. X-644-69-371**, 50p.

French B.M. (1970) Possible relations between meteorite impact and igneous petrogenesis, as indicated by the Sudbury Structure, Ontario, Canada. *Bull. Volcano.* **34-2**, 466-517.

French B.M. (1998) *Traces of Catastrophe: A Handbook of Shock-Metamorphic Effects in Terrestrial Meteorite Impact Structures.* LPI Contribution No. 954, Lunar and Planetary Institute, Houston, 120p.

Frost B.R. and Lindsley D.H. (1991) Occurrence of iron-titanium oxides in igneous rocks. *Rev. Mineral.* **25**, 433-468.

Fueten F. and Redmond D.J. (1997) Documentation of a 1450 Ma contractional orogeny preserved between the 1850 Ma Sudbury impact structure and the 1 Ga Grenville orogenic front, Ontario. *GSA Bull.* **109**, 268-279.

Gasparrini E. and Naldrett A.J. (1972) Magnetite and ilmenite in the Sudbury Nickel Irruptive. *Econ. Geol.* **67**, 605-621.

Ghiorso M.S. (1985) Chemical mass transfer in magmatic processes I. Thermodynamic relations and numerical algorithms. *Contrib. Mineral. Petrol.* **90**, 107-120.

Ghiorso M.S. (1994) Algorithms for the estimation of phase stability in heterogeneous thermodynamic systems. *Geochim. Cosmochim. Acta.* **58**, 5489-5501.

Ghiorso M.S. and Kelemen P.B. (1987) Evaluating reaction stoichiometry in magmatic systems evolving under generalized thermodynamic constraints: examples comparing isothermal and isenthalpic assimilation. *In* Magmatic processes: Physico-chemical principles (Mysen B.O., ed.), *Geochem. Soc. Sp. Publ.* **1**, 319-336.

Ghiorso M.S. and Sack R.O. (1995) Chemical mass transfer in magmatic processes. IV. A revised and internally consistent thermodynamic model for the interpolation and extrapolation of liquid-solid equilibria in magmatic systems at elevated temperatures and pressures. *Contr. Min. Pet.* **119**, 197-212.

Ghiorso M.S., Carmichael I.S.E., Rivers M.L. and Sack R.O. (1983) The Gibbs free energy of mixing of natural silicate liquids; an expanded regular solution approximation for the calculation of magmatic intensive variables. *Contrib. Mineral. Petrol.* **84**, 107-145.

Gibbins W.A. and McNutt R.H. (1975) The age of the Sudbury Nickel Irruptive and the Murray granite. *Can. J. Earth Sci.* **12**, 1970-1989.

Giblin P.E. (1984) History of Exploration and Development, of Geological Studies and Development of Geological Concepts. *In* The Geology and Ore Deposits of the Sudbury Structure (Pye E.G., Naldrett A.J. and Giblin P.E., eds.), *Ont. Geol. Surv. Sp. Vol.* **1**, 3-23.

Golightly J.P. (1994) The Sudbury Igneous Complex as an impact melt: Evolution and ore genesis. *Ont. Geol. Surv. Sp. Vol.* **5**, 105-117.

Grieve R.A.F. (1987) Terrestrial impact structure. *Ann. Rev. Earth Planet. Sci.* **15**, 245-270.

Grieve R.A.F. (1994) An impact model of the Sudbury Structure, Ontario. *Ont. Geol. Surv. Sp. Vol.* **5**, 119-132.

Grieve R.A.F. and Cintala M.J. (1992) An analysis of differential impact melt-crater scaling and implications for the terrestrial impact record. *Meteoritics* **27**, 526-538.

Grieve R.A.F. and Floran R.J. (1978) Manicouagan impact melt, Quebec 2. Chemical interrelations with basement and formational processes. *J. Geophys. Res.* **83**, 2761-2771.

Grieve R.A.F., Dence M.R. and Robertson P.B. (1977) Cratering processes: as interpreted from the occurrence of impact melts. *In* Impact and Explosion Cratering (Roddy D.J., Pepin R.O., Merill R.B., eds.), Pergamon Press, New York, pp. 794-814.

Grieve R.A.F., Stöffler D. and Deutsch A. (1991) The Sudbury Structure: Controversial or Misunderstood? *J. Geophys. Res.* **96**, 22,753-22,764.

Grieve R.A.F., Langenhorst F. and Stöffler D. (1996) Shock metamorphism of quartz in nature and experiment: II. Significance in geoscience. *Meteorit. & Planet. Sci.* **31**, 6-35.

Hall A. (1996) *Igneous Petrology*. Harlow, Essex, Longman, 551pp.

Harrigan D.B. and MacLean W.H. (1976) Petrography and geochemistry of epidote alteration patches in gabbro dykes at Matagami, Quebec. *Can. J. Earth Sci.* **13**, 500-511.

Harris P.G., Kennedy W.Q. and Scarfe C.M. (1970) Volcanism versus plutonism - the effect of chemical composition. *In* Mechanism of Igneous Intrusion (Newall G., Rast N., Flinn G.W. and Liverpool Geological Society, eds.), Gallery P., Liverpool, pp. 187-200.

Hawley J.E. (1962) The Sudbury ores: Their mineralogy and origin. *Can. Mineral.* **7**, 1-207.

Hess P.C. (1989) ***Origins of igneous rocks.*** **Cambridge, Mass., Harvard University, 336pp.**

Hewins R.H. (1970) Microprobe studies of the base of the Sudbury Nickel Irruptive, Ontario (abstr.). *Econ. Geol.* **65**, 737.

Hewins R.H. (1971) ***Petrology of some marginal mafic rocks along the North Range of the Sudbury Irruptive.*** **Ph.D. Thesis, University of Toronto, 147pp.**

Hewins R.H. (1974) Pyroxene crystallization trends and contrasting augite zoning in the Sudbury Nickel Irruptive. ***Am. Mineral.*** **59, 120-126.**

Hirt A.M., Lowrie W., Clendenen W.S. and Kligfield R. (1993) Correlation of strain and the anisotropy of magnetic susceptibility in the Onaping Formation: evidence for a near-circular origin of the Sudbury Basin. *Tectonophys.* **225**, 231-254.

Hoffman P.F. (1989) Precambrian geology and tectonic history of North America. *In* The geology of North America - An overview (Bailey A.W. and Palmer A.R., eds.), *Geol. Soc. Amer., Geology of North America* A, 447-512.

Ivanov B.A. and Deutsch A. (1999) Sudbury impact event: Cratering mechanics and thermal history. *In* Large Meteorite Impacts and Planetary Evolution II (Dressler B.O. and Sharpton V.L., eds.), Boulder, Colorado, *Geol. Soc. Amer. Sp. Pap.* **339**, 389-397.

Jaupart C. and Tait S. (1995) Dynamics of differentiation in magma reservoirs. *J. Geophys. Res.* **100**, 17,615-17,636.

Kamo S.L., Reimold W.U., Krogh T.E. and Colliston W.P. (1995) Shocked zircons in Vredefort pseudotachylite and the U-Pb zircon age of the Vredefort impact event (ext. abstract). *Cent. Congr. Geol. Soc. S. Afr.* **95th**, 566-569.

Knight C.W. (1917) Geology of the Sudbury area. *Royal Ontario Nickel Comm. Rept., Toronto, Ont.*, 105-211.

Knight C.W. (1923) The chemical composition of the norite-micropegmatite, Sudbury, Ontario. *Econ. Geol.* **18**, 592-594.

Koeberl C., Sharpton V.L, Schuraytz B.C., Shirey S.B., Blum J.D. and Marin L.E. (1994a) Evidence for a meteoritic component in impact melt rock from the Chicxulub structure. *Geochim. Cosmochim. Acta* **58**, 1679-1684.

Koeberl C., Reimold W.U., Shirey S.B. and LeRoux F.G. (1994b) Kalkkop Crater, Cape Province, South Africa: Confirmation of impact origin using osmium isotope systematics. *Geochim. Cosmochim. Acta* **58**, 1229-1234.

Koeberl C., Reimold W.U. and Shirey S.B. (1996) Re-Os isotope and geochemical study of the Vredefort Granophyre: clues to the origin of the Vredefort structure, South Africa. *Geology* **24**, 913-916.

Krogh T.E. (1994) Precise U-Pb ages for Grenvillian and pre-Grenvillian thrusting of Proterozoic and Archean metamorphic assemblages in the Grenville Front tectonic zone, Canada. *Tectonics* **13**, 963-982.

Krogh T.E., Davis D.W. and Corfu F. (1984) Precise U-Pb zircon and baddeleyite ages for the Sudbury area. *In* The Geology and Ore Deposits of the Sudbury Structure (Pye E.G., Naldrett A.J. and Giblin P.E., eds.), *Ont. Geol. Survey Sp. Vol.* **1**, 431-446.

Krogh T.E., Corfu F., Davis D.W., Dunning G.R., Heaman L.M., Kamo S.L., Machado N., Greenhough J.D. and Nakamura E. (1987) Precise U-Pb isotopic ages of diabase dykes and mafic to ultramafic rocks using trace amounts of baddeleyite and zircon. *In* Mafic dyke swarms (Halls H.C. and Fahrig W.F., eds.), *Geol. Ass. Can. Sp. Pap.* **34**, 147-152.

Kuo H.Y. and Crocket J.H. (1979) Rare earth elements in the Sudbury Nickel Irruptive: Comparison with layered gabbros and implications for Nickel Irruptive petrogenesis. *Econ. Geol.* **74**, 590-605.

Langford F.F. (1960) Geology of Levack Township and the northern part of Dowling Township, District of Sudbury. *Ont. Dept. Mines Prelim. Rep.* **1960-5**, 78p.

Leake B.E. *et al.* (1997) Nomenclature of amphiboles: Report of the subcommittee on amphiboles of the international mineralogical association, commission on new minerals and mineral names. *Can. Mineral.* **35**, 219-246.

Lentz D.R. and Fowler A.D. (1992) A dynamic model for graphic quartz-feldspar intergrowths in granitic pegmatites in the southwestern Grenville Province. *Can. Mineral.* **30**, 571-585.

Li C. and Naldrett A.J. (1993) High chlorite alteration minerals and calcium-rich brines in fluid inclusions from the Strathcona Deep Cooper Zone, Sudbury, Ontario. *Econ. Geol.* **88**, 1780-1796.

Lightfoot P.C., Keays R.R., Morrison G.G., Bite A. and Farrell K.P. (1997a) Geochemical relationships in the Sudbury Igneous Complex: Origin of the Main Mass and Offset Dikes. *Econ. Geol.* **92**, 289-307.

Lightfoot P.C., Keays R.R., Morrison G.G., Bite A. and Farrell K.P. (1997b) Geologic and Geochemical Relationships between the Contact Sublayer, Inclusions, and the Main Mass of the Sudbury Igneous Complex: A Case Study of the Whistle Mine Embayment. *Econ. Geol.* **92**, 647-673.

Lightfoot P.C., Doherty W., Farrell K., Keays R.R., Moore M. and Pekeski D. (1997c) Geochemistry of the Main Mass, Sublayer, Offsets, and inclusions from the Sudbury Igneous Complex, Ontario. *Ont. Geol. Surv. Open File Rept.* **5959**, 231p.

Lowenstern J.B., Clynne M.A. and Bullen T.D. (1997) Comagmatic A-type granophyre and rhyolite from the Alid volcanic center, Eritrea, Northeast Africa. *J. Petrol.* **38**, 1707-1721.

Maaløe S. (1985) *Principles of igneous petrology.* Springer-Verlag, New York, 374p.

Manning D.A.C. (1982) Chemical and morphological variation in tourmalines from the Hub Kapong batholith of peninsular Thailand. *Min. Mag.* **45**, 139-147.

Marsh B.D. and Zieg M. (1999) Solidification fronts of the Sudbury melt sheet. *Geol. Ass. Can. - Mineral. Ass. Can. Joint Ann. Meeting, Sudbury 1999, Guidebook Field Trip* **B9**, 34 p.

Marshall D., Watkinson D., Farrow C., Molnár F. and Fouillac A.-M. (1999) Multiple fluid generations in the Sudbury igneous complex: fluid inclusion, Ar, O, H, Rb and Sr evidence. *Chem. Geol.* **154**, 1-19.

Masaitis V.L. (1994) Impactites from Popigai crater. *In* Large Meteorite Impacts and Planetary Evolution (Dressler B.O., Grieve R.A.F. and Sharpton V.L., eds.), *Geol. Soc. Am. Sp. Pap.* **293**, 153-162.

McPherson Coombes C.L.A. (1996) *Petrographic and Geochemical Study of the Quartz Gabbro and the Norite Phases of the Sudbury Igneous Complex.* B.Sc. Thesis. Brock University, Ontario. 45pp.

Meldrum A., Abdel-Rahman A.-F.M., Martin R.F. and Wodicka N. (1997) The nature, age and petrogenesis of the Cartier Batholith, northern flank of the Sudbury Structure, Ontario, Canada. *Precambrian Res.* **82**, 265-285.

Melosh H.J. (1989) *Impact Cratering. A Geologic Process.* Oxford University Press, New York, 245p.

Molnár F., Watkinson D.H., Jones P.C. and Gatter I. (1997) Fluid inclusions evidence for hydrothermal enrichment of magmatic ore at the contact zone of the Ni-Cu-platinum-group element 4b deposit, Lindsley Mine, Sudbury, Canada. *Econ. Geol.* **92**, 674-685.

Molnár F., Watkinson D.H., and Everest J.O. (1999) Fluid-inclusion characteristics of hydrothermal Cu-Ni-PGE veins in granitic and metavolcanic rocks at the contact of the Little Stobie deposit, Sudbury, Canada. *Chem. Geol.* **154**, 279-301.

Morrison G.G. (1984) Morphological features of the Sudbury Structure in relation to an impact origin. *In* The geology and ore deposits of the Sudbury Structure (Pye E.G., Naldrett A.J. and Giblin P.E., eds.). *Ont. Geol. Surv. Sp. Vol.* **1**, 513-520.

Morse S.A. (1990) A discussion of Hunter and Sparks (Contrib. Mineral. Petrol. 95, 451-461). *Contr. Min. Pet.* **104**, 240-244.

Naldrett A.J. (1986) Geochemistry of the Sudbury Igneous Complex: A Model for the Complex and Its Ores. *In* Geology and Metallogeny of Copper Deposits (Friedrich G.H., Genkin A.D., Naldrett A.J., Ridge J.D., Sillitoe R.H. and Vokes F.M., eds.), Springer-Verlag Berlin Heidelberg, *Sp. Publ. Soc. Geol. Applied to Min. Deposits* **4**, 91-110.

Naldrett A.J. (1999) Summary: Development of ideas on Sudbury geology, 1992-1998. *In* Large Meteorite Impacts and Planetary Evolution II (Dressler B.O. and Sharpton V.L., eds.), Boulder, Colorado, *Geol. Soc. Amer. Sp. Pap.* **339**, 431-442.

Naldrett A.J. and Hewins R.H. (1984) The Main Mass of the Sudbury Igneous Complex. *In* The Geology and Ore Deposits of the Sudbury Structure (Pye E.G., Naldrett A.J. and Giblin P.E., eds.), *Ont. Geol. Surv. Sp. Vol.* **1**, 235-251.

Naldrett A.J. and Kullerud G. (1967) A study of the Strathcona Mine and its bearing on the origin of the Nickel-Copper Ores of the Sudbury District, Ontario. *J. Petrol.* **8**, 453-531.

Naldrett A.J., Bray J.G., Gasparrini E.L., Podolsky T. and Rucklidge J.C. (1970) Cryptic variation and petrology of the Sudbury Nickel Irruptive. *Econ. Geol.* **65**, 122-155.

Naldrett A.J., Rao B.V. and N.M. Evensen (1986) Contamination at Sudbury and its role in ore formation. *In* Metallogeny of basic and ultrabasic rocks, *London, Institute of Mining and Metallurgy*, 75-91.

NEWPET 8 1987-1994 Memorial University of Newfoundland, Department of Earth Sciences, Centre for Earth Resources Research. All rights reserved.

Norman M.C. (1994) Sudbury Igneous Complex: Impact melt or endogenous magma? Implications for lunar crustal evolution. *In* Large Meteorite Impacts and Planetary Evolution (Dressler B.O., Grieve R.A.F. and Sharpton V.L., eds.), *Geol. Soc. Am. Sp. Pap.* **293**, 331-341.

Onorato P.I.K., Ulhmann D.R. and Simonds C.H. (1978) The thermal history of the Manicouagan impact melt sheet, Quebec. *J. Geophys. Res.* **83**, 2789-2798.

Ostermann M. (1996) *Die Geochemie der Impaktschmeltzdecke (Sudbury Igneous Complex) im Multiring-Becken Sudbury (in German).* Ph.D. thesis, Institut für Planetologie, Münster, Germany, 168p.

Palme H. (1980) The meteoritic contamination of terrestrial and lunar impact melts and the problem of indigenous siderophiles in the lunar highland. *Proc. Lunar Planet. Sci. Conf.* **11**, 481-506.

Pattison E.F. (1979) The Sudbury Sublayer. *Can. Mineral.* **17**, 257-274.

Pearce T.H. (1968) A contribution to the theory of variation diagrams. *Contr. Min. Pet.* **19**, 142-157.

Pearce T.H. (1987) The identification and assessment of spurious trends in Pearce-type ratio variation diagrams: a discussion of some statistical arguments. *Contr. Min. Pet.* **97**, 529-534.

Peredery W.V. and Naldrett A. (1975) Petrology of the Upper Irruptive Rocks, Sudbury, Ontario. *Econ. Geol.* **70**, 164-175.

Phemister T.C. (1926) Igneous rocks of Sudbury and their relation to the ore deposits. *Ont. Dept. Mines, Ann. Rept. 1925* **34**, Part 8, 1-61.

Pilkington M., Hildebrand A.R. and Ortiz-Aleman C. (1994) Gravity and magnetic field modelling and structure of the Chicxulub crater, Mexico. *J. Geophys. Res.* **99**, 13,147-13,162

Prevec S.A. (2000) An examination of modal variation mechanisms in the contact sublayer of the Sudbury Igneous Complex, Canada. *Miner. and Petrol.* **68**, 141-157.

Reimold W.U., Koeberl C., Brandstätter F., Kruger F.J., Armstrong R.A. and Bootsman C. (1999) Morokweng impact structure, South Africa: Geologic, petrographic, and isotopic results, and implications for the size of the structure. *In* Large Meteorite Impacts and Planetary Evolution II (Dressler B.O. and Sharpton V.L., eds.), Boulder, Colorado, *Geol. Soc. Amer. Sp. Pap.* **339**, 61-90.

Reiners P.W., Nelson B.K. and Ghiorso M.S. (1995) Assimilation of felsic crust by basaltic magma: Thermal limits and extents of crustal contamination of mantle-derived magmas. *Geology* **23**, 563-566.

Riller U., Schwerdtner W.M., Halls H.C. and Card K.D. (1999) Transpressive tectonism in the eastern Penokean Orogen, Canada; consequences for Proterozoic crustal kinematics and continental fragmentation. *Precambrian Res.* **93**, 51-70.

Robertson P.B., Dence M.R. and Vos M.A. (1968) Deformation in rock-forming minerals from Canadian craters. *In* Shock Metamorphism of Natural Materials (French B.M. and Short N.M., eds.), Mono Book Corp., Baltimore, 433-452.

Roest W.R. and Pilkington M. (1994) Restoring post-impact deformation at Sudbury: A circular argument. *Geophys. Res. Lett.* **21**, 959-962.

Rousell D.H., Gibson H.L. and Jonasson I.R. (1997) The tectonic, magmatic and mineralization history of the Sudbury Structure. *Explor. Mining Geol.* **6**, 1-22.

Russell J.K. and Stanley C.R. (1990a) Theory and application of Pearce element ratios to geochemical data analysis. *Geol. Ass. Can., Vancouver, British Columbia, Short Course Volume* **8**, 315pp.

Russell J.K. and Stanley C.R. (1990b) A theoretical basis for the development and use of chemical variation diagrams. *Geochim. Cosmochim. Acta* **54**, 2419-2431.

Sazonova L.V. (1983) Structure of melt impactites as a reflector on the conditions of impact melt cooling (exemplified by the Yanisyarvi meteorite crater). Vestnik Moskovskogo Universiteta. *Geologiya* **38**, 40-46.

Schandl E.S., Martin R.F. and Stevenson J.S. (1986) Feldspar mineralogy of the Sudbury Igneous Complex and the Onaping Formation, Sudbury, Ontario. *Can. Mineral.* **24**, 747-759.

Scott R.G. and Spray J.G. (1999) Magnetic fabric constraints on friction melt flow regimes and ore emplacement direction within the South Range Breccia Belt, Sudbury Impact Structure. *Tectonophys.* **307**, 163-189.

Sonnenthal E.L. (1990) *Part I. Metasomatic replacement and the behavior of fluorine and chlorine during differentiation of the Skaergaard Intrusion, East Greenland. Part II. Geochemical and physical aspects of melt segregation in the Picture Gorge basalt, Oregon.* Ph.D. Thesis, University of Oregon, 258pp.

Spray J.G. and Thompson L.M. (1995) Friction melt distribution in a multi-ring impact basin. *Nature* **373**, 130-132.

Spray J.G., Kelley S.P. and Reimold W.U. (1995) Laser probe ^{40}Ar-^{39}Ar dating of coesite- and stishovite-bearing pseudotachylytes and the age of the Vredefort impact event. *Meteoritics* **30**, 335-343.

Stanley C.R. (1993) Effects of Non-Conserved Denominators on Pearce Element Ratio Diagrams. *Math. Geol.* **25**, 1049-1070.

Stevenson J.S. (1961) Recognition of the quartzite breccia in the Whitewater Series, Sudbury Basin, Ontario. *Royal Soc. Canada Trans., 3rd ser.* **55**, 57-66.

Stevenson J.S. (1963) The upper contact phase of the Sudbury Micropegmatite. *Can. Mineral.* **7**, 413-419.

Stevenson J.S. and Colgrove G.L. (1968) The Sudbury Irruptive: Some petrogenetic concepts based on recent field work. *Report of 23rd Inter. Geol. Congress, Czechoslavakia*, **5**, 27-35.

Stöffler D. and Langenhorst F. (1994) Shock metamorphism of quartz in nature and experiment: 1. Basic observation and theory. *Meteoritics* **29**, 155-181.

Stöffler D., Deutsch A., Avermann M., Bischoff L., Brockmeyer P., Buhl D., Lakomy R. and Müller-Mohr V. (1994) The formation of the Sudbury Structure, Canada: Toward a unified impact model. *In* Large Meteorite Impacts and Planetary Evolution (Dressler B.O., Grieve R.A.F. and Sharpton V.L., eds.), *Geol. Soc. Am. Sp. Pap.* **293**, 303-318.

Streckeisen A. (1976) To each plutonic rock its proper name. *Earth Sci. Rev.* **12**, 1-33.

Sun S.S. and McDonough W.F. (1989) Chemical and isotopic systematics of oceanic basalts; implications for mantle composition and processes. *Geol. Soc. London Sp. Publ.* **42**, 313-345.

Swanson S.E. and Fenn P.M. (1986) Quartz crystallization in igneous rocks. *Am. Mineral.* **71**, 331-342.

Taylor H.P.Jr (1967) Origin of Red-Rock Granophyres (abstract). *Trans. - Amer. Geophys. Union* **48**, 245-246.

Taylor R.W. (1964) Phase equilibria in the system FeO-Fe_2O_3-TiO_2 at 1300°C. *Am. Mineral.* **69**, 1016-1030.

Therriault A.M., Reimold W.U. and Reid A.M. (1996) Field relations and petrography of the Vredefort Granophyre. *S. Afr. J. Geol.* **99**, 1-21.

Therriault A.M., Grieve R.A.F. and Reimold W.U. (1997) Original size of the Vredefort Structure: Implications for the geological evolution of the Witwatersrand Basin. *Meteorit. & Planet. Sci.* **32**, 71-77.

Thode H.G., Dunford H.B. and Shima M. (1962) Sulfur isotope abundances in rocks of the Sudbury District and their geological significance. *Econ. Geol.* **57**, 565-578.

Thompson L.M., Spray J.G. and Kelley S.P. (1998) Laser probe argon-40/argon-39 dating of pseudotachylyte from the Sudbury Structure: Evidence for postimpact thermal overprinting in the North Range. *Meteor. & Planet. Sci.* **33**, 1259-1269.

Thomson J.E. (1969) A discussion of Sudbury geology and sulphide deposits. *Ont. Dept. Mines, Misc. Pap.* **30**, 22p.

van Schmus W.R. (1980) Chronology of igneous rocks associated with the Penokean Orogeny in Wisconsin. *Geol. Soc. of Amer. Sp. Pap.* **182**, 159-168.

von Foullon, H.B. (1892) Ueber einige Nickelerzvorkommen (*in German*). *Verhandlungen der Geologischen Bundersanstalt*, 223-310.

Walker R.J., Morgan J.W., Naldrett A.J., Li C. and Fassett J.D. (1991) Re-Os isotope systematics of Ni-Cu sulfide ores, Sudbury Igneous Complex, Ontario: evidence for a major crustal component. *Earth Planet. Sci. Lett.* **105**, 416-429.

Walker T.L. (1897) Geological and petrological studies of the Sudbury Nickel District, Canada. *Geol. Soc. of London, Quarterly Journ.* **53**, 40-66.

Warner S., Martin R.F., Abdel-Rahman A.-F. M. and Doig R. (1998) Apatite as a monitor of fractionation, degassing, and metamorphism in the Sudbury Igneous Complex, Ontario. *Can. Mineral.* **36**, 981-999.

Williams G.H. (1891) Notes on the microscopial character of rocks from the Sudbury Mining District, Canada. *In* Appendix I, *Geol. Surv. Can. Ann. Rept. New Series* **5**, Part 1, 55F-82F.

Williams H. (1957) Glowing avalanche deposits of the Sudbury Basin. *Ont. Dept. Mines Ann. Rept. 1956* **65**, Part 3, 57-89.

Wood C.R. and Spray J.G. (1998) Origin and emplacement of Offset Dykes in the Sudbury impact structure: Constraints from Hess. *Meteorit. & Planet. Sci.* **33**, 337-347.

Zhou M.-F., Lightfoot P.C., Keays R.R., Moore M.L. and Morrison G.G. (1997) Petrogenetic significance of chromian spinels from the Sudbury Igneous Complex, Ontario, Canada. *Can. J. Earth Sci.* **34**, 1405-1419.

Zolnai A.I., Price R.A. and Helmstaedt H. (1984) Regional cross section of the Southern Province adjacent to Lake Huron, Ontario: Implications for the tectonic significance of the Murray fault zone. *Can. J. Earth Sci.* **21**, 447-456.

APPENDIX A

Microprobe analysis of minerals carried out on various samples used in this study.

Mineral analysed	# of oxygens used in calculating the mineral formula	Data used in Figures	Page
Feldspar	8	Ab, An and Or in mol% used in Fig. 7; An/(An+Ab) used in Fig. 13	A2
Pyroxene	6	En, Wo and Fs in mol% used in Fig. 16	A33
Amphibole* pseudomorphs after pyroxene	23	-	A37
Amphibole*	23	-	A47
Various oxides	not calculated	-	A51
Titanite	not calculated	-	A52

Note: * = nomenclature according to Leake et al. (1997)

Abbreviations used in this appendix:

alter = alteration
B = bright phase in backscattered image
cl = clast or xenocryst
D = dark phase in backscattered image
graphic = micrographic or granophyric intergrowth
inc = micro-inclusion
Kf = alkali feldspar
L = light gray phase in backscattered image
lam = lamellae
over = overgrowth
Pl = plagioclase
px = pyroxene

Feldspars	Sample SUD-85-1994; Drill core 70011				Sample SUD-2-1994; Drill core 70011					
point	lath core	lath core	lath	lath rim	lath rim	lath core	lath rim	lath core	lath core	lath core
SiO_2	66.408	66.189	66.692	65.639	66.440	66.566	67.473	66.545	66.622	66.098
Al_2O_3	20.538	19.572	19.785	19.657	19.994	20.088	20.309	19.913	19.994	19.947
FeO	0.055	0.115	0.268	0.464	0.046	0.000	0.071	0.000	0.000	0.031
CaO	0.515	0.389	0.391	1.144	0.284	0.382	0.343	0.245	0.119	0.250
Na_2O	10.794	11.279	11.061	11.132	11.417	10.994	11.448	11.400	11.653	11.361
K_2O	0.081	0.121	0.083	0.159	0.054	0.005	0.052	0.045	0.080	0.034
BaO	0.219	0.101	0.189	0.000	0.000	0.192	0.083	0.000	0.000	0.137
SrO	0.041	0.239	0.000	0.000	0.103	0.143	0.205	0.000	0.000	0.143
Total	98.651	98.005	98.469	98.195	98.338	98.370	99.984	98.148	98.468	98.001
Si	2.946	2.963	2.966	2.941	2.957	2.961	2.957	2.964	2.960	2.955
Al	1.074	1.033	1.037	1.038	1.049	1.053	1.049	1.045	1.047	1.051
Fe2+	0.002	0.004	0.010	0.017	0.002	0.000	0.003	0.000	0.000	0.001
Ca	0.024	0.019	0.019	0.055	0.014	0.018	0.016	0.012	0.006	0.012
Na	0.928	0.979	0.954	0.967	0.985	0.948	0.973	0.984	1.004	0.985
K	0.005	0.007	0.005	0.009	0.003	0.000	0.003	0.003	0.005	0.002
Ba	0.004	0.002	0.003	0.000	0.000	0.003	0.001	0.000	0.000	0.002
Sr	0.001	0.006	0.000	0.000	0.003	0.004	0.005	0.000	0.000	0.004
Total	4.984	5.013	4.994	5.028	5.012	4.987	5.007	5.007	5.021	5.013
Ab	96.965	97.455	97.611	93.792	98.342	98.087	98.083	98.573	98.994	98.607
Or	0.479	0.688	0.482	0.881	0.306	0.029	0.293	0.256	0.447	0.194
An	2.557	1.857	1.907	5.326	1.352	1.883	1.624	1.171	0.559	1.199
An/(Ab+An)	2.569	1.870	1.916	5.374	1.356	1.884	1.629	1.174	0.561	1.201

Feldspars	SUD-2-1994; Drill core 70011 (cont'd)				Sample SUD-3-1994; Drill core 70011					
point	lath rim	lath rim	lath rim	graphic	Pl rim	Pl	Pl core	Pl rim	Pl over	Pl over
SiO_2	66.953	66.478	66.241	62.452	68.536	68.745	67.070	68.217	64.546	67.312
Al_2O_3	19.801	20.221	20.370	18.743	19.674	19.933	19.733	19.332	18.410	17.371
FeO	0.086	0.000	0.031	0.045	0.704	0.114	0.140	0.127	0.000	0.482
CaO	0.239	0.208	0.409	0.011	0.269	0.395	0.486	0.236	0.000	0.638
Na_2O	11.175	11.617	11.300	0.208	11.326	11.326	10.309	11.086	0.239	4.109
K_2O	0.105	0.039	0.066	16.297	0.081	0.069	0.105	0.098	16.857	9.684
BaO	0.028	0.275	0.000	1.075	0.246	0.370	0.492	0.083	0.248	0.330
SrO	0.082	0.184	0.041	0.000	0.000	0.075	0.000	0.000	0.000	0.024
Total	98.469	99.022	98.458	98.831	100.836	101.027	98.335	99.179	100.300	99.950
Si	2.972	2.948	2.944	2.954	2.982	2.981	2.982	3.002	2.990	3.047
Al	1.036	1.057	1.067	1.045	1.009	1.019	1.034	1.003	1.005	0.927
Fe2+	0.003	0.000	0.001	0.002	0.026	0.004	0.005	0.005	0.000	0.018
Ca	0.011	0.010	0.019	0.001	0.013	0.018	0.023	0.011	0.000	0.031
Na	0.962	0.999	0.974	0.019	0.956	0.952	0.889	0.946	0.021	0.361
K	0.006	0.002	0.004	0.984	0.004	0.004	0.006	0.006	0.996	0.559
Ba	0.000	0.005	0.000	0.020	0.004	0.006	0.009	0.001	0.005	0.006
Sr	0.002	0.005	0.001	0.000	0.000	0.002	0.000	0.000	0.000	0.001
Total	4.993	5.025	5.011	5.024	4.993	4.987	4.948	4.973	5.017	4.949
Ab	98.232	98.804	97.671	1.902	98.248	97.725	96.829	98.272	2.109	37.929
Or	0.607	0.218	0.375	98.043	0.462	0.392	0.649	0.572	97.891	58.817
An	1.161	0.978	1.954	0.056	1.289	1.883	2.523	1.156	0.000	3.254
An/(Ab+An)	1.168	0.980	1.961		1.295	1.891	2.539	1.163		

Feldspars	Sample SUD-3-1994; Drill core 70011 (continued)								SUD-4-1994	
point	Pl rim	Pl	Pl	Pl	Pl core	Pl	Pl	Pl rim	Pl rim	Pl
SiO_2	68.371	68.856	68.993	69.040	68.300	69.156	67.680	68.439	66.088	70.699
Al_2O_3	19.712	20.031	19.731	19.691	19.882	19.562	19.648	19.948	19.421	17.698
FeO	0.000	0.040	0.000	0.000	0.067	0.040	0.033	0.013	0.102	0.038
CaO	0.393	0.442	0.278	0.206	0.508	0.153	0.393	0.445	0.167	0.123
Na_2O	11.080	11.233	11.502	11.219	11.026	11.396	11.039	11.033	11.572	10.968
K_2O	0.071	0.098	0.048	0.088	0.114	0.112	0.078	0.057	0.078	0.047
BaO	0.370	0.000	0.083	0.288	0.000	0.000	0.000	0.000	0.953	0.000
SrO	0.025	0.000	0.123	0.000	0.000	0.098	0.000	0.000	0.000	0.000
Total	100.022	100.700	100.758	100.532	99.897	100.517	98.871	99.935	98.381	99.573
Si	2.990	2.984	2.992	2.999	2.984	3.002	2.987	2.986	2.963	3.082
Al	1.016	1.023	1.009	1.008	1.024	1.001	1.022	1.026	1.026	0.909
Fe2+	0.000	0.001	0.000	0.000	0.002	0.001	0.001	0.000	0.004	0.001
Ca	0.018	0.021	0.013	0.010	0.024	0.007	0.019	0.021	0.008	0.006
Na	0.939	0.944	0.967	0.945	0.934	0.959	0.944	0.933	1.006	0.927
K	0.004	0.005	0.003	0.005	0.006	0.006	0.004	0.003	0.004	0.003
Ba	0.006	0.000	0.001	0.005	0.000	0.000	0.000	0.000	0.017	0.000
Sr	0.001	0.000	0.003	0.000	0.000	0.002	0.000	0.000	0.000	0.000
Total	4.974	4.979	4.988	4.972	4.974	4.980	4.977	4.969	5.029	4.928
Ab	97.674	97.325	98.415	98.492	96.875	98.630	97.626	97.496	98.774	99.106
Or	0.412	0.559	0.270	0.508	0.659	0.638	0.454	0.331	0.438	0.279
An	1.914	2.116	1.314	0.999	2.466	0.732	1.921	2.173	0.788	0.614
An/(Ab+An)	1.922	2.128	1.318	1.004	2.483	0.736	1.929	2.180	0.791	0.616

Feldspars	Sample SUD-4-1994; Drill core 70011 (continued)							Sample SUD-5-1994		
point	Pl	Pl core	Pl core	Pl rim	Pl core	Pl rim	matrix	Pl1 rim	Pl2 rim	Pl4 rim
SiO_2	65.759	66.409	67.185	66.534	66.786	66.681	65.966	65.924	65.400	65.986
Al_2O_3	19.386	19.759	19.785	19.813	19.772	19.474	19.772	20.321	20.697	20.166
FeO	0.040	0.034	0.000	0.000	0.034	0.092	0.000	0.046	0.015	0.081
CaO	0.115	0.262	0.312	0.262	0.194	0.147	0.171	0.467	1.213	0.417
Na_2O	11.926	11.617	11.655	11.615	11.493	11.538	9.619	11.171	10.746	11.552
K_2O	0.048	0.049	0.045	0.067	0.043	0.049	3.716	0.028	0.108	0.145
BaO	0.598	0.000	0.041	0.027	0.000	0.000	0.150	0.000	0.000	0.000
SrO	0.151	0.121	0.030	0.030	0.121	0.075	0.075	0.061	0.164	0.020
Total	98.023	98.251	99.053	98.348	98.443	98.056	99.469	98.018	98.343	98.367
Si	2.958	2.961	2.969	2.962	2.968	2.975	2.950	2.943	2.918	2.942
Al	1.028	1.038	1.030	1.040	1.036	1.024	1.042	1.069	1.088	1.060
Fe2+	0.002	0.001	0.000	0.000	0.001	0.003	0.000	0.002	0.001	0.003
Ca	0.006	0.013	0.015	0.012	0.009	0.007	0.008	0.022	0.058	0.020
Na	1.040	1.004	0.999	1.003	0.990	0.998	0.834	0.967	0.930	0.999
K	0.003	0.003	0.003	0.004	0.002	0.003	0.212	0.002	0.006	0.008
Ba	0.011	0.000	0.001	0.000	0.000	0.000	0.003	0.000	0.000	0.000
Sr	0.004	0.003	0.001	0.001	0.003	0.002	0.002	0.002	0.004	0.001
Total	5.050	5.023	5.017	5.021	5.010	5.013	5.052	5.007	5.005	5.032
Ab	99.209	98.499	98.296	98.400	98.835	99.026	79.113	97.585	93.546	97.257
Or	0.283	0.273	0.250	0.373	0.243	0.277	20.110	0.161	0.619	0.803
An	0.529	1.228	1.454	1.227	0.922	0.697	0.777	2.254	5.835	1.940
An/(Ab+An)	0.530	1.231	1.458	1.231	0.924	0.699	0.973	2.258	5.871	1.956

Feldspars	SUD-5-1994 (continued)			Sample SUD-173-1995; Drill core 70011						
point	Pl6 core	Pl6 rim	Kf1	Pl1 core	Pl1 rim	Pl1 inc	Pl2 rim	Pl3 rim	Pl4 rim	Pl5 core
SiO_2	66.260	66.596	61.930	66.602	66.446	61.845	65.798	66.510	62.921	67.030
Al_2O_3	20.001	20.015	18.566	20.651	20.659	18.976	19.949	19.988	22.390	20.287
FeO	0.000	0.000	0.217	0.031	0.036	0.000	0.067	0.112	0.076	0.000
CaO	0.518	0.474	0.000	0.589	0.567	0.027	0.579	0.428	2.896	0.323
Na_2O	11.307	11.274	0.278	10.288	10.355	0.208	11.369	11.073	9.673	10.816
K_2O	0.099	0.033	16.958	0.100	0.111	15.912	0.071	0.299	0.106	0.067
BaO	0.083	0.000	0.249	0.000	0.028	1.574	0.083	0.165	0.468	0.083
SrO	0.143	0.205	0.000	0.061	0.000	0.059	0.123	0.144	0.041	0.000
Total	98.411	98.597	98.198	98.322	98.202	98.601	98.039	98.719	98.571	98.606
Si	2.952	2.957	2.948	2.953	2.950	2.940	2.945	2.956	2.824	2.965
Al	1.050	1.048	1.042	1.079	1.081	1.063	1.052	1.047	1.184	1.058
Fe2+	0.000	0.000	0.009	0.001	0.001	0.000	0.003	0.004	0.003	0.000
Ca	0.025	0.023	0.000	0.028	0.027	0.001	0.028	0.020	0.139	0.015
Na	0.977	0.971	0.026	0.884	0.891	0.019	0.987	0.954	0.842	0.928
K	0.006	0.002	1.030	0.006	0.006	0.965	0.004	0.017	0.006	0.004
Ba	0.001	0.000	0.005	0.000	0.000	0.029	0.001	0.003	0.008	0.001
Sr	0.004	0.005	0.000	0.002	0.000	0.002	0.003	0.004	0.001	0.000
Total	5.014	5.005	5.059	4.953	4.958	5.020	5.024	5.006	5.008	4.971
Ab	96.986	97.546	2.431	96.336	96.403	1.945	96.876	96.235	85.277	97.984
Or	0.559	0.188	97.569	0.616	0.680	97.915	0.398	1.710	0.615	0.399
An	2.455	2.266	0.000	3.048	2.917	0.140	2.726	2.056	14.108	1.617
An/(Ab+An)	2.469	2.271		3.067	2.937		2.737	2.091	14.196	1.623

Feldspars	SUD-173-1995		Sample SUD-87-1994; Drill core 70011							
point	graphic	graphic	lath rim	lath core	lath rim	lath rim	Pl	lath core	Pl	lath rim
SiO_2	61.810	62.247	68.176	67.652	65.104	68.705	69.079	68.921	68.752	68.257
Al_2O_3	18.873	18.694	19.636	19.538	19.799	20.127	19.355	20.014	19.706	19.562
FeO	0.060	0.117	0.121	0.013	3.336	0.060	0.048	0.000	0.027	0.169
CaO	0.000	0.007	0.565	0.539	0.459	0.749	0.250	0.330	0.208	0.388
Na_2O	0.229	0.767	11.101	10.114	10.540	10.924	11.109	11.241	11.346	11.171
K_2O	16.744	15.895	0.046	1.485	0.002	0.073	0.095	0.055	0.031	0.048
BaO	1.408	0.414	0.000	0.000	0.000	0.000	0.083	0.288	0.247	0.000
SrO	0.000	0.098	0.050	0.000	0.248	0.000	0.000	0.124	0.322	0.025
Total	99.124	98.239	99.695	99.341	99.488	100.638	100.019	100.973	100.639	99.620
Si	2.935	2.951	2.987	2.987	2.912	2.979	3.011	2.985	2.991	2.992
Al	1.056	1.044	1.014	1.017	1.044	1.029	0.994	1.022	1.010	1.010
Fe2+	0.002	0.005	0.004	0.000	0.125	0.002	0.002	0.000	0.001	0.006
Ca	0.000	0.000	0.027	0.025	0.022	0.035	0.012	0.015	0.010	0.018
Na	0.021	0.071	0.943	0.866	0.914	0.918	0.939	0.944	0.957	0.949
K	1.014	0.961	0.003	0.084	0.000	0.004	0.005	0.003	0.002	0.003
Ba	0.026	0.008	0.000	0.000	0.000	0.000	0.001	0.005	0.004	0.000
Sr	0.000	0.003	0.001	0.000	0.006	0.000	0.000	0.003	0.008	0.001
Total	5.055	5.043	4.979	4.979	5.023	4.968	4.964	4.977	4.983	4.979
Ab	2.036	6.830	97.007	88.805	97.638	95.943	98.226	98.093	98.821	97.845
Or	97.964	93.135	0.264	8.579	0.012	0.422	0.553	0.316	0.178	0.277
An	0.000	0.034	2.728	2.615	2.350	3.635	1.222	1.591	1.001	1.878
An/(Ab+An)			2.736	2.861	2.350	3.651	1.228	1.596	1.003	1.883

Feldspars	SUD-179-1995; Drill core 70011						SUD-89-1994; Drill core 70011				
point	Pl1 core	Pl1 rim	Pl2 rim	Pl3 core	Pl3 rim	Pl7 rim	Pl1 core	Pl1 rim	Pl1 rim	Pl2 core	Pl2 rim
SiO_2	66.031	66.245	66.361	66.889	65.969	66.042	56.263	55.615	61.468	54.520	59.134
Al_2O_3	20.493	20.498	20.931	20.045	20.487	20.383	26.244	26.873	23.238	27.340	24.279
FeO	0.086	0.382	0.091	0.198	0.112	0.072	0.464	0.673	0.328	0.790	0.291
CaO	0.883	0.791	0.786	0.344	0.791	0.744	8.210	8.767	4.484	10.081	5.924
Na_2O	11.014	11.127	10.952	11.328	11.315	11.110	6.488	6.333	9.128	5.579	7.628
K_2O	0.047	0.042	0.057	0.102	0.086	0.052	0.573	0.219	0.164	0.416	0.859
BaO	0.000	0.000	0.165	0.137	0.000	0.000	0.221	0.415	0.277	0.000	0.249
SrO	0.082	0.000	0.041	0.000	0.061	0.000	0.145	0.063	0.000	0.084	0.187
Total	98.636	99.085	99.384	99.043	98.821	98.403	98.608	98.958	99.087	98.810	98.551
Si	2.934	2.933	2.927	2.959	2.929	2.939	2.573	2.540	2.760	2.499	2.689
Al	1.073	1.069	1.088	1.045	1.072	1.069	1.415	1.446	1.230	1.477	1.301
Fe2+	0.003	0.014	0.003	0.007	0.004	0.003	0.018	0.026	0.012	0.030	0.011
Ca	0.042	0.038	0.037	0.016	0.038	0.035	0.402	0.429	0.216	0.495	0.289
Na	0.949	0.955	0.937	0.972	0.974	0.959	0.575	0.561	0.795	0.496	0.673
K	0.003	0.002	0.003	0.006	0.005	0.003	0.033	0.013	0.009	0.024	0.050
Ba	0.000	0.000	0.003	0.002	0.000	0.000	0.004	0.007	0.005	0.000	0.004
Sr	0.002	0.000	0.001	0.000	0.002	0.000	0.004	0.002	0.000	0.002	0.005
Total	5.006	5.011	4.999	5.007	5.024	5.007	5.024	5.024	5.027	5.023	5.022
Ab	95.501	95.991	95.870	97.780	95.819	96.146	56.903	55.937	77.925	48.838	66.522
Or	0.268	0.238	0.328	0.579	0.479	0.296	3.307	1.273	0.921	2.396	4.929
An	4.231	3.771	3.802	1.641	3.702	3.558	39.790	42.791	21.153	48.766	28.549
An/(Ab+An)	4.242	3.780	3.815	1.650	3.719	3.569	41.151	43.342	21.350	49.963	30.029

Feldspars	Sample SUD-89-1994; Drill core (continued)										
point	Pl3 core	Pl4 core	Pl4 rim	Pl5 core	Pl5 rim	Pl6 core	Pl6 rim	Pl7 core	Pl8 core	Pl8 rim	graphic
SiO_2	55.127	64.478	65.321	53.717	54.798	62.272	64.129	63.216	58.875	62.961	62.803
Al_2O_3	26.854	21.787	20.888	28.595	27.270	23.164	21.500	22.000	25.167	22.641	17.925
FeO	0.581	0.307	0.031	0.567	0.538	0.390	0.067	0.301	0.342	0.210	0.055
CaO	9.123	1.308	1.153	10.725	9.700	2.616	1.942	1.240	6.671	3.551	0.111
Na_2O	5.947	10.126	10.993	5.509	5.816	9.274	10.402	9.890	7.272	9.909	0.648
K_2O	0.413	0.693	0.065	0.177	0.381	0.985	0.040	1.476	0.748	0.055	14.200
BaO	0.000	0.221	0.083	0.166	0.056	0.000	0.138	0.000	0.083	0.111	3.112
SrO	0.000	0.041	0.000	0.252	0.168	0.000	0.000	0.310	0.021	0.000	0.040
Total	98.045	98.961	98.534	99.708	98.727	98.701	98.218	98.433	99.179	99.438	98.894
Si	2.534	2.874	2.910	2.447	2.510	2.795	2.873	2.847	2.657	2.804	2.984
Al	1.455	1.144	1.097	1.535	1.472	1.225	1.135	1.168	1.339	1.189	1.004
Fe2+	0.022	0.011	0.001	0.022	0.021	0.015	0.003	0.011	0.013	0.008	0.002
Ca	0.449	0.062	0.055	0.523	0.476	0.126	0.093	0.060	0.323	0.169	0.006
Na	0.530	0.875	0.950	0.487	0.517	0.807	0.904	0.864	0.636	0.856	0.060
K	0.024	0.039	0.004	0.010	0.022	0.056	0.002	0.065	0.043	0.003	0.861
Ba	0.000	0.004	0.001	0.003	0.001	0.000	0.002	0.000	0.001	0.002	0.058
Sr	0.000	0.001	0.000	0.007	0.004	0.000	0.000	0.006	0.001	0.000	0.001
Total	5.015	5.011	5.018	5.034	5.023	5.024	5.012	5.043	5.013	5.031	4.975
Ab	52.815	89.573	94.175	47.688	50.897	81.582	90.441	85.654	63.508	83.217	6.446
Or	2.413	4.034	0.366	1.008	2.194	5.701	0.229	8.411	4.298	0.304	92.944
An	44.772	6.394	5.458	51.304	46.909	12.717	9.331	5.935	32.194	16.479	0.610
An/(Ab+An)	45.879	6.662	5.478	51.826	47.961	13.486	9.352	6.480	33.640	16.530	

Feldspars	Sample SUD-89-1994; Drill core 70011 (cont'd)						Sample SUD-59-1994; Drill core 70011				
point	graphic	graphic	graphic	graphic	matrix	matrix	Pl rim	Pl rim	Pl core	Pl rim	Pl rim
SiO_2	63.841	63.150	63.438	63.209	64.057	57.979	65.847	53.487	55.127	55.200	61.419
Al_2O_3	18.654	18.841	18.870	18.395	21.980	25.322	19.976	27.591	26.295	26.306	22.265
FeO	0.138	0.244	0.000	0.046	0.117	0.470	0.511	0.567	0.628	0.639	0.392
CaO	0.239	0.239	0.008	0.000	2.358	6.715	1.835	10.750	9.749	9.433	4.414
Na_2O	2.370	1.263	2.100	0.213	10.257	7.633	11.222	5.470	5.928	6.254	9.563
K_2O	12.834	15.029	14.097	17.050	0.104	0.329	0.058	0.357	0.434	0.374	0.170
BaO	0.970	0.306	0.306	0.028	0.165	0.332	0.000	0.000	0.013	0.066	0.250
SrO	0.060	0.099	0.040	0.158	0.145	0.167	0.073	0.119	0.000	0.312	0.176
Total	99.106	99.171	98.859	99.099	99.183	98.947	99.522	98.341	98.174	98.584	98.649
Si	2.971	2.953	2.961	2.972	2.851	2.633	2.921	2.469	2.538	2.537	2.779
Al	1.023	1.039	1.038	1.019	1.153	1.355	1.044	1.501	1.427	1.425	1.187
Fe2+	0.005	0.010	0.000	0.002	0.004	0.018	0.019	0.022	0.024	0.025	0.015
Ca	0.012	0.012	0.000	0.000	0.112	0.327	0.087	0.532	0.481	0.465	0.214
Na	0.214	0.115	0.190	0.019	0.885	0.672	0.965	0.489	0.529	0.557	0.839
K	0.762	0.897	0.839	1.023	0.006	0.019	0.003	0.021	0.025	0.022	0.010
Ba	0.018	0.006	0.006	0.001	0.003	0.006	0.000	0.000	0.000	0.001	0.004
Sr	0.002	0.003	0.001	0.004	0.004	0.004	0.002	0.003	0.000	0.008	0.005
Total	5.006	5.033	5.035	5.040	5.018	5.035	5.041	5.036	5.025	5.040	5.052
Ab	21.651	11.193	18.454	1.863	88.206	66.028	91.428	46.972	51.100	53.395	78.942
Or	77.143	87.637	81.508	98.137	0.588	1.873	0.311	2.017	2.462	2.101	0.923
An	1.207	1.170	0.039	0.000	11.206	32.099	8.261	51.011	46.439	44.504	20.135
An/(Ab+An)					11.272	32.712	8.287	52.061	47.611	45.459	20.323

Feldspars	Sample SUD-59-1994 (continued)						Sample SUD-92-1994; Drill core 70011				
point	Pl core	Pl	altered	Pl rim	needle	matrix	Pl rim	Pl	Pl	Pl rim	Pl rim
SiO_2	53.727	57.884	56.895	73.174	72.022	63.598	60.887	53.297	53.805	54.685	53.596
Al_2O_3	27.104	24.684	25.219	15.226	15.937	17.894	23.699	28.400	27.396	27.099	28.619
FeO	0.671	0.494	0.587	0.063	0.199	0.156	0.367	0.616	0.525	0.569	0.627
CaO	10.828	7.248	8.110	0.831	0.926	0.023	5.180	10.740	10.145	9.610	11.037
Na_2O	5.117	7.456	6.787	8.833	9.392	0.353	8.855	5.243	5.564	5.651	5.192
K_2O	0.345	0.190	0.383	0.024	0.084	16.560	0.116	0.294	0.302	0.451	0.339
BaO	0.053	0.000	0.145	0.131	0.197	0.494	0.350	0.149	0.000	0.000	0.000
SrO	0.252	0.088	0.118	0.266	0.000	0.096	0.271	0.153	0.273	0.121	0.031
Total	98.097	98.044	98.244	98.548	98.757	99.174	99.725	98.892	98.010	98.186	99.441
Si	2.486	2.646	2.608	3.199	3.155	2.990	2.729	2.447	2.487	2.516	2.444
Al	1.478	1.330	1.363	0.785	0.823	0.992	1.252	1.537	1.492	1.469	1.538
Fe2+	0.026	0.019	0.023	0.002	0.007	0.006	0.014	0.024	0.020	0.022	0.024
Ca	0.537	0.355	0.398	0.039	0.043	0.001	0.249	0.528	0.502	0.474	0.539
Na	0.459	0.661	0.603	0.749	0.798	0.032	0.770	0.467	0.499	0.504	0.459
K	0.020	0.011	0.022	0.001	0.005	0.993	0.007	0.017	0.018	0.026	0.020
Ba	0.001	0.000	0.003	0.002	0.003	0.009	0.006	0.003	0.000	0.000	0.000
Sr	0.007	0.002	0.003	0.007	0.000	0.003	0.007	0.004	0.007	0.003	0.001
Total	5.014	5.025	5.023	4.784	4.835	5.027	5.033	5.027	5.025	5.015	5.026
Ab	45.173	64.352	58.912	94.897	94.307	3.134	75.082	46.107	48.941	50.194	45.093
Or	2.004	1.079	2.187	0.170	0.555	96.753	0.647	1.701	1.748	2.636	1.937
An	52.823	34.569	38.901	4.934	5.138	0.113	24.271	52.192	49.311	47.170	52.970
An/(Ab+An)	53.903	34.946	39.771	4.942	5.167		24.429	53.095	50.189	48.447	54.017

Feldspars	Sample SUD-92-1994; Drill core 70011 (continued)										
point	Pl	Pl	Pl core	Pl	Pl rim	Pl rim	Pl core	Pl rim	Pl rim	Pl core	Pl rim
SiO_2	54.409	54.187	54.570	53.729	61.383	54.986	53.734	60.016	56.131	54.243	54.154
Al_2O_3	27.543	27.370	27.114	27.239	22.159	27.179	27.417	22.489	25.883	27.663	27.652
FeO	0.604	0.631	0.654	0.862	0.652	0.588	0.796	1.160	0.846	0.566	0.561
CaO	10.178	10.282	9.965	10.234	4.241	9.404	10.143	5.943	8.690	10.139	9.878
Na_2O	5.771	5.462	5.760	5.748	9.641	6.019	5.869	8.770	6.214	5.765	5.651
K_2O	0.238	0.277	0.154	0.235	0.475	0.418	0.176	0.075	0.105	0.194	0.233
BaO	0.000	0.148	0.000	0.000	0.000	0.000	0.000	0.000	0.095	0.284	0.000
SrO	0.122	0.167	0.197	0.046	0.120	0.137	0.000	0.090	0.076	0.000	0.076
Total	98.865	98.524	98.414	98.093	98.671	98.731	98.135	98.543	98.040	98.854	98.205
Si	2.491	2.492	2.508	2.484	2.778	2.517	2.481	2.732	2.578	2.486	2.491
Al	1.486	1.484	1.468	1.484	1.182	1.466	1.492	1.207	1.401	1.494	1.499
Fe2+	0.023	0.024	0.025	0.033	0.025	0.023	0.031	0.044	0.032	0.022	0.022
Ca	0.499	0.507	0.491	0.507	0.206	0.461	0.502	0.290	0.428	0.498	0.487
Na	0.512	0.487	0.513	0.515	0.846	0.534	0.525	0.774	0.553	0.512	0.504
K	0.014	0.016	0.009	0.014	0.027	0.024	0.010	0.004	0.006	0.011	0.014
Ba	0.000	0.003	0.000	0.000	0.000	0.000	0.000	0.000	0.002	0.005	0.000
Sr	0.003	0.004	0.005	0.001	0.003	0.004	0.000	0.002	0.002	0.000	0.002
Total	5.029	5.017	5.019	5.039	5.067	5.029	5.041	5.054	5.002	5.029	5.018
Ab	49.957	48 225	50.669	49.732	78.400	52.382	50.639	72.459	56.057	50.150	50.174
Or	1.356	1.609	0.891	1.338	2.542	2.394	0.999	0.408	0.623	1.110	1.361
An	48.688	50.166	48.440	48.930	19.058	45.225	48.362	27.134	43.320	48.739	48.465
An/(Ab+An)	49.357	50.986	48.876	49.594	19.555	46.334	48.850	27.245	43.592	49.287	49.134

Feldspars	Sample SUD-92-1994; Drill core 70011 (continued)										
point	Pl over	Pl rim	Pl	Pl	Pl over	Pl rim	Pl rim	Pl core	hole	Pl core	Pl rim
SiO_2	60.936	57.308	54.982	56.259	68.775	60.103	54.726	54.363	64.954	52.977	53.526
Al_2O_3	22.315	25.793	27.346	26.262	18.981	23.595	27.023	27.570	21.153	28.098	27.811
FeO	0.588	0.391	0.609	0.465	0.206	0.770	0.609	0.592	0.060	0.574	0.635
CaO	4.407	7.484	9.610	8.364	1.344	6.459	9.590	10.275	1.713	11.191	10.556
Na_2O	9.262	7.156	5.922	6.804	10.396	7.894	6.156	5.487	10.754	5.138	5.240
K_2O	0.276	0.110	0.318	0.131	0.083	0.087	0.106	0.314	0.113	0.292	0.333
BaO	0.174	0.108	0.054	0.000	0.000	0.000	0.081	0.000	0.000	0.027	0.000
SrO	0.150	0.196	0.000	0.076	0.162	0.254	0.000	0.106	0.105	0.289	0.335
Total	98.108	98.546	98.841	98.361	99.947	99.162	98.291	98.707	98.852	98.586	98.436
Si	2.772	2.609	2.512	2.572	3.007	2.711	2.515	2.492	2.891	2.444	2.467
Al	1.196	1.384	1.473	1.415	0.978	1.254	1.464	1.489	1.110	1.527	1.511
Fe2+	0.022	0.015	0.023	0.018	0.008	0.029	0.023	0.023	0.002	0.022	0.024
Ca	0.215	0.365	0.470	0.410	0.063	0.312	0.472	0.505	0.082	0.553	0.521
Na	0.817	0.632	0.525	0.603	0.881	0.690	0.549	0.488	0.928	0.459	0.468
K	0.016	0.006	0.019	0.008	0.005	0.005	0.006	0.018	0.006	0.017	0.020
Ba	0.003	0.002	0.001	0.000	0.000	0.000	0.001	0.000	0.000	0.000	0.000
Sr	0.004	0.005	0.000	0.002	0.004	0.007	0.000	0.003	0.003	0.008	0.009
Total	5.046	5.018	5.023	5.026	4.946	5.009	5.031	5.017	5.022	5.031	5.021
Ab	77.970	62.971	51.758	59.103	92.877	68.521	53.413	48.252	91.329	44.623	46.403
Or	1.529	0.637	1.829	0.749	0.488	0.497	0.605	1.817	0.631	1.669	1.940
An	20.501	36.393	46.413	40.148	6.635	30.982	45.981	49.931	8.039	53.709	51.657
An/(Ab+An)	20.819	36.626	47.278	40.451	6.668	31.136	46.261	50.855	8.090	54.620	52.679

Feldspars	Sample SUD-92-1994; Drill core 70011 (continued)								SUD-60-1994		
point	Pl over	Pl rim	altered	rim alter	Pl core	Pl	Pl rim	Pl	Pl1 core	Pl1 rim	Pl2 core
SiO_2	58.680	57.235	53.289	55.338	64.301	61.233	60.903	58.318	55.121	53.805	54.976
Al_2O_3	24.531	25.423	27.977	26.651	21.548	22.591	24.093	23.809	27.036	28.559	27.852
FeO	0.457	0.551	0.576	0.496	0.108	0.834	0.346	0.562	0.617	0.528	0.642
CaO	6.599	7.681	10.682	8.732	2.179	4.615	2.122	6.747	9.783	11.285	10.637
Na_2O	7.614	7.187	5.268	6.473	10.321	9.002	8.474	7.961	5.774	5.085	5.429
K_2O	0.123	0.219	0.168	0.219	0.037	0.239	1.985	0.395	0.441	0.272	0.366
BaO	0.148	0.000	0.095	0.176	0.134	0.040	0.134	0.215	0.000	0.241	0.176
SrO	0.000	0.121	0.321	0.167	0.120	0.225	0.060	0.180	0.075	0.072	0.080
Total	98.152	98.417	98.376	98.252	98.748	98.779	98.117	98.187	98.846	99.847	100.158
Si	2.672	2.612	2.459	2.542	2.869	2.766	2.760	2.672	2.520	2.447	2.488
Al	1.316	1.368	1.521	1.443	1.133	1.203	1.287	1.286	1.457	1.531	1.486
Fe2+	0.017	0.021	0.022	0.019	0.004	0.032	0.013	0.022	0.024	0.020	0.024
Ca	0.322	0.376	0.528	0.430	0.104	0.223	0.103	0.331	0.479	0.550	0.516
Na	0.672	0.636	0.471	0.577	0.893	0.789	0.745	0.707	0.512	0.448	0.476
K	0.007	0.013	0.010	0.013	0.002	0.014	0.115	0.023	0.026	0.016	0.021
Ba	0.003	0.000	0.002	0.003	0.002	0.001	0.002	0.004	0.000	0.004	0.003
Sr	0.000	0.003	0.009	0.004	0.003	0.006	0.002	0.005	0.002	0.002	0.002
Total	5.010	5.028	5.021	5.031	5.011	5.033	5.026	5.050	5.020	5.019	5.017
Ab	67.134	62.087	46.696	56.570	89.363	76.878	77.369	66.623	50.338	44.219	47.016
Or	0.714	1.245	0.980	1.259	0.211	1.343	11.925	2.175	2.531	1.555	2.083
An	32.153	36.668	52.324	42.170	10.426	21.779	10.706	31.202	47.132	54.226	50.901
An/(Ab+An)	32.384	37.130	52.842	42.708	10.448	22.076	12.156	31.896	48.355	55.083	51.984

Feldspars	Sample SUD-60-1994; Drill core 70011 (continued)										
point	Pl2 core	Pl2 rim	Pl2 rim	Pl3 rim	Pl3 core	Pl3 core	Pl3 rim	Pl4 rim	Pl5 core	Pl5 rim	Pl6 core
SiO_2	54.983	53.394	54.258	55.739	53.416	53.343	53.965	53.920	53.769	53.795	54.328
Al_2O_3	27.558	28.358	27.647	27.003	28.168	28.395	27.842	27.668	28.305	28.091	27.968
FeO	0.621	0.571	0.546	0.566	0.586	0.601	0.678	0.589	0.598	0.623	0.549
CaO	10.492	11.127	10.237	9.209	11.376	11.045	10.422	10.747	11.188	10.808	10.650
Na_2O	5.453	5.202	5.768	6.410	5.093	5.100	5.484	5.531	5.166	5.233	5.412
K_2O	0.343	0.291	0.294	0.165	0.274	0.209	0.344	0.105	0.206	0.256	0.315
BaO	0.000	0.000	0.000	0.000	0.143	0.000	0.044	0.087	0.143	0.033	0.000
SrO	0.100	0.093	0.111	0.093	0.168	0.065	0.164	0.088	0.070	0.130	0.076
Total	99.550	99.035	98.860	99.186	99.224	98.758	98.942	98.736	99.445	98.969	99.297
Si	2.499	2.446	2.485	2.535	2.448	2.448	2.474	2.475	2.454	2.464	2.477
Al	1.476	1.531	1.492	1.447	1.521	1.536	1.504	1.497	1.522	1.516	1.503
Fe2+	0.024	0.022	0.021	0.022	0.022	0.023	0.026	0.023	0.023	0.024	0.021
Ca	0.511	0.546	0.502	0.449	0.559	0.543	0.512	0.529	0.547	0.530	0.520
Na	0.481	0.462	0.512	0.565	0.453	0.454	0.487	0.492	0.457	0.465	0.478
K	0.020	0.017	0.017	0.010	0.016	0.012	0.020	0.006	0.012	0.015	0.018
Ba	0.000	0.000	0.000	0.000	0.003	0.000	0.001	0.002	0.003	0.001	0.000
Sr	0.003	0.002	0.003	0.002	0.004	0.002	0.004	0.002	0.002	0.003	0.002
Total	5.013	5.027	5.033	5.029	5.026	5.017	5.028	5.026	5.020	5.018	5.020
Ab	47.511	45.067	49.649	55.226	44.060	44.968	47.814	47.935	44.985	46.011	47.042
Or	1.968	1.661	1.662	0.935	1.557	1.213	1.974	0.596	1.180	1.479	1.799
An	50.520	53.272	48.689	43.839	54.383	53.819	50.212	51.469	53.835	52.509	51.158
An/(Ab+An)	51.535	54.171	49.512	44.253	55.243	54.480	51.223	51.778	54.478	53.298	52.096

Feldspars	Sample SUD-60-1994 (cont'd)					Sample SUD-61-1994; Drill core 70011				
point	Pl6 rim	Pl7 core	Pl7 core	Pl7 rim	Pl7 rim	Pl1 rim	Pl1	Pl1	Pl1 core	Pl1
SiO_2	53.422	53.523	53.534	54.190	55.296	57.234	54.485	53.660	52.498	53.204
Al_2O_3	28.190	27.510	27.996	27.965	27.283	26.614	28.181	29.107	28.653	28.695
FeO	0.563	0.630	0.591	0.481	0.604	0.518	0.499	0.711	0.494	0.807
CaO	10.814	10.580	10.941	10.837	9.622	8.664	10.389	11.720	11.815	11.434
Na_2O	5.243	5.429	5.354	5.297	5.887	6.861	5.981	4.866	5.148	4.974
K_2O	0.249	0.374	0.353	0.203	0.297	0.183	0.252	0.311	0.035	0.329
BaO	0.000	0.066	0.000	0.000	0.000	0.246	0.109	0.000	0.028	0.219
SrO	0.098	0.098	0.040	0.109	0.159	0.267	0.000	0.000	0.228	0.083
Total	98.580	98.208	98.808	99.083	99.149	100.587	99.896	100.375	98.899	99.745
Si	2.456	2.473	2.458	2.475	2.519	2.569	2.472	2.427	2.415	2.429
Al	1.527	1.498	1.515	1.505	1.465	1.408	1.507	1.552	1.554	1.544
Fe2+	0.022	0.024	0.023	0.018	0.023	0.019	0.019	0.027	0.019	0.031
Ca	0.533	0.524	0.538	0.530	0.470	0.417	0.505	0.568	0.582	0.559
Na	0.467	0.486	0.477	0.469	0.520	0.597	0.526	0.427	0.459	0.440
K	0.015	0.022	0.021	0.012	0.017	0.010	0.015	0.018	0.002	0.019
Ba	0.000	0.001	0.000	0.000	0.000	0.004	0.002	0.000	0.001	0.004
Sr	0.003	0.003	0.001	0.003	0.004	0.007	0.000	0.000	0.006	0.002
Total	5.022	5.032	5.033	5.013	5.017	5.031	5.045	5.019	5.038	5.029
Ab	46.062	47.119	46.027	46.389	51.642	58.297	50.312	42.140	44.000	43.219
Or	1.439	2.137	1.994	1.172	1.714	1.023	1.395	1.772	0.197	1.881
An	52.498	50.744	51.979	52.440	46.644	40.680	48.293	56.087	55.803	54.900
An/(Ab+An)	53.265	51.852	53.037	53.061	47.458	41.101	48.976	57.099	55.913	55.953

Feldspars	Sample SUD-61-1994; Drill core 70011 (continued)									
point	Pl over	Pl1	Pl1 rim	Pl over	Pl2 rim	Pl2 rim	Pl2	Pl2	Pl2	Pl2
SiO_2	67.447	52.487	53.104	53.559	56.069	53.754	53.617	53.379	53.386	54.107
Al_2O_3	20.763	29.203	29.152	28.814	27.361	28.965	28.814	28.474	28.634	28.689
FeO	0.096	0.722	0.549	0.782	0.471	0.756	0.596	0.606	0.717	0.666
CaO	0.653	11.941	11.465	11.227	8.322	11.268	11.360	11.622	11.381	11.111
Na_2O	11.683	4.710	5.219	5.195	6.687	5.271	5.381	5.188	4.966	5.529
K_2O	0.057	0.305	0.304	0.330	0.512	0.290	0.133	0.317	0.326	0.219
BaO	0.000	0.000	0.164	0.000	0.028	0.055	0.000	0.220	0.109	0.109
SrO	0.000	0.435	0.228	0.000	0.021	0.352	0.063	0.124	0.145	0.124
Total	100.699	99.803	100.185	99.907	99.471	100.711	99.964	99.930	99.664	100.554
Si	2.937	2.399	2.415	2.435	2.539	2.430	2.435	2.434	2.436	2.445
Al	1.065	1.573	1.562	1.544	1.460	1.543	1.542	1.530	1.540	1.528
Fe2+	0.003	0.028	0.021	0.030	0.018	0.029	0.023	0.023	0.027	0.025
Ca	0.030	0.585	0.559	0.547	0.404	0.546	0.553	0.568	0.556	0.538
Na	0.986	0.417	0.460	0.458	0.587	0.462	0.474	0.459	0.439	0.484
K	0.003	0.018	0.018	0.019	0.030	0.017	0.008	0.018	0.019	0.013
Ba	0.000	0.000	0.003	0.000	0.000	0.001	0.000	0.004	0.002	0.002
Sr	0.000	0.012	0.006	0.000	0.001	0.009	0.002	0.003	0.004	0.003
Total	5.025	5.032	5.043	5.032	5.039	5.037	5.035	5.039	5.023	5.039
Ab	96.703	40.924	44.400	44.722	57.534	45.096	45.811	43.896	43.297	46.804
Or	0.310	1.744	1.702	1.869	2.899	1.632	0.745	1.765	1.870	1.220
An	2.987	57.333	53.899	53.409	39.567	53.272	53.444	54.339	54.833	51.976
An/(Ab+An)	2.996	58.350	54.832	54.426	40.748	54.156	53.845	55.316	55.878	52.618

Feldspars	Sample SUD-61-1994; Drill core 70011 (continued)									
point	Pl2	Pl2	Pl2	Pl2 rim	Pl2 over	Pl2 over	Pl2 over	Pl2 over	Pl2 over	Pl2 over
SiO_2	54.126	53.942	54.394	54.584	67.009	66.652	66.153	64.271	67.512	64.568
Al_2O_3	28.394	28.192	28.058	27.975	20.559	20.069	20.039	21.649	20.366	21.808
FeO	0.615	0.596	0.575	0.727	0.102	0.117	0.148	0.127	0.362	0.265
CaO	11.024	10.923	10.733	10.406	0.617	0.357	0.495	2.211	0.215	2.555
Na_2O	5.440	5.528	5.547	5.971	11.892	12.053	12.175	10.935	11.902	10.755
K_2O	0.404	0.229	0.452	0.094	0.046	0.035	0.080	0.071	0.161	0.089
BaO	0.000	0.109	0.109	0.000	0.164	0.000	0.000	0.055	0.000	0.083
SrO	0.144	0.186	0.351	0.041	0.000	0.061	0.000	0.000	0.000	0.144
Total	100.147	99.705	100.219	99.798	100.389	99.344	99.090	99.319	100.518	100.267
Si	2.455	2.458	2.468	2.478	2.934	2.946	2.936	2.857	2.948	2.850
Al	1.518	1.514	1.501	1.497	1.061	1.045	1.048	1.134	1.048	1.134
Fe2+	0.023	0.023	0.022	0.028	0.004	0.004	0.005	0.005	0.013	0.010
Ca	0.536	0.533	0.522	0.506	0.029	0.017	0.024	0.105	0.010	0.121
Na	0.478	0.488	0.488	0.525	1.009	1.033	1.048	0.943	1.008	0.920
K	0.023	0.013	0.026	0.005	0.003	0.002	0.005	0.004	0.009	0.005
Ba	0.000	0.002	0.002	0.000	0.003	0.000	0.000	0.001	0.000	0.001
Sr	0.004	0.005	0.009	0.001	0.000	0.002	0.000	0.000	0.000	0.004
Total	5.037	5.036	5.038	5.040	5.042	5.049	5.066	5.049	5.036	5.046
Ab	46.111	47.188	47.106	50.674	96.973	98.205	97.391	89.605	98.147	87.972
Or	2.253	1.286	2.526	0.525	0.247	0.188	0.421	0.383	0.874	0.479
An	51.636	51.525	50.368	48.801	2.780	1.607	2.188	10.012	0.980	11.549
An/(Ab+An)	52.826	52.197	51.673	49.059	2.787	1.610	2.197	10.050	0.988	11.604

Feldspars	Sample SUD-61-1994; Drill core 70011 (continued)									
point	Pl3 over	Pl3 core	Pl3	Pl3 rim	Pl3 over	Pl3 over	Pl3	Pl3 over	matrix-D	matrix-L
SiO_2	66.326	53.365	53.889	53.236	63.813	65.644	63.111	66.545	52.977	63.254
Al_2O_3	20.013	28.498	27.873	28.596	21.891	21.324	18.943	20.145	28.406	18.923
FeO	0.421	0.576	0.500	0.521	0.102	0.699	0.086	1.459	0.545	0.095
CaO	0.418	10.592	10.541	10.891	2.586	1.363	0.000	1.638	11.177	0.000
Na_2O	11.979	5.528	5.896	5.585	10.751	11.231	0.588	10.045	5.498	0.394
K_2O	0.061	0.094	0.157	0.166	0.023	0.242	16.277	0.060	0.325	16.297
BaO	0.191	0.109	0.000	0.000	0.000	0.000	0.303	0.055	0.109	0.000
SrO	0.000	0.104	0.083	0.083	0.164	0.000	0.000	0.082	0.145	0.000
Total	99.409	98.866	98.939	99.078	99.330	100.503	99.308	100.029	99.182	98.963
Si	2.939	2.447	2.469	2.438	2.841	2.884	2.955	2.933	2.432	2.962
Al	1.045	1.540	1.505	1.543	1.148	1.104	1.045	1.046	1.537	1.044
Fe2+	0.016	0.022	0.019	0.020	0.004	0.026	0.003	0.054	0.021	0.004
Ca	0.020	0.520	0.517	0.534	0.123	0.064	0.000	0.077	0.550	0.000
Na	1.029	0.491	0.524	0.496	0.928	0.957	0.053	0.858	0.489	0.036
K	0.003	0.005	0.009	0.010	0.001	0.014	0.972	0.003	0.019	0.974
Ba	0.003	0.002	0.000	0.000	0.000	0.000	0.006	0.001	0.002	0.000
Sr	0.000	0.003	0.002	0.002	0.004	0.000	0.000	0.002	0.004	0.000
Total	5.055	5.031	5.045	5.043	5.050	5.049	5.035	4.975	5.054	5.020
Ab	97.787	48.309	49.864	47.684	88.158	92.486	5.204	91.404	46.247	3.544
Or	0.328	0.541	0.874	0.933	0.124	1.311	94.796	0.359	1.799	96.456
An	1.886	51.150	49.263	51.384	11.718	6.202	0.000	8.236	51.954	0.000
An/(Ab+An)	1.892	51.428	49.697	51.867	11.733	6.285		8.266	52.906	

Feldspars	Sample SUD-61-1994 (continued)					Sample SUD-174-1995; Drill core 70011					
point	matrix-D	matrix-L	matrix-D	matrix-D	matrix-L	Pl1 core	Pl2 core	Pl2 rim	Pl2 over	Pl3 rim	Pl3 over
SiO_2	62.921	63.719	60.600	53.129	63.588	53.422	53.399	55.970	58.537	55.519	60.257
Al_2O_3	22.133	19.130	25.309	28.929	18.730	28.179	28.162	27.024	24.697	26.607	23.678
FeO	0.172	0.000	0.774	0.669	0.035	0.499	0.706	0.548	0.481	0.684	0.286
CaO	3.122	0.000	1.798	11.314	0.000	10.534	10.851	8.983	6.463	9.246	5.166
Na_2O	10.513	0.375	7.321	5.412	0.314	5.093	5.275	6.236	7.768	6.193	8.909
K_2O	0.067	16.881	3.263	0.169	16.637	0.264	0.304	0.190	0.198	0.206	0.094
BaO	0.000	0.137	0.192	0.137	0.000	0.028	0.056	0.000	0.056	0.000	0.249
SrO	0.164	0.156	0.103	0.021	0.000	0.000	0.000	0.168	0.147	0.000	0.104
Total	99.092	100.398	99.360	99.780	99.304	98.019	98.753	99.119	98.347	98.455	98.743
Si	2.815	2.955	2.726	2.422	2.971	2.464	2.453	2.543	2.663	2.543	2.723
Al	1.167	1.045	1.342	1.554	1.031	1.532	1.525	1.447	1.324	1.436	1.261
Fe2+	0.006	0.000	0.029	0.026	0.001	0.019	0.027	0.021	0.018	0.026	0.011
Ca	0.150	0.000	0.087	0.553	0.000	0.520	0.534	0.437	0.315	0.454	0.250
Na	0.912	0.034	0.639	0.478	0.028	0.455	0.470	0.549	0.685	0.550	0.781
K	0.004	0.999	0.187	0.010	0.992	0.016	0.018	0.011	0.011	0.012	0.005
Ba	0.000	0.002	0.003	0.002	0.000	0.001	0.001	0.000	0.001	0.000	0.004
Sr	0.004	0.004	0.003	0.001	0.000	0.000	0.000	0.004	0.004	0.000	0.003
Total	5.059	5.039	5.016	5.045	5.024	5.006	5.028	5.013	5.023	5.020	5.039
Ab	85.595	3.266	69.980	45.961	2.788	45.933	45.984	55.064	67.726	54.145	75.337
Or	0.359	96.734	20.523	0.944	97.212	1.567	1.744	1.104	1.136	1.185	0.523
An	14.046	0.000	9.497	53.095	0.000	52.500	52.272	43.832	31.138	44.670	24.140
An/(Ab+An	14.097		11.950	53.601		53.336	53.200	44.321	31.496	45.206	24.267

Feldspars	Sample SUD-174-1995; Drill core 70011 (continued)										
point	Pl4 rim	Pl6 rim	Pl7 rim	Pl7 over	Pl8 core	Pl9 core	Pl9 over	Pl10 core	Pl10 rim	graphic1	graphic3
SiO_2	65.244	64.339	58.368	61.712	63.635	52.629	59.359	62.968	60.910	62.003	62.300
Al_2O_3	21.222	21.668	25.095	23.068	21.851	27.914	24.238	22.172	23.089	18.547	18.694
FeO	0.021	0.112	0.419	0.241	0.306	0.719	0.394	0.103	0.378	0.203	0.041
CaO	1.701	2.456	6.715	4.091	2.467	11.076	5.839	2.826	4.358	0.143	0.000
Na_2O	10.323	10.029	7.361	9.035	10.404	5.140	8.058	9.742	9.077	0.325	0.682
K_2O	0.082	0.102	0.214	0.078	0.052	0.342	0.114	0.112	0.073	16.015	16.125
BaO	0.028	0.083	0.277	0.332	0.221	0.084	0.304	0.056	0.056	1.111	1.167
SrO	0.124	0.103	0.000	0.000	0.041	0.125	0.208	0.063	0.063	0.040	0.140
Total	98.745	98.892	98.449	98.557	98.977	98.029	98.514	98.042	98.004	98.387	99.149
Si	2.900	2.866	2.653	2.778	2.844	2.442	2.694	2.833	2.760	2.951	2.946
Al	1.112	1.138	1.344	1.224	1.151	1.527	1.296	1.176	1.233	1.040	1.042
Fe2+	0.001	0.004	0.016	0.009	0.011	0.028	0.015	0.004	0.014	0.008	0.002
Ca	0.081	0.117	0.327	0.197	0.118	0.551	0.284	0.136	0.212	0.007	0.000
Na	0.890	0.866	0.649	0.789	0.901	0.462	0.709	0.850	0.798	0.030	0.063
K	0.005	0.006	0.012	0.004	0.003	0.020	0.007	0.006	0.004	0.972	0.973
Ba	0.000	0.001	0.005	0.006	0.004	0.002	0.005	0.001	0.001	0.021	0.022
Sr	0.003	0.003	0.000	0.000	0.001	0.003	0.005	0.002	0.002	0.001	0.004
Total	4.991	5.001	5.006	5.007	5.033	5.036	5.016	5.007	5.024	5.030	5.051
Ab	91.217	87.564	65.650	79.625	88.158	44.752	70.935	85.626	78.703	2.970	6.040
Or	0.477	0.586	1.256	0.452	0.290	1.959	0.660	0.648	0.416	96.307	93.960
An	8.306	11.850	33.094	19.923	11.552	53.289	28.404	13.726	20.881	0.722	0.000
An/(Ab+An	8.346	11.920	33.515	20.014	11.585	54.354	28.593	13.815	20.968		

Feldspars	174-1995	Sample SUD-175-1995; Drill core 70011								
point	graphic5	Pl1 core	Pl1 rim	Pl2 core	Pl2over	Pl3 rim	Pl4 rim	Pl7 core	Pl7 rim	Pl8 rim
SiO_2	62.801	66.596	66.350	66.440	66.744	65.849	65.946	64.305	64.589	64.859
Al_2O_3	18.412	20.487	20.933	19.924	19.943	20.566	20.187	21.675	21.296	21.468
FeO	0.041	0.124	0.237	0.082	0.093	0.005	0.000	0.235	0.041	0.072
CaO	0.000	0.733	0.905	0.264	0.309	0.662	0.630	1.883	1.956	1.813
Na_2O	0.355	11.064	10.677	11.463	11.437	11.165	11.317	10.157	10.575	10.003
K_2O	16.297	0.061	0.055	0.037	0.107	0.051	0.034	0.088	0.092	0.070
BaO	0.138	0.000	0.000	0.028	0.055	0.056	0.000	0.000	0.000	0.000
SrO	0.000	0.000	0.000	0.103	0.103	0.063	0.000	0.000	0.000	0.103
Total	98.044	99.065	99.157	98.341	98.791	98.417	98.114	98.343	98.549	98.388
Si	2.973	2.942	2.928	2.958	2.960	2.932	2.943	2.873	2.882	2.891
Al	1.027	1.067	1.089	1.046	1.042	1.079	1.062	1.141	1.120	1.128
Fe2+	0.002	0.005	0.009	0.003	0.003	0.000	0.000	0.009	0.002	0.003
Ca	0.000	0.035	0.043	0.013	0.015	0.032	0.030	0.090	0.094	0.087
Na	0.033	0.948	0.914	0.990	0.983	0.964	0.979	0.880	0.915	0.864
K	0.984	0.003	0.003	0.002	0.006	0.003	0.002	0.005	0.005	0.004
Ba	0.003	0.000	0.000	0.000	0.001	0.001	0.000	0.000	0.000	0.000
Sr	0.000	0.000	0.000	0.003	0.003	0.002	0.000	0.000	0.000	0.003
Total	5.022	5.000	4.986	5.015	5.014	5.012	5.016	4.999	5.018	4.979
Ab	3.205	96.132	95.217	98.537	97.935	96.546	96.830	90.241	90.258	90.517
Or	96.795	0.349	0.323	0.209	0.603	0.290	0.191	0.514	0.517	0.417
An	0.000	3.519	4.460	1.254	1.462	3.163	2.979	9.245	9.225	9.066
An/(Ab+An)		3.532	4.474	1.257	1.471	3.173	2.984	9.293	9.273	9.104

Feldspars	SUD-175-1995 (continued)			Sample SUD-130-1995; Drill core 70011					SUD-153-1995	
point	Pl10 core	Pl10 rim	matrix6	Pl over	Pl	Pl core	Pl	Pl rim	Pl2 core	Pl2 rim
SiO_2	52.306	52.547	63.580	66.830	67.179	67.012	67.382	57.427	54.020	53.344
Al_2O_3	28.464	28.978	21.915	19.220	18.878	19.204	18.950	24.874	28.062	28.300
FeO	0.740	0.495	0.163	0.031	0.031	0.029	0.011	0.274	0.600	0.558
CaO	11.571	11.444	2.775	0.540	0.235	0.209	0.170	7.218	10.959	10.988
Na_2O	4.675	4.859	9.607	11.285	11.853	11.790	11.754	7.866	5.346	5.208
K_2O	0.337	0.304	0.107	0.039	0.009	0.028	0.023	0.304	0.372	0.255
BaO	0.056	0.028	0.028	0.094	0.000	0.000	0.107	0.175	0.000	0.000
SrO	0.315	0.000	0.000	0.000	0.000	0.044	0.000	0.136	0.137	0.102
Total	98.464	98.655	98.175	98.039	98.185	98.316	98.397	98.274	99.496	98.755
Si	2.420	2.417	2.851	2.983	2.994	2.983	2.996	2.629	2.464	2.449
Al	1.552	1.571	1.158	1.011	0.992	1.008	0.993	1.342	1.509	1.531
Fe2+	0.029	0.019	0.006	0.001	0.001	0.001	0.000	0.010	0.023	0.021
Ca	0.574	0.564	0.133	0.026	0.011	0.010	0.008	0.354	0.536	0.541
Na	0.419	0.433	0.835	0.977	1.024	1.018	1.013	0.698	0.473	0.464
K	0.020	0.018	0.006	0.002	0.001	0.002	0.001	0.018	0.022	0.015
Ba	0.001	0.001	0.000	0.002	0.000	0.000	0.002	0.003	0.000	0.000
Sr	0.008	0.000	0.000	0.000	0.000	0.001	0.000	0.004	0.004	0.003
Total	5.023	5.023	4.991	5.001	5.023	5.022	5.014	5.058	5.029	5.024
Ab	41.405	42.687	85.694	97.209	98.867	98.877	99.081	65.253	45.902	45.492
Or	1.964	1.757	0.628	0.221	0.049	0.155	0.128	1.659	2.100	1.464
An	56.631	55.556	13.678	2.570	1.083	0.969	0.792	33.088	51.998	53.044
An/(Ab+An)	57.765	56.550	13.765	2.576	1.084	0.970	0.793	33.646	53.113	53.832

Feldspars	Sample SUD-153-1995; Drill core 70011 (continued)										
point	Pl2 core	Pl2 rim	Pl3 rim	Pl3 core	Pl3 rim	Pl4 core	Pl4 rim	Pl4 rim	Pl4 core	Pl5 rim	Pl5 core
SiO_2	52.367	55.469	52.757	52.935	53.953	53.245	53.671	54.098	53.970	53.581	52.815
Al_2O_3	28.767	27.450	28.736	28.718	28.196	27.822	28.234	28.292	28.309	28.360	28.832
FeO	0.713	0.585	0.615	0.560	0.560	0.603	0.676	0.529	0.663	0.392	0.525
CaO	11.867	10.215	11.639	11.622	10.843	11.135	9.143	10.304	11.109	10.980	11.705
Na_2O	4.879	5.639	4.896	4.997	5.408	5.347	5.316	5.585	5.305	5.479	4.895
K_2O	0.271	0.377	0.252	0.289	0.281	0.170	1.157	0.382	0.326	0.090	0.256
BaO	0.231	0.111	0.000	0.066	0.022	0.197	0.000	0.011	0.111	0.044	0.088
SrO	0.127	0.063	0.103	0.085	0.090	0.108	0.162	0.094	0.058	0.142	0.114
Total	99.222	99.908	98.997	99.273	99.353	98.626	98.360	99.295	99.851	99.068	99.229
Si	2.408	2.512	2.422	2.425	2.462	2.455	2.473	2.467	2.455	2.451	2.420
Al	1.559	1.465	1.555	1.550	1.516	1.512	1.533	1.521	1.518	1.529	1.557
Fe2+	0.027	0.022	0.024	0.021	0.021	0.023	0.026	0.020	0.025	0.015	0.020
Ca	0.585	0.496	0.572	0.570	0.530	0.550	0.451	0.503	0.541	0.538	0.575
Na	0.435	0.495	0.436	0.444	0.478	0.478	0.475	0.494	0.468	0.486	0.435
K	0.016	0.022	0.015	0.017	0.016	0.010	0.068	0.022	0.019	0.005	0.015
Ba	0.004	0.002	0.000	0.001	0.000	0.004	0.000	0.000	0.002	0.001	0.002
Sr	0.003	0.002	0.003	0.002	0.002	0.003	0.004	0.002	0.002	0.004	0.003
Total	5.038	5.014	5.026	5.031	5.027	5.034	5.032	5.030	5.030	5.030	5.026
Ab	42.007	48.899	42.596	43.041	46.681	46.049	47.765	48.438	45.504	47.209	42.448
Or	1.534	2.151	1.442	1.639	1.595	0.962	6.839	2.178	1.842	0.511	1.460
An	56.459	48.950	55.962	55.320	51.724	52.989	45.396	49.384	52.654	52.280	56.093
An/(Ab+An)	57.339	50.026	56.780	56.242	52.562	53.504	48.729	50.484	53.642	52.549	56.924

Feldspars	Sample SUD-153-1995; Drill core 70011 (continued)							SUD-63-1994; Drill core 70011		
point	Pl5 core	Pl5 rim	Pl5 over	Pl6 core	Pl6 rim	Pl6 over	Pl6 over	altered	altered	Pl over
SiO_2	52.933	59.148	66.728	52.562	57.253	65.830	68.403	65.269	59.671	62.005
Al_2O_3	28.958	24.819	19.919	28.668	25.798	21.079	19.588	20.772	23.901	22.535
FeO	0.548	0.282	0.292	0.658	0.488	0.126	0.114	0.074	0.359	0.214
CaO	11.505	6.295	1.018	11.785	7.897	1.912	0.199	1.619	5.990	4.045
Na_2O	5.044	8.092	11.711	4.611	7.071	10.654	11.977	10.595	8.214	9.584
K_2O	0.126	0.328	0.076	0.256	0.058	0.060	0.102	0.400	0.090	0.077
BaO	0.000	0.065	0.000	0.000	0.152	0.033	0.011	0.079	0.131	0.236
SrO	0.026	0.096	0.019	0.115	0.148	0.038	0.025	0.073	0.029	0.146
Total	99.140	99.125	99.763	98.655	98.865	99.731	100.419	98.881	98.385	98.842
Si	2.422	2.669	2.943	2.421	2.602	2.902	2.983	2.906	2.706	2.789
Al	1.562	1.320	1.035	1.556	1.382	1.095	1.007	1.090	1.277	1.194
Fe2+	0.021	0.011	0.011	0.025	0.019	0.005	0.004	0.003	0.014	0.008
Ca	0.564	0.304	0.048	0.582	0.385	0.090	0.009	0.077	0.291	0.195
Na	0.448	0.708	1.001	0.412	0.623	0.911	1.013	0.915	0.722	0.836
K	0.007	0.019	0.004	0.015	0.003	0.003	0.008	0.023	0.005	0.004
Ba	0.000	0.001	0.000	0.000	0.003	0.001	0.000	0.001	0.002	0.004
Sr	0.001	0.003	0.000	0.003	0.004	0.001	0.001	0.002	0.001	0.004
Total	5.024	5.034	5.043	5.014	5.020	5.008	5.023	5.017	5.019	5.034
Ab	43.920	68.655	95.030	40.834	61.628	90.669	98.544	90.148	70.912	80.742
Or	0.725	1.829	0.405	1.494	0.334	0.337	0.551	2.239	0.511	0.427
An	55.355	29.515	4.565	57.672	38.038	8.994	0.905	7.612	28.576	18.831
An/(Ab+An)	55.759	30.065	4.583	58.546	38.165	9.024	0.910	7.787	28.723	18.912

Feldspars	Sample SUD-64-1994; Drill core 70011										
point	Pl core	Pl core	Pl core	Pl core	Pl	Pl	Pl	Pl	Pl	Pl	Pl rim
SiO_2	53.300	53.400	54.100	54.400	55.400	61.500	53.200	55.900	55.700	56.600	61.300
Al_2O_3	28.400	28.500	28.300	28.200	27.800	23.800	27.800	26.700	26.900	26.400	23.700
FeO	0.800	0.500	0.300	0.600	0.500	0.400	0.400	0.600	0.600	0.500	0.300
CaO	12.000	11.400	10.900	11.000	10.000	5.500	11.200	9.500	9.500	8.900	5.200
Na_2O	4.900	4.900	5.200	5.300	5.800	8.800	5.300	6.300	6.000	6.600	8.700
K_2O	0.100	0.200	0.100	0.100	0.100	0.100	0.200	0.100	0.200	0.200	0.100
BaO	0.100	0.200	0.100	0.100	0.000	0.000	0.000	0.100	0.100	0.000	0.200
SrO	0.100	0.100	0.100	0.100	0.100	0.100	0.100	0.000	0.100	0.100	0.000
Total	99.700	99.200	99.100	99.800	99.700	100.200	98.200	99.200	99.100	99.300	99.500
Si	2.433	2.444	2.468	2.469	2.506	2.734	2.457	2.542	2.536	2.567	2.741
Al	1.528	1.537	1.522	1.509	1.482	1.247	1.513	1.431	1.444	1.411	1.249
Fe2+	0.031	0.019	0.011	0.023	0.019	0.015	0.015	0.023	0.023	0.019	0.011
Ca	0.587	0.559	0.533	0.535	0.485	0.262	0.554	0.463	0.464	0.432	0.249
Na	0.434	0.435	0.460	0.466	0.509	0.758	0.475	0.556	0.530	0.580	0.754
K	0.006	0.012	0.006	0.006	0.006	0.006	0.012	0.006	0.012	0.012	0.006
Ba	0.002	0.004	0.002	0.002	0.000	0.000	0.000	0.002	0.002	0.000	0.004
Sr	0.003	0.003	0.003	0.003	0.003	0.003	0.003	0.000	0.003	0.003	0.000
Total	5.023	5.011	5.004	5.012	5.010	5.025	5.029	5.023	5.012	5.024	5.014
Ab	42.252	43.243	46.062	46.311	50.914	73 918	45.608	54.238	52.718	56.654	74.747
Or	0.567	1.181	0.583	0.575	0.578	0.553	1.132	0.566	1.156	1.130	0.565
An	57.180	55.595	53.355	53.114	48.509	25.529	53.259	45.196	46.126	42.217	24.688
An/(Ab+An)	57.507	56.249	53.668	53.421	48.790	25.671	53.869	45.453	46.665	42.699	24.828

Feldspars	Sample SUD-64-1994; Drill core 70011 (continued)										
point	Pl over	Pl over	Pl over	Pl over	Pl over	Pl rim	Pl rim	Pl rim	Pl rim	Pl	Pl
SiO_2	63.900	63.300	62.700	63.600	63.700	59.200	56.400	53.600	53.200	59.800	55.500
Al_2O_3	18.700	18.700	19.200	18.900	18.800	25.300	26.900	28.800	28.800	24.700	27.400
FeO	0.100	0.100	0.200	0.100	0.200	0.300	0.600	0.600	0.500	0.400	0.600
CaO	0.100	0.100	0.500	0.200	0.200	7.300	9.400	11.400	11.400	6.700	9.900
Na_2O	0.600	0.700	1.800	0.900	1.300	7.700	6.100	5.000	4.900	7.700	5.800
K_2O	14.800	14.500	12.900	13.600	13.300	0.100	0.300	0.200	0.200	0.200	0.200
BaO	1.700	2.400	2.000	2.000	2.200	0.200	0.200	0.000	0.000	0.100	0.200
SrO	0.000	0.000	0.000	0.100	0.100	0.000	0.100	0.100	0.100	0.000	0.000
Total	99.900	99.800	99.300	99.400	99.800	100.100	100.000	99.700	99.100	99.600	99.600
Si	2.977	2.966	2.937	2.970	2.968	2.649	2.547	2.438	2.434	2.681	2.517
Al	1.027	1.033	1.060	1.040	1.032	1.334	1.432	1.544	1.553	1.305	1.465
Fe2+	0.004	0.004	0.008	0.004	0.008	0.011	0.023	0.023	0.019	0.015	0.023
Ca	0.005	0.005	0.025	0.010	0.010	0.350	0.455	0.556	0.559	0.322	0.481
Na	0.054	0.064	0.163	0.081	0.117	0.668	0.534	0.441	0.435	0.669	0.510
K	0.880	0.867	0.771	0.810	0.791	0.006	0.017	0.012	0.012	0.011	0.012
Ba	0.031	0.044	0.037	0.037	0.040	0.004	0.004	0.000	0.000	0.002	0.004
Sr	0.000	0.000	0.000	0.003	0.003	0.000	0.003	0.003	0.003	0.000	0.000
Total	4.977	4.983	5.000	4.956	4.970	5.021	5.013	5.016	5.013	5.006	5.011
Ab	5.773	6.799	17.039	9.037	12.793	65.255	53.081	43.740	43.243	66.759	50.867
Or	93.695	92.664	80.346	89.853	86.119	0.558	1.718	1.151	1.161	1.141	1.154
An	0.532	0.537	2.615	1.110	1.088	34.187	45.201	55.109	55.595	32.100	47.979
An/(Ab+An)						34.379	45.991	55.751	56.249	32.470	48.539

Feldspars	Sample SUD-64-1994; Drill core 70011 (continued)										
point	Pl	Pl	Pl	Pl	Pl	Pl	Pl	Pl	Pl	Pl1 core	Pl1 core
SiO_2	52.500	53.400	52.700	53.800	54.900	53.800	53.700	53.100	53.400	54.775	53.532
Al_2O_3	29.200	29.200	29.200	28.300	28.100	28.700	29.100	29.000	28.600	27.407	28.065
FeO	0.500	0.600	0.500	0.500	0.600	0.700	0.400	0.500	0.500	0.568	0.559
CaO	11.600	11.800	12.000	11.000	10.700	11.300	11.600	11.600	11.100	10.297	10.399
Na_2O	4.700	4.500	4.500	5.100	5.500	4.900	4.700	4.800	5.100	5.820	5.574
K_2O	0.300	0.200	0.200	0.200	0.100	0.300	0.200	0.200	0.100	0.243	0.269
BaO	0.000	0.200	0.200	0.000	0.100	0.000	0.100	0.100	0.100	0.011	0.000
SrO	0.100	0.100	0.100	0.100	0.000	0.100	0.100	0.000	0.100	0.119	0.126
Total	98.900	100.000	99.400	99.000	100.000	99.800	99.900	99.300	99.000	99.240	98.524
Si	2.410	2.425	2.410	2.460	2.483	2.445	2.436	2.426	2.444	2.499	2.462
Al	1.580	1.563	1.574	1.525	1.498	1.537	1.555	1.561	1.543	1.473	1.521
Fe2+	0.019	0.023	0.019	0.019	0.023	0.027	0.015	0.019	0.019	0.022	0.021
Ca	0.571	0.574	0.588	0.539	0.519	0.550	0.564	0.568	0.544	0.503	0.512
Na	0.418	0.396	0.399	0.452	0.482	0.432	0.413	0.425	0.453	0.515	0.497
K	0.018	0.012	0.012	0.012	0.006	0.017	0.012	0.012	0.006	0.014	0.016
Ba	0.000	0.004	0.004	0.000	0.002	0.000	0.002	0.002	0.002	0.000	0.000
Sr	0.003	0.003	0.003	0.003	0.000	0.003	0.003	0.000	0.003	0.003	0.003
Total	5.018	4.998	5.008	5.009	5.012	5.011	4.999	5.012	5.014	5.029	5.034
Ab	41.565	40.351	39.955	45.092	47.915	43.203	41.808	42.321	45.134	49.874	48.480
Or	1.746	1.180	1.168	1.164	0.573	1.740	1.171	1.160	0.582	1.372	1.541
An	56.689	58.469	58.877	53.744	51.512	55.056	57.021	56.518	54.284	48.754	49.979
An/(Ab+An)	57.696	59.168	59.573	54.377	51.809	56.032	57.696	57.182	54.602	49.432	50.761

Feldspars	Sample SUD-64-1994; Drill core 70011 (continued)										
point	Pl1 rim	Pl2 core	Pl2 rim	Pl2 core	Pl3 core	Pl3 rim	Pl3 rim	Pl3 core	Pl3 rim	Pl3 core	Pl3 core
SiO_2	52.649	53.989	53.529	53.167	52.503	60.470	59.074	52.033	58.117	51.105	52.106
Al_2O_3	28.958	28.292	28.291	28.788	28.894	23.884	25.154	28.749	25.293	28.321	28.992
FeO	0.339	0.510	0.401	0.434	0.580	0.232	0.507	0.493	0.388	1.326	0.645
CaO	11.412	10.894	10.948	11.234	11.935	5.284	7.137	11.663	7.273	12.919	11.775
Na_2O	5.165	5.547	5.453	5.231	4.698	8.822	7.705	5.055	7.436	4.444	4.673
K_2O	0.278	0.165	0.136	0.188	0.233	0.130	0.253	0.095	0.315	0.112	0.236
BaO	0.000	0.000	0.255	0.155	0.188	0.099	0.110	0.144	0.319	0.199	0.055
SrO	0.094	0.113	0.130	0.115	0.048	0.062	0.066	0.103	0.122	0.128	0.087
Total	98.895	99.510	99.142	99.310	99.080	98.982	100.006	98.334	99.263	98.553	98.570
Si	2.417	2.459	2.451	2.431	2.412	2.722	2.649	2.408	2.632	2.380	2.404
Al	1.567	1.519	1.527	1.552	1.564	1.267	1.329	1.568	1.350	1.555	1.577
Fe2+	0.013	0.019	0.015	0.017	0.022	0.009	0.019	0.019	0.015	0.052	0.025
Ca	0.561	0.532	0.537	0.550	0.587	0.255	0.343	0.578	0.353	0.645	0.582
Na	0.460	0.490	0.484	0.464	0.418	0.770	0.670	0.454	0.653	0.401	0.418
K	0.016	0.010	0.008	0.011	0.014	0.007	0.014	0.006	0.018	0.007	0.014
Ba	0.000	0.000	0.005	0.003	0.003	0.002	0.002	0.003	0.006	0.004	0.001
Sr	0.003	0.003	0.003	0.003	0.001	0.002	0.002	0.003	0.003	0.003	0.002
Total	5.037	5.031	5.031	5.030	5.022	5.033	5.028	5.038	5.029	5.046	5.023
Ab	44.318	47.506	47.040	45.239	41.042	74.589	65.209	43.718	63.760	38.127	41.227
Or	1.571	0.932	0.773	1.068	1.341	0.721	1.409	0.541	1.779	0.632	1.370
An	54.110	51.562	52.186	53.692	57.616	24.690	33.381	55.740	34.461	61.241	57.403
An/(Ab+An)	54.974	52.047	52.593	54.272	58.400	24.869	33.858	56.044	35.085	61.631	58.200

Feldspars	Sample SUD-64-1994; Drill core 70011 (continued)										
point	Pl3 core	Pl3 core	Pl3 rim	Pl3 rim	Pl4 rim	Pl4 core	Pl4 core	Pl4 rim	Pl4 core	Pl4 core	Pl5 core
SiO_2	53.004	52.107	56.079	52.581	54.475	52.149	52.972	51.243	51.303	51.823	51.656
Al_2O_3	28.483	29.039	26.556	28.951	27.031	28.399	28.074	28.720	29.317	28.986	28.750
FeO	0.443	0.545	0.470	0.735	0.545	0.586	0.563	0.771	0.671	0.634	0.640
CaO	11.275	12.068	9.054	11.576	9.697	11.874	10.761	12.354	12.397	12.146	11.826
Na_2O	4.973	4.743	6.601	5.120	6.095	4.682	5.588	4.532	4.503	4.537	4.893
K_2O	0.415	0.244	0.178	0.108	0.086	0.316	0.142	0.301	0.250	0.347	0.317
BaO	0.077	0.088	0.099	0.033	0.263	0.000	0.187	0.209	0.033	0.155	0.000
SrO	0.055	0.041	0.035	0.061	0.082	0.118	0.085	0.122	0.131	0.090	0.089
Total	98.725	98.875	99.071	99.165	98.272	98.124	98.373	98.253	98.605	98.716	98.171
Si	2.438	2.399	2.552	2.411	2.509	2.418	2.447	2.385	2.374	2.394	2.398
Al	1.544	1.576	1.424	1.565	1.467	1.552	1.528	1.575	1.599	1.578	1.573
Fe2+	0.017	0.021	0.018	0.028	0.021	0.023	0.022	0.030	0.026	0.024	0.025
Ca	0.556	0.595	0.442	0.569	0.479	0.590	0.533	0.616	0.615	0.601	0.588
Na	0.443	0.423	0.583	0.455	0.544	0.421	0.500	0.409	0.404	0.406	0.440
K	0.024	0.014	0.010	0.006	0.005	0.019	0.008	0.018	0.015	0.020	0.019
Ba	0.001	0.002	0.002	0.001	0.005	0.000	0.003	0.004	0.001	0.003	0.000
Sr	0.001	0.001	0.001	0.002	0.002	0.003	0.002	0.003	0.004	0.002	0.002
Total	5.024	5.032	5.032	5.037	5.032	5.026	5.044	5.041	5.036	5.030	5.045
Ab	43.335	40.986	56.318	44.186	52.954	40.886	48.056	39.214	39.096	39.530	42.049
Or	2.376	1.389	0.998	0.612	0.490	1.815	0.805	1.716	1.427	1.989	1.791
An	54.288	57.625	42.684	55.202	46.556	57.300	51.139	59.070	59.477	58.481	56.162
An/(Ab+An)	55.610	58.437	43.114	55.542	46.785	58.359	51.554	60.101	60.338	59.667	57.186

Feldspars	Sample SUD-64-1994; Drill core 70011 (continued)										
point	Pl5 rim	Pl5 core	Pl5 rim	Pl5 core	Pl6 rim	Pl6 core	Pl6 core	Pl6 rim	Pl6 core	Pl6 core	Pl6 rim
SiO_2	60.857	52.233	52.622	52.850	64.821	53.677	54.617	53.300	52.667	52.801	54.314
Al_2O_3	23.044	28.784	28.518	28.186	20.711	27.902	26.779	28.294	28.280	28.487	26.717
FeO	0.234	0.544	0.677	0.503	0.064	0.500	0.600	0.418	0.557	0.588	0.861
CaO	4.728	11.681	11.381	11.127	1.593	10.471	9.659	10.896	11.087	10.962	9.913
Na_2O	9.333	5.006	5.026	5.183	11.065	5.674	6.143	5.538	5.200	5.217	6.103
K_2O	0.215	0.140	0.158	0.301	0.068	0.209	0.283	0.213	0.204	0.143	0.299
BaO	0.076	0.000	0.066	0.210	0.087	0.111	0.230	0.000	0.077	0.077	0.277
SrO	0.000	0.125	0.142	0.102	0.050	0.062	0.037	0.065	0.107	0.107	0.111
Total	98.488	98.513	98.591	98.463	98.459	98.606	98.348	98.723	98.178	98.383	98.593
Si	2.752	2.411	2.426	2.441	2.899	2.467	2.516	2.448	2.436	2.435	2.505
Al	1.228	1.566	1.550	1.534	1.092	1.512	1.454	1.532	1.542	1.549	1.452
Fe2+	0.009	0.021	0.026	0.019	0.002	0.019	0.023	0.016	0.022	0.023	0.033
Ca	0.229	0.578	0.562	0.551	0.076	0.516	0.477	0.536	0.550	0.542	0.490
Na	0.818	0.448	0.449	0.464	0.960	0.506	0.549	0.493	0.466	0.467	0.546
K	0.012	0.008	0.009	0.018	0.004	0.012	0.017	0.012	0.012	0.008	0.018
Ba	0.001	0.000	0.001	0.004	0.002	0.002	0.004	0.000	0.001	0.001	0.005
Sr	0.000	0.003	0.004	0.003	0.001	0.002	0.001	0.002	0.003	0.003	0.003
Total	5.050	5.035	5.028	5.033	5.036	5.036	5.040	5.039	5.032	5.028	5.051
Ab	77.213	43.330	44.014	44.954	92.283	48.926	52.651	47.336	45.372	45.889	51.820
Or	1.172	0.798	0.912	1.720	0.374	1.184	1.596	1.196	1.168	0.829	1.669
An	21.615	55.872	55.073	53.326	7.342	49.890	45.752	51.468	53.459	53.281	46.511
An/(Ab+An)	21.871	56.321	55.580	54.259	7.370	50.488	46.494	52.091	54.091	53.727	47.300

Feldspars	Sample SUD-64-1994; Drill core 70011 (cont'd)						SUD-7-1994; Drill core 70011				
point	Pl6 hole	Pl6 hole	matrix B	matrix B	matrix B	matrix L	Pl1	Pl1	Pl1	Pl1	Pl1
SiO_2	69.225	55.351	66.207	63.718	64.740	63.814	51.486	59.303	55.063	55.636	54.759
Al_2O_3	18.589	27.131	20.054	19.141	19.380	18.012	29.715	24.973	28.175	27.699	27.837
FeO	0.000	0.559	0.049	0.052	0.499	0.165	0.594	0.439	0.418	0.403	0.427
CaO	1.027	9.380	0.994	0.388	1.891	0.033	11.629	5.661	9.653	9.299	8.962
Na_2O	10.583	6.299	11.462	6.688	10.180	0.367	4.664	7.964	6.023	6.275	5.610
K_2O	0.080	0.213	0.080	7.301	1.908	15.122	0.141	0.117	0.124	0.136	1.244
BaO	0.033	0.132	0.174	0.861	0.261	0.721	0.164	0.354	0.082	0.164	0.000
SrO	0.076	0.086	0.040	0.050	0.061	0.072	0.021	0.061	0.166	0.166	0.267
Total	99.613	99.151	99.060	98.199	98.919	98.306	98.414	98.872	99.704	99.778	99.106
Si	3.030	2.523	2.939	2.942	2.919	3.004	2.379	2.678	2.493	2.516	2.502
Al	0.959	1.457	1.049	1.042	1.030	0.999	1.618	1.329	1.504	1.477	1.499
Fe2+	0.000	0.021	0.002	0.002	0.019	0.006	0.023	0.017	0.016	0.015	0.016
Ca	0.048	0.458	0.047	0.019	0.091	0.002	0.576	0.274	0.468	0.451	0.439
Na	0.898	0.557	0.986	0.599	0.890	0.034	0.418	0.697	0.529	0.550	0.497
K	0.004	0.012	0.005	0.430	0.110	0.908	0.008	0.007	0.007	0.008	0.073
Ba	0.001	0.002	0.003	0.016	0.005	0.013	0.003	0.006	0.001	0.003	0.000
Sr	0.002	0.002	0.001	0.001	0.002	0.002	0.001	0.002	0.004	0.004	0.007
Total	4.942	5.033	5.032	5.051	5.066	4.968	5.025	5.009	5.023	5.024	5.033
Ab	94.464	54.194	95.010	57.131	81.569	3.554	41.706	71.303	52.654	54.550	49.293
Or	0.468	1.208	0.437	41.040	10.058	96.268	0.830	0.689	0.713	0.778	7.192
An	5.068	44.598	4.553	1.830	8.373	0.178	57.464	28.008	46.633	44.672	43.515
An/(Ab+An)	5.092	45.143	4.573		9.309		57.945	28.202	46.968	45.022	46.887

Feldspars	Sample SUD-7-1994; Drill core 70011 (continued)										
point	Pl1	Pl1	Pl1	Pl1	Pl1	Pl1	Pl2 core	Pl2 rim	Pl3 core	Pl3 rim	Pl4 core
SiO_2	55.200	51.713	52.466	52.440	53.138	53.876	54.402	53.596	52.032	65.612	52.808
Al_2O_3	27.606	29.775	29.877	30.031	28.827	28.094	28.523	28.311	29.577	21.386	29.467
FeO	0.418	0.458	0.437	0.517	0.759	0.533	0.731	0.540	0.560	0.147	0.630
CaO	9.542	11.914	11.869	11.137	10.122	10.288	10.838	10.628	12.307	1.464	12.148
Na_2O	5.907	4.648	4.587	4.499	4.870	5.709	5.372	5.493	4.729	11.140	4.734
K_2O	0.172	0.140	0.243	0.744	0.873	0.086	0.273	0.163	0.229	0.072	0.240
BaO	0.355	0.000	0.000	0.491	0.136	0.191	0.109	0.109	0.083	0.000	0.000
SrO	0.083	0.124	0.104	0.145	0.144	0.310	0.207	0.063	0.248	0.082	0.063
Total	99.283	98.772	99.583	100.004	98.869	99.087	100.455	98.903	99.765	99.903	100.090
Si	2.512	2.379	2.392	2.391	2.441	2.467	2.459	2.456	2.380	2.890	2.400
Al	1.481	1.615	1.605	1.614	1.561	1.516	1.519	1.529	1.594	1.110	1.578
Fe2+	0.016	0.018	0.017	0.020	0.029	0.020	0.028	0.021	0.021	0.005	0.024
Ca	0.465	0.587	0.580	0.544	0.498	0.505	0.525	0.522	0.603	0.069	0.592
Na	0.521	0.415	0.405	0.398	0.434	0.507	0.471	0.488	0.419	0.951	0.417
K	0.010	0.008	0.014	0.043	0.051	0.005	0.016	0.010	0.013	0.004	0.014
Ba	0.006	0.000	0.000	0.009	0.002	0.003	0.002	0.002	0.001	0.000	0.000
Sr	0.002	0.003	0.003	0.004	0.004	0.008	0.005	0.002	0.007	0.002	0.002
Total	5.013	5.025	5.016	5.022	5.021	5.031	5.025	5.028	5.039	5.032	5.026
Ab	52.306	41.046	40.572	40.376	44.121	49.857	46.548	47.876	40.486	92.861	40.793
Or	1.002	0.813	1.414	4.393	5.204	0.494	1.556	0.935	1.290	0.395	1.361
An	46.691	58.140	58.013	55.231	50.675	49.649	51.895	51.189	58.224	6.744	57.846
An/(Ab+An)	47.164	58.617	58.846	57.769	53.457	49.895	52.716	51.672	58.985	6.770	58.644

Feldspars	Sample SUD-7-1994; Drill core 70011 (continued)										
point	Pl4	Pl4 rim	Pl4 over	Pl5 core	Pl5 rim	Pl6 rim	Pl6 core	Pl7 over	Pl7 over	Pl7 rim	Pl7
SiO_2	52.661	54.905	62.294	52.823	54.361	62.904	64.215	67.512	66.566	63.047	52.817
Al_2O_3	29.201	28.058	19.127	29.857	28.602	22.847	22.864	20.504	20.555	23.128	29.388
FeO	0.499	0.359	0.090	0.508	0.347	0.307	0.181	0.000	0.050	0.202	0.548
CaO	11.829	9.945	0.013	12.039	10.547	3.417	3.317	0.402	0.937	3.748	11.819
Na_2O	4.884	6.090	0.390	4.718	5.843	9.804	10.019	11.532	9.746	9.928	4.822
K_2O	0.198	0.092	16.179	0.254	0.102	0.077	0.088	0.155	0.170	0.045	0.139
BaO	0.028	0.000	1.667	0.383	0.192	0.000	0.109	0.000	0.000	0.246	0.192
SrO	0.063	0.083	0.176	0.166	0.000	0.225	0.184	0.000	0.000	0.225	0.166
Total	99.363	99.532	99.936	100.748	99.994	99.581	100.977	100.105	98.024	100.569	99.891
Si	2.408	2.490	2.932	2.391	2.461	2.799	2.815	2.952	2.957	2.786	2.406
Al	1.574	1.500	1.061	1.593	1.526	1.198	1.181	1.057	1.076	1.204	1.578
Fe2+	0.019	0.014	0.004	0.019	0.013	0.011	0.007	0.000	0.002	0.007	0.021
Ca	0.580	0.483	0.001	0.584	0.512	0.163	0.156	0.019	0.045	0.177	0.577
Na	0.433	0.536	0.036	0.414	0.513	0.846	0.852	0.978	0.839	0.851	0.426
K	0.012	0.005	0.972	0.015	0.006	0.004	0.005	0.009	0.010	0.003	0.008
Ba	0.001	0.000	0.031	0.007	0.003	0.000	0.002	0.000	0.000	0.004	0.003
Sr	0.002	0.002	0.005	0.004	0.000	0.006	0.005	0.000	0.000	0.006	0.004
Total	5.027	5.030	5.041	5.027	5.035	5.027	5.022	5.013	4.929	5.038	5.023
Ab	42.282	52.292	3.532	40.891	49.777	83.489	84.123	97.266	93.932	82.536	42.133
Or	1.128	0.520	96.403	1.449	0.572	0.431	0.486	0.860	1.078	0.246	0.799
An	56.590	47.188	0.065	57.660	49.651	16.080	15.390	1.874	4.990	17.218	57.068
An/(Ab+An)	57.236	47.435		58.508	49.937	16.149	15.466	1.890	5.045	17.261	57.527

Feldspars	Sample SUD-7-1994; Drill	Sample SUD-7-1994; Drill core 70011 (continued)									
point	Pl7 core	Pl8	Pl8	Pl8	Pl8	Pl8	Pl8	Pl8	Pl8	Pl8	Pl8
SiO_2	52.725	58.298	55.266	54.948	53.534	54.169	54.019	54.329	54.560	54.806	55.224
Al_2O_3	29.473	25.804	27.164	26.819	28.202	28.298	28.496	28.474	28.120	28.105	27.578
FeO	0.634	0.449	0.464	0.560	0.636	0.570	0.722	0.549	0.585	0.423	0.499
CaO	11.801	6.964	9.159	9.335	10.527	10.732	10.774	10.441	10.434	10.028	9.645
Na_2O	5.001	7.782	6.380	6.380	5.529	5.670	5.401	5.440	5.602	5.980	6.075
K_2O	0.142	0.109	0.310	0.345	0.194	0.248	0.314	0.235	0.160	0.112	0.375
BaO	0.109	0.109	0.137	0.028	0.000	0.000	0.109	0.356	0.000	0.164	0.247
SrO	0.331	0.268	0.103	0.186	0.104	0.186	0.083	0.124	0.000	0.124	0.041
Total	100.216	99.782	98.983	98.601	98.726	99.873	99.918	99.948	99.461	99.742	99.684
Si	2.398	2.622	2.523	2.522	2.457	2.461	2.454	2.466	2.480	2.486	2.507
Al	1.580	1.368	1.461	1.451	1.526	1.515	1.526	1.523	1.506	1.502	1.476
Fe2+	0.024	0.017	0.018	0.021	0.024	0.022	0.027	0.021	0.022	0.016	0.019
Ca	0.575	0.336	0.448	0.459	0.518	0.522	0.524	0.508	0.508	0.487	0.469
Na	0.441	0.679	0.565	0.568	0.492	0.499	0.476	0.479	0.494	0.526	0.535
K	0.008	0.006	0.018	0.020	0.011	0.014	0.018	0.014	0.009	0.006	0.022
Ba	0.002	0.002	0.002	0.001	0.000	0.000	0.002	0.006	0.000	0.003	0.004
Sr	0.009	0.007	0.003	0.005	0.003	0.005	0.002	0.003	0.000	0.003	0.001
Total	5.037	5.036	5.038	5.047	5.031	5.039	5.030	5.019	5.019	5.030	5.033
Ab	43.054	66.505	54.786	54.226	48.188	48.199	46.716	47.869	48.827	51.573	52.139
Or	0.804	0.607	1.752	1.929	1.113	1.387	1.787	1.361	0.918	0.636	2.118
An	56.142	32.888	43.462	43.844	50.700	50.414	51.497	50.770	50.255	47.791	45.743
An/(Ab+An)	56.597	33.089	44.237	44.707	51.270	51.123	52.434	51.471	50.721	48.097	46.733

Feldspars	Sample SUD-7-1994; Drill core 70011 (continued)										
point	Pl8	Pl8	Pl8	Pl8 rim	Pl8 rim	Pl8 rim	Pl8 rim	Pl8 rim	Pl8	Pl8 over	Pl8 over
SiO_2	55.641	56.973	55.433	61.763	64.611	59.581	61.109	61.821	61.701	61.673	62.219
Al_2O_3	27.009	26.354	27.348	23.448	21.560	24.697	24.077	23.416	22.943	19.157	18.970
FeO	0.610	0.504	0.480	0.136	0.050	0.223	0.349	0.247	0.944	0.055	0.021
CaO	9.230	8.094	9.132	4.188	2.299	6.007	4.932	4.262	5.149	0.017	0.000
Na_2O	6.379	7.079	6.311	9.453	10.730	8.337	9.095	9.521	9.480	0.279	0.298
K_2O	0.141	0.100	0.102	0.080	0.051	0.063	0.107	0.043	0.055	15.750	16.193
BaO	0.137	0.028	0.247	0.109	0.000	0.027	0.027	0.000	0.082	2.352	1.506
SrO	0.124	0.000	0.104	0.020	0.082	0.103	0.144	0.206	0.000	0.000	0.000
Total	99.271	99.132	99.157	99.197	99.383	99.038	99.840	99.516	100.354	99.283	99.207
Si	2.532	2.581	2.523	2.763	2.866	2.683	2.726	2.760	2.750	2.928	2.942
Al	1.448	1.407	1.467	1.236	1.127	1.311	1.266	1.232	1.205	1.072	1.057
Fe2+	0.023	0.019	0.018	0.005	0.002	0.008	0.013	0.009	0.035	0.002	0.001
Ca	0.450	0.393	0.445	0.201	0.109	0.290	0.236	0.204	0.246	0.001	0.000
Na	0.563	0.622	0.557	0.820	0.923	0.728	0.787	0.824	0.819	0.026	0.027
K	0.008	0.006	0.006	0.005	0.003	0.004	0.006	0.002	0.003	0.954	0.977
Ba	0.002	0.000	0.004	0.002	0.000	0.000	0.000	0.000	0.001	0.044	0.028
Sr	0.003	0.000	0.003	0.001	0.002	0.003	0.004	0.005	0.000	0.000	0.000
Total	5.030	5.029	5.024	5.031	5.033	5.027	5.037	5.037	5.059	5.026	5.032
Ab	55.123	60.934	55.241	79.975	89.164	71.269	76.488	79.978	76.690	2.619	2.721
Or	0.802	0.566	0.587	0.445	0.279	0.354	0.592	0.238	0.293	97.292	97.279
An	44.075	38.500	44.171	19.580	10.557	28.377	22.920	19.784	23.018	0.088	0.000
An/(Ab+An)	44.431	38.719	44.432	19.667	10.587	28.477	23.057	19.831	23.085		

Feldspars	Sample SUD-7-1994; Drill core 70011 (continued)								SUD-94-1994		
point	Pl8 over	Kf1	Kf1	Kf1	Kf2	matrix1	matrix2	matrix3	Pl	Pl	Pl
SiO_2	61.436	62.771	62.091	63.137	62.649	66.973	67.073	67.546	59.666	47.589	55.249
Al_2O_3	19.045	18.847	19.040	18.934	18.811	20.304	20.462	20.517	25.082	28.793	28.124
FeO	0.232	0.080	0.015	0.000	0.000	0.076	0.000	0.005	0.295	1.707	0.615
CaO	0.197	0.077	0.000	0.000	0.046	0.562	0.430	0.757	5.930	17.598	11.303
Na_2O	0.310	0.208	0.262	0.247	0.278	11.699	11.811	11.343	6.733	3.052	4.869
K_2O	16.179	16.598	17.084	17.007	16.684	0.066	0.102	0.075	1.467	0.402	0.358
BaO	1.096	0.493	0.548	0.192	0.849	0.082	0.000	0.000	0.124	0.124	0.000
SrO	0.000	0.039	0.156	0.137	0.000	0.000	0.000	0.000	0.000	0.101	0.225
Total	98.495	99.113	99.196	99.654	99.317	99.762	99.878	100.243	99.297	99.366	100.743
Si	2.926	2.954	2.934	2.954	2.951	2.945	2.943	2.949	2.685	2.244	2.484
Al	1.069	1.045	1.060	1.044	1.044	1.052	1.058	1.056	1.330	1.600	1.490
Fe2+	0.009	0.003	0.001	0.000	0.000	0.003	0.000	0.000	0.011	0.067	0.023
Ca	0.010	0.004	0.000	0.000	0.002	0.026	0.020	0.035	0.286	0.889	0.545
Na	0.029	0.019	0.024	0.022	0.025	0.997	1.005	0.960	0.587	0.279	0.424
K	0.983	0.996	1.030	1.015	1.003	0.004	0.006	0.004	0.084	0.024	0.021
Ba	0.020	0.009	0.010	0.004	0.016	0.001	0.000	0.000	0.002	0.002	0.000
Sr	0.000	0.001	0.004	0.004	0.000	0.000	0.000	0.000	0.000	0.003	0.006
Total	5.046	5.031	5.063	5.043	5.041	5.029	5.033	5.005	4.986	5.108	4.993
Ab	2.802	1.862	2.278	2.160	2.464	97.063	97.485	96.040	61.348	23.403	42.896
Or	96.214	97.757	97.722	97.840	97.310	0.360	0.554	0.418	8.795	2.028	2.075
An	0.984	0.381	0.000	0.000	0.225	2.577	1.961	3.542	29.858	74.569	55.028
An/(Ab+An)						2.586	1.972	3.557	32.737	76.113	56.194

Feldspars	SUD-94-1994; Drill core 70011 (continued)						SUD-8-1994; Drill core 70011				
point	Pl	Pl	Pl	Pl	Pl	Pl	Pl1 core	Pl1 core	Pl1 core	Pl1 rim	Pl1 over
SiO_2	55.155	54.629	54.158	50.459	54.751	56.740	52.786	53.643	53.346	52.851	61.462
Al_2O_3	27.784	28.202	28.812	27.827	28.313	27.017	28.982	28.496	28.708	28.898	23.888
FeO	0.449	0.569	0.623	1.303	0.709	0.435	0.364	0.451	0.559	0.450	0.145
CaO	11.080	11.805	11.883	14.969	11.641	10.122	11.706	11.342	11.301	11.399	5.194
Na_2O	4.994	4.742	4.669	4.061	4.598	5.632	4.853	5.150	4.962	5.029	8.749
K_2O	0.267	0.216	0.225	0.101	0.323	0.177	0.253	0.308	0.265	0.192	0.060
BaO	0.041	0.000	0.000	0.000	0.000	0.083	0.033	0.000	0.155	0.111	0.000
SrO	0.000	0.101	0.000	0.101	0.200	0.000	0.063	0.125	0.055	0.053	0.039
Total	99.770	100.264	100.370	98.821	100.535	100.206	99.040	99.514	99.350	98.981	99.536
Si	2.497	2.469	2.445	2.357	2.469	2.549	2.419	2.446	2.437	2.424	2.741
Al	1.483	1.502	1.533	1.532	1.505	1.431	1.565	1.531	1.546	1.562	1.256
Fe2+	0.017	0.022	0.024	0.051	0.027	0.016	0.014	0.017	0.021	0.017	0.005
Ca	0.537	0.572	0.575	0.749	0.562	0.487	0.575	0.554	0.553	0.560	0.248
Na	0.438	0.415	0.409	0.368	0.402	0.491	0.431	0.455	0.440	0.447	0.756
K	0.015	0.012	0.013	0.006	0.019	0.010	0.015	0.018	0.015	0.011	0.003
Ba	0.001	0.000	0.000	0.000	0.000	0.001	0.001	0.000	0.003	0.002	0.000
Sr	0.000	0.003	0.000	0.003	0.005	0.000	0.002	0.003	0.001	0.001	0.001
Total	4.989	4.994	4.999	5.065	4.989	4.986	5.021	5.025	5.017	5.025	5.011
Ab	44.224	41.569	41.015	32.752	40.895	49.657	42.246	44.319	43.601	43.906	75.046
Or	1.556	1.246	1.301	0.536	1.890	1.027	1.447	1.744	1.531	1.101	0.336
An	54.220	57.185	57.684	66.712	57.214	49.316	56.307	53.937	54.868	54.994	24.618
An/(Ab+An)	55.077	57.907	58.444	67.072	58.317	49.828	57.134	54.895	55.721	55.608	24.701

Feldspars	Sample SUD-8-1994; Drill core 70011 (continued)										
point	Pl1 core	Pl1 rim	Pl2 core	Pl2 rim	Pl2 rim	Pl2 core	Pl2 core	Pl3 core	Pl3 core	Pl4 rim	Pl4 core
SiO_2	51.959	54.348	53.036	52.755	53.944	54.656	52.786	52.246	51.778	52.741	53.013
Al_2O_3	29.079	27.980	28.235	29.316	28.900	27.838	29.200	29.283	29.294	29.946	28.512
FeO	0.544	0.228	0.538	0.471	0.388	0.575	0.542	0.522	0.447	0.401	0.462
CaO	12.190	10.194	10.837	11.828	11.418	10.287	12.307	12.020	12.275	12.389	11.172
Na_2O	4.519	6.043	5.605	4.776	5.403	5.624	4.598	4.614	4.652	4.678	5.177
K_2O	0.249	0.058	0.099	0.249	0.057	0.394	0.321	0.278	0.259	0.103	0.326
BaO	0.011	0.100	0.000	0.000	0.000	0.044	0.112	0.000	0.000	0.177	0.000
SrO	0.044	0.040	0.097	0.066	0.102	0.126	0.120	0.108	0.133	0.034	0.121
Total	98.597	98.991	98.505	99.460	100.212	99.545	99.985	99.072	98.839	100.470	98.782
Si	2.397	2.481	2.443	2.408	2.440	2.487	2.405	2.398	2.386	2.388	2.436
Al	1.581	1.506	1.536	1.577	1.541	1.493	1.568	1.584	1.591	1.598	1.544
Fe2+	0.021	0.009	0.021	0.018	0.015	0.022	0.021	0.020	0.017	0.015	0.018
Ca	0.603	0.499	0.535	0.579	0.553	0.501	0.601	0.591	0.606	0.601	0.550
Na	0.404	0.535	0.500	0.423	0.474	0.496	0.406	0.411	0.416	0.411	0.461
K	0.015	0.003	0.006	0.015	0.003	0.023	0.019	0.016	0.015	0.006	0.019
Ba	0.000	0.002	0.000	0.000	0.000	0.001	0.002	0.000	0.000	0.003	0.000
Sr	0.001	0.001	0.003	0.002	0.003	0.003	0.003	0.003	0.004	0.001	0.003
Total	5.022	5.035	5.043	5.021	5.028	5.026	5.024	5.023	5.034	5.022	5.032
Ab	39.575	51.586	48.075	41.617	45.981	48.621	39.607	40.335	40.086	40.359	44.763
Or	1.437	0.326	0.560	1.428	0.317	2.240	1.817	1.599	1.467	0.583	1.853
An	58.988	48.088	51.365	56.955	53.702	49.139	58.576	58.066	58.447	59.058	53.384
An/(Ab+An)	59.848	48.245	51.654	57.780	53.873	50.265	59.660	59.009	59.318	59.404	54.392

Feldspars	Sample SUD-8-1994; Drill core 70011 (continued)										
point	Pl4 core	Pl5 core	Pl5 core	Pl5 core	Pl5 rim	Pl6 rim	Pl6 rim	Pl6 rim	Pl6 core	Pl6 core	Pl6 core
SiO_2	52.756	52.037	51.732	59.440	54.776	51.210	54.239	59.981	53.863	52.105	53.063
Al_2O_3	29.106	29.389	29.403	24.271	28.060	29.317	27.037	23.463	28.208	29.452	28.910
FeO	0.599	0.559	0.546	0.546	0.470	0.626	0.643	0.392	0.491	0.621	0.533
CaO	11.606	12.416	12.352	5.732	10.277	12.295	9.486	5.379	10.698	12.326	11.462
Na_2O	4.889	4.527	4.366	8.291	5.873	4.404	6.303	8.876	5.450	4.643	5.113
K_2O	0.309	0.215	0.308	0.316	0.102	0.309	0.202	0.154	0.149	0.259	0.299
BaO	0.055	0.178	0.066	0.000	0.000	0.055	0.165	0.121	0.000	0.056	0.144
SrO	0.134	0.075	0.070	0.075	0.074	0.030	0.083	0.078	0.114	0.117	0.036
Total	99.453	99.397	98.844	98.671	99.632	98.245	98.157	98.445	98.972	99.579	99.560
Si	2.413	2.386	2.384	2.692	2.485	2.376	2.503	2.721	2.464	2.385	2.423
Al	1.569	1.588	1.597	1.295	1.500	1.603	1.471	1.255	1.521	1.589	1.556
Fe2+	0.023	0.021	0.021	0.021	0.018	0.024	0.025	0.015	0.019	0.024	0.020
Ca	0.569	0.610	0.610	0.278	0.499	0.611	0.469	0.261	0.524	0.605	0.561
Na	0.433	0.403	0.390	0.728	0.517	0.396	0.564	0.781	0.483	0.412	0.453
K	0.018	0.013	0.018	0.018	0.006	0.018	0.012	0.009	0.009	0.015	0.017
Ba	0.001	0.003	0.001	0.000	0.000	0.001	0.003	0.002	0.000	0.001	0.003
Sr	0.004	0.002	0.002	0.002	0.002	0.001	0.002	0.002	0.003	0.003	0.001
Total	5.029	5.027	5.022	5.034	5.026	5.030	5.049	5.046	5.022	5.034	5.034
Ab	42.493	39.264	38.316	71.069	50.546	38.626	53.974	74.276	47.558	39.939	43.911
Or	1.764	1.228	1.777	1.783	0.577	1.781	1.139	0.849	0.853	1.468	1.691
An	55.742	59.509	59.907	27.148	48.877	59.593	44.887	24.875	51.588	58.593	54.398
An/(Ab+An)	56.743	60.248	60.991	27.641	49.161	60.673	45.404	25.088	52.032	59.466	55.334

Feldspars	Sample SUD-8-1994; Drill core 70011 (continued)										
point	Pl6 rim	Pl6 core	Pl6 rim	Pl6 core	Pl6 core	Pl6 rim	Pl6 rim	Pl7 core	Pl7 core	Pl7 core	Pl7 rim
SiO_2	55.592	51.252	53.784	51.276	52.395	55.416	57.219	51.829	52.714	52.454	51.032
Al_2O_3	27.342	29.579	28.012	29.255	29.579	28.065	26.045	29.512	28.578	28.484	29.742
FeO	0.579	0.582	0.581	0.622	0.528	0.574	0.342	0.511	0.490	0.595	0.678
CaO	9.623	12.514	10.822	12.200	12.433	10.301	8.286	12.417	11.575	11.611	12.607
Na_2O	5.348	4.497	5.424	4.528	4.494	5.748	7.126	4.482	5.089	4.975	4.396
K_2O	0.169	0.279	0.283	0.255	0.269	0.313	0.061	0.215	0.103	0.341	0.210
BaO	0.100	0.078	0.000	0.110	0.066	0.166	0.000	0.100	0.155	0.000	0.088
SrO	0.049	0.137	0.068	0.071	0.121	0.029	0.130	0.055	0.112	0.087	0.066
Total	98.800	98.918	98.974	98.316	99.886	100.611	99.210	99.120	98.817	98.549	98.820
Si	2.532	2.365	2.464	2.378	2.389	2.493	2.591	2.381	2.425	2.422	2.357
Al	1.467	1.609	1.512	1.599	1.589	1.488	1.390	1.598	1.550	1.550	1.619
Fe2+	0.022	0.022	0.022	0.024	0.020	0.022	0.013	0.020	0.019	0.023	0.026
Ca	0.470	0.619	0.531	0.606	0.607	0.497	0.402	0.611	0.571	0.574	0.624
Na	0.472	0.402	0.482	0.407	0.397	0.501	0.626	0.399	0.454	0.445	0.394
K	0.010	0.016	0.017	0.015	0.016	0.018	0.004	0.013	0.006	0.020	0.012
Ba	0.002	0.001	0.000	0.002	0.001	0.003	0.000	0.002	0.003	0.000	0.002
Sr	0.001	0.004	0.002	0.002	0.003	0.001	0.003	0.001	0.003	0.002	0.002
Total	4.976	5.040	5.029	5.034	5.023	5.022	5.029	5.026	5.030	5.036	5.036
Ab	49.625	38.783	46.795	39.588	38.936	49.355	60.673	39.026	44.050	42.831	38.227
Or	1.030	1.581	1.606	1.469	1.533	1.771	0.344	1.231	0.588	1.934	1.199
An	49.346	59.636	51.598	58.943	59.531	48.874	38.983	59.743	55.363	55.235	60.574
An/(Ab+An)	49.859	60.594	52.441	59.822	60.458	49.755	39.117	60.488	55.690	56.324	61.309

Feldspars	Sample SUD-8-1994; Drill core 70011 (continued)										
point	Pl7 rim	Pl7 rim	Pl7 rim	Pl8 core	Pl8 rim	Pl8 rim	Pl8 core	Pl8 core	Pl8 rim	Pl8 core	Pl8 rim
SiO_2	51.023	52.602	51.963	51.105	53.849	56.823	52.060	51.699	60.981	51.027	59.191
Al_2O_3	29.687	28.581	29.254	29.582	28.083	25.844	29.457	29.281	24.013	29.801	24.341
FeO	0.664	0.378	0.478	0.484	0.454	0.481	0.472	0.533	0.200	0.554	0.279
CaO	12.623	11.302	12.209	12.435	10.435	8.275	12.448	11.794	5.326	12.455	6.046
Na_2O	4.481	5.178	4.603	4.430	5.676	7.272	4.399	4.705	9.072	4.381	8.280
K_2O	0.194	0.066	0.218	0.239	0.339	0.095	0.237	0.300	0.068	0.247	0.306
BaO	0.089	0.066	0.133	0.077	0.044	0.176	0.000	0.165	0.000	0.166	0.055
SrO	0.093	0.095	0.051	0.099	0.113	0.108	0.025	0.092	0.044	0.112	0.090
Total	98.854	98.269	98.909	98.450	98.993	99.076	99.097	98.569	99.704	98.743	98.588
Si	2.357	2.428	2.392	2.366	2.466	2.585	2.389	2.389	2.723	2.359	2.684
Al	1.616	1.555	1.587	1.614	1.516	1.386	1.593	1.595	1.264	1.623	1.301
Fe2+	0.026	0.015	0.018	0.019	0.017	0.018	0.018	0.021	0.007	0.021	0.011
Ca	0.625	0.559	0.602	0.617	0.512	0.403	0.612	0.584	0.255	0.617	0.294
Na	0.401	0.463	0.411	0.398	0.504	0.641	0.391	0.422	0.785	0.393	0.728
K	0.011	0.004	0.013	0.014	0.020	0.006	0.014	0.018	0.004	0.015	0.018
Ba	0.002	0.001	0.002	0.001	0.001	0.003	0.000	0.003	0.000	0.003	0.001
Sr	0.002	0.003	0.001	0.003	0.003	0.003	0.001	0.002	0.001	0.003	0.002
Total	5.041	5.028	5.027	5.032	5.038	5.046	5.017	5.033	5.040	5.033	5.038
Ab	38.682	45.153	40.049	38.664	48.657	61.071	38.473	41.200	75.223	38.345	70.038
Or	1.104	0.381	1.251	1.370	1.911	0.528	1.361	1.730	0.374	1.421	1.705
An	60.213	54.466	58.700	59.966	49.432	38.402	60.165	57.070	24.403	60.234	28.257
An/(Ab+An)	60.886	54.675	59.444	60.799	50.395	38.605	60.996	58.075	24.494	61.103	28.747

Feldspars	Sample SUD-8-1994; Drill core 70011 (continued)										
point	Pl9 over	Pl9 rim	Pl9 core	Pl9 core	Pl9 rim	Pl9 core	Pl9 rim	Pl9 rim	Pl9 core	Pl10 core	Pl10 core
SiO_2	57.007	52.083	51.582	51.382	52.486	52.212	53.124	53.712	54.896	51.596	51.680
Al_2O_3	25.474	28.707	29.395	29.422	29.085	29.245	28.123	27.962	27.572	29.393	29.572
FeO	0.258	0.391	0.661	0.523	0.414	0.530	0.637	0.551	0.494	0.609	0.516
CaO	7.753	11.619	12.491	12.222	11.970	12.033	10.858	10.353	10.172	12.604	12.780
Na_2O	7.153	4.903	4.276	4.566	4.909	4.757	5.495	5.765	5.758	4.428	4.268
K_2O	0.349	0.222	0.246	0.267	0.129	0.299	0.207	0.214	0.222	0.270	0.253
BaO	0.154	0.100	0.177	0.077	0.111	0.000	0.232	0.132	0.033	0.000	0.000
SrO	0.050	0.042	0.085	0.053	0.056	0.076	0.093	0.073	0.048	0.080	0.039
Total	98.197	98.068	98.915	98.513	99.159	99.152	98.769	98.762	99.195	98.980	99.107
Si	2.609	2.413	2.379	2.376	2.407	2.396	2.446	2.466	2.501	2.377	2.375
Al	1.374	1.568	1.598	1.604	1.572	1.582	1.526	1.513	1.480	1.596	1.602
Fe2+	0.010	0.015	0.026	0.020	0.016	0.020	0.025	0.021	0.019	0.023	0.020
Ca	0.380	0.577	0.617	0.606	0.588	0.592	0.536	0.509	0.496	0.622	0.629
Na	0.635	0.441	0.382	0.409	0.436	0.423	0.491	0.513	0.509	0.395	0.380
K	0.020	0.013	0.014	0.016	0.008	0.017	0.012	0.013	0.013	0.016	0.015
Ba	0.003	0.002	0.003	0.001	0.002	0.000	0.004	0.002	0.001	0.000	0.000
Sr	0.001	0.001	0.002	0.001	0.001	0.002	0.002	0.002	0.001	0.002	0.001
Total	5.032	5.030	5.021	5.034	5.030	5.033	5.042	5.040	5.020	5.031	5.022
Ab	61.310	42.749	37.704	39.721	42.289	41.001	47.244	49.581	49.964	38.271	37.126
Or	1.967	1.272	1.429	1.529	0.729	1.693	1.169	1.213	1.265	1.533	1.445
An	36.723	55.979	60.867	58.750	56.982	57.306	51.587	49.206	48.770	60.196	61.429
An/(Ab+An)	37.460	56.700	61.749	59.662	57.401	58.293	52.197	49.810	49.395	61.133	62.330

Feldspars	Sample SUD-8-1994; Drill core 70011 (continued)							Sample SUD-66-1994			
point	Pl10 rim	Pl10 core	Pl11 core	Pl11 core	Pl11 rim	Pl11 core	Pl11 rim	Pl1 rim	Pl1	Pl1	Pl1
SiO_2	58.853	51.889	50.896	52.206	54.972	51.955	51.985	53.369	53.033	51.828	51.991
Al_2O_3	24.861	28.999	29.462	28.696	27.040	29.307	29.341	28.666	29.044	29.655	29.496
FeO	0.377	0.575	0.612	0.618	0.577	0.744	0.623	0.540	0.418	0.352	0.352
CaO	6.645	12.137	12.597	11.809	9.680	12.159	12.567	11.392	11.079	12.064	11.862
Na_2O	7.785	4.622	4.320	4.845	5.943	4.373	4.569	5.687	5.097	4.636	4.727
K_2O	0.264	0.259	0.226	0.304	0.319	0.274	0.195	0.084	0.267	0.253	0.093
BaO	0.240	0.143	0.099	0.000	0.154	0.144	0.000	0.192	0.109	0.000	0.109
SrO	0.074	0.104	0.107	0.148	0.040	0.114	0.112	0.000	0.311	0.104	0.270
Total	99.100	98.729	98.318	98.626	98.724	99.068	99.392	99.930	99.358	98.892	98.900
Si	2.661	2.395	2.363	2.410	2.518	2.390	2.384	2.430	2.425	2.383	2.391
Al	1.325	1.578	1.612	1.561	1.460	1.589	1.586	1.538	1.565	1.607	1.599
Fe2+	0.014	0.022	0.024	0.024	0.022	0.029	0.024	0.021	0.016	0.014	0.014
Ca	0.322	0.600	0.627	0.584	0.475	0.599	0.617	0.556	0.543	0.594	0.584
Na	0.682	0.414	0.389	0.434	0.528	0.390	0.406	0.502	0.452	0.413	0.421
K	0.015	0.015	0.013	0.018	0.019	0.016	0.011	0.005	0.016	0.015	0.005
Ba	0.004	0.003	0.002	0.000	0.003	0.003	0.000	0.003	0.002	0.000	0.002
Sr	0.002	0.003	0.003	0.004	0.001	0.003	0.003	0.000	0.008	0.003	0.007
Total	5.026	5.030	5.032	5.035	5.025	5.019	5.032	5.055	5.026	5.028	5.023
Ab	66.936	40.194	37.794	41.872	51.671	38.795	39.245	47.244	44.730	40.422	41.673
Or	1.494	1.483	1.301	1.729	1.822	1.597	1.099	0.459	1.542	1.451	0.539
An	31.570	58.323	60.904	56.399	46.507	59.608	59.656	52.297	53.728	58.127	57.788
An/(Ab+An)	32.049	59.201	61.707	57.391	47.370	60.575	60.319	52.538	54.569	58.983	58.101

Feldspars	Sample SUD-66-1994; Drill core 70011 (continued)										
point	Pl1	Pl1	Pl1	Pl1	Pl1	Pl1 over	Pl1 over	Pl2 rim	Pl2 rim	Pl2	Pl2
SiO_2	52.336	52.408	52.840	56.013	61.053	65.866	64.318	63.385	61.254	52.475	52.205
Al_2O_3	30.140	30.036	29.507	26.994	23.903	21.551	22.620	22.473	23.892	30.085	30.019
FeO	0.383	0.368	0.494	0.392	0.307	0.262	0.157	0.243	0.500	0.277	0.437
CaO	12.337	12.559	11.834	8.739	4.507	1.619	2.593	3.271	4.922	12.201	12.595
Na_2O	4.766	4.544	4.936	6.879	9.558	10.676	10.611	9.707	9.127	4.522	4.432
K_2O	0.101	0.208	0.213	0.118	0.087	0.596	0.064	0.043	0.083	0.163	0.147
BaO	0.000	0.137	0.000	0.300	0.000	0.000	0.272	0.055	0.055	0.164	0.301
SrO	0.250	0.124	0.104	0.330	0.061	0.163	0.266	0.041	0.020	0.104	0.394
Total	100.313	100.384	99.928	99.765	99.476	100.733	100.901	99.218	99.853	99.991	100.530
Si	2.375	2.378	2.403	2.539	2.732	2.886	2.825	2.822	2.732	2.385	2.372
Al	1.612	1.606	1.581	1.442	1.260	1.113	1.171	1.179	1.256	1.611	1.607
Fe2+	0.015	0.014	0.019	0.015	0.011	0.010	0.006	0.009	0.019	0.011	0.017
Ca	0.600	0.610	0.577	0.424	0.216	0.076	0.122	0.156	0.235	0.594	0.613
Na	0.419	0.400	0.435	0.605	0.829	0.907	0.904	0.838	0.789	0.398	0.390
K	0.006	0.012	0.012	0.007	0.005	0.033	0.004	0.002	0.005	0.009	0.009
Ba	0.000	0.002	0.000	0.005	0.000	0.000	0.005	0.001	0.001	0.003	0.005
Sr	0.007	0.003	0.003	0.009	0.002	0.004	0.007	0.001	0.001	0.003	0.010
Total	5.032	5.025	5.030	5.046	5.055	5.028	5.043	5.009	5.037	5.014	5.024
Ab	40.910	39.102	42.495	58.367	78.954	89.243	87.796	84.095	76.688	39.766	38.577
Or	0.570	1.178	1.207	0.659	0.473	3.278	0.348	0.245	0.459	0.943	0.842
An	58.519	59.721	56.299	40.974	20.573	7.479	11.856	15.660	22.853	59.291	60.581
An/(Ab+An)	58.855	60.432	56.987	41.246	20.671	7.732	11.897	15.698	22.959	59.855	61.095

Feldspars	Sample SUD-66-1994; Drill core 70011 (continued)										
point	Pl2	Pl2 rim	Pl2 over	Pl2	Pl2 core	Pl2 rim	Pl3 core	Pl3 rim	Pl3 over	matrix	matrix
SiO_2	54.941	58.045	64.326	55.765	52.460	52.915	62.724	64.010	52.128	56.588	62.852
Al_2O_3	27.803	25.883	22.356	27.431	29.260	28.969	22.303	21.158	29.853	26.486	18.760
FeO	0.368	0.383	0.055	0.262	0.373	0.318	0.207	0.288	0.409	0.374	0.126
CaO	9.859	7.463	2.789	9.195	11.538	11.192	3.082	2.207	12.434	8.024	0.035
Na_2O	6.124	7.609	10.172	6.525	4.952	5.280	10.124	10.989	4.471	7.286	1.131
K_2O	0.071	0.146	0.081	0.069	0.242	0.154	0.053	0.065	0.226	0.066	15.197
BaO	0.109	0.464	0.027	0.164	0.109	0.000	0.000	0.027	0.303	0.192	0.768
SrO	0.083	0.000	0.246	0.041	0.311	0.187	0.000	0.000	0.104	0.041	0.000
Total	99.358	99.993	100.052	99.452	99.245	99.015	98.493	98.744	99.928	99.057	98.869
Si	2.498	2.611	2.839	2.527	2.405	2.424	2.816	2.865	2.378	2.571	2.956
Al	1.490	1.372	1.163	1.465	1.581	1.564	1.180	1.116	1.605	1.418	1.040
Fe2+	0.014	0.014	0.002	0.010	0.014	0.012	0.008	0.011	0.016	0.014	0.005
Ca	0.480	0.360	0.132	0.446	0.567	0.549	0.148	0.106	0.608	0.391	0.002
Na	0.540	0.664	0.870	0.573	0.440	0.469	0.881	0.954	0.395	0.642	0.103
K	0.004	0.008	0.005	0.004	0.014	0.009	0.003	0.004	0.013	0.004	0.912
Ba	0.002	0.008	0.000	0.003	0.002	0.000	0.000	0.000	0.005	0.003	0.014
Sr	0.002	0.000	0.006	0.001	0.008	0.005	0.000	0.000	0.003	0.001	0.000
Total	5.029	5.038	5.017	5.029	5.032	5.033	5.036	5.056	5.024	5.043	5.032
Ab	52.708	64.324	86.449	56.001	43.109	45.851	85.348	89.696	38.910	61.937	10.144
Or	0.402	0.812	0.453	0.390	1.386	0.876	0.294	0.349	1.294	0.369	89.683
An	46.890	34.864	13.098	43.609	55.505	53.473	14.358	9.955	59.796	37.693	0.173
An/(Ab+An)	47.080	35.149	13.158	43.780	56.285	53.946	14.400	9.990	60.580	37.833	

Feldspars	Sample SUD-66-1994 (cont'd)				Sample SUD-155-1995; Drill core 70011						
point	Kf1	Kf2	Kf4	Kf4	Pl1 core	Pl1 core	Pl1 rim	Pl1 over	Pl1 rim	Pl1 rim	Pl2 core
SiO_2	66.778	63.841	62.546	67.137	52.004	51.495	52.246	54.742	59.342	58.883	53.647
Al_2O_3	20.296	19.044	18.807	20.166	29.468	29.040	28.908	27.002	24.153	23.964	28.418
FeO	0.000	0.096	0.201	0.000	0.536	0.542	0.658	0.656	0.374	0.470	0.508
CaO	0.495	0.122	0.000	0.413	12.366	12.206	10.977	9.321	6.320	6.281	11.193
Na_2O	11.646	3.476	1.697	11.851	4.536	4.584	5.091	6.465	8.315	7.645	4.998
K_2O	0.375	11.894	14.691	0.161	0.304	0.217	1.038	0.085	0.075	0.848	0.388
BaO	0.000	0.467	0.851	0.027	0.033	0.055	0.144	0.121	0.120	0.229	0.155
SrO	0.061	0.059	0.020	0.163	0.110	0.096	0.185	0.178	0.083	0.089	0.103
Total	99.651	98.999	98.813	99.918	99.358	98.234	99.246	98.570	98.782	98.409	99.408
Si	2.943	2.957	2.946	2.950	2.385	2.388	2.407	2.514	2.687	2.686	2.450
Al	1.054	1.040	1.044	1.044	1.592	1.587	1.569	1.461	1.289	1.289	1.530
Fe2+	0.000	0.004	0.008	0.000	0.021	0.021	0.025	0.025	0.014	0.018	0.019
Ca	0.023	0.006	0.000	0.019	0.608	0.606	0.542	0.459	0.307	0.307	0.548
Na	0.995	0.312	0.155	1.010	0.403	0.412	0.455	0.576	0.730	0.676	0.443
K	0.021	0.703	0.883	0.009	0.018	0.013	0.061	0.005	0.004	0.049	0.023
Ba	0.000	0.008	0.016	0.000	0.001	0.001	0.003	0.002	0.002	0.004	0.003
Sr	0.002	0.002	0.001	0.004	0.003	0.003	0.005	0.005	0.002	0.002	0.003
Total	5.038	5.031	5.051	5.037	5.030	5.031	5.066	5.046	5.036	5.032	5.018
Ab	95.724	30.573	14.934	97.258	39.205	39.960	42.998	55.387	70.126	65.491	43.695
Or	2.028	68.834	85.066	0.869	1.732	1.243	5.769	0.482	0.418	4.777	2.230
An	2.248	0.593	0.000	1.873	59.064	58.796	51.233	44.131	29.457	29.732	54.075
An/(Ab+An)	2.295			1.889	60.104	59.538	54.370	44.345	29.580	31.223	55.308

Feldspars	Sample SUD-155-1995; Drill core 70011 (continued)										
point	Pl2 core	Pl2 core	Pl2 core	Pl2 core	Pl2 core	Pl2 core	Pl2 rim	Pl2 rim	Pl2 rim	Pl3 core	Pl3 core
SiO_2	51.866	51.978	52.851	51.214	52.145	51.418	50.797	53.945	53.120	51.299	53.278
Al_2O_3	28.687	28.706	28.510	29.363	29.227	28.961	29.466	27.781	28.209	29.306	28.485
FeO	0.719	0.565	0.397	0.655	0.500	0.512	0.461	0.390	0.542	0.714	0.594
CaO	11.661	11.773	11.435	12.747	11.812	11.988	12.542	10.246	10.903	12.537	11.316
Na_2O	4.711	4.923	4.930	4.197	4.785	4.716	4.437	5.662	5.226	4.303	5.066
K_2O	0.196	0.586	0.370	0.296	0.416	0.353	0.467	0.354	0.370	0.367	0.384
BaO	0.088	0.144	0.000	0.000	0.033	0.000	0.000	0.011	0.000	0.067	0.055
SrO	0.121	0.140	0.078	0.063	0.108	0.155	0.084	0.071	0.146	0.102	0.101
Total	98.050	98.815	98.572	98.534	99.026	98.104	98.254	98.461	98.516	98.695	99.279
Si	2.408	2.403	2.433	2.371	2.397	2.389	2.361	2.479	2.447	2.373	2.439
Al	1.569	1.564	1.547	1.602	1.584	1.586	1.614	1.505	1.532	1.598	1.537
Fe2+	0.028	0.022	0.015	0.025	0.019	0.020	0.018	0.015	0.021	0.028	0.023
Ca	0.580	0.583	0.564	0.632	0.582	0.597	0.624	0.505	0.538	0.621	0.555
Na	0.424	0.441	0.440	0.377	0.427	0.425	0.400	0.505	0.467	0.386	0.450
K	0.012	0.035	0.022	0.017	0.024	0.021	0.028	0.021	0.022	0.022	0.022
Ba	0.002	0.003	0.000	0.000	0.001	0.000	0.000	0.000	0.000	0.001	0.001
Sr	0.003	0.004	0.002	0.002	0.003	0.004	0.002	0.002	0.004	0.003	0.003
Total	5.025	5.053	5.024	5.026	5.036	5.041	5.046	5.031	5.031	5.032	5.029
Ab	41.749	41.671	42.898	36.702	41.300	40.750	38.003	48.993	45.467	37.508	43.779
Or	1.144	3.262	2 120	1.702	2.362	2.009	2.634	2.018	2.116	2.104	2.186
An	57.107	55.067	54.982	61.596	56.339	57.241	59.363	48.989	52.417	60.388	54.035
An/(Ab+An)	57.767	56.924	56.173	62.662	57.702	58.415	60.969	49.998	53.550	61.686	55.243

Feldspars	Sample SUD-155-1995; Drill core 70011 (continued)										
point	Pl4 core	Pl4 core	Pl4 rim	Pl5 core	Pl5 core	Pl5 rim	Pl5 rim	Pl5 over	Pl6 core	Pl6 core	Pl6 rim
SiO_2	51.929	51.724	51.693	53.655	54.046	58.832	59.669	58.898	51.311	50.900	57.453
Al_2O_3	28.879	29.102	29.280	27.837	27.653	24.600	23.482	24.130	29.370	29.549	25.707
FeO	1.516	0.525	0.465	0.546	0.539	0.416	0.551	0.366	0.692	0.704	0.456
CaO	11.392	12.178	12.127	10.847	10.566	6.592	5.321	6.021	12.827	13.075	7.455
Na_2O	4.695	4.563	4.472	5.496	5.474	8.080	8.731	8.371	4.314	4.159	7.771
K_2O	0.557	0.298	0.293	0.228	0.395	0.097	0.046	0.099	0.296	0.300	0.069
BaO	0.198	0.242	0.044	0.011	0.133	0.143	0.099	0.033	0.133	0.133	0.154
SrO	0.061	0.089	0.112	0.119	0.084	0.083	0.136	0.126	0.126	0.088	0.086
Total	99.227	98.721	98.485	98.739	98.891	98.843	98.034	98.044	99.069	98.908	99.152
Si	2.396	2.390	2.389	2.465	2.479	2.666	2.718	2.685	2.368	2.354	2.605
Al	1.570	1.585	1.595	1.507	1.495	1.314	1.261	1.297	1.597	1.611	1.374
Fe2+	0.058	0.020	0.018	0.021	0.021	0.016	0.021	0.014	0.027	0.027	0.017
Ca	0.563	0.603	0.600	0.534	0.519	0.320	0.260	0.294	0.634	0.648	0.362
Na	0.420	0.409	0.401	0.490	0.487	0.710	0.771	0.740	0.386	0.373	0.683
K	0.033	0.018	0.017	0.013	0.023	0.006	0.003	0.006	0.017	0.018	0.004
Ba	0.004	0.004	0.001	0.000	0.002	0.003	0.002	0.001	0.002	0.002	0.003
Sr	0.002	0.002	0.003	0.003	0.002	0.002	0.004	0.003	0.003	0.002	0.002
Total	5.046	5.031	5.023	5.033	5.028	5.035	5.039	5.039	5.035	5.036	5.051
Ab	41.339	39.718	39.349	47.218	47.299	68.550	74.614	71.160	37.197	35.912	65.106
Or	3.230	1.707	1.693	1.288	2.245	0.542	0.260	0.554	1.681	1.702	0.381
An	55.432	58.574	58.958	51.493	50.456	30.908	25.126	28.285	61.122	62.385	34.513
An/(Ab+An)	57.282	59.592	59.973	52.165	51.615	31.077	25.191	28.443	62.167	63.466	34.645

Feldspars	Sample SUD-155-1995; Drill core 70011 (continued)										
point	Pl6 rim	Pl6 core	Pl6 rim	Pl7 rim	Pl7 core	Pl7 core	Pl7 core	Pl7 core	Pl8 rim	Pl8 core	Pl8 core
SiO_2	55.659	51.293	59.399	53.808	51.336	51.552	50.515	51.366	56.689	51.008	53.089
Al_2O_3	26.493	29.434	23.821	27.738	29.731	29.343	29.377	29.604	25.681	29.294	28.757
FeO	0.331	0.564	0.420	0.366	0.595	0.491	0.652	0.630	0.363	0.547	0.493
CaO	8.771	12.844	5.949	10.319	12.557	12.409	13.065	12.612	8.361	12.526	11.554
Na_2O	6.862	4.188	8.363	5.773	4.339	4.441	4.277	4.145	6.898	4.390	5.096
K_2O	0.086	0.270	0.244	0.079	0.182	0.287	0.124	0.267	0.197	0.290	0.093
BaO	0.199	0.056	0.000	0.000	0.000	0.000	0.000	0.088	0.000	0.132	0.221
SrO	0.088	0.127	0.076	0.074	0.087	0.102	0.060	0.056	0.121	0.146	0.079
Total	98.490	98.775	98.272	98.157	98.827	98.624	98.070	98.768	98.311	98.334	99.382
Si	2.549	2.369	2.701	2.478	2.366	2.381	2.353	2.370	2.593	2.369	2.428
Al	1.430	1.602	1.277	1.506	1.615	1.597	1.613	1.610	1.384	1.603	1.550
Fe2+	0.013	0.022	0.016	0.014	0.023	0.019	0.025	0.024	0.014	0.021	0.019
Ca	0.430	0.636	0.290	0.509	0.620	0.614	0.652	0.624	0.410	0.623	0.566
Na	0.609	0.375	0.737	0.516	0.388	0.398	0.386	0.371	0.612	0.395	0.452
K	0.005	0.016	0.014	0.005	0.011	0.017	0.007	0.016	0.011	0.017	0.005
Ba	0.004	0.001	0.000	0.000	0.000	0.000	0.000	0.002	0.000	0.002	0.004
Sr	0.002	0.003	0.002	0.002	0.002	0.003	0.002	0.001	0.003	0.004	0.002
Total	5.043	5.025	5.037	5.029	5.025	5.028	5.038	5.018	5.027	5.036	5.026
Ab	58.324	36.536	70.807	50.082	38.070	38.661	36.940	36.712	59.223	38.167	44.154
Or	0.482	1.548	1.359	0.449	1.048	1.642	0.706	1.558	1.112	1.659	0.531
An	41.195	61.917	27.833	49.468	60.882	59.698	62.354	61.730	39.664	60.174	55.315
An/(Ab+An)	41.394	62.890	28.217	49.692	61.527	60.694	62.797	62.707	40.111	61.189	55.610

Feldspars	Sample SUD-155-1995; Drill core 70011 (continued)										
point	Pl8 core	Pl8 core	Pl8 core	Pl8 core	Pl8 rim	Pl8 rim	Pl9 core	Pl9 core	Pl9 core	Pl9 rim	Pl9 rim
SiO_2	54.486	52.002	51.570	51.540	56.694	60.963	52.042	52.897	51.885	52.905	56.356
Al_2O_3	27.205	28.902	29.067	29.089	26.072	23.248	29.472	28.376	29.094	28.836	26.748
FeO	0.501	0.533	0.413	0.455	0.567	0.197	0.468	0.428	0.429	0.407	0.537
CaO	10.211	11.964	12.254	12.200	8.418	5.604	12.334	11.728	11.913	11.436	8.998
Na_2O	5.823	4.779	4.544	4.568	6.663	8.833	4.492	5.001	4.701	5.149	6.596
K_2O	0.316	0.177	0.195	0.279	0.319	0.062	0.097	0.239	0.205	0.105	0.114
BaO	0.077	0.055	0.188	0.000	0.000	0.033	0.210	0.133	0.055	0.110	0.000
SrO	0.062	0.164	0.091	0.068	0.055	0.177	0.123	0.072	0.080	0.099	0.125
Total	98.681	98.577	98.321	98.198	98.788	99.117	99.237	98.874	98.362	99.047	99.474
Si	2.500	2.402	2.389	2.389	2.582	2.741	2.388	2.432	2.398	2.425	2.553
Al	1.471	1.573	1.587	1.589	1.399	1.232	1.594	1.538	1.585	1.558	1.428
Fe2+	0.019	0.021	0.016	0.018	0.022	0.007	0.018	0.016	0.017	0.016	0.020
Ca	0.502	0.592	0.608	0.606	0.411	0.270	0.606	0.578	0.590	0.562	0.437
Na	0.518	0.428	0.408	0.410	0.588	0.770	0.400	0.446	0.421	0.458	0.579
K	0.019	0.010	0.012	0.016	0.019	0.004	0.006	0.014	0.012	0.006	0.007
Ba	0.001	0.001	0.003	0.000	0.000	0.001	0.004	0.002	0.001	0.002	0.000
Sr	0.002	0.004	0.002	0.002	0.001	0.005	0.003	0.002	0.002	0.003	0.003
Total	5.032	5.031	5.027	5.030	5.022	5.030	5.018	5.029	5.026	5.028	5.026
Ab	49.884	41.533	39.709	39.745	57.813	73.789	39.500	42.964	41.170	44.630	56.652
Or	1.783	1.013	1.122	1.596	1.824	0.341	0.560	1.354	1.179	0.596	0.645
An	48.333	57.454	59.169	58.659	40.363	25.870	59.940	55.682	57.650	54.774	42.704
An/(Ab+An)	49.211	58.042	59.841	59.611	41.113	25.959	60.277	56.446	58.338	55.102	42.981

Feldspars	Sample SUD-155-1995; Drill core 70011 (continued)									
point	Pl9 rim	Pl10 core	Pl11 core	Pl11 core	Pl11 rim	Pl11 rim	Pl11 core	Pl11 rim	Pl11 rim	Pl12 core
SiO_2	57.038	53.236	51.689	51.824	53.044	52.660	51.526	56.490	51.656	51.579
Al_2O_3	26.496	28.132	29.232	29.417	28.633	28.620	29.690	26.541	29.407	29.648
FeO	0.341	0.483	0.650	0.665	0.411	0.499	0.611	0.519	0.472	0.575
CaO	8.365	10.899	12.680	12.400	11.213	11.662	12.396	8.782	12.324	12.639
Na_2O	7.028	5.328	4.374	4.376	5.175	4.897	4.374	6.807	4.592	4.335
K_2O	0.068	0.362	0.226	0.317	0.072	0.218	0.339	0.088	0.065	0.208
BaO	0.000	0.265	0.000	0.011	0.000	0.000	0.055	0.000	0.089	0.222
SrO	0.109	0.033	0.164	0.101	0.096	0.068	0.083	0.089	0.098	0.098
Total	99.445	98.737	99.014	99.112	98.645	98.624	99.075	99.315	98.701	99.304
Si	2.577	2.450	2.381	2.383	2.436	2.425	2.371	2.561	2.382	2.370
Al	1.411	1.526	1.587	1.594	1.550	1.553	1.610	1.418	1.598	1.606
Fe2+	0.013	0.019	0.025	0.026	0.016	0.019	0.024	0.020	0.018	0.022
Ca	0.405	0.537	0.626	0.611	0.552	0.575	0.611	0.427	0.609	0.622
Na	0.616	0.475	0.391	0.390	0.461	0.437	0.390	0.598	0.411	0.386
K	0.004	0.021	0.013	0.019	0.004	0.013	0.020	0.005	0.004	0.012
Ba	0.000	0.005	0.000	0.000	0.000	0.000	0.001	0.000	0.002	0.004
Sr	0.003	0.001	0.004	0.003	0.003	0.002	0.002	0.002	0.003	0.003
Total	5.028	5.035	5.027	5.025	5.021	5.024	5.029	5.031	5.026	5.026
Ab	60.095	45.974	37.939	38.261	45.319	42.636	38.211	58.091	40.120	37.839
Or	0.381	2.053	1.287	1.824	0.417	1.252	1.951	0.495	0.372	1.194
An	39.524	51.973	60.774	59.915	54.264	56.112	59.838	41.413	59.507	60.967
An/(Ab+An)	39.675	53.062	61.567	61.028	54.491	56.823	61.029	41.620	59.730	61.704

Feldspars	Sample SUD-155-1995; Drill core 70011 (continued)									
point	Pl12 core	Pl12 core	Pl12 core	Pl12 rim	Pl12 rim	Pl12 rim	Pl12 rim	matrix L	matrix L	matrix L
SiO_2	50.699	52.264	51.821	54.026	51.019	55.304	64.895	63.312	62.286	62.999
Al_2O_3	29.833	29.183	29.502	27.658	29.944	27.554	21.600	21.863	22.002	21.687
FeO	0.615	0.611	0.454	0.440	0.572	0.394	0.090	0.035	0.064	0.069
CaO	13.150	11.908	12.128	10.071	12.972	10.079	2.549	3.103	3.079	3.203
Na_2O	3.919	4.816	4.505	5.914	4.076	5.887	10.395	9.912	10.244	10.116
K_2O	0.264	0.117	0.270	0.020	0.228	0.398	0.073	0.051	0.249	0.061
BaO	0.156	0.022	0.000	0.011	0.177	0.122	0.098	0.011	0.154	0.250
SrO	0.074	0.091	0.117	0.107	0.101	0.104	0.108	0.223	0.178	0.262
Total	98.710	99.012	98.797	98.247	99.089	99.842	99.808	98.510	98.256	98.648
Si	2.347	2.400	2.386	2.485	2.351	2.506	2.868	2.839	2.814	2.833
Al	1.628	1.580	1.601	1.499	1.627	1.472	1.125	1.155	1.172	1.149
Fe2+	0.024	0.023	0.017	0.017	0.022	0.015	0.003	0.001	0.002	0.003
Ca	0.652	0.586	0.598	0.496	0.641	0.489	0.121	0.149	0.149	0.154
Na	0.352	0.429	0.402	0.527	0.364	0.517	0.891	0.862	0.897	0.882
K	0.016	0.007	0.016	0.001	0.013	0.023	0.004	0.003	0.014	0.004
Ba	0.003	0.000	0.000	0.000	0.003	0.002	0.002	0.000	0.003	0.004
Sr	0.002	0.002	0.003	0.003	0.003	0.003	0.003	0.006	0.005	0.007
Total	5.023	5.028	5.023	5.030	5.024	5.028	5.017	5.016	5.056	5.035
Ab	34.499	41.974	39.575	51.460	35.774	50.238	87.709	85.006	84.594	84.620
Or	1.528	0.670	1.558	0.117	1.318	2.233	0.406	0.287	1.353	0.339
An	63.974	57.356	58.867	48.423	62.908	47.529	11.885	14.707	14.053	14.841
An/(Ab+An)	64.966	57.743	59.798	48.480	63.748	48.614	11.933	14.749	14.245	14.891

Feldspars	Sample SUD-155-1995; Drill core 70011 (continued)									SUD-71-1994
point	matrix B	matrix D	matrix B	cl1 core	cl1 rim	cl2 core	cl2 rim	cl3 core	cl3 rim	Pl1 rim
SiO_2	63.235	63.124	63.741	52.251	54.770	52.574	55.071	54.743	55.603	56.109
Al_2O_3	21.783	21.691	22.113	29.592	28.424	29.382	27.262	27.544	26.916	27.401
FeO	0.084	0.102	0.032	0.480	0.333	0.597	0.601	0.503	0.508	0.524
CaO	2.820	3.052	3.238	12.223	10.716	11.999	9.741	10.588	9.628	9.703
Na_2O	10.409	9.826	10.037	4.822	5.683	4.778	6.008	5.581	6.099	6.142
K_2O	0.022	0.040	0.052	0.068	0.108	0.311	0.411	0.396	0.323	0.257
BaO	0.000	0.242	0.132	0.000	0.145	0.245	0.033	0.100	0.044	0.220
SrO	0.209	0.228	0.249	0.103	0.084	0.149	0.122	0.154	0.098	0.152
Total	98.563	98.304	99.595	99.539	100.263	100.034	99.250	99.608	99.220	100.508
Si	2.837	2.841	2.832	2.387	2.472	2.397	2.511	2.492	2.531	2.525
Al	1.152	1.151	1.158	1.593	1.512	1.579	1.465	1.478	1.444	1.453
Fe2+	0.003	0.004	0.001	0.018	0.013	0.023	0.023	0.019	0.019	0.020
Ca	0.136	0.147	0.154	0.598	0.518	0.586	0.476	0.516	0.470	0.468
Na	0.906	0.858	0.865	0.427	0.497	0.422	0.531	0.493	0.538	0.536
K	0.001	0.002	0.003	0.004	0.006	0.018	0.024	0.023	0.019	0.015
Ba	0.000	0.004	0.002	0.000	0.003	0.004	0.001	0.002	0.001	0.004
Sr	0.005	0.006	0.006	0.003	0.002	0.004	0.003	0.004	0.003	0.004
Total	5.040	5.013	5.022	5.031	5.023	5.034	5.034	5.027	5.025	5.024
Ab	86.872	85.157	84.624	41.496	48.673	41.144	51.522	47.734	52.430	52.620
Or	0.122	0.227	0.287	0.383	0.609	1.760	2.319	2.230	1.830	1.448
An	13.006	14.616	15.089	58.120	50.718	57.096	46.159	50.037	45.740	45.932
An/(Ab+An)	13.022	14.650	15.132	58.344	51.029	58.119	47.255	51.178	46.593	46.607

Feldspars	Sample SUD-71-1994; Drill core 70011 (continued)									
point	Pl1 core	Pl1 rim	Pl1 core	Pl2 rim	Pl3 core	Pl3 rim	Pl4 rim	Pl4 core	Pl4 core	Pl4 rim
SiO_2	52.994	56.236	53.925	56.473	51.655	57.854	59.984	51.500	51.485	57.699
Al_2O_3	29.813	28.313	28.832	27.022	30.796	26.714	25.163	30.453	29.995	26.389
FeO	0.731	0.492	0.488	0.412	0.597	0.434	0.409	0.600	0.559	0.505
CaO	12.463	10.052	11.353	9.321	13.557	9.038	6.811	13.458	13.119	8.402
Na_2O	4.465	5.733	5.034	6.230	3.659	6.335	7.988	3.933	3.945	6.754
K_2O	0.296	0.386	0.299	0.237	0.235	0.346	0.060	0.220	0.262	0.416
BaO	0.000	0.299	0.000	0.077	0.000	0.188	0.165	0.000	0.132	0.066
SrO	0.071	0.099	0.074	0.067	0.113	0.112	0.105	0.119	0.072	0.098
Total	100.833	101.609	100.004	99.839	100.612	101.020	100.684	100.283	99.568	100.329
Si	2.392	2.504	2.444	2.548	2.341	2.579	2.666	2.344	2.359	2.588
Al	1.586	1.486	1.540	1.437	1.645	1.403	1.318	1.633	1.620	1.395
Fe2+	0.028	0.018	0.018	0.016	0.023	0.016	0.015	0.023	0.021	0.019
Ca	0.603	0.479	0.551	0.451	0.658	0.432	0.324	0.656	0.644	0.404
Na	0.391	0.495	0.442	0.545	0.321	0.547	0.688	0.347	0.350	0.587
K	0.017	0.022	0.017	0.014	0.014	0.020	0.003	0.013	0.015	0.024
Ba	0.000	0.005	0.000	0.001	0.000	0.003	0.003	0.000	0.002	0.001
Sr	0.002	0.003	0.002	0.002	0.003	0.003	0.003	0.003	0.002	0.003
Total	5.019	5.012	5.016	5.013	5.004	5.003	5.021	5.019	5.014	5.020
Ab	38.667	49.674	43.756	54.001	32.364	54.816	67.746	34.153	34.706	57.871
Or	1.686	2.201	1.708	1.353	1.369	1.968	0.332	1.260	1.516	2.346
An	59.647	48.125	54.536	44.645	66.267	43.216	31.922	64.588	63.778	39.783
An/(Ab+An)	60.670	49.208	55.484	45.258	67.186	44.084	32.028	65.412	64.760	40.739

Feldspars	SUD-71-1994 (continued)			Sample SUD-97-1994; Drill core 70011						
point	Pl5 core	Pl5	Pl5 over	Pl	Pl	Pl	Pl	Pl	Pl	Pl
SiO_2	51.699	52.104	51.358	54.329	53.980	53.364	53.859	53.965	54.113	54.023
Al_2O_3	30.386	30.476	30.079	28.568	28.736	28.404	28.802	28.664	28.910	28.576
FeO	0.570	0.581	0.624	0.503	0.422	0.422	0.603	0.576	0.650	0.516
CaO	13.128	13.184	13.015	11.826	12.387	11.869	12.190	12.132	12.426	11.743
Na_2O	4.003	4.164	4.031	4.636	4.425	4.474	4.478	4.359	4.315	4.473
K_2O	0.264	0.269	0.112	0.387	0.383	0.482	0.395	0.367	0.370	0.383
BaO	0.011	0.000	0.033	0.000	0.165	0.000	0.000	0.413	0.165	0.083
SrO	0.069	0.081	0.107	0.150	0.351	0.376	0.000	0.101	0.000	0.426
Total	100.130	100.860	99.359	100.399	100.849	99.391	100.327	100.577	100.949	100.223
Si	2.353	2.356	2.356	2.454	2.437	2.441	2.437	2.442	2.436	2.450
Al	1.630	1.624	1.626	1.521	1.529	1.531	1.536	1.529	1.534	1.527
Fe2+	0.022	0.022	0.024	0.019	0.016	0.016	0.023	0.022	0.024	0.020
Ca	0.640	0.639	0.640	0.572	0.599	0.582	0.591	0.588	0.599	0.570
Na	0.353	0.365	0.359	0.406	0.387	0.397	0.393	0.382	0.377	0.393
K	0.015	0.016	0.007	0.022	0.022	0.028	0.023	0.021	0.021	0.022
Ba	0.000	0.000	0.001	0.000	0.003	0.000	0.000	0.007	0.003	0.001
Sr	0.002	0.002	0.003	0.004	0.009	0.010	0.000	0.003	0.000	0.011
Total	5.016	5.023	5.014	4.999	5.003	5.006	5.003	4.995	4.995	4.995
Ab	35.018	35.813	35.685	40.575	38.405	39.419	39.027	38.559	37.768	39.887
Or	1.522	1.522	0.652	2.229	2.187	2.794	2.265	2.136	2.131	2.247
An	63.460	62.665	63.663	57.196	59.408	57.787	58.708	59.304	60.101	57.866
An/(Ab+An)	64.441	63.634	64.061	58.500	60.737	59.448	60.068	60.599	61.410	59.196

Feldspars	Sample SUD-97-1994; Drill core 70011 (continued)									
point	Pl	Pl	Pl	Pl	Pl	Pl	Pl	Pl	Pl	Pl
SiO_2	54.152	58.986	54.646	53.448	52.795	53.694	53.538	54.746	55.741	54.776
Al_2O_3	28.355	25.670	28.339	29.112	29.294	29.127	28.691	28.419	27.682	27.536
FeO	0.570	0.369	0.717	0.449	0.702	0.650	0.529	0.470	0.590	0.455
CaO	12.000	8.307	11.820	12.789	13.322	12.292	11.853	11.769	10.579	10.574
Na_2O	4.853	6.581	4.793	4.074	3.994	4.230	4.510	4.815	5.412	5.488
K_2O	0.112	0.195	0.485	0.332	0.318	0.306	0.281	0.313	0.231	0.165
BaO	0.124	0.000	0.165	0.248	0.289	0.000	0.207	0.000	0.041	0.330
SrO	0.000	0.075	0.000	0.050	0.000	0.000	0.150	0.000	0.050	0.000
Total	100.166	100.183	100.965	100.502	100.714	100.299	99.759	100.532	100.326	99.324
Si	2.453	2.635	2.460	2.419	2.394	2.428	2.438	2.466	2.510	2.497
Al	1.514	1.351	1.504	1.553	1.566	1.553	1.540	1.509	1.469	1.479
Fe2+	0.022	0.014	0.027	0.017	0.027	0.025	0.020	0.018	0.022	0.017
Ca	0.582	0.398	0.570	0.620	0.647	0.596	0.578	0.568	0.510	0.516
Na	0.426	0.570	0.418	0.358	0.351	0.371	0.398	0.421	0.472	0.485
K	0.006	0.011	0.028	0.019	0.018	0.018	0.016	0.018	0.013	0.010
Ba	0.002	0.000	0.003	0.004	0.005	0.000	0.004	0.000	0.001	0.006
Sr	0.000	0.002	0.000	0.001	0.000	0.000	0.004	0.000	0.001	0.000
Total	5.006	4.980	5.011	4.992	5.006	4.990	4.999	4.999	4.999	5.011
Ab	41.989	58.240	41.163	35.864	34.535	37.687	40.107	41.781	47.432	47.973
Or	0.638	1.135	2.741	1.823	1.809	1.794	1.644	1.787	1.332	0.949
An	57.374	40.624	56.096	62.213	63.655	60.519	58.249	56.432	51.236	51.078
An/(Ab+An)	57.742	41.091	57.677	63.433	64.828	61.624	59.222	57.459	51.927	51.567

Feldspars	Sample SUD-97-1994; Drill core 70011 (continued)									
point	Pl	Pl	Pl	Pl	Pl	Pl	Pl	Pl	Pl	Pl
SiO_2	54.693	54.030	54.851	54.858	55.172	56.571	57.354	54.751	58.263	57.972
Al_2O_3	28.695	28.895	28.302	28.190	27.523	27.140	26.635	28.253	26.546	26.193
FeO	0.457	0.623	0.718	0.476	0.482	0.536	0.645	0.516	0.443	0.536
CaO	11.500	12.049	11.388	11.345	10.607	10.197	9.702	11.672	8.933	9.112
Na_2O	4.629	4.413	4.610	4.717	5.036	5.520	5.280	4.735	6.384	6.230
K_2O	0.388	0.351	0.361	0.460	0.346	0.172	1.077	0.304	0.059	0.159
BaO	0.207	0.496	0.207	0.330	0.041	0.454	0.165	0.000	0.330	0.165
SrO	0.101	0.351	0.175	0.201	0.000	0.125	0.050	0.226	0.200	0.025
Total	100.670	101.208	100.612	100.577	99.207	100.715	100.908	100.457	101.158	100.392
Si	2.462	2.436	2.473	2.476	2.509	2.540	2.569	2.470	2.591	2.596
Al	1.523	1.535	1.504	1.500	1.475	1.436	1.406	1.502	1.392	1.382
Fe2+	0.017	0.023	0.027	0.018	0.018	0.020	0.024	0.019	0.016	0.020
Ca	0.555	0.582	0.550	0.549	0.517	0.490	0.466	0.564	0.426	0.437
Na	0.404	0.386	0.403	0.413	0.444	0.480	0.458	0.414	0.551	0.541
K	0.022	0.020	0.021	0.026	0.020	0.010	0.062	0.017	0.003	0.009
Ba	0.004	0.009	0.004	0.006	0.001	0.008	0.003	0.000	0.006	0.003
Sr	0.003	0.009	0.005	0.005	0.000	0.003	0.001	0.006	0.005	0.001
Total	4.990	5.000	4.987	4.993	4.985	4.988	4.988	4.994	4.990	4.988
Ab	41.186	39.045	41.380	41.784	45.267	48.988	46.520	41.590	56.201	54.794
Or	2.271	2.043	2.132	2.681	2.046	1.004	6.244	1.757	0.342	0.920
An	56.542	58.911	56.487	55.535	52.687	50.007	47.236	56.653	43.457	44.286
An/(Ab+An)	57.856	60.140	57.718	57.064	53.787	50.515	50.382	57.666	43.606	44.697

Feldspars	Sample SUD-43-1994; Drill core 52848						Sample SUD-166-1995			
point	Pl1 rim	Pl1 core	Pl2 core	Pl2 rim	Pl3 core	Pl4 core	Pl1 rim	Pl1	Pl1	Pl1 rim
SiO_2	62.94	59.35	60.35	62.92	64.30	66.77	61.278	62.929	59.605	61.851
Al_2O_3	21.68	24.15	22.99	21.76	18.26	19.62	23.952	22.681	25.305	23.467
FeO	0.21	0.37	0.28	0.22	0.03	0.06	0.283	0.217	0.476	0.603
CaO	3.32	5.94	4.67	3.21	0.05	0.41	4.042	1.924	1.329	1.042
Na_2O	8.67	7.73	8.40	9.18	1.10	11.46	9.553	10.333	8.254	9.464
K_2O	1.18	0.68	0.93	0.98	14.41	0.05	0.383	0.791	2.990	2.220
BaO	0.32	0.23	0.25	0.09	0.43	0.09	0.000	0.055	0.000	0.000
SrO	0.11	0.09	0.13	0.04	0.04	0.03	0.000	0.020	0.186	0.144
Total	98.434	98.538	97.995	98.402	98.608	98.483	99.491	98.950	98.145	98.791
Si	2.840	2.696	2.751	2.835	3.001	2.969	2.739	2.816	2.713	2.788
Al	1.153	1.293	1.235	1.156	1.005	1.028	1.262	1.196	1.357	1.247
Fe2+	0.008	0.014	0.011	0.008	0.001	0.002	0.011	0.008	0.018	0.023
Ca	0.160	0.289	0.228	0.155	0.002	0.019	0.194	0.092	0.065	0.050
Na	0.759	0.681	0.742	0.802	0.099	0.988	0.828	0.897	0.728	0.827
K	0.068	0.039	0.054	0.056	0.858	0.003	0.022	0.045	0.174	0.128
Ba	0.006	0.004	0.004	0.002	0.008	0.002	0.000	0.001	0.000	0.000
Sr	0.003	0.002	0.003	0.001	0.001	0.001	0.000	0.001	0.005	0.004
Total	4.997	5.018	5.030	5.016	4.975	5.012	5.055	5.056	5.060	5.066
Ab	76.878	67.439	72.449	79.167	10.334	97.819	79.353	86.711	75.339	82.292
Or	6.879	3.905	5.282	5.532	89.429	0.269	2.093	4.368	17.957	12.701
An	16.243	28.656	22.269	15.302	0.237	1.911	18.554	8.922	6.703	5.007
An/(Ab+An)	17.443	29.821	23.511	16.198		1.917	18.950	9.329	8.171	5.735

Feldspars	Sample SUD-166-1995; Drill core 52848 (continued)										
point	Pl2 over	Pl2	Pl2	Pl2 rim	Pl2 over	Pl2 over	Pl3 rim	Pl3	Pl3	Pl3	Pl3 rim
SiO_2	62.814	58.749	61.656	61.930	67.993	61.977	61.117	60.769	60.011	65.479	64.052
Al_2O_3	22.571	26.276	22.225	22.923	19.429	19.266	21.498	24.835	25.434	20.859	21.413
FeO	0.274	0.688	0.405	0.350	0.229	0.136	2.079	0.678	0.278	0.107	0.967
CaO	3.792	0.956	4.316	3.554	0.677	0.087	5.308	1.447	1.729	1.076	1.142
Na_2O	9.029	7.092	9.933	8.659	11.154	0.930	9.816	8.332	8.484	11.316	10.928
K_2O	1.114	4.009	0.147	1.984	0.070	14.923	0.061	2.661	2.702	0.096	0.275
BaO	0.192	0.055	0.000	0.165	0.000	1.345	0.000	0.082	0.000	0.109	0.000
SrO	0.226	0.268	0.083	0.041	0.143	0.059	0.000	0.166	0.020	0.020	0.164
Total	100.012	98.093	98.765	99.606	99.695	98.723	99.879	98.970	98.658	99.062	98.941
Si	2.800	2.683	2.781	2.780	2.986	2.930	2.759	2.739	2.712	2.908	2.865
Al	1.186	1.414	1.182	1.213	1.005	1.074	1.144	1.319	1.355	1.092	1.129
Fe2+	0.010	0.026	0.015	0.013	0.008	0.005	0.078	0.026	0.011	0.004	0.036
Ca	0.181	0.047	0.209	0.171	0.032	0.004	0.257	0.070	0.084	0.051	0.055
Na	0.780	0.628	0.869	0.754	0.950	0.085	0.859	0.728	0.743	0.974	0.948
K	0.063	0.234	0.008	0.114	0.004	0.900	0.004	0.153	0.156	0.005	0.016
Ba	0.003	0.001	0.000	0.003	0.000	0.025	0.000	0.001	0.000	0.002	0.000
Sr	0.006	0.007	0.002	0.001	0.004	0.002	0.000	0.004	0.001	0.001	0.004
Total	5.029	5.040	5.066	5.048	4.988	5.026	5.101	5.041	5.060	5.036	5.052
Ab	76.146	69.135	80.010	72.592	96.370	8.613	76.751	76.563	75.633	94.507	93.083
Or	6.182	25.715	0.779	10.944	0.398	90.941	0.314	16.089	15.849	0.528	1.541
An	17.672	5.150	19.211	16.464	3.232	0.445	22.935	7.348	8.518	4.966	5.375
An/(Ab+An)	18.837	6.933	19.362	18.488	3.245		23.007	8.757	10.122	4.992	5.460

Feldspars	Sample SUD-166-1995; Drill core 52848 (continued)										
point	Pl3 rim	Pl3 over	Pl4 rim	Pl4 rim	Pl5 rim	Pl5	Pl5 rim	Pl6 rim	Pl6 core	Pl7 rim	Pl7 core
SiO_2	63.137	64.052	61.393	62.938	61.291	63.605	63.518	56.715	59.408	59.588	59.932
Al_2O_3	22.881	21.133	23.280	23.121	23.416	22.371	22.632	27.907	25.738	24.835	25.148
FeO	0.193	0.207	0.360	0.304	0.334	0.359	0.136	0.974	0.409	0.409	0.419
CaO	1.892	1.431	4.419	3.386	3.327	1.776	2.344	0.796	1.991	5.980	6.133
Na_2O	10.510	10.532	8.822	9.944	9.197	9.969	10.298	6.190	8.193	7.861	7.797
K_2O	0.807	0.903	0.752	0.464	0.906	0.948	0.517	5.120	2.868	0.766	0.907
BaO	0.000	0.246	0.109	0.055	0.274	0.164	0.000	0.355	0.083	0.301	0.356
SrO	0.164	0.246	0.000	0.123	0.083	0.103	0.329	0.145	0.268	0.309	0.164
Total	99.584	98.750	99.135	100.335	98.828	99.295	99.774	98.202	98.958	100.049	100.856
Si	2.811	2.876	2.758	2.787	2.763	2.837	2.820	2.609	2.689	2.675	2.669
Al	1.200	1.118	1.233	1.207	1.244	1.176	1.184	1.513	1.373	1.314	1.320
Fe2+	0.007	0.008	0.014	0.011	0.013	0.013	0.005	0.037	0.015	0.015	0.016
Ca	0.090	0.069	0.213	0.161	0.161	0.085	0.112	0.039	0.097	0.288	0.293
Na	0.907	0.917	0.769	0.854	0.804	0.862	0.887	0.552	0.719	0.684	0.673
K	0.046	0.052	0.043	0.026	0.052	0.054	0.029	0.300	0.166	0.044	0.052
Ba	0.000	0.004	0.002	0.001	0.005	0.003	0.000	0.006	0.001	0.005	0.006
Sr	0.004	0.006	0.000	0.003	0.002	0.003	0.006	0.004	0.007	0.008	0.004
Total	5.066	5.050	5.031	5.050	5.043	5.033	5.045	5.061	5.067	5.033	5.033
Ab	86.956	88.379	75.025	82.043	79.069	86.131	86.295	61.908	73.281	67.363	66.172
Or	4.393	4.986	4.208	2.519	5.125	5.389	2.851	33.693	16.879	4.319	5.065
An	8.650	6.636	20.767	15.438	15.806	8.479	10.854	4.399	9.841	28.318	28.763
An/(Ab+An)	9.048	6.984	21.679	15.837	16.660	8.962	11.173		11.839	29.596	30.297

Feldspars	Sample SUD-166-1995; Drill core 52848 (cont'd)						SUD-140-1995; Drill core 52848				
point	Pl8 rim	Pl8 core	Pl8 over	Pl9 core	Pl9 rim	matrix	Pl1 core	Pl2 rim	Pl3 core	Pl3 rim	matrix
SiO_2	56.141	62.538	62.243	63.364	63.729	61.511	55.659	54.777	54.938	61.806	63.516
Al_2O_3	29.205	24.258	19.442	23.465	21.932	19.727	26.697	27.327	26.750	22.639	19.058
FeO	0.702	0.329	0.081	0.345	0.396	0.090	0.325	0.313	0.476	0.331	0.125
CaO	0.596	1.221	0.069	1.622	2.965	0.495	8.939	9.375	9.471	4.335	0.531
Na_2O	5.560	9.358	0.526	9.778	10.466	1.748	5.898	5.749	5.733	8.348	3.086
K_2O	5.645	2.255	15.379	1.344	0.216	13.726	0.510	0.362	0.461	0.861	10.737
BaO	0.301	0.192	1.566	0.000	0.000	1.427	0.011	0.120	0.154	0.055	1.700
SrO	0.000	0.000	0.039	0.020	0.164	0.000	0.143	0.091	0.129	0.089	0.170
Total	98.150	100.151	99.345	99.938	99.868	98.724	98.183	98.115	98.112	98.464	96.922
Si	2.578	2.777	2.930	2.807	2.831	2.903	2.552	2.517	2.530	2.789	2.954
Al	1.580	1.270	1.079	1.225	1.148	1.097	1.443	1.480	1.452	1.204	1.045
Fe2+	0.027	0.012	0.003	0.013	0.015	0.004	0.012	0.012	0.018	0.012	0.005
Ca	0.029	0.058	0.003	0.077	0.141	0.025	0.439	0.462	0.467	0.210	0.026
Na	0.495	0.806	0.048	0.840	0.901	0.160	0.524	0.512	0.512	0.730	0.278
K	0.331	0.128	0.924	0.076	0.012	0.826	0.030	0.021	0.027	0.050	0.637
Ba	0.005	0.003	0.029	0.000	0.000	0.026	0.000	0.002	0.003	0.001	0.031
Sr	0.000	0.000	0.001	0.001	0.004	0.000	0.004	0.002	0.003	0.002	0.005
Total	5.045	5.054	5.017	5.038	5.052	5.042	5.004	5.009	5.013	4.999	4.981
Ab	57.895	81.258	4.924	84.595	85.461	15.815	52.788	51.479	50.869	73.808	29.544
Or	38.676	12.884	94.719	7.651	1.161	81.710	3.003	2.131	2.693	5.009	67.646
An	3.429	5.859	0.357	7.755	13.379	2.475	44.208	46.389	46.438	21.182	2.810
An/(Ab+An)		6.725		8.397	13.536		45.577	47.400	47.723	22.299	

Feldspars	Sample SUD-48-1994; Drill core 52848			
point	Pl3 core	Pl3 rim	Pl4 core	Pl4 rim
SiO_2	53.625	53.274	53.680	53.423
Al_2O_3	28.007	27.878	27.591	27.814
FeO	0.475	0.518	0.588	0.395
CaO	11.053	10.973	10.857	10.840
Na_2O	4.960	4.984	4.996	5.078
K_2O	0.382	0.401	0.452	0.352
BaO	0.219	0.033	0.000	0.098
SrO	0.078	0.078	0.098	0.147
Total	98.797	98.140	98.263	98.148
Si	2.463	2.461	2.476	2.467
Al	1.516	1.518	1.500	1.514
Fe2+	0.018	0.020	0.023	0.015
Ca	0.544	0.543	0.537	0.536
Na	0.442	0.446	0.447	0.455
K	0.022	0.024	0.027	0.021
Ba	0.004	0.001	0.000	0.002
Sr	0.002	0.002	0.003	0.004
Total	5.011	5.015	5.011	5.014
Ab	43.819	44.062	44.239	44.941
Or	2.221	2.335	2.633	2.051
An	53.960	53.603	53.128	53.008
An/(Ab+An)	55.185	54.885	54.565	54.118

Pyroxene	66-1994	71-1994	Sample SUD-97-1994; Drill core 70011							
point	main2	core1	px1 lam	px1 L la	px1 edg	px1 main	px1 main	px2 rim	px2 core	px3 rim
SiO_2	52.280	49.903	50.577	51.411	53.144	51.568	51.108	52.851	51.786	52.325
TiO_2	0.097	0.494	0.550	0.666	0.065	0.667	0.504	0.350	0.349	0.325
Al_2O_3	0.368	1.700	2.065	2.322	0.650	2.296	1.629	0.854	0.962	0.941
FeO	10.590	10.814	9.523	9.385	6.034	9.288	16.310	20.770	20.027	20.175
MgO	12.808	13.043	13.588	13.667	14.901	13.667	17.606	22.557	22.781	22.834
MnO	0.329	0.477	0.262	0.174	0.252	0.207	0.333	0.400	0.420	0.436
CaO	22.674	21.787	21.600	21.718	23.990	21.998	11.262	1.256	1.587	1.381
Na_2O	0.129	0.283	0.364	0.387	0.146	0.375	0.225	0.023	0.043	0.030
K_2O	0.013	0.000	0.002	0.013	0.010	0.000	0.016	0.012	0.000	0.008
Cr_2O_3	0.025	0.018	0.113	0.232	0.121	0.194	0.180	0.039	0.079	0.067
NiO	0.017	-	0.060	0.004	0.025	0.017	0.043	0.090	0.018	0.060
Total	99.330	98.518	98.644	99.975	99.313	100.260	99.173	99.112	98.034	98.522
Si	1.985	1.918	1.924	1.925	1.980	1.925	1.934	1.975	1.958	1.966
Ti	0.003	0.014	0.016	0.019	0.002	0.019	0.014	0.010	0.010	0.009
Al	0.016	0.077	0.093	0.102	0.029	0.101	0.073	0.038	0.043	0.042
Fe^{2+}	0.336	0.348	0.303	0.294	0.188	0.290	0.516	0.649	0.633	0.634
Mg	0.725	0.747	0.770	0.763	0.828	0.761	0.993	1.257	1.284	1.279
Mn	0.011	0.016	0.008	0.006	0.008	0.007	0.011	0.013	0.013	0.014
Ca	0.922	0.897	0.880	0.871	0.958	0.880	0.457	0.050	0.064	0.056
Na	0.009	0.021	0.027	0.028	0.011	0.027	0.017	0.002	0.003	0.002
K	0.001	0.000	0.000	0.001	0.000	0.000	0.001	0.001	0.000	0.000
Cr	0.001	0.001	0.003	0.007	0.004	0.006	0.005	0.001	0.002	0.002
Ni	0.001	-	-	-	-	-	-	-	-	-
Total	4.009	4.039	4.024	4.016	4.007	4.015	4.020	3.994	4.011	4.003
Wo	46.500	45.037	45.057	45.190	48.530	45.579	23.226	2.571	3.244	2.824
En	36.548	37.515	39.438	39.568	41.942	39.400	50.520	64.244	64.799	64.972
Fs	16.952	17.448	15.505	15.242	9.528	15.021	26.254	33.185	31.957	32.204
En	68.314	68.254	71.779	72.191	81.489	72.399	65.803	65.940	66.972	66.860
Fs	31.686	31.746	28.221	27.809	18.511	27.601	34.197	34.060	33.028	33.140

Note: 66-1994 = SUD-66-1994; Drill core 70011, and 71-1994 = SUD-71-1994; Drill core 70011.

Pyroxene	Sample SUD-97-1994; Drill core 70011 (continued)							Sample SUD-166-1995		
point	px3 core	px4 main	px5 core	px6 rim	px6 core	px7 main	px8 main	px1 core	px1 rim	px2 core
SiO_2	51.749	52.994	52.644	53.431	53.215	51.655	51.001	50.868	50.474	52.126
TiO_2	0.377	0.362	0.282	0.314	0.182	0.702	0.706	0.590	0.540	0.190
Al_2O_3	1.056	0.988	1.011	1.085	1.576	2.347	2.356	1.321	1.128	0.837
FeO	20.144	20.532	20.005	19.445	18.722	9.381	9.043	15.388	15.471	14.369
MgO	22.582	23.133	23.219	23.488	23.910	13.626	13.425	10.878	10.921	11.457
MnO	0.400	0.385	0.359	0.346	0.269	0.222	0.222	0.324	0.333	0.278
CaO	1.857	1.354	1.410	2.026	1.473	21.971	21.739	20.250	20.410	20.743
Na_2O	0.042	0.032	0.009	0.035	0.022	0.404	0.396	0.371	0.390	0.298
K_2O	0.004	0.007	0.000	0.008	0.000	0.004	0.000	0.014	0.018	0.037
Cr_2O_3	0.070	0.063	0.096	0.152	0.297	0.155	0.145	0.026	0.056	0.006
NiO	0.025	0.011	0.010	0.037	0.015	0.025	0.055	0.010	0.000	0.039
Total	98.281	99.850	99.035	100.330	99.666	100.467	99.033	100.030	99.741	100.341
Si	1.954	1.965	1.964	1.964	1.959	1.925	1.926	1.951	1.947	1.980
Ti	0.011	0.010	0.008	0.009	0.005	0.020	0.020	0.017	0.016	0.005
Al	0.047	0.043	0.044	0.047	0.068	0.103	0.105	0.060	0.051	0.037
Fe^{2+}	0.636	0.637	0.624	0.598	0.576	0.292	0.286	0.494	0.499	0.457
Mg	1.271	1.279	1.292	1.287	1.312	0.757	0.756	0.622	0.628	0.649
Mn	0.013	0.012	0.011	0.011	0.008	0.007	0.007	0.011	0.011	0.009
Ca	0.075	0.054	0.056	0.080	0.058	0.877	0.880	0.832	0.843	0.844
Na	0.003	0.002	0.001	0.002	0.002	0.029	0.029	0.028	0.029	0.022
K	0.000	0.000	0.000	0.000	0.000	0.000	0.000	0.001	0.001	0.002
Cr	0.002	0.002	0.003	0.004	0.009	0.005	0.004	0.001	0.002	0.000
Ni	-	-	-	-	-	-	-	0.000	0.000	0.001
Total	4.012	4.004	4.004	4.002	3.998	4.015	4.012	4.016	4.026	4.007
Wo	3.790	2.732	2.858	4.061	2.985	45.533	45.789	42.725	42.805	43.305
En	64.122	64.936	65.489	65.513	67.407	39.292	39.344	31.934	31.869	33.280
Fs	32.088	32.332	31.653	30.426	29.609	15.175	14.867	25.342	25.326	23.415
En	66.648	66.760	67.416	68.286	69.480	72.139	72.576	55.755	55.720	58.700
Fs	33.352	33.240	32.584	31.714	30.520	27.861	27.424	44.245	44.280	41.300

Pyroxene	SUD-166-1995; Drill core 52848			Sample SUD-48-1994; Drill core 52848				
point	px4 main	px5 core	px11 main	px4 rim	px5 core	px6 core	px6 rim	px7 core
SiO_2	50.613	50.637	49.914	51.185	49.799	50.293	49.981	49.545
TiO_2	0.280	0.217	0.824	0.378	0.733	0.677	0.751	0.696
Al_2O_3	0.633	1.425	1.710	0.863	1.652	1.743	1.821	1.556
FeO	15.125	16.596	12.840	23.515	12.555	11.557	11.389	12.861
MgO	11.097	10.467	11.888	19.996	13.706	13.287	13.443	11.548
MnO	0.300	0.261	0.294	0.577	0.341	0.296	0.309	0.350
CaO	20.010	17.915	21.163	1.920	19.081	20.230	20.595	21.150
Na_2O	0.333	0.317	0.326	0.000	0.276	0.309	0.252	0.295
K_2O	0.029	0.076	0.002	0.016	0.000	0.002	0.007	0.041
Cr_2O_3	0.038	0.058	0.006	0.027	0.000	0.000	0.016	0.056
NiO	0.024	0.037	0.006	-	-	-	-	-
Total	98.458	97.969	98.967	98.479	98.142	98.393	98.563	98.098
Si	1.971	1.980	1.922	1.962	1.921	1.930	1.917	1.928
Ti	0.008	0.006	0.024	0.011	0.021	0.020	0.022	0.020
Al	0.029	0.066	0.078	0.039	0.075	0.079	0.082	0.071
Fe^{2+}	0.493	0.543	0.414	0.754	0.405	0.371	0.365	0.419
Mg	0.644	0.610	0.682	1.143	0.788	0.760	0.768	0.670
Mn	0.010	0.009	0.010	0.019	0.011	0.010	0.010	0.012
Ca	0.835	0.750	0.873	0.079	0.789	0.832	0.846	0.882
Na	0.025	0.024	0.024	0.000	0.021	0.023	0.019	0.022
K	0.001	0.004	0.000	0.001	0.000	0.000	0.000	0.002
Cr	0.001	0.002	0.000	0.001	0.000	0.000	0.000	0.002
Ni	0.001	0.001	0.000	-	-	-	-	-
Total	4.019	3.994	4.027	4.008	4.031	4.023	4.030	4.027
Wo	42.344	39.432	44.343	3.992	39.792	42.378	42.738	44.755
En	32.674	32.056	34.658	57.846	39.772	38.726	38.815	34.001
Fs	24.983	28.512	20.999	38.161	20.437	18.897	18.448	21.244
En	56.670	52.925	62.270	60.252	66.057	67.206	67.784	61.546
Fs	43.330	47.075	37.730	39.748	33.943	32.794	32.216	38.454

Pyroxene	SUD-140-1995, Drill core 52848					Sample SUD-43-1994, Drill core 52848					60-1994
point	rim1	over3	rim4	core5	core6	core1	core2	rim2	core4	core5	alter2
SiO_2	50.581	50.548	50.369	50.738	49.638	50.119	50.380	50.031	49.320	49.809	48.286
TiO_2	0.409	0.222	0.362	0.332	0.707	0.479	0.150	0.148	0.733	0.641	2.728
Al_2O_3	1.162	0.563	0.789	0.786	1.774	1.087	0.490	0.510	1.346	1.546	4.026
FeO	13.887	15.073	15.047	14.806	13.230	15.592	18.030	16.445	15.671	13.659	17.326
MnO	0.356	0.407	0.378	0.385	0.355	0.498	0.567	0.612	0.544	0.363	0.259
MgO	11.660	11.757	11.451	11.532	12.722	9.088	8.133	8.693	9.733	11.788	9.455
CaO	19.464	18.996	19.492	19.539	19.538	21.045	20.540	21.364	20.678	20.131	14.902
Na_2O	0.311	0.318	0.325	0.323	0.307	0.170	0.176	0.163	0.203	0.238	0.835
K_2O	0.004	0.000	0.000	0.022	0.003	0.049	0.013	0.000	0.000	0.021	0.338
P_2O_5	0.000	0.029	0.000	0.000	0.072	0.101	0.000	0.043	0.043	0.101	0.044
F	0.000	0.000	0.000	0.000	0.000	0.000	0.000	0.000	0.000	0.000	0.000
Cl	0.000	0.013	0.038	0.000	0.020	0.075	0.033	0.092	0.013	0.016	0.145
BaO	0.000	0.172	0.000	0.000	0.000	0.022	0.000	0.086	0.303	0.065	0.128
RbO_2	0.021	0.000	0.002	0.000	0.060	0.000	0.000	0.022	0.052	0.000	0.000
SrO	0.000	0.000	0.000	0.001	0.000	0.057	0.000	0.000	0.000	0.000	0.000
NiO	0.000	0.000	0.000	0.000	0.000	0.003	0.003	0.000	0.000	0.003	0.000
ZnO	0.175	0.046	0.059	0.036	0.059	0.069	0.000	0.062	0.000	0.073	0.000
Cr_2O_3	0.000	0.035	0.067	0.031	0.000	0.000	0.066	0.022	0.000	0.000	0.000
V_2O_3	0.092	0.000	0.042	0.000	0.078	0.000	0.105	0.049	0.000	0.098	0.058
Total	98.121	98.181	98.421	98.533	98.564	98.453	98.686	98.346	98.640	98.552	98.530
Si	1.964	1.972	1.961	1.969	1.916	1.965	1.989	1.976	1.936	1.930	1.881
Ti	0.012	0.007	0.011	0.010	0.021	0.014	0.004	0.004	0.022	0.019	0.080
Al	0.053	0.026	0.036	0.036	0.081	0.050	0.023	0.024	0.062	0.071	0.185
Fe^{2+}	0.451	0.492	0.490	0.481	0.427	0.511	0.595	0.543	0.514	0.443	0.564
Mn	0.012	0.013	0.012	0.013	0.012	0.017	0.019	0.020	0.018	0.012	0.009
Mg	0.675	0.684	0.664	0.667	0.732	0.531	0.478	0.512	0.569	0.681	0.549
Ca	0.810	0.794	0.813	0.813	0.808	0.884	0.869	0.904	0.870	0.836	0.622
Na	0.023	0.024	0.025	0.024	0.023	0.013	0.013	0.013	0.015	0.018	0.063
K	0.000	0.000	0.000	0.001	0.000	0.002	0.001	0.000	0.000	0.001	0.017
P	0.000	0.001	0.000	0.000	0.002	0.003	0.000	0.001	0.001	0.003	0.001
F	0.000	0.000	0.000	0.000	0.000	0.000	0.000	0.000	0.000	0.000	0.000
Cl	0.000	0.001	0.002	0.000	0.001	0.005	0.002	0.006	0.001	0.001	0.010
Ba	0.000	0.003	0.000	0.000	0.000	0.000	0.000	0.001	0.005	0.001	0.002
Rb	0.000	0.000	0.000	0.000	0.001	0.000	0.000	0.000	0.001	0.000	0.000
Sr	0.000	0.000	0.000	0.000	0.000	0.001	0.000	0.000	0.000	0.000	0.000
Ni	0.000	0.000	0.000	0.000	0.000	0.000	0.000	0.000	0.000	0.000	0.000
Zn	0.005	0.001	0.002	0.001	0.002	0.002	0.000	0.002	0.000	0.002	0.000
Cr	0.000	0.001	0.002	0.001	0.000	0.000	0.002	0.001	0.000	0.000	0.000
V	0.003	0.000	0.001	0.000	0.002	0.000	0.003	0.002	0.000	0.003	0.002
Total	4.008	4.018	4.020	4.015	4.028	3.999	3.999	4.010	4.015	4.019	3.984
Wo	43.243	41.452	42.384	42.590	42.951	46.026	43.980	45.941	44.872	44.167	35.752
En	25.905	25.656	24.898	25.137	27.966	19.875	17.415	18.694	21.122	25.864	22.682
Fs	30.852	32.892	32.718	32.272	29.082	34.099	38.605	35.364	34.006	29.969	41.565

Note: 60-1994 = SUD-60-1994; Drill core 70011

Amphibole after px	Sample SUD-3-1994; Drill core 70011		Sample SUD-87-1994; Drill core 70011							
point	core	rim	core	rim	rim	rim	contact	main	core	main
SiO_2	51.680	51.166	44.976	43.667	43.263	43.554	42.730	50.690	45.845	50.464
Al_2O_3	1.063	1.530	4.652	5.867	5.821	5.570	6.422	0.722	3.949	0.707
TiO_2	0.037	0.032	0.497	1.243	1.283	1.391	1.456	0.257	0.859	0.057
FeO	21.351	22.506	31.492	30.017	29.765	29.239	29.914	29.728	29.143	28.058
MnO	0.370	0.280	0.373	0.324	0.353	0.292	0.362	0.516	0.420	0.300
MgO	9.913	9.462	3.816	3.801	3.768		3.617	4.726	6.134	5.933
CaO	13.050	12.136	9.980	10.434	10.725	10.428	10.530	12.083	9.884	12.149
Na_2O	0.172	0.285	0.837	1.655	1.002	1.562	0.962	0.123	0.675	0.113
K_2O	0.066	0.114	0.864	1.100	1.102	1.067	1.174	0.083	0.778	0.120
Cr_2O_3	0.027	0.024	0.004	0.041	0.009	0.000	0.019	0.039	0.012	0.019
NiO	0.032	0.018	0.009	0.003	0.008	0.000	0.000	0.000	0.013	0.003
Total	97.761	97.553	97.500	98.152	97.099	93.103	97.186	98.967	97.712	97.923
Si	7.795	7.760	7.217	6.967	6.971	6.972	6.887	7.848	7.242	7.839
Al	0.189	0.273	0.880	1.103	1.105	1.051	1.220	0.132	0.735	0.129
Ti	0.004	0.004	0.060	0.149	0.155	0.167	0.176	0.030	0.102	0.007
Fe2+	2.693	2.855	4.226	4.005	4.011	3.914	4.032	3.849	3.850	3.645
Mn	0.047	0.036	0.051	0.044	0.048	0.040	0.049	0.068	0.056	0.039
Mg	2.229	2.139	0.913	0.904	0.905	1.052	0.869	1.091	1.444	1.374
Ca	2.109	1.972	1.716	1.784	1.852	1.788	1.818	2.004	1.673	2.022
Na	0.050	0.084	0.260	0.512	0.313	0.485	0.301	0.037	0.207	0.034
K	0.013	0.022	0.177	0.224	0.227	0.218	0.241	0.016	0.157	0.024
Cr	0.003	0.003	0.001	0.005	0.001	0.000	0.002	0.005	0.001	0.002
Ni	0.004	0.002	0.001	0.000	0.001	0.000	0.000	0.000	0.002	0.000
Total	15.136	15.151	15.501	15.698	15.590	15.687	15.596	15.080	15.469	15.117
Name	1	1	2	3	3	3	3	1	2	1

1 = ferro-actinolite; 2 = ferrohornblende; 3 = ferro-edenite

Amphibole Sample SUD-87-1994; Drill core 70011 (continued)										SUD-149-1995	
after px											
point	rim	rim	main	core	main	rim	main	main	main	core1	rim1
SiO_2	48.605	47.931	46.773	51.031	46.493	45.988	45.749	48.923	45.886	46.369	50.333
Al_2O_3	1.035	2.658	3.563	0.357	3.843	4.327	5.001	2.526	4.166	6.409	3.244
TiO_2	0.030	0.662	0.781	0.047	0.756	0.661	0.073	0.460	1.136	0.175	0.269
FeO	32.767	26.397	28.529	27.684	29.158	27.973	27.744	27.205	29.769	24.447	22.086
MnO	0.491	0.455	0.444	0.329	0.331	0.420	0.212	0.439	0.451	0.288	0.269
MgO	2.880	7.358	6.126	6.005	5.154	6.335	4.978	7.646	5.000	7.195	8.956
CaO	11.785	10.879	10.168	12.276	10.932	9.811	11.782	9.992	9.808	11.950	12.222
Na_2O	0.202	0.464	0.541	0.063	0.491	0.853	0.723	0.429	0.838	0.751	0.363
K_2O	0.135	0.577	0.725	0.042	0.722	0.746	0.671	0.657	0.848	0.546	0.269
Cr_2O_3	0.035	0.029	0.018	0.037	0.047	0.041	0.034	0.018	0.031	0.067	0.048
NiO	0.034	0.033	0.000	0.028	0.000	0.036	0.048	0.018	0.018	0.004	0.031
Total	97.999	97.443	97.668	97.899	97.927	97.191	97.015	98.313	97.951	98.201	98.090
Si	7.754	7.473	7.354	7.906	7.326	7.259	7.253	7.547	7.254	7.124	7.588
Al	0.195	0.488	0.660	0.065	0.714	0.805	0.934	0.459	0.776	1.160	0.576
Ti	0.004	0.078	0.092	0.005	0.090	0.078	0.009	0.053	0.135	0.020	0.030
Fe2+	4.372	3.442	3.751	3.587	3.842	3.693	3.678	3.510	3.936	3.141	2.785
Mn	0.066	0.060	0.059	0.043	0.044	0.056	0.028	0.057	0.060	0.037	0.034
Mg	0.685	1.710	1.436	1.387	1.211	1.491	1.176	1.758	1.178	1.648	2.013
Ca	2.014	1.817	1.713	2.038	1.846	1.659	2.001	1.651	1.661	1.967	1.974
Na	0.062	0.140	0.165	0.019	0.150	0.261	0.222	0.128	0.257	0.224	0.106
K	0.027	0.115	0.145	0.008	0.145	0.150	0.136	0.129	0.171	0.107	0.052
Cr	0.004	0.004	0.002	0.005	0.006	0.005	0.004	0.002	0.004	0.008	0.006
Ni	0.004	0.004	0.000	0.003	0.000	0.005	0.006	0.002	0.002	0.000	0.004
Total	15.188	15.331	15.378	15.067	15.372	15.463	15.448	15.296	15.435	15.437	15.169
Name	1	2	2	1	2	2	2	1	2	2	1

1 = ferro-actinolite; 2 = ferrohornblende

Amph. Sample SUD-149-1995; Drill core 70011 (continued)

after px point	rim2	core2	D2	main3	core3	main3	rim tip3	rim tip4	main4	main4	main5	main6
SiO_2	49.488	49.032	50.767	51.884	50.363	50.378	51.345	47.315	46.643	46.294	49.644	50.036
Al_2O_3	3.904	3.866	3.975	2.105	3.129	3.739	2.220	4.376	4.546	4.646	3.760	2.743
TiO_2	0.227	0.656	0.704	0.207	0.072	0.060	0.028	0.752	1.173	0.869	0.062	0.058
FeO	22.863	21.873	18.259	21.470	22.748	26.640	21.844	24.461	23.413	25.257	22.387	23.440
MnO	0.318	0.300	0.324	0.291	0.324	0.479	0.271	0.424	0.218	0.429	0.256	0.225
MgO	8.364	8.547	11.634	9.797	9.152	7.179	9.331	8.290	9.008	8.397	8.814	8.321
CaO	11.675	12.541	11.244	12.190	10.918	7.854	12.434	8.892	9.745	9.124	12.323	12.275
Na_2O	0.445	0.507	0.884	0.256	0.375	0.291	0.302	1.992	1.754	2.108	0.464	0.319
K_2O	0.773	0.284	0.308	0.163	0.696	0.620	0.142	0.554	0.612	0.635	0.252	0.214
Cr_2O_3	0.032	0.001	0.028	0.028	0.009	0.031	0.000	0.007	0.019	0.026	0.025	0.056
NiO	0.000	0.017	0.000	0.032	0.000	0.000	0.048	0.062	0.006	0.046	0.000	0.027
Total	98.089	97.624	98.127	98.423	97.786	97.271	97.965	97.125	97.137	97.831	97.987	97.714
Si	7.511	7.454	7.502	7.745	7.630	7.726	7.728	7.326	7.208	7.175	7.514	7.627
Al	0.698	0.693	0.692	0.370	0.559	0.676	0.394	0.799	0.828	0.849	0.671	0.493
Ti	0.026	0.075	0.078	0.023	0.008	0.007	0.003	0.088	0.136	0.101	0.007	0.007
Fe2+	2.902	2.781	2.257	2.680	2.882	3.417	2.750	3.167	3.026	3.274	2.834	2.968
Mn	0.041	0.039	0.041	0.037	0.042	0.062	0.035	0.056	0.029	0.056	0.033	0.029
Mg	1.892	1.937	2.563	2.180	2.067	1.641	2.094	1.914	2.075	1.940	1.969	1.891
Ca	1.898	2.043	1.780	1.950	1.772	1.291	2.005	1.475	1.613	1.515	1.998	2.005
Na	0.131	0.149	0.253	0.074	0.110	0.087	0.088	0.598	0.526	0.633	0.136	0.094
K	0.150	0.055	0.058	0.031	0.135	0.121	0.027	0.109	0.121	0.126	0.049	0.042
Cr	0.004	0.000	0.003	0.003	0.001	0.004	0.000	0.001	0.002	0.003	0.003	0.007
Ni	0.000	0.002	0.000	0.004	0.000	0.000	0.006	0.008	0.001	0.006	0.000	0.003
Total	15.253	15.227	15.228	15.098	15.205	15.031	15.129	15.540	15.564	15.678	15.234	15.185
Name	1	1	4	1	1	1	1	2	2	2	1	1

1 = ferro-actinolite; 2 = ferrohornblende; 4 = actinolite

Amphibole Sample SUD-59-1994; Drill core 70011 after px										SUD-92-1994	
point	D-spot	L-spot rim	core L	rim2	rim3	rim3	core4	rim5	core6	core	rim
SiO_2	48.890	49.369	47.542	49.568	49.285	49.450	49.858	49.221	50.115	51.687	49.069
Al_2O_3	3.883	4.003	5.268	4.078	4.417	4.283	3.461	4.038	3.875	1.206	3.785
TiO_2	0.081	0.051	0.089	0.118	1.336	1.064	0.083	0.062	0.078	0.182	0.110
FeO	20.746	21.762	23.168	21.244	17.788	18.684	20.329	20.528	20.097	22.502	21.201
MnO	0.301	0.207	0.199	0.410	0.306	0.341	0.334	0.340	0.329	0.749	0.272
MgO	10.155	9.359	8.189	9.706	11.978	12.351	10.407	10.099	10.273	11.992	9.622
CaO	12.284	12.267	12.070	11.877	10.645	9.796	12.225	12.316	12.065	9.239	12.197
Na_2O	0.474	0.489	0.586	0.492	1.143	1.425	0.430	0.501	0.442	0.279	0.538
K_2O	0.240	0.346	0.374	0.324	0.504	0.389	0.265	0.235	0.254	0.095	0.243
Cr_2O_3	0.069	0.081	0.063	0.054	0.032	0.035	0.064	0.072	0.072	0.034	0.071
NiO	0.070	0.000	0.020	0.000	0.038	0.023	0.000	0.000	0.003	0.000	0.013
Total	97.193	97.934	97.568	97.871	97.472	97.841	97.456	97.412	97.603	97.965	97.121
Si	7.426	7.463	7.284	7.472	7.347	7.358	7.519	7.443	7.524	7.751	7.467
Al	0.695	0.713	0.951	0.724	0.776	0.751	0.615	0.720	0.686	0.213	0.679
Ti	0.009	0.006	0.010	0.013	0.150	0.119	0.009	0.007	0.009	0.021	0.013
Fe2+	2.635	2.751	2.969	2.678	2.218	2.325	2.564	2.596	2.523	2.822	2.698
Mn	0.039	0.027	0.026	0.052	0.039	0.043	0.043	0.044	0.042	0.095	0.035
Mg	2.299	2.109	1.870	2.181	2.662	2.740	2.340	2.277	2.299	2.681	2.183
Ca	1.999	1.987	1.981	1.918	1.700	1.562	1.975	1.995	1.941	1.484	1.989
Na	0.140	0.143	0.174	0.144	0.330	0.411	0.126	0.147	0.129	0.081	0.159
K	0.047	0.067	0.073	0.062	0.096	0.074	0.051	0.045	0.049	0.018	0.047
Cr	0.008	0.010	0.008	0.006	0.004	0.004	0.008	0.009	0.009	0.004	0.009
Ni	0.009	0.000	0.002	0.000	0.005	0.003	0.000	0.000	0.000	0.000	0.002
Total	15.306	15.275	15.350	15.252	15.326	15.388	15.249	15.282	15.209	15.170	15.279
Name	1	1	2	1	5	5	1	1	1	0	1

0 = cannot be classified; 1 = ferro-actinolite; 2 = ferrohornblende; 5 = magnesio-hornblende

Amphibole Sample SUD-92-1994; Drill core 70011 (continued)

after px											
point	rim	core	core	main	rim	core	rim	rim	main	main	core
SiO_2	48.303	51.495	51.561	51.621	48.523	53.006	51.540	51.769	51.133	51.178	51.705
Al_2O_3	4.552	1.673	2.266	1.574	4.369	1.193	1.777	1.812	2.036	2.316	2.004
TiO_2	0.079	0.136	0.063	0.187	0.090	0.123	0.206	0.156	0.132	0.143	0.080
FeO	21.939	19.533	18.856	19.526	21.072	16.540	20.830	18.996	19.528	19.555	19.138
MnO	0.253	0.332	0.308	0.380	0.288	0.302	0.465	0.343	0.358	0.320	0.265
MgO	9.021	11.275	11.562	11.409	9.843	13.075	10.914	11.441	11.353	11.061	11.654
CaO	12.087	12.249	12.487	12.150	12.217	12.559	10.771	12.399	12.055	11.944	12.264
Na_2O	0.590	0.278	0.257	0.234	0.541	0.191	0.383	0.258	0.328	0.314	0.266
K_2O	0.347	0.107	0.142	0.097	0.248	0.056	0.162	0.120	0.146	0.168	0.108
Cr_2O_3	0.058	0.040	0.054	0.012	0.082	0.044	0.027	0.022	0.032	0.047	0.031
NiO	0.000	0.022	0.000	0.067	0.000	0.000	0.007	0.022	0.022	0.042	0.018
Total	97.229	97.140	97.556	97.257	97.273	97.089	97.082	97.338	97.123	97.088	97.533
Si	7.377	7.736	7.687	7.743	7.376	7.834	7.765	7.739	7.686	7.690	7.712
Al	0.819	0.296	0.398	0.278	0.783	0.208	0.316	0.319	0.361	0.410	0.352
Ti	0.009	0.015	0.007	0.021	0.010	0.014	0.023	0.018	0.015	0.016	0.009
Fe2+	2.802	2.454	2.351	2.449	2.679	2.044	2.624	2.375	2.455	2.457	2.387
Mn	0.033	0.042	0.039	0.048	0.037	0.038	0.059	0.043	0.046	0.041	0.033
Mg	2.054	2.525	2.570	2.551	2.230	2.881	2.451	2.550	2.544	2.478	2.591
Ca	1.978	1.972	1.995	1.953	1.990	1.989	1.739	1.986	1.942	1.923	1.960
Na	0.175	0.081	0.074	0.068	0.159	0.055	0.112	0.075	0.096	0.091	0.077
K	0.068	0.021	0.027	0.019	0.048	0.011	0.031	0.023	0.028	0.032	0.021
Cr	0.007	0.005	0.006	0.001	0.010	0.005	0.003	0.003	0.004	0.006	0.004
Ni	0.000	0.003	0.000	0.008	0.000	0.000	0.001	0.003	0.003	0.005	0.002
Total	15.322	15.149	15.154	15.140	15.322	15.078	15.124	15.132	15.178	15.148	15.149
Name	1	4	4	4	1	4	1	4	4	4	4

1 = ferro-actinolite; 4 = actinolite

Amph. Sample SUD-92-1994; Drill core 70011 (continued)

after px point	main	over	rim	main	main	core	main	over	rim	core	core	rim
SiO_2	51.504	52.114	50.640	50.949	51.074	50.791	51.072	51.539	51.566	46.619	50.254	46.724
Al_2O_3	1.805	1.558	2.379	2.345	2.238	2.303	2.188	1.974	2.124	5.811	2.942	5.149
TiO_2	0.105	0.118	0.145	0.140	0.146	0.155	0.151	0.148	0.109	0.869	0.056	1.338
FeO	19.110	18.699	20.112	19.485	20.303	19.810	19.614	19.066	18.937	20.599	20.249	18.764
MnO	0.305	0.361	0.305	0.327	0.329	0.306	0.336	0.319	0.299	0.316	0.303	0.254
MgO	11.658	11.806	10.980	11.234	10.895	11.037	11.159	11.542	11.483	9.628	10.632	11.613
CaO	12.351	12.361	12.131	12.151	12.045	12.063	12.055	12.285	12.324	11.730	12.400	10.760
Na_2O	0.305	0.224	0.391	0.371	0.385	0.380	0.332	0.279	0.306	1.243	0.393	1.657
K_2O	0.102	0.108	0.163	0.156	0.148	0.169	0.142	0.132	0.137	0.228	0.188	0.714
Cr_2O_3	0.027	0.017	0.037	0.034	0.022	0.045	0.024	0.008	0.031	0.066	0.054	0.015
NiO	0.010	0.043	0.014	0.006	0.000	0.000	0.006	0.051	0.000	0.028	0.006	0.031
Total	97.282	97.409	97.297	97.198	97.585	97.059	97.079	97.343	97.316	97.137	97.477	97.019
Si	7.712	7.769	7.628	7.654	7.667	7.654	7.681	7.708	7.707	7.116	7.570	7.097
Al	0.319	0.274	0.422	0.415	0.396	0.409	0.388	0.348	0.374	1.045	0.522	0.922
Ti	0.012	0.013	0.016	0.016	0.016	0.018	0.017	0.017	0.012	0.100	0.006	0.153
Fe2+	2.393	2.331	2.534	2.448	2.549	2.497	2.467	2.385	2.367	2.629	2.551	2.384
Mn	0.039	0.046	0.039	0.042	0.042	0.039	0.043	0.040	0.038	0.041	0.039	0.033
Mg	2.602	2.624	2.466	2.516	2.438	2.480	2.502	2.573	2.559	2.191	2.388	2.630
Ca	1.981	1.974	1.958	1.956	1.937	1.948	1.943	1.969	1.974	1.918	2.001	1.751
Na	0.089	0.065	0.114	0.108	0.112	0.111	0.097	0.081	0.089	0.368	0.115	0.488
K	0.019	0.021	0.031	0.030	0.028	0.032	0.027	0.025	0.026	0.044	0.036	0.138
Cr	0.003	0.002	0.004	0.004	0.003	0.005	0.003	0.001	0.004	0.008	0.006	0.002
Ni	0.001	0.005	0.002	0.001	0.000	0.000	0.001	0.006	0.000	0.003	0.001	0.004
Total	15.170	15.123	15.215	15.189	15.188	15.193	15.168	15.154	15.149	15.464	15.235	15.601
Name	4	4	1	4	1	4	4	4	4	2	1	6

1 = ferro-actinolite; 2 = ferrohornblende; 4 = actinolite; 6 = edenite

Amphibole 130-1995 after px	Sample SUD-63-1994; Drill core 70011									
point	bright	core	core	core	rim	rim	rim	over	dark	bright	dark
SiO_2	44.475	53.276	51.159	50.345	51.176	49.669	53.281	52.658	50.329	46.631	53.999
Al_2O_3	5.960	1.859	3.392	3.742	3.395	4.055	1.520	1.357	3.337	5.728	0.989
TiO_2	1.361	0.116	0.208	0.365	0.261	0.533	0.075	0.053	0.523	1.236	0.058
FeO	23.406	17.081	15.439	16.057	16.226	16.240	19.211	17.431	16.675	19.822	13.568
MnO	0.320	0.601	0.257	0.265	0.259	0.241	0.816	0.310	0.200	0.251	0.383
MgO	8.660	15.259	15.311	14.807	14.781	14.368	15.294	12.779	13.664	11.277	15.397
CaO	9.978	9.376	10.881	10.638	10.591	10.832	7.624	12.529	11.308	10.592	12.990
Na_2O	2.039	0.289	0.749	0.777	0.736	0.986	0.238	0.143	0.740	1.289	0.073
K_2O	0.850	0.121	0.315	0.382	0.302	0.421	0.065	0.049	0.351	0.769	0.042
Cr_2O_3	0.016	0.044	0.063	0.054	0.040	0.038	0.053	0.019	0.007	0.042	0.024
NiO	0.000	0.000	0.000	0.027	0.000	0.046	0.053	0.000	0.000	0.032	0.046
Total	97.065	98.022	97.774	97.459	97.767	97.429	98.230	97.328	97.134	97.669	97.569
Si	6.934	7.755	7.483	7.420	7.503	7.350	7.782	7.799	7.473	7.055	7.834
Al	1.095	0.319	0.585	0.650	0.587	0.707	0.262	0.237	0.584	1.021	0.169
Ti	0.160	0.013	0.023	0.040	0.029	0.059	0.008	0.006	0.058	0.141	0.006
Fe2+	3.052	2.079	1.889	1.979	1.990	2.010	2.347	2.159	2.071	2.508	1.646
Mn	0.042	0.074	0.032	0.033	0.032	0.030	0.101	0.039	0.025	0.032	0.047
Mg	2.013	3.311	3.339	3.253	3.231	3.170	3.330	2.821	3.025	2.544	3.330
Ca	1.667	1.462	1.705	1.680	1.664	1.717	1.193	1.988	1.799	1.717	2.019
Na	0.616	0.082	0.212	0.222	0.209	0.283	0.067	0.041	0.213	0.378	0.021
K	0.169	0.022	0.059	0.072	0.056	0.079	0.012	0.009	0.066	0.148	0.008
Cr	0.002	0.005	0.007	0.006	0.005	0.004	0.006	0.002	0.001	0.005	0.003
Ni	0.000	0.000	0.000	0.003	0.000	0.005	0.006	0.000	0.000	0.004	0.005
Total	15.750	15.122	15.334	15.359	15.305	15.416	15.115	15.101	15.316	15.554	15.088
Name	2	0	5	5	5	5	0	4	5	6	4

0 = cannot be classified; 2 = ferrohornblende; 4 = actinolite; 5 = magnesio-hornblende; 6 = edenite

Note: 130-1995 = Sample SUD-130-1995; Drill core 70011

Amphibole after px	Sample SUD-63-1994; Drill core 70011 (continued)								Sample SUD-66-1994; Drill core 70011		
point	bright	over?	bright	dark	dark	core	core	core	main1	rim1	core1
SiO_2	52.080	51.622	52.719	53.430	51.745	52.972	53.129	50.758	53.739	54.714	54.691
Al_2O_3	1.401	1.307	1.306	1.913	2.468	1.105	1.044	3.738	0.406	1.757	1.181
TiO_2	0.214	0.132	0.177	0.193	0.313	0.163	0.250	0.079	0.035	0.165	0.062
FeO	23.346	23.462	22.121	13.644	15.613	20.314	18.515	15.296	10.813	12.740	12.817
MnO	0.716	0.489	0.630	0.178	0.215	0.882	0.898	0.176	0.325	0.214	0.207
MgO	16.021	17.502	15.564	15.135	14.801	16.342	12.280	13.891	12.294	15.170	15.052
CaO	3.353	2.495	4.859	12.939	11.192	4.936	12.372	12.658	21.112	12.046	12.730
Na_2O	0.259	0.257	0.219	0.174	0.502	0.153	0.097	0.409	0.127	0.186	0.119
K_2O	0.063	0.030	0.046	0.073	0.189	0.060	0.069	0.171	0.034	0.131	0.066
Cr_2O_3	0.052	0.037	0.029	0.063	0.034	0.064	0.041	0.057	0.025	0.028	0.079
NiO	0.000	0.073	0.004	0.040	0.013	0.019	0.027	0.056	0.031	0.042	0.047
Total	97.505	97.406	97.674	97.782	97.085	97.010	98.722	97.289	98.941	97.193	97.051
Si	7.732	7.664	7.786	7.737	7.616	7.820	7.808	7.480	7.788	7.891	7.920
Al	0.245	0.229	0.227	0.326	0.428	0.192	0.181	0.649	0.069	0.299	0.202
Ti	0.024	0.015	0.020	0.021	0.035	0.018	0.028	0.009	0.004	0.018	0.007
Fe2+	2.899	2.913	2.732	1.652	1.922	2.508	2.276	1.885	1.310	1.537	1.552
Mn	0.090	0.061	0.079	0.022	0.027	0.110	0.112	0.022	0.040	0.026	0.025
Mg	3.546	3.874	3.427	3.267	3.247	3.596	2.691	3.052	2.656	3.262	3.249
Ca	0.533	0.397	0.769	2.007	1.765	0.781	1.948	1.999	3.278	1.861	1.975
Na	0.075	0.074	0.063	0.049	0.143	0.044	0.028	0.117	0.036	0.052	0.033
K	0.012	0.006	0.009	0.013	0.035	0.011	0.013	0.032	0.006	0.024	0.012
Cr	0.006	0.004	0.003	0.007	0.004	0.007	0.005	0.007	0.003	0.003	0.009
Ni	0.000	0.009	0.000	0.005	0.002	0.002	0.003	0.007	0.004	0.005	0.005
Total	15.162	15.245	15.115	15.107	15.223	15.090	15.091	15.258	15.193	14.978	14.991
Name	7	7	8	4	5	8	4	5	9	4	4

4 = actinolite; 5 = magnesio-hornblende; 7 = cummingtonite/anthophyllite;
8 = calcian cummingtonite/anthophyllite; 9 = cannilloite

Amphibole after px	Sample SUD-66-1994 (cont'd)				SUD-71-1994; Drill core 70011		Sample SUD-166-1995; Drill core 52848				
point	main1	main2	main2	main6	core2	rim2	rim2	main9	main12	main13	main14
SiO_2	54.802	52.534	54.190	52.680	52.889	54.315	51.146	49.937	52.102	45.975	52.252
Al_2O_3	0.884	1.175	0.399	1.908	2.945	1.677	2.677	3.333	2.167	6.224	1.239
TiO_2	0.075	0.277	0.027	0.130	0.119	0.061	0.048	0.055	0.175	1.506	0.063
FeO	13.383	19.063	15.864	20.323	12.632	10.960	20.438	22.117	17.762	21.002	20.015
MnO	0.210	0.474	0.309	0.544	0.437	0.393	0.151	0.199	0.139	0.380	0.190
MgO	14.991	11.336	13.452	16.311	15.981	17.332	10.412	9.235	12.497	9.276	10.721
CaO	12.970	12.071	12.958	4.871	12.051	12.286	12.636	12.275	12.384	10.975	12.236
Na_2O	0.094	0.181	0.031	0.287	0.297	0.126	0.345	0.407	0.360	1.347	0.208
K_2O	0.065	0.099	0.005	0.102	0.033	0.023	0.199	0.190	0.113	0.725	0.067
Cr_2O_3	0.091	0.057	0.044	0.006	0.103	0.060	0.048	0.048	0.019	0.045	0.029
NiO	0.004	0.025	0.000	0.000	-	-	0.041	0.051	0.014	0.041	0.027
Total	97.569	97.292	97.279	97.162	97.486	97.233	98.141	97.847	97.732	97.496	97.047
Si	7.920	7.843	7.955	7.753	7.638	7.789	7.642	7.554	7.700	7.024	7.851
Al	0.151	0.207	0.069	0.331	0.501	0.283	0.471	0.594	0.377	1.121	0.219
Ti	0.008	0.031	0.003	0.014	0.013	0.007	0.005	0.006	0.019	0.173	0.007
Fe2+	1.618	2.380	1.948	2.501	1.526	1.314	2.554	2.798	2.195	2.683	2.515
Mn	0.026	0.060	0.038	0.068	0.053	0.048	0.019	0.025	0.017	0.049	0.024
Mg	3.230	2.523	2.944	3.579	3.441	3.705	2.319	2.083	2.753	2.113	2.401
Ca	2.008	1.931	2.038	0.768	1.865	1.888	2.023	1.989	1.961	1.796	1.970
Na	0.026	0.052	0.009	0.082	0.083	0.035	0.100	0.119	0.103	0.399	0.061
K	0.012	0.019	0.001	0.019	0.006	0.004	0.038	0.037	0.021	0.141	0.013
Cr	0.010	0.007	0.005	0.001	0.012	0.007	0.006	0.006	0.002	0.005	0.003
Ni	0.000	0.003	0.000	0.000	-	-	0.005	0.006	0.002	0.005	0.003
Total	15.010	15.055	15.010	15.117	15.137	15.079	15.183	15.218	15.153	15.510	15.067
Name	4	4	4	8	4	4	1	1	4	2	1

1 = ferro-actinolite; 2 = ferrohornblende; 4 = actinolite; 8 = calcian cummingtonite/anthophyllite

Amphibole Sample SUD-166-1995; Drill core 52848 (continued)

after px							
point	main15	main16	main17	main18	main19	main20	main21
SiO_2	52.436	52.460	47.597	51.696	50.207	54.004	51.112
Al_2O_3	1.204	1.307	4.327	2.307	3.118	1.141	2.783
TiO_2	0.088	0.075	1.086	0.043	0.087	0.193	0.282
FeO	20.230	18.852	21.511	20.482	21.134	14.922	20.445
MnO	0.223	0.178	0.347	0.152	0.183	0.142	0.368
MgO	10.590	11.530	10.082	10.505	9.566	14.107	11.692
CaO	12.719	12.542	10.397	12.394	12.537	12.262	9.783
Na_2O	0.183	0.201	1.485	0.291	0.396	0.483	1.019
K_2O	0.084	0.083	0.534	0.133	0.176	0.232	0.275
Cr_2O_3	0.042	0.018	0.012	0.051	0.077	0.034	0.007
NiO	0.008	0.045	0.000	0.020	0.048	0.000	0.037
Total	97.807	97.291	97.378	98.074	97.529	97.520	97.803
Si	7.834	7.825	7.263	7.712	7.587	7.874	7.629
Al	0.212	0.230	0.778	0.406	0.555	0.196	0.490
Ti	0.010	0.008	0.125	0.005	0.010	0.021	0.032
Fe2+	2.528	2.352	2.745	2.555	2.671	1.820	2.552
Mn	0.028	0.022	0.045	0.019	0.023	0.018	0.047
Mg	2.359	2.564	2.294	2.336	2.155	3.066	2.602
Ca	2.036	2.004	1.700	1.981	2.030	1.916	1.565
Na	0.053	0.058	0.439	0.084	0.116	0.137	0.295
K	0.016	0.016	0.104	0.025	0.034	0.043	0.052
Cr	0.005	0.002	0.001	0.006	0.009	0.004	0.001
Ni	0.001	0.005	0.000	0.002	0.006	0.000	0.004
Total	15.082	15.087	15.494	15.132	15.196	15.094	15.268
Name	1	4	2	1	1	4	4

1 = ferro-actinolite; 2 = ferrohornblende; 4 = actinolite

Amphibole Sample SUD-60-1994; Drill core 70011

point	core1	core1	lam1	rim1	lam2	lam3	core2	core2	core2	rim2
SiO_2	53.453	51.682	51.999	52.742	52.814	53.055	52.015	51.465	51.855	51.249
Al_2O_3	2.046	2.265	3.220	1.710	2.115	1.533	1.915	2.990	1.879	1.577
TiO_2	0.093	0.064	0.376	0.134	0.140	0.109	0.262	0.256	0.337	1.245
Cr_2O_3	0.105	0.000	0.044	0.066	0.026	0.000	0.031	0.031	0.057	0.031
FeO	16.527	16.602	17.309	15.771	16.899	15.869	17.764	17.573	17.023	17.831
MnO	0.307	0.376	0.350	0.357	0.358	0.304	0.404	0.388	0.351	0.376
MgO	13.381	13.515	12.746	13.890	13.234	13.927	12.694	11.812	13.097	12.681
CaO	11.978	12.472	11.905	11.843	11.821	12.254	12.338	12.077	12.271	12.149
Na_2O	0.164	0.152	0.226	0.103	0.197	0.133	0.159	0.252	0.167	0.057
K_2O	0.127	0.113	0.167	0.087	0.095	0.067	0.136	0.141	0.145	0.117
Cl	0.039	0.045	0.102	0.043	0.057	0.041	0.098	0.000	0.018	0.035
F	0.000	0.000	0.000	0.000	0.000	0.000	0.000	0.000	0.000	0.000
P_2O_5	0.000	0.000	0.074	0.104	0.015	0.015	0.000	0.015	0.104	0.015
NiO	0.000	0.000	0.010	0.000	0.026	0.050	0.018	0.026	0.000	0.000
BaO	0.213	0.464	0.191	0.000	0.000	0.000	0.000	0.000	0.000	0.000
SO_2	0.000	0.000	0.000	0.000	0.000	0.037	0.130	0.000	0.121	0.000
SrO	0.000	0.000	0.000	0.013	0.061	0.039	0.000	0.000	0.012	0.034
ZnO	0.023	0.049	0.073	0.099	0.096	0.023	0.000	0.050	0.162	0.109
V_2O_3	0.030	0.073	0.127	0.110	0.061	0.098	0.177	0.159	0.079	0.000
Total	98.487	97.872	98.919	97.070	98.014	97.556	98.142	97.235	97.678	97.503
Si	7.777	7.631	7.580	7.760	7.737	7.776	7.666	7.646	7.657	7.622
Al	0.351	0.394	0.553	0.297	0.365	0.265	0.333	0.524	0.327	0.276
Ti	0.010	0.007	0.041	0.015	0.015	0.012	0.029	0.029	0.037	0.139
Cr	0.012	0.000	0.005	0.008	0.003	0.000	0.004	0.004	0.007	0.004
Fe^{2+}	2.011	2.050	2.110	1.940	2.070	1.945	2.189	2.183	2.102	2.217
Mn	0.038	0.047	0.043	0.044	0.044	0.038	0.050	0.049	0.044	0.047
Mg	2.901	2.974	2.769	3.045	2.889	3.041	2.788	2.615	2.882	2.810
Ca	1.867	1.973	1.859	1.867	1.855	1.924	1.948	1.922	1.941	1.936
Na	0.046	0.044	0.064	0.029	0.056	0.038	0.045	0.073	0.048	0.016
K	0.024	0.021	0.031	0.016	0.018	0.013	0.026	0.027	0.027	0.022
Cl	0.010	0.011	0.025	0.011	0.014	0.010	0.024	0.000	0.004	0.009
F	0.000	0.000	0.000	0.000	0.000	0.000	0.000	0.000	0.000	0.000
P	0.000	0.000	0.009	0.013	0.002	0.002	0.000	0.002	0.013	0.002
Ni	0.000	0.000	0.001	0.000	0.003	0.006	0.002	0.003	0.000	0.000
Ba	0.012	0.027	0.011	0.000	0.000	0.000	0.000	0.000	0.000	0.000
S	0.000	0.000	0.000	0.000	0.000	0.005	0.018	0.000	0.017	0.000
Sr	0.000	0.000	0.000	0.001	0.005	0.003	0.000	0.000	0.001	0.003
Zn	0.002	0.005	0.008	0.011	0.010	0.003	0.000	0.005	0.018	0.012
V	0.004	0.009	0.015	0.013	0.007	0.012	0.021	0.019	0.009	0.000
Total	15.064	15.193	15.125	15.070	15.094	15.091	15.144	15.099	15.135	15.116
Name	4	4	4	4	4	4	4	4	4	4

4 = actinolite

Amphibole Sample SUD-60-1994; Drill core 70011 (continued)

point	core3	core3	rim4	core4	rim6	rim7	core7	core7	rim8
SiO_2	51.557	52.140	51.769	52.235	52.495	52.651	51.864	46.819	46.642
Al_2O_3	2.294	2.163	2.288	2.228	1.163	1.982	2.682	4.937	5.076
TiO_2	0.102	0.104	0.224	0.208	0.701	0.141	0.096	0.813	1.261
Cr_2O_3	0.009	0.035	0.000	0.026	0.066	0.026	0.000	0.039	0.000
FeO	17.089	16.934	18.112	17.512	14.628	16.585	16.657	20.731	21.081
MnO	0.268	0.342	0.400	0.334	0.469	0.253	0.346	0.371	0.224
MgO	12.942	12.873	12.241	12.613	15.805	13.353	12.840	11.308	11.227
CaO	12.179	12.155	12.080	12.128	11.198	12.106	12.165	10.109	9.940
Na_2O	0.204	0.241	0.152	0.261	0.210	0.163	0.190	0.794	0.977
K_2O	0.104	0.095	0.184	0.137	0.171	0.137	0.159	0.634	0.693
Cl	0.090	0.045	0.055	0.095	0.039	0.035	0.071	0.346	0.259
F	0.000	0.000	0.000	0.000	0.000	0.000	0.000	0.000	0.000
P_2O_5	0.148	0.000	0.000	0.000	0.045	0.045	0.000	0.000	0.000
NiO	0.081	0.024	0.016	0.000	0.000	0.016	0.000	0.000	0.000
BaO	0.128	0.128	0.000	0.000	0.000	0.000	0.000	0.273	0.000
SO_2	0.000	0.000	0.063	0.155	0.000	0.086	0.083	0.000	0.000
SrO	0.000	0.001	0.001	0.000	0.000	0.000	0.000	0.000	0.000
ZnO	0.036	0.106	0.142	0.007	0.000	0.037	0.000	0.039	0.056
V_2O_3	0.128	0.055	0.091	0.000	0.041	0.068	0.000	0.033	0.111
Total	97.359	97.441	97.818	97.939	97.030	97.682	97.152	97.247	97.548
Si	7.640	7.710	7.668	7.688	7.696	7.729	7.668	7.136	7.088
Al	0.401	0.377	0.399	0.387	0.201	0.343	0.467	0.887	0.909
Ti	0.011	0.012	0.025	0.023	0.077	0.016	0.011	0.093	0.144
Cr	0.001	0.004	0.000	0.003	0.008	0.003	0.000	0.005	0.000
Fe^{2+}	2.118	2.094	2.243	2.155	1.793	2.036	2.059	2.642	2.679
Mn	0.034	0.043	0.050	0.042	0.058	0.031	0.043	0.048	0.029
Mg	2.858	2.837	2.701	2.766	3.453	2.921	2.829	2.568	2.542
Ca	1.934	1.926	1.917	1.912	1.759	1.904	1.927	1.651	1.618
Na	0.059	0.069	0.044	0.074	0.060	0.046	0.054	0.235	0.288
K	0.020	0.018	0.035	0.026	0.032	0.026	0.030	0.123	0.134
Cl	0.023	0.011	0.014	0.024	0.010	0.009	0.018	0.089	0.067
F	0.000	0.000	0.000	0.000	0.000	0.000	0.000	0.000	0.000
P	0.019	0.000	0.000	0.000	0.006	0.006	0.000	0.000	0.000
Ni	0.010	0.003	0.002	0.000	0.000	0.002	0.000	0.000	0.000
Ba	0.007	0.007	0.000	0.000	0.000	0.000	0.000	0.016	0.000
S	0.000	0.000	0.009	0.021	0.000	0.012	0.011	0.000	0.000
Sr	0.000	0.000	0.000	0.000	0.000	0.000	0.000	0.000	0.000
Zn	0.004	0.012	0.016	0.001	0.000	0.004	0.000	0.004	0.006
V	0.015	0.007	0.011	0.000	0.005	0.008	0.000	0.004	0.013
Total	15.151	15.128	15.133	15.123	15.157	15.094	15.118	15.502	15.518
Name	4	4	4	4	4	4	4	5	5

4 = actinolite; 5 = magnesio-hornblende

Amphibole	SUD-153-1995; Drill core 70011								Sample SUD-94-1994		
point	alter2	core3	core3	rim4	rim5	core6	core9	core9	-	-	-
SiO_2	52.084	46.028	53.306	48.400	51.357	54.355	44.688	44.494	50.856	45.869	50.909
Al_2O_3	2.934	5.715	0.564	4.042	3.223	0.805	5.980	5.874	2.108	4.911	2.150
TiO_2	0.118	1.251	0.866	1.966	0.032	0.112	1.490	1.464	0.000	1.274	0.160
Cr_2O_3	0.018	0.004	0.018	0.030	0.074	0.092	0.030	0.043	0.036	0.035	0.024
FeO	16.103	21.912	13.941	16.873	15.894	14.163	22.388	21.927	19.757	19.765	20.464
MnO	0.294	0.363	0.359	0.304	0.353	0.508	0.276	0.242	0.316	0.241	0.306
MgO	14.035	9.643	14.916	13.182	13.354	16.033	9.503	9.603	11.113	10.963	10.902
CaO	11.956	10.155	12.512	12.355	12.233	11.062	9.922	10.050	12.033	10.510	11.490
Na_2O	0.250	0.935	0.090	0.177	0.252	0.161	1.428	2.107	0.351	1.702	0.369
K_2O	0.118	0.757	0.044	0.261	0.086	0.066	0.748	0.796	0.157	0.670	0.157
Cl	0.051	0.400	0.080	0.083	0.041	0.000	0.368	0.434	0.073	0.216	0.057
F	0.000	0.000	0.000	0.000	0.000	0.000	0.000	0.000	0.000	1.326	0.137
P_2O_5	0.000	0.029	0.163	0.044	0.074	0.000	0.132	0.000	0.025	0.050	0.051
NiO	0.071	0.021	0.000	0.036	0.029	0.044	0.018	0.026	0.043	0.000	0.000
BaO	0.000	0.000	0.000	0.147	0.149	0.000	0.084	0.146	0.072	0.159	0.000
SO_2	0.000	0.000	0.000	0.000	0.095	0.000	0.010	0.054	0.006	0.032	0.038
SrO	0.000	0.000	0.000	0.000	0.000	0.000	0.000	0.000	0.000	0.000	0.000
ZnO	0.010	0.128	0.093	0.065	0.181	0.171	0.003	0.098	0.149	0.008	0.008
V_2O_3	0.061	0.128	0.102	0.029	0.098	0.000	0.007	0.000	-	-	-
Total	98.101	97.469	97.054	97.992	97.524	97.573	97.074	97.357	97.095	97.731	97.222
Si	7.604	7.043	7.794	7.186	7.563	7.873	6.907	6.878	7.669	6.869	7.654
Al	0.505	1.031	0.097	0.707	0.559	0.137	1.090	1.070	0.375	0.867	0.381
Ti	0.013	0.144	0.095	0.219	0.003	0.012	0.173	0.170	0.000	0.143	0.018
Cr	0.002	0.001	0.002	0.004	0.009	0.011	0.004	0.005	0.004	0.004	0.003
Fe^{2+}	1.966	2.803	1.704	2.095	1.957	1.715	2.893	2.834	2.491	2.475	2.573
Mn	0.036	0.047	0.044	0.038	0.044	0.062	0.036	0.032	0.040	0.031	0.039
Mg	3.053	2.199	3.250	2.916	2.930	3.460	2.189	2.212	2.497	2.446	2.442
Ca	1.870	1.665	1.960	1.965	1.930	1.717	1.643	1.664	1.944	1.686	1.851
Na	0.071	0.277	0.026	0.051	0.072	0.045	0.428	0.631	0.103	0.494	0.108
K	0.022	0.148	0.008	0.049	0.016	0.012	0.148	0.157	0.030	0.128	0.030
Cl	0.013	0.104	0.020	0.021	0.010	0.000	0.096	0.114	0.019	0.055	0.015
F	0.000	0.000	0.000	0.000	0.000	0.000	0.000	0.000	0.000	0.628	0.065
P	0.000	0.004	0.020	0.005	0.009	0.000	0.017	0.000	0.003	0.006	0.006
Ni	0.008	0.003	0.000	0.004	0.003	0.005	0.002	0.003	0.005	0.000	0.000
Ba	0.000	0.000	0.000	0.009	0.009	0.000	0.005	0.009	0.004	0.009	0.000
S	0.000	0.000	0.000	0.000	0.013	0.000	0.001	0.008	0.001	0.004	0.005
Sr	0.000	0.000	0.000	0.000	0.000	0.000	0.000	0.000	0.000	0.000	0.000
Zn	0.001	0.014	0.010	0.007	0.020	0.018	0.000	0.011	0.017	0.001	0.001
V	0.007	0.016	0.012	0.003	0.012	0.000	0.001	0.000	-	-	-
Total	15.172	15.497	15.042	15.280	15.160	15.069	15.633	15.800	15.202	15.849	15.190
Name	4	2	4	5	4	4	3	3	4	3*	4

2 = ferrohornblende; 3 = ferro-edenite; 3* = fluorian-ferro-edenite;
4 = actinolite; 5 = magnesio-hornblende

Amphibole 94-1994 (cont'd)			Sample SUD-71-1994; Drill core 70011							43-1994
point	-	-	1	2	3	4	5	core2	rim2	px over
SiO_2	50.277	49.348	55.071	54.352	54.709	52.894	53.171	52.889	54.315	48.341
Al_2O_3	2.274	3.520	1.364	1.400	1.407	3.088	2.814	2.945	1.677	5.881
TiO_2	0.045	0.229	0.026	0.017	0.026	0.102	0.087	0.119	0.061	0.476
Cr_2O_3	0.028	0.068	0.288	0.401	0.193	0.335	0.272	0.103	0.060	0.000
FeO	20.433	20.326	10.741	12.066	11.746	11.610	11.500	12.632	10.960	18.346
MnO	0.410	0.237	0.284	0.222	0.240	0.466	0.346	0.437	0.393	0.320
MgO	10.837	10.666	17.099	16.581	17.259	16.512	16.849	15.981	17.332	12.414
CaO	12.084	11.234	12.637	12.113	12.073	11.834	11.752	12.051	12.286	10.567
Na_2O	0.306	0.428	0.050	0.087	0.014	0.397	0.236	0.297	0.126	1.591
K_2O	0.174	0.721	0.007	0.033	0.062	0.037	0.030	0.033	0.023	0.601
Cl	0.107	0.078	0.129	0.018	0.077	0.069	0.039	-	-	0.099
F	0.082	0.110	0.000	0.000	0.000	0.000	0.000	-	-	0.000
P_2O_5	0.031	0.000	0.000	0.030	0.000	0.120	0.000	-	-	0.030
NiO	0.005	0.000	0.018	0.000	0.000	0.092	0.000	-	-	0.076
BaO	0.000	0.095	0.000	0.022	0.000	0.129	0.280	-	-	0.085
SO_2	0.000	0.026	0.031	0.120	0.085	0.007	0.088	-	-	0.000
SrO	0.000	0.000	0.072	0.022	0.000	0.046	0.016	-	-	0.056
ZnO	0.123	0.000	0.000	0.000	0.063	0.000	0.000	-	-	0.000
V_2O_3	-	-	0.019	0.000	0.069	0.000	0.000	-	-	0.059
Total	97.216	97.086	97.837	97.485	98.022	97.737	97.480	97.486	97.233	98.942
Si	7.597	7.472	7.839	7.809	7.800	7.597	7.645	7.639	7.789	7.146
Al	0.405	0.628	0.229	0.237	0.236	0.523	0.477	0.501	0.283	1.025
Ti	0.005	0.026	0.003	0.002	0.003	0.011	0.009	0.013	0.007	0.053
Cr	0.003	0.008	0.032	0.046	0.022	0.038	0.031	0.012	0.007	0.000
Fe^{2+}	2.582	2.573	1.278	1.450	1.400	1.394	1.382	1.525	1.314	2.268
Mn	0.052	0.030	0.034	0.027	0.029	0.057	0.042	0.053	0.048	0.040
Mg	2.440	2.406	3.627	3.550	3.667	3.534	3.610	3.439	3.704	2.735
Ca	1.956	1.822	1.927	1.864	1.844	1.821	1.810	1.865	1.888	1.674
Na	0.090	0.126	0.014	0.024	0.004	0.111	0.066	0.083	0.035	0.456
K	0.034	0.139	0.001	0.006	0.011	0.007	0.006	0.006	0.004	0.113
Cl	0.027	0.020	0.031	0.004	0.019	0.017	0.010	-	-	0.025
F	0.039	0.053	0.000	0.000	0.000	0.000	0.000	-	-	0.000
P	0.004	0.000	0.000	0.004	0.000	0.015	0.000	-	-	0.004
Ni	0.001	0.000	0.002	0.000	0.000	0.011	0.000	-	-	0.009
Ba	0.000	0.006	0.000	0.001	0.000	0.007	0.016	-	-	0.005
S	0.000	0.004	0.004	0.016	0.011	0.001	0.012	-	-	0.000
Sr	0.000	0.000	0.006	0.002	0.000	0.004	0.001	-	-	0.005
Zn	0.014	0.000	0.000	0.000	0.007	0.000	0.000	-	-	0.000
V	-	-	0.002	0.000	0.008	0.000	0.000	-	-	0.007
Total	15.249	15.313	15.030	15.042	15.060	15.147	15.116	15.137	15.079	15.564
Name	4	2	4	4	4	4	4	4	4	6

2 = ferrohornblende; 4 = actinolite; 6 = edenite

Note: 43-1994 = Sample SUD-43-1994; Drill core 52848

Oxides	87-1994	Sample SUD-84-1994, Drill core 70011							
SiO_2	0.000	0.1	0.1	0.2	0.0	0.0	0.2	0.0	0.1
TiO_2	46.057	52.1	52.8	52.9	53.4	53.4	52.4	52.1	53.1
Al_2O_3	0.826	0.1	0.0	0.0	0.1	0.0	0.1	0.0	0.0
FeO	51.708	43.6	43.6	43.4	43.0	42.2	42.9	43.3	41.8
MgO	0.158	0.0	0.1	0.1	0.1	0.1	0.1	0.0	0.1
MnO	2.283	2.5	2.5	2.6	2.8	3.0	3.1	2.6	2.8
CaO	0.041	0.1	0.0	0.0	0.2	0.3	0.5	0.0	0.1
V_2O_3	0.306	0.7	0.7	0.3	0.3	0.3	0.3	0.8	0.4
Cr_2O_3	0.289	0.0	0.0	0.0	0.0	0.0	0.1	0.0	0.1
NiO	0.017	0.1	0.0	0.0	0.1	0.0	0.0	0.0	0.0
ZnO	0.115	0.0	0.0	0.0	0.1	0.0	0.2	0.0	0.0
As_2O_3	-	0.0	0.1	0.0	0.0	0.0	0.0	0.0	0.0
CO_2	0.113	0.1	0.0	0.1	0.0	0.1	0.0	0.1	0.1
Total	101.911	99.4	99.9	99.6	100.1	99.4	99.9	98.9	98.6

Oxides	Sample SUD-154-1995			Sample SUD-155-1995, Drill core 70011						
point	-	-	-	L1	L2	L2	L2	L1	L2	L3
SiO_2	0.100	0.100	0.000	0.053	0.123	0.042	0.000	0.076	0.000	0.031
TiO_2	50.700	51.000	51.000	5.096	2.873	33.674	36.983	43.133	42.762	52.309
Al_2O_3	0.100	0.000	0.100	0.067	0.026	0.042	0.058	0.034	0.069	0.016
FeO	44.000	43.600	43.700	85.659	87.182	62.265	59.341	53.123	53.368	43.537
MgO	0.200	0.300	0.300	0.030	0.112	0.083	0.036	0.000	0.048	0.046
MnO	2.500	2.500	2.500	0.344	0.183	1.771	1.887	2.348	2.207	2.789
CaO	0.100	0.300	0.100	0.035	0.021	0.014	0.000	0.000	0.000	0.098
V_2O_3	0.300	0.300	0.400	0.665	0.916	0.342	0.411	0.310	0.348	0.250
Cr_2O_3	0.100	0.100	0.000	0.359	0.717	0.258	0.371	0.185	0.124	0.000
NiO	0.000	0.000	0.000	0.018	0.085	0.190	0.049	0.046	0.000	0.056
ZnO	0.100	0.100	0.000	0.032	0.000	0.003	0.006	0.060	0.101	0.000
As_2O_3	0.000	0.000	0.000	0.000	0.000	0.000	0.000	0.000	0.000	0.000
SO_3	0.000	0.000	0.000	0.035	0.000	0.000	0.084	0.000	0.039	0.083
CO_2	0.000	0.100	0.000	0.054	0.069	0.023	0.000	0.073	0.000	0.076
O	-	-	-	7.553	7.693	1.293	0.775	0.612	0.935	0.709
Total	98.100	98.300	98.100	100.000	100.000	100.000	100.000	100.000	100.000	100.000

Note: 87-1994 = Sample SUD-87-1994; Drill core 70011 and
Sample SUD-154-1995 is also from drill core 70011

Oxides	Sample SUD-155-1995, Drill core 70011 (continued)			
point	L3	D3	D3	B3
SiO_2	0.102	0.160	1.215	0.031
TiO_2	52.632	52.576	53.230	52.470
Al_2O_3	0.041	0.128	0.092	0.056
FeO	43.931	42.978	41.452	45.065
MgO	0.055	0.047	0.018	0.034
MnO	2.838	2.751	3.032	2.796
CaO	0.160	0.677	1.410	0.073
V_2O_3	0.216	0.359	0.299	0.165
Cr_2O_3	0.000	0.000	0.008	0.000
NiO	0.000	0.000	0.033	0.031
ZnO	0.013	0.072	0.101	0.013
As_2O_3	0.000	0.024	0.000	0.000
SO_3	0.000	0.049	0.033	0.000
CO_2	0.023	0.053	0.000	0.072
O	0.000	0.125	0.000	0.000
Total	100.011	100.000	100.924	100.806

Titanite	SUD-87-1994		SUD-64-1994		154-1994	SUD-155-1995
SiO_2	32.437	31.795	29.800	34.000	31.400	28.173
TiO_2	33.309	33.813	38.200	36.900	37.200	39.498
Al_2O_3	4.268	3.509	1.100	1.200	1.100	0.313
FeO	1.913	2.524	2.400	1.100	0.600	3.567
MgO	0.138	0.269	0.100	0.100	0.000	0.067
MnO	0.034	0.000	0.100	0.000	0.100	0.150
CaO	27.668	27.757	26.900	27.700	29.600	26.605
SO_2	0.012	0.000	0.000	0.000	0.000	0.040
NiO	0.084	0.022	0.000	0.000	0.000	0.013
ZnO	0.000	0.091	0.000	0.000	0.000	0.013
Cr_2O_3	0.000	0.104	0.000	0.000	0.200	0.191
CO_2	0.014	0.034	0.000	0.100	0.000	0.000
As_2O_3	-	-	0.000	0.000	0.000	0.025
V_2O_3	0.231	0.115	0.600	0.600	0.600	0.246
Total	100.108	100.032	99.200	101.700	100.800	98.902

Note: All samples from drill core 70011

APPENDIX B

Whole-rock geochemical analysis for samples used in this study. Major elements are listed from page B2 to B7; whereas trace and rare earth elements are listed from page B8 to B16.

Analytical precision is as follows:

1) major elements (XRF):

SiO_2	± 0.50; ± 1%; determ. limit 0.50%	CaO	± 0.10; ± 1%; determ. limit 0.10%
TiO_2	± 0.02; ± 1%; determ. limit 0.02%	Na_2O	± 0.50; ± 1%; determ. limit 0.50%
Al_2O_3	± 0.40; ± 1%; determ. limit 0.40%	K_2O	± 0.05; ± 1%; determ. limit 0.05%
Fe_2O_3T	± 0.10; ± 1%; determ. limit 0.10%	H_2OT	± 0.10; ± 5%; determ. limit 0.10%
FeO	± 0.20; ± 5%; determ. limit 0.20%	CO_2T	± 0.10; ± 3%; determ. limit 0.10%
MnO	± 0.01; ± 1%; determ. limit 0.01%	P_2O_5	± 0.02; ± 1%; determ. limit 0.02%
MgO	± 0.10; ± 1%; determ. limit 0.10%	S	± 0.02; ± 5%; determ. limit 0.02%

2) trace and rare earth elements:

Ag	± 0.1 ppm (ICP-MS)	Nd	± 0.1 ppm (ICP-MS)
Ba	± 20 ppm; ± 10% of conc. (ICP-TR1)	Ni	± 10 ppm; ± 5% of conc. (ICP-TR1)
Be	± 0.5 ppm; ± 5% of conc. (ICP-TR1)	Pb	± 2 ppm (ICP-MS)
Bi	± 0.5 ppm (ICP-MS)	Pr	± 0.02 ppm (ICP-MS)
Cd	± 0.2 ppm (ICP-MS)	Rb	± 0.05 ppm (ICP-MS)
Ce	± 0.1 ppm (ICP-MS)	Sc	± 0.5 ppm; ± 5% of conc. (ICP-TR1)
Co	± 5 ppm; ± 5% of conc. (ICP-TR1)	Sm	± 0.02 ppm (ICP-MS)
Cr	± 10 ppm; ± 5% of conc. (ICP-TR1)	Sr	± 10 ppm; ± 5% of conc. (ICP-TR1)
Cs	± 0.02 ppm (ICP-MS)	Ta	± 0.2 ppm (ICP-MS)
Cu	± 10 ppm; ± 5% of conc. (ICP-TR1)	Tb	± 0.02 ppm (ICP-MS)
Dy	± 0.02 ppm (ICP-MS)	Th	± 0.02 ppm (ICP-MS)
Er	± 0.02 ppm (ICP-MS)	Tl	± 0.02 ppm (ICP-MS)
Eu	± 0.02 ppm (ICP-MS)	Tm	± 0.02 ppm (ICP-MS)
Ga	± 0.1 ppm (ICP-MS)	U	± 0.02 ppm (ICP-MS)
Gd	± 0.02 ppm (ICP-MS)	V	± 5 ppm; ± 5% of conc. (ICP-TR1)
Hf	± 0.05 ppm (ICP-MS)	Y	± 0.02 ppm (ICP-MS)
Ho	± 0.02 ppm (ICP-MS)	Yb	± 0.05 ppm (ICP-MS)
In	± 0.05 ppm (ICP-MS)	Zn	± 5 ppm; ± 5% of conc. (ICP-TR1)
La	± 0.1 ppm (ICP-MS)	Zr	± 0.5 ppm (ICP-MS)
Lu	± 0.02 ppm (ICP-MS)		
Mo	± 0.2 ppm (ICP-MS)		
Nb	± 0.05 ppm (ICP-MS)		

Drill core 70011

sample	189	191	193	195	83	143a	143b	177	178	197	198	199
depth (m)	15.2	45.7	76.2	79.2	82.3	83.9	83.9	89.9	93.0	121.9	152.4	182.9
SiO_2	65.30	67.60	70.80	73.20	72.10	68.90	68.30	77.40	74.60	70.00	69.90	68.60
TiO_2	0.53	0.46	0.31	0.31	0.18	0.27	0.30	0.15	0.51	0.80	0.81	0.83
Al_2O_3	12.40	13.20	14.00	13.80	14.80	15.60	15.40	12.40	11.60	12.30	12.40	12.40
Fe_2O_3T	6.70	4.80	3.10	1.90	1.70	2.80	3.40	0.90	3.00	5.50	5.90	5.80
Fe_2O_3	0.80	1.30	0.60	0.60	0.70	1.80	0.80	0.40	1.30	1.60	2.40	2.90
FeO	5.30	3.20	2.20	1.10	0.90	0.90	2.30	0.40	1.50	3.50	3.10	2.60
MnO	0.07	0.06	0.03	0.02	0.01	0.03	0.03	0.01	0.03	0.06	0.06	0.04
MgO	4.38	3.45	2.20	1.62	0.69	0.85	1.90	0.50	0.78	0.97	0.88	1.33
CaO	3.30	2.71	0.99	1.32	2.04	3.31	1.77	1.23	2.32	1.80	1.81	1.76
Na_2O	3.70	4.50	4.90	6.60	6.30	6.10	5.00	4.30	3.90	3.00	3.00	3.10
K_2O	1.69	1.87	2.15	0.34	0.64	0.93	2.36	1.53	1.52	3.99	3.99	4.21
H_2OT	2.10	1.60	1.60	1.00	0.80	0.90	1.40	0.70	1.00	1.40	1.20	1.00
CO_2T	0.10	0.10	0.10	0.10	0.30	0.10	0.10	0.10	0.60	0.10	0.10	0.30
P_2O_5	0.13	0.12	0.09	0.11	0.06	0.12	0.13	0.02	0.08	0.17	0.17	0.17
S	0.80	0.19	0.01	0.01	0.10	0.01	0.00	0.01	0.00	0.05	0.02	0.10
LoI	0.00	0.00	0.00	0.00	-	-	-	-	-	0.00	0.00	0.00
Total	101.20	100.66	100.28	100.33	99.60	99.80	99.70	99.20	99.70	100.14	100.24	99.64

Drill core 70011

sample	50	200	144	145	167	168	52	146	147	169	201	53
depth (m)	243.8	304.8	456.6	609.6	640.1	670.6	853.4	893.1	967.7	990.6	1066.8	1158.2
SiO_2	69.30	69.40	68.56	68.47	67.77	68.49	69.90	66.63	70.43	69.90	70.70	68.90
TiO_2	0.80	0.85	0.96	0.95	0.92	0.81	0.68	0.65	0.70	0.67	0.79	0.69
Al_2O_3	12.50	12.50	13.07	12.65	13.11	12.86	12.70	13.39	12.59	12.70	12.60	13.10
Fe_2O_3T	5.90	6.10	5.19	6.22	6.51	5.88	6.30	7.29	5.39	6.30	5.30	6.10
Fe_2O_3	2.40	1.60	1.20	1.61	1.90	1.89	1.40	2.20	1.30	1.20	1.20	1.50
FeO	3.20	4.00	3.59	4.22	4.10	3.59	4.40	4.60	3.70	4.60	3.70	4.10
MnO	0.07	0.07	0.06	0.08	0.05	0.07	0.07	0.08	0.06	0.07	0.06	0.08
MgO	0.88	0.75	1.25	0.90	1.72	0.91	1.05	0.96	0.85	0.85	0.94	0.65
CaO	2.17	2.18	2.51	2.49	1.16	2.52	1.37	2.71	1.64	1.13	2.20	2.15
Na_2O	3.10	3.40	4.59	3.61	3.30	3.19	3.50	3.50	3.30	3.50	3.50	3.50
K_2O	3.85	3.70	2.47	3.21	3.87	4.00	3.40	3.38	4.04	3.92	3.61	3.66
H_2OT	1.20	1.20	1.20	1.41	1.70	1.20	1.40	1.50	1.20	1.30	1.10	1.40
CO_2T	0.80	0.10	0.10	0.20	0.10	0.10	0.30	0.20	0.10	0.10	0.10	0.30
P_2O_5	0.18	0.19	0.27	0.23	0.24	0.18	0.13	0.12	0.13	0.13	0.15	0.13
S	0.05	0.05	0.01	0.01	0.02	0.05	0.02	0.14	0.01	0.04	0.09	0.09
LoI	-	0.00	1.58	1.85	0.00	0.00	-	1.96	1.44	0.00	0.00	-
Total	100.50	100.49	101.82	102.30	100.48	100.26	100.40	102.50	101.87	100.61	101.14	100.30

Note: Sample = SUD-##-1994, SUD-1##-1995, SUD-2##-1997

Drill core 70011

sample	202	54	55	170	171	172	173	148	56	179	180
depth (m)	1219.2	1463.0	1493.5	1501.7	1502.4	1503.0	1503.6	1504.2	1524.0	1562.1	1566.7
SiO_2	70.50	69.40	67.90	67.27	67.10	67.57	67.00	66.63	65.70	62.20	61.40
TiO_2	0.66	0.66	0.80	0.84	0.90	0.95	0.89	0.94	1.06	1.38	1.46
Al_2O_3	12.50	12.80	13.20	13.11	13.00	13.11	13.12	12.76	13.50	13.60	13.60
Fe_2O_3T	5.50	5.40	6.40	7.01	7.30	6.91	7.06	7.64	8.00	9.50	10.20
Fe_2O_3	1.30	1.70	1.90	1.70	1.80	2.00	1.61	1.81	1.90	2.60	2.60
FeO	3.80	3.30	4.10	4.80	5.00	4.40	4.84	5.33	5.50	6.20	6.90
MnO	0.08	0.07	0.08	0.09	0.10	0.10	0.08	0.09	0.12	0.14	0.15
MgO	0.52	0.39	0.54	0.67	0.73	0.64	1.01	0.80	0.81	1.11	1.27
CaO	2.11	2.36	2.48	2.68	2.79	3.02	2.57	2.80	3.19	4.37	4.43
Na_2O	3.50	3.30	3.80	4.20	3.50	4.10	3.43	3.32	3.80	3.40	3.20
K_2O	3.98	3.99	3.41	2.91	3.44	2.66	3.46	3.57	2.82	2.45	2.46
H_2OT	1.30	1.30	1.40	1.40	1.30	1.10	1.61	1.71	1.60	1.90	2.00
CO_2T	0.10	0.30	0.30	0.10	0.10	0.10	0.10	0.10	0.20	0.40	0.60
P_2O_5	0.13	0.15	0.17	0.18	0.19	0.21	0.19	0.21	0.23	0.38	0.41
S	0.03	0.03	0.02	0.03	0.01	0.00	0.03	0.04	0.01	0.04	0.03
LoI	0.00	-	-	0.00	0.00	0.00	0.00	2.06	-	-	-
Total	100.91	99.80	100.10	100.50	100.46	100.48	100.57	102.68	100.40	100.20	100.50

Drill core 70011

sample	149	203	204	59	150	151	61	62	174	175	93
depth (m)	1615.4	1646.0	1661.2	1676.4	1723.6	1726.7	1752.6	1799.8	1810.5	1812.0	1813.6
SiO_2	56.79	53.90	53.80	55.40	56.32	56.85	58.40	59.00	59.22	59.32	58.10
TiO_2	1.82	1.85	1.85	1.38	1.15	0.99	0.54	0.58	0.59	0.59	0.67
Al_2O_3	13.37	13.20	13.70	14.70	14.73	15.28	15.90	15.80	15.63	15.75	16.60
Fe_2O_3T	11.88	14.20	14.10	12.40	10.65	10.12	7.50	7.60	7.62	6.78	6.70
Fe_2O_3	2.79	4.30	4.50	4.00	2.59	2.28	1.10	1.50	1.40	1.69	1.50
FeO	8.18	8.90	8.60	7.50	7.26	7.04	5.80	5.50	5.51	4.59	4.60
MnO	0.16	0.16	0.15	0.14	0.12	0.12	0.12	0.12	0.12	0.12	0.12
MgO	2.39	3.57	3.68	3.57	3.58	3.43	3.82	3.69	3.67	3.82	3.69
CaO	5.95	7.14	7.74	7.24	7.59	7.08	7.93	6.75	7.10	6.54	5.54
Na_2O	3.79	3.10	2.70	3.10	3.08	2.78	3.60	3.10	3.31	5.58	6.70
K_2O	2.13	1.64	1.63	1.68	1.46	2.07	1.21	1.97	1.71	0.55	0.37
H_2OT	1.80	1.90	2.00	1.90	1.79	1.79	1.40	1.60	1.50	1.30	1.60
CO_2T	0.10	0.10	0.10	0.00	0.10	0.10	0.20	0.40	0.10	0.00	0.40
P_2O_5	0.55	0.73	0.31	0.15	0.13	0.13	0.18	0.11	0.16	0.15	0.15
S	0.12	0.13	0.13	0.08	0.10	0.07	0.04	0.02	0.04	0.01	0.01
LoI	2.56	0.00	0.00	0.00	2.12	2.08	-	-	0.00	0.00	-
Total	103.39	101.62	101.89	101.74	102.93	102.89	100.20	100.10	100.77	100.51	100.10

Note: Sample = SUD-##-1994, SUD-1##-1995, SUD-2##-1997

Drill core 70011

sample	176	152	153	63	64	65	205	66	154	155	187
depth (m)	1816.6	1826.7	1831.8	1905.0	1920.2	2045.2	2164.1	2199.1	2249.4	2255.5	2257.3
SiO_2	59.54	54.94	59.34	58.50	58.30	57.50	58.30	59.40	59.04	52.15	52.50
TiO_2	0.56	0.59	0.65	0.67	0.50	0.48	0.63	0.44	0.60	0.54	0.54
Al_2O_3	15.66	15.25	16.28	16.40	16.00	17.40	16.40	16.90	15.88	15.72	15.00
Fe_2O_3T	7.33	8.18	7.19	7.70	7.80	7.30	7.20	6.90	7.49	10.31	10.80
Fe_2O_3	1.31	1.20	1.40	1.40	1.30	1.00	1.50	1.30	1.10	1.50	2.90
FeO	5.42	6.28	5.19	5.60	5.90	5.70	5.10	5.10	5.79	7.91	7.10
MnO	0.11	0.11	0.12	0.12	0.12	0.10	0.11	0.09	0.11	0.14	0.13
MgO	3.71	3.89	3.82	4.35	4.80	4.90	4.39	4.15	4.74	7.75	8.82
CaO	6.78	5.80	5.35	6.11	6.33	6.85	5.37	6.09	6.38	8.04	7.30
Na_2O	3.11	4.79	4.10	3.20	2.90	3.00	3.50	3.10	2.90	2.30	2.50
K_2O	1.88	0.78	1.38	1.23	1.58	1.33	1.91	1.92	1.74	1.58	1.07
H_2OT	1.61	2.79	1.90	2.20	1.80	1.60	2.10	1.40	1.50	2.00	2.00
CO_2T	0.10	3.39	0.30	0.40	0.80	0.30	0.10	0.20	0.10	0.20	0.20
P_2O_5	0.11	0.11	0.11	0.17	0.14	0.10	0.12	0.13	0.13	0.09	0.09
S	0.04	0.15	0.02	0.04	0.07	0.09	0.10	0.05	0.04	0.13	0.27
LoI	0.00	6.44	2.33	-	-	-	0.00	-	1.77	2.42	-
Total	100.54	107.20	102.89	100.40	100.50	100.40	100.23	100.30	102.42	103.37	100.40

Drill core 52847

sample	206	207	208	209	136	13	156	157	158	137	159
depth (m)	250	500	750	1000	3560	3720	3840	3860	3880	3900	3970
SiO_2	67.80	66.20	67.70	64.80	67.74	62.60	63.79	61.99	62.70	61.79	61.44
TiO_2	0.47	0.52	0.50	0.51	0.95	1.30	0.67	0.78	0.72	0.75	0.72
Al_2O_3	11.70	12.80	12.10	12.10	12.73	13.30	14.19	14.64	14.21	14.54	15.18
Fe_2O_3T	6.40	4.60	5.90	6.90	6.71	9.20	7.24	7.72	7.66	7.72	7.39
Fe_2O_3	0.70	0.50	1.00	1.50	1.50	2.80	1.49	1.91	1.61	1.91	1.20
FeO	5.10	3.70	4.40	4.90	4.71	5.80	5.16	5.32	5.44	5.32	5.59
MnO	0.10	0.08	0.07	0.12	0.08	0.12	0.10	0.10	0.11	0.11	0.11
MgO	4.36	4.01	3.74	4.03	0.85	1.56	2.40	2.52	2.44	2.58	3.30
CaO	2.81	3.25	3.01	3.86	2.46	4.77	4.55	5.54	5.13	5.25	4.57
Na_2O	4.00	5.00	3.50	3.30	3.31	3.40	3.67	3.31	3.33	3.31	5.09
K_2O	1.36	1.96	1.84	2.64	3.62	2.58	2.15	2.33	2.49	2.34	0.59
H_2OT	2.00	1.40	2.00	1.80	1.40	1.80	1.59	1.40	1.51	1.71	1.80
CO_2T	0.10	0.10	0.10	0.10	0.50	0.10	0.10	0.00	0.10	0.10	0.20
P_2O_5	0.11	0.13	0.12	0.13	0.20	0.45	0.21	0.18	0.20	0.24	0.20
S	0.01	0.00	0.14	0.39	0.03	0.01	0.01	0.07	0.04	0.05	0.00
LoI	0.00	0.00	0.00	0.00	2.13	0.00	0.00	0.00	0.00	0.00	0.00
Total	101.22	100.05	100.72	100.68	102.72	101.19	100.67	100.58	100.65	100.48	100.59

Note: Sample = SUD-##-1994, SUD-1##-1995, SUD-2##-1997

Drill core 52847

sample	138	139	22	210	26
depth (m)	4050	4070	4100	4300	4960
SiO_2	60.88	60.12	59.50	59.90	60.60
TiO_2	0.63	0.58	0.65	0.54	0.27
Al_2O_3	15.47	15.75	16.00	17.10	18.00
Fe_2O_3T	7.29	7.58	7.90	6.30	4.00
Fe_2O_3	1.40	1.30	1.60	1.80	1.10
FeO	5.29	5.68	5.60	4.00	2.60
MnO	0.11	0.12	0.13	0.10	0.05
MgO	3.24	3.46	3.84	3.58	3.96
CaO	5.66	5.84	6.01	6.35	4.26
Na_2O	3.09	2.99	2.90	3.70	5.40
K_2O	2.07	1.87	1.81	1.58	1.47
H_2OT	1.90	1.99	2.30	2.00	2.20
CO_2T	0.10	0.10	0.10	0.10	0.30
P_2O_5	0.11	0.15	0.16	0.10	0.06
S	0.03	0.04	0.03	0.01	0.02
LoI	2.14	2.28	0.00	0.00	0.00
Total	102.70	102.88	101.33	101.36	100.59

Drill core 52848

sample	211	212	213	214	215	37	44	160	161	162	163
depth (m)	500	1500	2500	3000	3500	4096	4375	4500	4575	4640	4646
SiO_2	68.80	69.80	69.50	69.20	57.90	66.60	67.10	56.00	53.58	53.21	68.64
TiO_2	0.80	0.68	0.72	0.77	1.20	1.35	0.92	1.96	2.91	2.64	0.82
Al_2O_3	12.90	12.70	12.80	12.90	14.70	12.60	14.00	14.20	13.60	12.93	13.63
Fe_2O_3T	5.50	6.00	6.20	6.30	10.00	6.70	6.00	11.00	12.29	13.03	4.91
Fe_2O_3	2.40	2.00	1.80	2.00	3.70	1.30	1.70	2.70	2.92	2.30	1.00
FeO	2.80	3.60	4.00	3.90	5.70	4.90	3.90	7.50	8.36	9.62	3.51
MnO	0.08	0.09	0.08	0.08	0.18	0.10	0.08	0.13	0.15	0.18	0.06
MgO	0.65	0.51	0.59	0.41	0.95	1.37	1.19	2.78	3.24	3.84	1.22
CaO	3.15	1.68	2.09	2.10	2.41	2.93	2.74	7.03	6.88	6.06	2.60
Na_2O	3.30	3.40	3.50	3.80	5.80	4.30	4.10	3.20	3.12	3.91	3.81
K_2O	3.90	4.29	3.93	3.69	3.46	3.23	3.37	1.76	1.89	1.30	3.45
H_2OT	1.10	1.30	1.30	1.10	2.50	1.00	1.10	1.70	1.71	2.10	1.00
CO_2T	0.00	0.10	0.10	0.10	1.20	0.20	0.20	0.40	0.00	0.20	0.10
P_2O_5	0.16	0.13	0.14	0.15	0.31	0.37	0.19	1.08	1.36	1.56	0.16
S	0.05	0.01	0.03	0.00	0.01	0.01	0.01	0.07	0.10	0.20	0.04
LoI	0.00	0.00	0.00	0.00	0.00	0.00	0.00	0.00	0.00	0.00	0.00
Total	100.39	100.69	100.98	100.60	100.62	100.76	101.00	100.40	100.83	101.15	100.43

Note: Sample = SUD-##-1994, SUD-1##-1995, SUD-2##-1997

Drill core 52848

sample	164	165	166g3	166g2	166g1	166q1	166q2	140	216	217	45
depth (m)	4650	4663	4677.1	4677.2	4677.3	4677.4	4677.5	4700	4800	4900	5005
SiO_2	66.57	67.30	68.37	62.34	61.64	51.30	52.00	52.63	52.90	54.80	53.00
TiO_2	1.20	1.04	0.95	1.81	1.81	3.43	3.28	2.93	2.98	2.15	2.57
Al_2O_3	13.57	13.24	13.11	13.39	13.49	13.43	13.60	13.01	13.20	14.40	13.30
Fe_2O_3T	6.49	6.42	4.40	7.59	7.89	14.03	13.50	13.31	13.20	11.60	13.50
Fe_2O_3	1.60	2.51	1.40	1.80	2.00	3.71	3.40	9.24	3.70	3.00	3.70
FeO	4.39	3.51	2.70	5.19	5.29	9.32	9.10	3.67	8.60	7.70	8.80
MnO	0.07	0.06	0.05	0.11	0.10	0.21	0.21	0.16	0.18	0.15	0.16
MgO	1.12	1.11	1.34	2.33	2.36	3.63	3.55	3.55	3.78	3.70	4.01
CaO	2.69	3.34	4.25	4.91	4.89	6.81	6.60	7.30	7.79	7.09	7.53
Na_2O	4.39	5.52	5.01	5.00	4.80	3.21	3.20	2.98	2.90	3.10	2.80
K_20	3.12	1.12	1.44	1.29	1.39	1.42	1.54	1.43	1.27	1.70	1.48
H_2OT	0.90	0.80	0.70	1.00	1.30	1.90	2.00	1.69	1.70	1.60	1.60
CO_2T	0.10	0.10	0.40	0.10	0.10	0.10	0.10	0.20	0.10	0.10	0.10
P_2O_5	0.28	0.34	0.27	0.60	0.65	1.44	1.34	1.12	1.28	0.88	1.17
S	0.06	0.00	0.02	0.11	0.11	0.17	0.13	0.11	0.14	0.10	0.12
LoI	0.00	0.00	0.00	0.00	0.00	0.00	0.00	3.12	0.00	0.00	0.00
Total	100.56	100.40	100.32	100.56	100.51	101.08	101.05	103.53	101.42	101.37	101.34

Drill core 52848

sample	141	142	47	218	219	48	49	220	221	222	223
depth (m)	5150	5375	5510	6000	6500	6910	7285	7550	7750	8050	8350
SiO_2	52.18	51.24	52.50	51.10	52.40	45.00	54.80	57.10	56.60	56.80	56.30
TiO_2	3.13	2.89	3.19	2.66	1.74	4.16	0.77	0.47	0.44	0.43	0.38
Al_2O_3	13.39	13.80	13.50	14.80	16.30	13.70	6.00	17.60	17.50	17.90	18.30
Fe_2O_3T	13.39	13.51	13.60	13.30	12.00	17.00	16.70	7.40	7.20	7.20	6.80
Fe_2O_3	5.46	10.03	3.50	3.90	3.80	5.80	4.70	1.00	0.80	1.10	1.10
FeO	7.14	3.18	9.10	8.50	7.40	10.10	10.80	5.70	5.80	5.50	5.20
MnO	0.18	0.16	0.17	0.15	0.13	0.18	0.18	0.12	0.12	0.12	0.11
MgO	3.72	3.84	3.86	4.14	4.29	5.46	13.01	5.40	5.70	5.90	5.77
CaO	7.60	8.13	7.89	8.62	8.89	10.26	4.87	7.34	7.32	7.41	7.63
Na_2O	2.88	2.88	2.90	2.90	2.80	2.50	0.40	2.90	2.90	2.80	2.90
K_2O	1.31	1.23	1.36	1.04	1.13	0.54	1.24	1.16	1.06	1.14	1.11
H_2OT	1.39	1.19	1.40	1.10	1.20	0.70	3.30	1.30	1.20	1.20	1.10
CO_2T	0.20	0.10	0.10	0.10	0.10	0.10	0.10	0.10	0.20	0.10	0.10
P_2O_5	1.17	1.18	1.32	1.36	0.32	1.67	0.12	0.09	0.04	0.09	0.07
S	0.13	0.11	0.10	0.12	0.14	0.16	0.11	0.08	0.06	0.07	0.06
LoI	2.89	2.58	0.00	0.00	0.00	0.00	0.00	0.00	0.00	0.00	0.00
Total	103.56	102.85	101.89	101.39	101.44	101.43	101.60	101.06	100.34	101.16	100.63

Note: Sample = SUD-##-1994, SUD-1##-1995, SUD-2##-1997

Duplicates sample	145	151	154	173	174	175	140	161	162	163	164	165
depth (m)	2000	5665	7380	4933	5940	5945	4700	4575	4640	4646	4650	4663
SiO_2	68.90	56.10	59.40	66.20	58.60	58.60	54.10	53.40	52.80	67.80	66.20	67.80
TiO_2	0.82	1.03	0.58	0.91	0.59	0.63	2.75	2.72	2.32	0.76	1.17	0.92
Al_2O_3	12.90	15.40	16.00	13.30	15.70	16.00	13.50	13.60	12.40	13.50	13.50	13.80
Fe_2O_3T	5.90	9.90	7.40	7.10	7.70	6.90	12.50	12.10	14.10	4.90	6.50	6.20
Fe_2O_3	1.80	2.40	1.00	1.60	1.40	1.60	3.20	2.90	2.80	0.90	1.60	2.50
FeO	3.70	6.80	5.70	5.00	5.70	4.80	8.40	8.30	10.20	3.60	4.40	3.30
MnO	0.07	0.12	0.11	0.09	0.12	0.13	0.15	0.15	0.16	0.06	0.08	0.06
MgO	0.90	3.47	4.67	0.73	3.75	3.86	3.32	3.32	4.08	1.34	1.07	1.13
CaO	2.67	7.24	6.38	2.85	7.13	6.28	7.14	6.85	6.15	2.52	2.50	3.33
Na_2O	3.40	2.90	2.90	3.40	3.10	5.50	3.10	3.10	3.50	3.70	4.40	5.80
K_20	3.20	1.96	1.72	3.42	1.68	0.81	1.52	1.90	1.40	3.56	3.01	1.04
H_2OT	1.40	1.90	1.40	1.60	1.70	1.50	1.70	1.90	2.40	1.20	1.00	0.90
CO_2T	0.20	0.10	0.10	0.30	0.30	0.30	0.10	0.30	0.30	0.30	0.20	0.30
P_2O_5	0.20	0.14	0.14	0.20	0.21	0.20	1.11	1.29	1.57	0.15	0.27	0.35
S	0.01	0.06	0.04	0.03	0.06	0.01	0.09	0.08	0.28	0.04	0.04	0.00
LoI	-999.00	-999.00	-999.00	-999.00	-999.00	-999.00	-999.00	-999.00	-999.00	-999.00	-999.00	-999.00
Total	100.10	99.60	100.20	99.60	100.00	100.20	100.10	99.80	100.30	99.50	99.40	i01.20

Note: Sample = SUD-##-1994, SUD-1##-1995, SUD-2##-1997

Drill core 70011														
sample	189	191	193	195	83	143a	143b	177	178	197	198	199	50	200
depth (m)	15.2	45.7	76.2	79.2	82.3	83.9	83.9	89.9	93.0	121.9	152.4	182.9	243.8	304.8
Ba	710	590	1100	140	410	510	1200	1600	550	1200	1100	1200	1100	1000
Be	1.3	1.3	1.1	1.3	1.1	1	1.3	1.3	2	1.9	1.8	1.7	2	1.9
Co	41	18	10	10	6	6	8	-5	6	11	12	12	12	13
Cr	110	100	53	35	12	27	40	-10	-10	-10	-10	-10	12	-10
Cu	170	39	13	-10	-10	-10	-10	-10	-10	-10	-10	-10	-10	15
Ni	160	80	31	24	110	17	29	-10	-10	-10	-10	-10	-10	-10
Sc	12	11	5.8	5.2	1.1	2.2	5.1	0.9	7.4	12	12	12	12	13
Sr	200	120	270	170	490	560	390	590	280	180	170	180	170	200
V	110	86	38	35	16	28	38	7	21	63	70	69	62	77
Zn	11	13	17	15	10	23	26	9	36	29	31	38	34	39
Ce	52	40	62	68	32	36	64	26	95	100	100	110	100	110
Dy	2.7	2.6	1.6	1.8	0.45	0.86	1.6	0.6	4.3	4.7	4.7	4.2	5	4.9
Er	1.5	1.3	0.75	0.9	0.15	0.27	0.71	0.3	2.5	2.4	2.4	2.2	2.4	2.6
Eu	0.52	0.75	0.55	1.1	1	1.1	0.79	0.31	1.2	0.69	0.74	0.76	0.88	0.91
Gd	3.6	3.1	2.3	3	0.68	1.3	2.3	0.68	5	5.9	5.9	5.5	5.6	6
Ho	0.54	0.49	0.28	0.35	0.08	0.14	0.3	0.11	0.91	0.96	0.95	0.87	0.94	1
La	24	20	34	35	19	19	33	16	48	49	51	51	52	51
Lu	0.26	0.22	0.13	0.16	0.04	0.05	0.13	0.07	0.41	0.38	0.37	0.38	0.38	0.39
Nd	24	20	23	28	9.9	14	24	8.7	39	43	42	44	43	45
Pr	6.2	5.1	6.7	7.5	3	3.6	6.4	2.5	11	11	11	11	12	11
Sm	4.2	3.7	3.4	4.1	1.2	2.1	3.7	1.2	6.7	7.4	7.3	6.9	7.2	7.6
Tb	0.5	0.43	0.29	0.34	0.08	0.14	0.28	0.09	0.71	0.8	0.81	0.8	0.78	0.84
Tm	0.23	0.2	0.12	0.14	0.03	0.05	0.13	0.05	0.4	0.38	0.37	0.32	0.38	0.38
Y	19	16	8.9	11	2.4	4.2	9.2	3.9	28	29	28	26	30	29
Yb	1.7	1.5	0.86	1	0.18	0.26	0.79	0.37	2.6	2.6	2.7	2.3	2.5	2.6
Ag	-0.1	-0.1	-0.1	0.1	-0.1	2.2	-0.1	0.2	0.2	-0.1	0.1	0.2	0.2	-0.1
Bi	-0.5	-0.5	-0.5	-0.5	0.7	0.7	0.6	0.6	0.8	-0.5	-0.5	-0.5	0.8	-0.5
Cd	-0.2	-0.2	-0.2	-0.2	-0.2	-0.2	-0.2	-0.2	-0.2	-0.2	-0.2	-0.2	-0.2	-0.2
Cs	0.3	0.22	0.35	0.12	0.22	0.12	0.46	0.6	0.17	0.62	0.49	0.81	0.49	0.65
Ga	15	14	14	13	16	19	17	12	17	16	17	16	18	17
Hf	3.7	3.5	3.8	4.2	2.6	2.5	3.8	3.3	7.3	6.3	6.3	6	6.2	6.3
In	-0.05	-0.05	-0.05	-0.05	-0.05	-0.05	-0.05	-0.05	-0.05	-0.05	-0.05	-0.05	-0.05	-0.05
Mo	5.6	3.6	0.8	-0.2	0.9	-0.2	0.5	-0.2	0.2	1	1.6	1.8	2	1.6
Nb	7.8	6.5	3.6	3.9	1.4	1.8	3.6	1.5	12	13	12	12	13	12
Pb	6	2	-2	21	-2	3	3	3	4	4	5	3	7	5
Rb	53	53	60	8.1	20	25	73	60	38	94	96	130	130	96
Sn	1.6	1.9	1.2	3	-	-	-	-	-	0.6	1.7	1.8	-	3.4
Ta	0.5	0.4	-0.2	-0.2	-0.2	-0.2	0.2	-0.2	0.8	0.8	0.8	0.8	0.8	0.8
Th	7.3	8	7	8.4	0.26	0.54	5	1.1	16	13	13	12	13	13
Tl	0.28	0.3	0.32	0.07	0.04	0.06	0.34	0.22	0.15	0.46	0.55	0.7	0.42	0.5
U	2.4	2	1.2	1.2	0.36	0.37	1.1	0.42	4.4	3.3	3.3	3	3.1	3.3
Zr	150	150	160	170	100	100	150	120	310	260	260	240	250	250

Note: Sample = SUD-##-1994, SUD-1##-1995, SUD-2##-1997

Drill core 70011												
sample	144	145	167	168	52	146	147	169	201	53	202	54
depth (m)	456.6	609.6	640.1	670.6	853.4	893.1	967.7	990.6	1066.8	1158.2	1219.2	1463.0
Ba	660	880	1000	1200	1100	850	1100	1200	1100	950	1000	1000
Be	1.9	2	2.1	2.2	2.2	2	1.8	2.1	2.7	2	2.1	2.3
Co	46	39	9	7	13	31	34	6	10	13	10	9
Cr	21	25	15	11	12	29	16	10	-10	13	-10	12
Cu	<10	<10	<10	10	-10	<10	<10	10	-10	-10	-10	-10
Ni	13	17	<10	<10	-10	23	11	<10	-10	-10	-10	-10
Sc	14	12	14	12	10	9.4	10	10	12	10	10	12
Sr	240	180	110	170	110	270	140	120	180	150	170	160
V	110	63	54	39	15	30	27	10	8	10	7	-5
Zn	8	22	39	31	63	43	23	51	52	56	56	73
Ce	98	94	120	120	140	150	110	140	140	87	110	110
Dy	5.7	5	5.4	5.4	7	7.8	5.2	6.3	6.1	5.7	5.9	6.1
Er	3.2	3	3.2	3.2	3.7	4.4	3.1	3.6	3.2	3.2	3.2	3.3
Eu	1.8	1.6	1.3	1.3	1.3	2.3	1.6	1.2	1.2	1.4	1	1.3
Gd	7	6	6.9	6.9	7.8	9.5	6.7	7.8	7.7	5.9	6.9	6.9
Ho	1.2	1.1	1.2	1.3	1.4	1.6	1.1	1.3	1.2	1.1	1.2	1.2
La	45	50	56	62	78	83	54	67	71	45	55	56
Lu	0.48	0.46	0.53	0.54	0.59	0.66	0.48	0.53	0.54	0.5	0.5	0.5
Nd	48	41	48	49	59	66	44	58	59	40	47	50
Pr	12	11	13	14	16	18	12	16	16	10	12	13
Sm	8.9	7.4	9	9.4	10	12	8.1	10	9.5	7.1	7.9	8.6
Tb	1.1	0.94	0.95	0.97	1.2	1.6	0.97	1.1	1.1	0.92	0.96	1
Tm	0.49	0.45	0.51	0.51	0.59	0.67	0.46	0.57	0.5	0.48	0.49	0.52
Y	33	30	36	37	40	48	30	40	36	35	37	37
Yb	3	3	3.4	3.3	4	4.3	3.1	3.7	3.4	3.3	3.4	3.5
Ag	0.1	0.2	0.7	0.9	0.4	0.2	0.1	0.8	-0.1	1	-0.1	0.1
Bi	<0.5	<0.5	<0.5	<0.5	0.8	<0.5	<0.5	0.5	-0.5	0.7	-0.5	0.6
Cd	<0.2	<0.2	<0.2	<0.2	-0.2	<0.2	<0.2	<0.2	-0.2	-0.2	-0.2	-0.2
Cs	0.34	0.45	3	0.62	0.54	0.64	0.37	0.48	0.34	0.79	0.92	0.81
Ga	18	17	18	19	19	23	17	19	18	19	18	19
Hf	6.1	5.9	7.9	7.9	9.1	9.2	7	8.5	7.8	6.9	8.1	7
In	0.07	0.06	<0.05	<0.05	0.06	0.1	<0.5	0.05	0.06	-0.05	0.05	0.09
Mo	2.3	3.7	2.7	1.4	1.1	5	4.4	2.1	1.1	2.5	1.4	1.8
Nb	15	16	17	16	18	19	16	17	16	15	16	16
Pb	28	35	4	7	10	6	6	10	13	11	14	10
Rb	60	78	140	120	120	140	120	130	95	95	85	76
Sn	7.9	4.7	2.4	1.8	-	3.3	2	5.1	1.6	-	4.5	-
Ta	2.3	2.1	0.9	0.8	1	1.9	2	0.8	1	0.8	0.9	0.8
Th	14	12	15	17	18	23	15	19	15	13	15	14
Tl	0.23	0.27	0.54	0.43	0.35	0.53	0.45	0.66	0.42	0.35	0.33	0.18
U	2.6	2.7	3.5	3.6	4.3	4.8	3.2	3.9	3.4	3	3.6	3.3
Zr	280	270	310	330	380	430	310	370	310	300	330	300

Note: Sample = SUD-##-1994, SUD-1##-1995, SUD-2##-1997

Drill core 70011											
sample	55	170	171	172	173	148	56	179	180	149	203
depth (m)	1493.5	1501.7	1502.4	1503.0	1503.6	1504.2	1524.0	1562.1	1566.7	1615.4	1646.0
Ba	940	800	1100	810	880	950	880	950	860	780	500
Be	2.5	2.1	2.3	2	2.1	1.8	2.1	1.8	1.9	1.4	1.1
Co	10	6	7	6	8	31	18	20	21	44	58
Cr	13	<10	<10	10	<10	17	16	17	19	21	10
Cu	-10	<10	<10	<10	<10	<10	-10	-10	-10	22	22
Ni	-10	<10	<10	<10	<10	14	-10	-10	-10	14	-10
Sc	14	14	15	16	14	16	17	21	22	24	31
Sr	170	180	180	210	180	210	180	300	300	370	340
V	5	9	9	11	10	32	14	26	28	460	710
Zn	60	78	63	46	45	43	74	82	94	69	86
Ce	110	140	120	130	130	130	130	100	110	88	77
Dy	5.8	6.4	6.4	6.2	6.2	6.3	6.1	5.8	6.3	5	4.6
Er	3.1	3.7	3.3	3.3	3.3	3.5	3.1	3	3.3	2.7	2.4
Eu	1.5	2.1	1.5	1.7	1.7	2	2	2	2.2	2.1	1.5
Gd	6.5	7.5	8.1	7.8	8	8	7.1	6.8	7.8	6.4	6.1
Ho	1.2	1.3	1.3	1.3	1.3	1.3	1.2	1.1	1.2	1	0.91
La	54	64	60	59	62	64	67	50	56	45	35
Lu	0.51	0.54	0.56	0 56	0.49	0.53	0.52	0.41	0.48	0.38	0.33
Nd	50	55	51	53	54	54	56	48	53	42	38
Pr	13	15	14	14	15	14	15	12	14	11	8.9
Sm	8.6	10	10	10	10	9.7	9.1	9.2	10	7.5	7.2
Tb	0.96	1	1.1	1	1	1.2	1.1	1	1.1	0.95	0.79
Tm	0.51	0.55	0.55	0.51	0.5	0.52	0.52	0.47	0.5	0.38	0.33
Y	34	39	39	39	38	37	37	34	37	28	27
Yb	3.2	3.7	3.6	3.5	3.1	3.4	3.4	3	3.2	2.4	2.1
Ag	0.3	0.8	1	0.5	3.3	1.2	0.2	0.2	1	0.1	-0.1
Bi	0.8	<0.5	<0.5	<0.5	<0.5	<0.5	0.7	0.5	0.7	0.6	-0.5
Cd	-0.2	<0.2	<0.2	<0.2	<0.2	<0.2	-0.2	-0.2	-0.2	<0.2	-0.2
Cs	0.86	1.1	1.1	0.92	1.2	1.1	1.1	1.5	1.7	1.4	0.89
Ga	18	20	18	21	19	19	18	19	19	20	20
Hf	6.4	7.8	7.8	7.1	6.8	6.6	6.9	5.2	6	4	3.3
In	-0.05	<0.05	<0.05	0.06	<0.05	0.06	0.06	-0.05	0.11	0.07	-0.05
Mo	1.5	1.4	1.4	2.4	2.3	4.3	1.3	1.9	2	3.2	0.8
Nb	16	17	16	19	18	18	17	15	16	11	7.4
Pb	8	10	10	10	8	10	9	10	15	8	3
Rb	68	87	92	65	97	90	62	91	130	130	60
Sn	-	1.9	2.4	3.8	3.9	12	-	-	-	4.6	1.3
Ta	0.8	0.9	0.8	0.7	0.5	1.8	0.9	0.8	0.9	1	0.4
Th	12	15	15	14	14	15	13	9.9	11	8.2	5.8
Tl	0.21	0.49	0.53	0.31	0.55	0.4	0.16	0.43	0.6	0.66	0.38
U	2.8	3.3	3.3	3.1	2.9	3.1	3.1	2.4	2.6	1.7	1.3
Zr	260	330	330	300	290	310	280	210	230	170	120

Note: Sample = SUD-##-1994, SUD-1##-1995, SUD-2##-1997

Drill core 70011											
sample	204	59	150	151	61	62	174	175	93	176	152
depth (m)	1661.2	1676.4	1723.6	1726.7	1752.6	1799.8	1810.5	1812.0	1813.6	1816.6	1826.7
Ba	490	700	450	660	460	640	560	250	160	620	260
Be	1	1.1	1	1.1	1.2	1.3	1.2	1.3	1.2	1.3	0.7
Co	57	48	50	42	32	29	23	20	24	23	30
Cr	-10	-10	28	25	20	27	32	31	29	33	49
Cu	26	13	17	<10	-10	-10	13	<10	-10	11	12
Ni	-10	-10	16	11	-10	-10	<10	<10	-10	<10	22
Sc	33	29	27	26	25	23	21	22	22	22	15
Sr	370	400	390	400	380	380	370	350	320	380	200
V	820	750	700	670	140	130	140	150	130	140	130
Zn	88	74	36	38	42	50	56	43	38	48	81
Ce	59	56	57	56	61	61	69	59	62	60	58
Dy	3.6	3.2	3.3	3.3	3.8	3.6	3.7	3.4	3.8	3.3	2.9
Er	1.9	1.7	1.9	1.9	2	2	2.1	2	2	1.9	1.7
Eu	1.3	1	1.3	1.3	1.5	1.3	1.3	1.4	1.6	1.1	1.3
Gd	4.7	3.8	4.1	3.9	4.2	3.8	4.4	4.3	4.6	3.9	3.6
Ho	0.71	0.63	0.7	0.66	0.75	0.74	0.77	0.76	0.78	0.72	0.61
La	28	27	29	28	28	30	35	27	30	30	30
Lu	0.3	0.26	0.28	0.28	0.29	0.29	0.31	0.3	0.31	0.29	0.26
Nd	27	25	25	25	28	26	30	25	27	24	25
Pr	6.6	6.5	6.7	6.6	7	7	7.9	6.8	6.7	6.5	6.7
Sm	5.1	4.5	4.8	4.6	5.5	4.9	5.7	5	5.3	4.9	4.1
Tb	0.62	0.58	0.62	0.6	0.62	0.61	0.62	0.54	0.64	0.55	0.54
Tm	0.27	0.27	0.28	0.28	0.29	0.3	0.32	0.32	0.31	0.28	0.25
Y	22	21	19	19	21	21	24	23	20	21	17
Yb	1.9	1.7	1.8	1.8	2	1.9	2.1	2	2	1.9	1.6
Ag	-0.1	0.1	<0.1	0.2	0.6	0.4	1.6	0.5	0.3	1.9	0.3
Bi	-0.5	-0.5	<0.5	0.6	1	0.6	<0.5	<0.5	0.6	<0.5	0.8
Cd	-0.2	-0.2	<0.2	<0.2	-0.2	-0.2	<0.2	<0.2	-0.2	<0.2	<0.2
Cs	0.79	0.81	0.67	1	0.25	0.3	0.3	0.12	0.08	0.22	0.31
Ga	20	22	20	20	20	20	22	20	17	20	18
Hf	3.1	3	3.4	3	3.7	3.9	4.3	4.2	4	3.9	3
In	-0.05	-0.05	0.05	0.08	-0.05	0.05	<0.05	<0.05	-0.05	<0.05	<0.5
Mo	0.6	0.6	2.9	1.9	0.5	0.7	1.5	0.6	0.3	1	2.9
Nb	6.7	6.7	7.3	6.8	6.4	7.8	8.3	8	7.8	7.6	7.5
Pb	3	3	6	6	7	7	10	8	7	11	6
Rb	54	66	55	86	40	60	56	20	12	58	24
Sn	2.7	1.5	4.1	13	-	-	1.3	1.7	-	2	2.8
Ta	0.4	0.4	1	0.8	0.3	0.4	<0.2	0.3	0.4	0.4	0.8
Th	5.2	5.5	6.3	6	6.2	7.2	7.4	7.7	7	7.2	6.8
Tl	0.34	0.38	0.31	0.43	0.13	0.22	0.28	0.13	-0.02	0.25	0.14
U	1.2	1.2	1.4	1.3	1.5	1.7	1.7	1.6	1.6	1.6	1.5
Zr	120	120	120	110	120	140	140	140	140	140	130

Note: Sample = SUD-##-1994, SUD-1##-1995, SUD-2##-1997

Drill core 70011									
sample	153	63	64	65	205	66	154	155	187
depth (m)	1831.8	1905.0	1920.2	2045.2	2164.1	2199.1	2249.4	2255.5	2257.3
Ba	610	480	480	460	810	570	510	490	440
Be	1.4	1.3	1.2	1.1	1.1	1.2	1.1	0.5	0.6
Co	28	35	32	32	32	28	32	47	49
Cr	45	45	54	78	74	74	160	270	630
Cu	<10	10	13	20	28	11	12	40	150
Ni	18	10	11	17	20	13	39	220	270
Sc	15	15	17	16	16	14	16	19	20
Sr	440	380	350	380	410	360	410	410	370
V	140	110	110	91	100	88	120	150	140
Zn	52	63	82	73	70	49	51	69	81
Ce	61	60	56	51	53	61	61	30	31
Dy	3	3.4	3.3	2.8	2.7	3.2	3	1.8	1.4
Er	1.8	1.7	1.8	1.6	1.4	1.8	1.7	1	0.74
Eu	1.4	1.2	1.2	1.3	0.66	1.3	1.3	1	0.76
Gd	3.6	3.8	3.8	3	3.4	3.6	3.9	2.2	1.5
Ho	0.66	0.64	0.64	0.58	0.55	0.67	0.62	0.38	0.28
La	32	30	28	24	27	30	32	15	17
Lu	0.3	0.27	0.26	0.25	0.23	0.29	0.28	0.17	0.13
Nd	25	27	24	20	23	24	26	14	13
Pr	7	6.8	6.1	5.3	5.8	6.4	7	3.5	3.4
Sm	4.2	4.7	4.3	3.9	4.2	4.5	4.4	2.5	2.3
Tb	0.57	0.54	0.57	0.48	0.46	0.54	0.59	0.32	0.24
Tm	0.28	0.27	0.27	0.24	0.22	0.28	0.26	0.17	0.12
Y	18	19	18	16	18	19	17	10	8.5
Yb	1.9	1.8	1.8	1.6	1.7	2	1.7	1	0.88
Ag	0.2	0.4	0.5	0.3	-0.1	0.7	0.2	0.2	1.1
Bi	<0.5	0.9	0.5	0.9	-0.5	0.6	0.7	1.3	0.5
Cd	<0.2	-0.2	-0.2	0.2	-0.2	-0.2	<0.2	<0.2	-0.2
Cs	0.45	0.58	1.4	1.3	0.42	1.7	1.4	1.8	1.4
Ga	19	19	18	19	18	19	18	17	17
Hf	6.2	3.9	3.3	3.7	3.1	5.2	4.2	1.8	1.6
In	0.06	-0.05	0.07	-0.05	-0.05	-0.05	<0.5	0.06	0.06
Mo	2.2	1.5	1	1.1	0.2	0.7	3.9	2.7	0.6
Nb	8.5	8.4	6.3	6.1	7.6	5.7	7.5	2.7	2.3
Pb	6	8	8	10	9	8	8	5	10
Rb	53	34	63	43	45	67	61	50	31
Sn	2.1	-	-	-	2.8	-	37	13	-
Ta	0.8	0.6	0.3	0.3	0.5	0.3	0.9	0.6	-0.2
Th	7.1	6.9	6.2	5.8	6.1	7.4	7	1.8	2.2
Tl	0.25	0.13	0.32	0.17	0.18	0.25	0.26	0.29	0.22
U	1.6	1.7	1.5	1.4	1.4	1.9	1.5	0.42	0.36
Zr	140	130	120	120	130	210	140	70	74

Note: Sample = SUD-##-1994, SUD-1##-1995, SUD-2##-1997

Drill core 52847

sample	206	207	208	209	136	13	156	157	158	137	159	138	139	22	210	26
depth (m)	250	500	750	1000	3560	3720	3840	3860	3880	3900	3970	4050	4070	4100	4300	4960
Ba	320	320	720	730	1100	770	820	740	730	780	290	570	610	610	500	320
Be	1.4	1.4	1.2	1.4	2	1.7	1.8	1.5	1.6	1.5	1.8	1.3	1.2	1.3	1.2	0.7
Co	19	18	19	22	28	26	16	20	17	19	20	34	36	29	17	11
Cr	110	110	110	120	20	-10	17	17	18	19	28	37	41	27	35	110
Cu	13	-10	34	45	<10	-10	<10	16	12	13	<10	<10	13	17	10	-10
Ni	58	57	56	66	17	-10	<10	<10	<10	<10	<10	14	16	10	13	35
Sc	11	12	12	13	13	19	19	21	20	21	21	15	14	16	15	6.9
Sr	110	55	380	270	180	260	260	280	270	280	220	380	420	380	430	350
V	100	100	100	120	54	200	180	190	160	170	160	120	110	120	97	31
Zn	17	8	14	45	33	58	88	110	75	130	77	42	77	91	43	43
Ce	53	27	45	53	110	110	99	82	95	86	88	63	66	71	57	24
Dy	2.8	2.6	2.6	3.2	5.9	5.3	4.5	4.3	4.5	4.2	4.1	3.2	3.3	3.5	2.8	0.8
Er	1.6	1.4	1.5	1.7	3.3	2.8	2.6	2.4	2.5	2.4	2.4	1.7	1.8	1.8	1.5	0.35
Eu	0.79	0.75	0.48	0.55	2	1.4	0.91	1.2	1.1	1.3	1.4	1.3	1.4	1	1	0.84
Gd	3.3	3.2	3.3	4.2	7	7.1	5.5	5.3	5.3	5.2	4.8	3.7	4	4.1	3.3	1.3
Ho	0.58	0.55	0.51	0.66	1.2	1.1	0.93	0.92	0.92	0.85	0.87	0.66	0.69	0.7	0.56	0.15
La	26	11	22	26	58	53	50	41	48	42	45	33	34	36	29	12
Lu	0.24	0.25	0.24	0.29	0.54	0.43	0.41	0.37	0.41	0.36	0.36	0.29	0.3	0.28	0.24	0.06
Nd	22	16	20	24	49	46	41	34	39	36	37	27	29	30	24	11
Pr	5.9	3.7	5.1	6.2	13	12	11	9.3	11	9.9	10	7.3	7.5	8.4	6.2	2.9
Sm	3.8	3.5	3.6	4.7	9	8.1	7.7	6.8	7.6	6.6	6.7	4.7	5.1	5	4	1.7
Tb	0.45	0.44	0.47	0.56	1.1	0.92	0.76	0.74	0.73	0.73	0.72	0.59	0.64	0.61	0.46	0.16
Tm	0.22	0.23	0.22	0.26	0.51	0.45	0.4	0.39	0.41	0.37	0.36	0.28	0.28	0.28	0.22	0.05
Y	19	17	17	21	35	34	29	27	29	28	28	18	20	21	18	4.1
Yb	1.6	1.6	1.5	1.9	3.3	2.9	2.6	2.5	2.6	2.2	2.4	1.8	1.8	1.9	1.7	0.35
Ag	-0.1	0.1	0.1	-0.1	<0.1	0.2	0.5	4.4	4.8	0.5	1.2	0.2	0.3	-0.1	0.2	-0.1
Bi	-0.5	-0.5	-0.5	-0.5	<0.5	-0.5	0.5	0.6	0.6	<0.5	0.6	0.6	0.7	-0.5	-0.5	-0.5
Cd	-0.2	-0.2	-0.2	-0.2	0.3	-0.2	<0.2	<0.2	<0.2	<0.2	<0.2	<0.2	<0.2	-0.2	-0.2	-0.2
Cs	0.28	0.14	0.3	0.28	0.93	1.2	0.34	0.38	0.42	0.45	0.34	0.43	0.88	0.77	0.63	0.52
Ga	14	14	13	14	20	20	19	19	20	19	20	19	19	20	20	18
Hf	3.4	3.6	3.5	3.5	7	5.7	5.2	4.9	5.5	4.3	4.5	4	4.1	3.6	3.4	1.8
In	-0.1	-0.1	-0.1	-0.1	<0.5	0.06	0.05	<0.05	<0.05	0.05	<0.05	0.06	<0.5	-0.1	0.06	-0.1
Mo	4.4	0.4	5.9	4.8	3.2	2	1.3	1.7	1.4	1.7	1.3	1.9	2.8	0.8	1.2	-0.2
Nb	7.6	8.8	7.7	8.2	17	13	11	10	11	10	11	8.7	8.3	8.5	7	1.8
Pb	-2	-2	-2	8	12	12	9	8	12	17	13	34	38	13	8	8
Rb	56	75	72	83	110	82	62	77	83	81	26	62	63	55	46	50
Sn	-0.5	1.7	-0.5	0.5	2.2	2.4	1.6	7.5	3.1	1.7	17	4.8	2.9	1.4	3.1	1.5
Ta	0.5	0.6	0.5	0.6	1.6	0.7	0.6	0.5	0.5	0.5	0.5	1	0.9	0.5	0.4	-0.2
Th	7.4	7.6	7.9	8	15	11	11	9.8	11	9	9.8	8.4	7.8	6.8	6.5	0.57
Tl	0.28	0.37	0.41	0.37	0.4	0.39	0.3	0.36	0.42	0.38	0.13	0.3	0.34	0.31	0.18	0.25
U	3.3	3.2	3.6	3.4	3.3	2.4	2.5	2.2	2.5	2	2.1	1.8	1.7	1.6	1.5	0.22
Zr	130	140	140	140	300	230	230	190	220	190	200	160	150	150	140	78

Note: Sample = SUD-##-1994, SUD-1##-1995, SUD-2##-1997

Drill core 52848

sample	211	212	213	214	215	37	44	160	161	162	163	164	165	166g3	166g2
depth (m)	500	1500	2500	3000	3500	4096	4375	4500	4575	4640	4646	4650	4663	4677.1	4677.2
Ba	920	1000	1200	1100	750	650	1100	670	940	630	1100	810	270	240	500
Be	1.9	2.3	2.3	2.5	2.7	1.9	2	1.4	1.1	1.7	1.9	2	2.1	1.4	1.9
Co	8	10	8	10	15	18	13	40	31	42	8	9	9	8	18
Cr	-10	-10	-10	-10	-10	-10	15	20	21	27	17	11	14	13	20
Cu	11	-10	-10	-10	-10	-10	14	13	24	28	17	10	<10	<10	<10
Ni	-10	-10	-10	-10	-10	-10	-10	-10	<10	<10	<10	<10	<10	<10	<10
Sc	12	11	13	14	23	19	14	26	28	29	11	15	15	14	23
Sr	170	150	180	170	130	150	230	330	290	200	190	180	300	310	210
V	18	8	-5	-5	-5	57	66	320	440	390	81	89	91	81	160
Zn	100	81	63	42	46	46	54	69	84	100	42	42	31	26	46
Ce	110	130	120	130	140	120	110	92	100	140	110	130	100	77	100
Dy	6	5.9	6.1	6.1	6.8	6	5.2	6	5.2	6.8	5.2	6.2	4.7	3.5	5.4
Er	3.2	3.3	3.2	3.1	3.5	3.3	2.7	2.8	2.6	3.6	3	3.2	2.7	1.9	3
Eu	1.1	1.2	1.2	1.2	1.8	1.2	1.2	2.4	1.9	2.1	0.95	1.5	2.4	1.9	1.5
Gd	7.6	7.1	7.5	7.6	8.9	7.4	6.3	7.9	7	8.7	6.1	8.3	6	4.4	7.1
Ho	1.2	1.2	1.2	1.2	1.3	1.2	1	1.2	1.1	1.4	1.1	1.3	1	0.74	1.2
La	58	63	61	63	72	60	55	42	47	70	60	62	55	40	48
Lu	0.49	0.51	0.51	0.5	0.57	0.53	0.42	0.4	0.36	0.46	0.47	0.51	0.43	0.3	0.42
Nd	47	52	53	53	64	56	48	45	50	64	47	55	41	30	49
Pr	12	14	14	14	16	15	13	11	13	16	13	14	11	8.1	12
Sm	8.7	8.9	9	9.2	11	9.5	8	9.4	9.4	12	8.8	10	7.4	5.7	9.2
Tb	0.99	0.98	1	1	1.2	1.1	0.92	1.1	0.9	1.2	0.87	1	0.78	0.6	0.95
Tm	0.46	0.47	0.48	0.47	0.54	0.5	0.41	0.43	0.37	0.51	0.45	0.53	0.42	0.29	0.44
Y	37	38	39	38	44	38	33	32	35	44	34	39	31	21	35
Yb	3.2	3.5	3.4	3.4	3.8	3.5	2.8	2.6	2.2	3.1	2.9	3.3	2.7	2	2.7
Ag	0.1	-0.1	0.2	-0.1	0.3	-0.1	0.1	0.3	4.1	0.7	0.8	0.5	0.6	1	0.4
Bi	-0.5	-0.5	-0.5	-0.5	-0.5	-0.5	-0.5	0.6	<0.5	0.6	<0.5	<0.5	<0.5	<0.5	<0.5
Cd	-0.2	-0.2	-0.2	-0.2	-0.2	-0.2	-0.2	-0.2	<0.2	<0.2	<0.2	<0.2	<0.2	<0.2	<0.2
Cs	0.6	1.1	0.69	0.42	2.7	0.22	0.39	0.36	0.35	0.37	0.34	0.16	0.16	0.11	0.18
Ga	19	18	18	19	19	15	19	19	20	17	19	19	20	18	19
Hf	7.1	7.7	7.4	7.1	7.1	7.3	5.6	5.2	4.5	3.5	6.9	6.4	7.9	5.4	5.2
In	-0.05	-0.05	-0.05	-0.05	-0.05	0.11	-0.05	-0.05	0.06	<0.05	<0.05	<0.05	<0.05	<0.05	0.05
Mo	1.4	2.1	1.5	1.7	1	1.2	1.6	1.1	1	0.9	1.5	1.8	1.7	1.3	1.1
Nb	15	16	16	17	18	17	14	8.5	12	11	16	19	7.2	8.2	17
Pb	93	37	14	98	3	-2	8	10	10	7	10	6	4	35	55
Rb	100	110	100	93	97	82	94	51	61	39	100	67	27	31	35
Sn	2.2	3.4	1.5	2.6	1.3	4.4	2		12	2.2	4.1	2.5	2.8	3	2.2
Ta	0.9	0.9	0.9	0.9	1	0.9	0.8	0.3	0.5	0.6	0.5	0.6	0.3	<0.2	0.7
Th	14	15	14	13	13	12	9	6.4	7.3	6.4	14	14	15	14	11
Tl	0.47	0.52	0.46	0.42	0.31	0.43	0.5	0.25	0.29	0.21	0.57	0.36	0.15	0.19	0.19
U	3.2	3.4	3	3	3	2.8	2	1.6	1.6	1.3	3.1	3	3.4	2.9	2.3
Zr	290	340	310	300	310	300	230	210	180	150	310	280	380	210	220

Note: Sample = SUD-##-1994, SUD-1##-1995, SUD-2##-1997

Drill core 52848

sample	166g1	166q1	166q2	140	216	217	45	141	142	47	218	219	48	49
depth (m)	4677	4677	4678	4700	4800	4900	5085	5150	5375	5510	6000	6500	6910	7285
Ba	750	620	720	620	530	630	570	530	500	500	370	340	250	180
Be	1.7	1.5	1.5	1.1	1.1	1.1	1	1	0.9	0.9	0.8	0.6	-0.5	0.6
Co	18	37	35	46	54	49	57	48	45	58	60	57	86	110
Cr	20	25	25	37	-10	22	22	24	31	10	13	51	-10	130
Cu	<10	22	23	40	20	30	30	23	24	24	31	37	39	30
Ni	<10	<10	<10	21	-10	-10	-10	10	16	-10	-10	-10	-10	15
Sc	22	30	30	29	33	28	29	29	30	32	29	28	36	36
Sr	230	290	300	370	380	380	360	390	430	400	460	430	430	48
V	190	400	390	410	370	380	490	430	450	410	480	590	850	630
Zn	51	89	91	47	83	87	120	71	64	93	98	87	96	110
Ce	110	110	92	82	78	73	75	75	78	76	66	32	47	43
Dy	5.8	6.2	5.1	4.8	4.8	4	4.2	4.4	4.6	4.6	4.1	2	3.2	2.6
Er	3.1	3.1	2.8	2.5	2.3	2	2.1	2.3	2.4	2.2	1.9	1	1.5	1.5
Eu	1.1	2.1	2.1	2.1	1.7	1.5	1.7	1.9	2	1.9	1.7	0.77	1.4	0.36
Gd	7.8	8.8	6.9	6.4	6.8	5.3	6.2	6.2	6.4	6.8	5.9	2.6	5	2.8
Ho	1.2	1.3	1.1	0.97	0.94	0.76	0.83	0.87	0.93	0.92	0.78	0.38	0.59	0.54
La	54	52	42	40	36	35	37	37	39	36	31	15	22	22
Lu	0.47	0.44	0.37	0.34	0.32	0.27	0.29	0.32	0.35	0.31	0.24	0.13	0.19	0.29
Nd	52	54	44	44	41	37	39	39	41	40	36	16	28	19
Pr	13	13	11	11	9.6	9	9.4	9.5	11	9.7	8.1	3.9	6.5	5.1
Sm	10	10	8.8	8.1	7.6	6.4	7.1	7.4	7.5	7.7	6.6	3	5.4	3.3
Tb	0.97	1.1	0.94	0.95	0.87	0.73	0.8	0.89	0.92	0.89	0.73	0.36	0.63	0.44
Tm	0.48	0.47	0.38	0.35	0.33	0.27	0.29	0.32	0.34	0.31	0.26	0.13	0.2	0.27
Y	37	38	31	28	28	26	26	25	25	28	24	12	19	18
Yb	3	2.8	2.6	2.2	2.1	2	2	2	2.1	2.1	1.8	0.99	1.3	1.9
Ag	1.7	0.9	1.1	0.2	0.1	0.3	-0.1	0.2	0.2	-0.1	0.1	-0.1	-0.1	0.3
Bi	0.6	0.6	0.7	0.6	-0.5	-0.5	-0.5	0.7	<0.5	-0.5	-0.5	-0.5	-0.5	-0.5
Cd	<0.2	<0.2	<0.2	<0.2	-0.2	-0.2	-0.2	<0.2	<0.2	-0.2	-0.2	-0.2	-0.2	-0.2
Cs	0.23	0.44	0.45	0.54	0.61	0.97	0.94	0.97	0.96	1.2	1.2	0.56	0.54	2.2
Ga	20	21	20	19	18	19	19	19	19	19	20	20	19	10
Hf	6.4	3.6	3.9	3.6	3.3	3.2	3.1	3.1	2.9	3.1	2.3	1.9	1.3	2.8
In	<0.05	0.07	0.06	0.09	-0.05	0.06	-0.05	0.06	0.05	-0.05	-0.05	-0.05	-0.05	0.07
Mo	1	0.9	1	4.4	0.6	0.8	0.8	2.2	2.6	0.7	0.4	0.3	-0.2	0.6
Nb	16	12	11	11	8.7	7.9	8.1	10	8.3	9.1	6.2	3.1	4.5	6.3
Pb	18	13	14	34	7	6	6	33	35	6	6	6	2	5
Rb	43	61	58	45	30	53	46	40	37	41	31	30	14	73
Sn	12	2.2	8.9	2.8	1.1	2	2.1	4	3.3	0.6	-0.5	1.8	0.9	10
Ta	0.6	0.6	0.6	1	0.5	0.5	0.5	1.1	0.8	0.5	0.4	-0.2	0.3	0.4
Th	13	5.5	5.8	6.2	5.7	5.2	4.8	5.7	4.8	5.1	4	3	1.8	5.4
Tl	0.22	0.3	0.31	0.23	0.18	0.27	0.25	0.23	0.22	0.27	0.18	0.15	0.09	0.47
U	2.8	1.2	1.3	1.3	1.2	1.1	1.1	1.2	1.1	1.2	0.91	0.56	0.45	1.1
Zr	280	150	160	130	140	140	120	120	110	120	91	76	52	110

Note: Sample = SUD-##-1994, SUD-1##-1995, SUD-2##-1997

Drill core 52848					Duplicates											
sample	220	221	222	223	145	151	154	173	174	175	140	161	162	163	164	165
depth (m)	7550	7750	8050	8350	2000	5665	7380	4933	5940	5945	4700	4575	4640	4646	4650	4663
Ba	360	370	360	390	910	660	580	940	540	340	680	930	800	1100	960	260
Be	0.9	0.9	0.8	0.8	2.1	1.3	1.2	2.2	1.3	1.3	1.2	1.4	2	1.9	2.1	2.2
Co	33	34	32	30	11	40	23	13	28	23	46	44	59	13	15	13
Cr	57	53	100	130	34	19	130	15	27	28	22	22	29	19	13	12
Cu	18	28	23	18	-10	10	23	-10	12	-10	21	14	-10	13	13	-10
Ni	18	25	26	28	12	-10	24	-10	-10	-10	-10	-10	-10	-10	-10	-10
Sc	16	15	15	14	12	27	16	15	21	23	29	28	31	11	14	15
Sr	430	440	440	440	160	340	340	190	370	310	320	300	190	210	180	260
V	87	88	84	78	40	640	100	7	130	130	320	370	410	65	71	74
Zn	63	61	61	59	36	73	55	54	50	36	70	75	90	37	46	28
Ce	37	33	39	36	110	56	64	110	65	67	78	95	120	100	120	100
Dy	2	1.7	1.9	1.8	5.5	3.2	3.3	6.3	3.7	4	5	5.4	7.5	5.7	6.4	4.9
Er	1.1	1	1.1	1	2.8	1.8	1.7	3.3	2	2.1	2.3	2.4	3.8	3.1	3.3	2.6
Eu	0.82	0.81	0.87	0.85	1.4	1.1	1.2	1.9	1.2	1.5	2.1	2.2	2.3	1.1	1.6	2.3
Gd	2.3	1.9	2.3	2.2	6.3	3.7	3.8	7.5	4.5	4.5	6.8	7.2	9.6	6.4	7.7	5.7
Ho	0.38	0.36	0.38	0.36	1.1	0.65	0.64	1.2	0.73	0.75	0.94	1	1.4	1.1	1.2	0.99
La	20	18	20	19	53	26	32	53	31	33	38	43	58	51	56	51
Lu	0.16	0.18	0.17	0.16	0.5	0.27	0.27	0.5	0.3	0.3	0.33	0.36	0.5	0.5	0.47	0.38
Nd	17	13	16	15	47	24	27	50	29	31	40	49	58	46	54	43
Pr	4.3	3.6	4.3	4.1	12	6.2	7.1	13	7.7	7.9	9.4	12	14	12	14	11
Sm	2.8	2.3	2.9	2.5	8.2	4.7	5	9.8	5.6	5.6	7.5	9.1	12	8.3	9.7	7.4
Tb	0.34	0.29	0.31	0.31	0.91	0.54	0.57	1.1	0.66	0.62	0.87	0.95	1.3	0.98	1.1	0.85
Tm	0.16	0.16	0.17	0.15	0.48	0.28	0.28	0.5	0.31	0.31	0.36	0.38	0.58	0.47	0.49	0.39
Y	12	11	12	12	33	19	20	37	22	22	27	31	41	32	35	30
Yb	1.3	1.2	1.2	1.1	3.2	1.8	1.8	3.3	2	2	2.2	2.3	3.3	3.2	3.2	2.6
Ag	-0.1	-0.1	-0.1	-0.1	0.1	-0.1	0.5	0.5	0.9	0.2	1.8	0.8	0.2	0.1	0.3	0.7
Bi	-0.5	-0.5	-0.5	-0.5	0.7	0.9	0.6	0.9	0.5	0.5	0.5	0.8	0.7	0.6	0.6	0.5
Cd	-0.2	-0.2	-0.2	-0.2	-0.2	-0.2	-0.2	-0.2	-0.2	-0.2	-0.2	-0.2	-0.2	-0.2	-0.2	-0.2
Cs	1.1	1.1	0.97	0.97	0.43	0.95	1.5	1.1	0.31	0.14	0.53	0.32	0.35	0.35	0.17	0.15
Ga	19	19	19	20	17	20	19	19	19	19	18	20	16	18	20	18
Hf	2.2	2.4	2.2	2.3	7.2	3.3	3.8	6.8	3.8	4	3.6	4.2	4.6	11	6.3	7.7
In	-0.1	-0.1	-0.1	-0.1	-0.1	-0.1	0.1	-0.1	0.06	-0.1	-0.1	0.07	-0.1	-0.1	0.06	0.06
Mo	0.4	0.4	0.3	0.3	1.6	0.7	1	1.9	0.9	0.4	0.9	1	0.8	2.9	2	1.5
Nb	5.2	4.9	4.8	4.4	15	6.5	7.8	17	7.3	7.5	9.6	11	6.5	14	17	5.2
Pb	7	5	5	4	9	11	7	8	7	5	7	10	7	10	6	5
Rb	33	34	37	34	79	78	63	97	51	28	46	57	38	97	64	22
Sn	-0.5	0.7	5.3	-0.5												
Ta	0.3	0.3	0.3	0.3	0.9	0.4	0.3	0.9	0.4	0.3	0.5	0.7	0.5	0.5	0.8	0.4
Th	4.1	4.3	4	3.8	15	5.8	7.3	13	6.8	7	5.6	8	6.1	14	13	16
Tl	0.18	0.2	0.21	0.18	0.29	0.37	0.3	0.44	0.23	0.14	0.17	0.25	0.2	0.54	0.35	0.15
U	0.89	0.9	0.86	0.83	3.6	1.4	1.7	3	1.7	1.7	1.3	1.9	1.5	3.7	2.8	3.7
Zr	90	95	85	91	310	120	150	270	130	140	140	150	180	450	270	330

Note: Sample = SUD-##-1994, SUD-1##-1995, SUD-2##-1997

APPENDIX C

Normalized whole-rock geochemical analyses and molar proportions for samples from drill core 70011.

sample	189	191	193	195	83	143a	143b	177	178	197	198	199	50	200
depth (m)	15.2	45.7	76.2	79.2	82.3	83.9	83.9	89.9	93.0	121.9	152.4	182.9	243.8	304.8
SiO_2	66.50	68.44	71.83	73.78	73.18	69.66	69.28	78.63	75.86	71.00	70.66	69.83	70.18	70.00
TiO_2	0.54	0.47	0.31	0.31	0.18	0.27	0.30	0.15	0.52	0.81	0.82	0.84	0.81	0.86
Al_2O_3	12.63	13.36	14.20	13.91	15.02	15.77	15.62	12.60	11.80	12.48	12.54	12.62	12.66	12.61
FeOT	6.82	4.86	3.14	1.91	1.73	2.83	3.45	0.91	3.05	5.58	5.96	5.90	5.97	6.15
MnO	0.07	0.06	0.03	0.02	0.01	0.03	0.03	0.01	0.03	0.06	0.06	0.04	0.07	0.07
MgO	4.46	3.49	2.23	1.63	0.70	0.86	1.93	0.51	0.79	0.98	0.89	1.35	0.89	0.76
CaO	3.36	2.74	1.00	1.33	2.07	3.35	1.80	1.25	2.36	1.83	1.83	1.79	2.20	2.20
Na_2O	3.77	4.56	4.97	6.65	6.39	6.17	5.07	4.37	3.97	3.04	3.03	3.16	3.14	3.43
K_2O	1.72	1.89	2.18	0.34	0.65	0.94	2.39	1.55	1.55	4.05	4.03	4.29	3.90	3.73
P_2O_5	0.13	0.12	0.09	0.11	0.06	0.12	0.13	0.02	0.08	0.17	0.17	0.17	0.18	0.19
LoI	0.00	0.00	0.00	0.00	-	-	-	-	-	0.00	0.00	0.00	-	0.00
Total	100.00	100.00	100.00	100.00	100.00	100.00	100.00	100.00	100.00	100.00	100.00	100.00	100.00	100.00
SiO_2	1.1067	1.1391	1.1954	1.2279	1.2180	1.1594	1.1530	1.3086	1.2625	1.1817	1.1761	1.1622	1.1680	1.1651
TiO_2	0.0068	0.0058	0.0039	0.0039	0.0023	0.0034	0.0038	0.0019	0.0065	0.0102	0.0102	0.0106	0.0101	0.0107
Al_2O_3	0.1238	0.1311	0.1393	0.1364	0.1473	0.1547	0.1532	0.1235	0.1157	0.1224	0.1229	0.1238	0.1241	0.1237
FeOT	0.0427	0.0304	0.0197	0.0120	0.0108	0.0177	0.0216	0.0057	0.0191	0.0349	0.0373	0.0370	0.0374	0.0385
MnO	0.0010	0.0009	0.0004	0.0003	0.0001	0.0004	0.0004	0.0001	0.0004	0.0009	0.0009	0.0006	0.0010	0.0010
MgO	0.1107	0.0867	0.0554	0.0405	0.0174	0.0213	0.0478	0.0126	0.0197	0.0244	0.0221	0.0336	0.0221	0.0188
CaO	0.0599	0.0489	0.0179	0.0237	0.0369	0.0597	0.0320	0.0223	0.0421	0.0326	0.0326	0.0319	0.0392	0.0392
Na_2O	0.0608	0.0735	0.0802	0.1073	0.1032	0.0995	0.0818	0.0705	0.0640	0.0491	0.0489	0.0509	0.0507	0.0553
K_2O	0.0183	0.0201	0.0232	0.0036	0.0069	0.0100	0.0254	0.0165	0.0164	0.0430	0.0428	0.0455	0.0414	0.0396
P_2O_5	0.0009	0.0009	0.0006	0.0008	0.0004	0.0009	0.0009	0.0001	0.0006	0.0012	0.0012	0.0012	0.0013	0.0014

Note: Samples = SUD-##-1994; SUD-1##-1995; SUD-2##-1997

Normalized whole-rock geochemical analyses and molar proportions for samples from drill core 70011.

sample	144	145	167	168	52	146	147	169	201	53	202	54	55	170
depth (m)	456.6	609.6	640.1	670.6	853.4	893.1	967.7	990.6	1066.8	1158.2	1219.2	1463.0	1493.5	1501.7
SiO_2	68.22	68.01	68.69	69.25	70.53	66.20	70.04	70.49	70.81	69.62	70.87	70.44	68.74	67.97
TiO_2	0.95	0.95	0.93	0.82	0.69	0.65	0.70	0.68	0.79	0.70	0.66	0.67	0.81	0.85
Al_2O_3	13.01	12.56	13.29	13.00	12.82	13.30	12.52	12.81	12.62	13.24	12.57	12.99	13.36	13.25
FeOT	5.16	6.18	6.59	5.95	6.36	7.24	5.36	6.35	5.31	6.16	5.53	5.48	6.48	7.08
MnO	0.06	0.08	0.05	0.07	0.07	0.08	0.06	0.07	0.06	0.08	0.08	0.07	0.08	0.09
MgO	1.24	0.90	1.75	0.92	1.06	0.95	0.84	0.86	0.94	0.66	0.52	0.40	0.55	0.68
CaO	2.50	2.47	1.18	2.55	1.38	2.69	1.63	1.14	2.20	2.17	2.12	2.40	2.51	2.71
Na_2O	4.57	3.59	3.35	3.23	3.53	3.47	3.28	3.53	3.51	3.54	3.52	3.35	3.85	4.25
K_2O	2.45	3.19	3.93	4.04	3.43	3.35	4.01	3.95	3.62	3.70	4.00	4.05	3.45	2.94
P_2O_5	0.27	0.23	0.24	0.18	0.13	0.12	0.13	0.13	0.15	0.13	0.13	0.15	0.17	0.18
LoI	1.57	1.83	0.00	0.00	-	1.95	1.43	0.00	0.00	-	0.00	-	-	0.00
Total	100.00	100.00	100.00	100.00	100.00	100.00	100.00	100.00	100.00	100.00	100.00	100.00	100.00	100.00
SiO_2	1.1353	1.1319	1.1432	1.1525	1.1739	1.1017	1.1657	1.1731	1.1784	1.1588	1.1795	1.1724	1.1440	1.1312
TiO_2	0.0119	0.0119	0.0117	0.0102	0.0086	0.0081	0.0087	0.0085	0.0099	0.0087	0.0083	0.0084	0.0101	0.0106
Al_2O_3	0.1276	0.1232	0.1304	0.1275	0.1257	0.1304	0.1228	0.1256	0.1238	0.1298	0.1232	0.1274	0.1311	0.1299
FeOT	0.0323	0.0387	0.0413	0.0372	0.0398	0.0454	0.0336	0.0398	0.0332	0.0386	0.0346	0.0343	0.0406	0.0443
MnO	0.0008	0.0011	0.0007	0.0010	0.0010	0.0011	0.0008	0.0010	0.0008	0.0011	0.0011	0.0010	0.0011	0.0013
MgO	0.0308	0.0223	0.0433	0.0228	0.0263	0.0236	0.0210	0.0213	0.0234	0.0163	0.0130	0.0098	0.0136	0.0168
CaO	0.0446	0.0441	0.0210	0.0455	0.0247	0.0480	0.0291	0.0203	0.0393	0.0387	0.0378	0.0427	0.0448	0.0483
Na_2O	0.0737	0.0579	0.0540	0.0520	0.0570	0.0560	0.0529	0.0569	0.0566	0.0571	0.0568	0.0540	0.0621	0.0685
K_2O	0.0260	0.0339	0.0417	0.0429	0.0364	0.0356	0.0426	0.0420	0.0384	0.0393	0.0425	0.0430	0.0366	0.0312
P_2O_5	0.0019	0.0016	0.0017	0.0013	0.0009	0.0008	0.0009	0.0009	0.0011	0.0009	0.0009	0.0011	0.0012	0.0013

Note: Samples = SUD-##-1994; SUD-1##-1995; SUD-2##-1997

Normalized whole-rock geochemical analyses and molar proportions for samples from drill core 70011.

sample	171	172	173	148	56	179	180	149	203	204	59	150	151	61
depth (m)	1502.4	1503.0	1503.6	1504.2	1524.0	1562.1	1566.7	1615.4	1646.0	1661.2	1676.4	1723.6	1726.7	1752.6
SiO_2	67.74	68.06	67.80	66.08	66.21	63.13	62.28	56.01	54.18	53.98	55.53	55.80	56.32	58.87
TiO_2	0.91	0.96	0.90	0.94	1.07	1.40	1.48	1.79	1.86	1.86	1.38	1.14	0.98	0.54
Al_2O_3	13.12	13.21	13.27	12.66	13.60	13.80	13.80	13.19	13.27	13.75	14.74	14.59	15.14	16.03
FeOT	7.37	6.96	7.15	7.58	8.06	9.64	10.35	11.71	14.27	14.15	12.43	10.55	10.03	7.56
MnO	0.10	0.10	0.08	0.09	0.12	0.14	0.15	0.16	0.16	0.15	0.14	0.12	0.12	0.12
MgO	0.74	0.65	1.02	0.80	0.82	1.13	1.29	2.35	3.59	3.69	3.58	3.55	3.40	3.85
CaO	2.82	3.04	2.60	2.78	3.21	4.44	4.49	5.87	7.18	7.77	7.26	7.52	7.02	7.99
Na_2O	3.53	4.13	3.47	3.29	3.83	3.45	3.25	3.74	3.12	2.71	3.11	3.06	2.75	3.63
K_2O	3.47	2.68	3.50	3.54	2.84	2.49	2.50	2.10	1.65	1.64	1.68	1.45	2.05	1.22
P_2O_5	0.19	0.21	0.19	0.21	0.23	0.39	0.42	0.54	0.73	0.31	0.15	0.13	0.13	0.18
LoI	0.00	0.00	0.00	2.04	-	-	-	2.53	0.00	0.00	0.00	2.10	2.06	-
Total	100.00	100.00	100.00	100.00	100.00	100.00	100.00	100.00	100.00	100.00	100.00	100.00	100.00	100.00
SiO_2	1.1275	1.1327	1.1285	1.0998	1.1019	1.0507	1.0366	0.9323	0.9017	0.8985	0.9243	0.9286	0.9374	0.9798
TiO_2	0.0114	0.0120	0.0112	0.0117	0.0134	0.0175	0.0185	0.0224	0.0233	0.0232	0.0173	0.0143	0.0123	0.0068
Al_2O_3	0.1287	0.1295	0.1302	0.1241	0.1334	0.1354	0.1353	0.1294	0.1301	0.1348	0.1445	0.1431	0.1485	0.1572
FeOT	0.0462	0.0436	0.0448	0.0474	0.0505	0.0604	0.0648	0.0734	0.0894	0.0886	0.0778	0.0661	0.0628	0.0473
MnO	0.0014	0.0014	0.0012	0.0013	0.0017	0.0020	0.0021	0.0022	0.0023	0.0021	0.0020	0.0017	0.0017	0.0017
MgO	0.0183	0.0160	0.0253	0.0198	0.0203	0.0280	0.0320	0.0584	0.0890	0.0916	0.0888	0.0881	0.0844	0.0955
CaO	0.0502	0.0543	0.0464	0.0496	0.0573	0.0791	0.0801	0.1046	0.1280	0.1385	0.1294	0.1341	0.1251	0.1425
Na_2O	0.0570	0.0667	0.0560	0.0531	0.0618	0.0557	0.0524	0.0604	0.0503	0.0437	0.0501	0.0493	0.0444	0.0586
K_2O	0.0369	0.0285	0.0372	0.0376	0.0302	0.0264	0.0265	0.0223	0.0175	0.0174	0.0179	0.0154	0.0218	0.0129
P_2O_5	0.0014	0.0015	0.0014	0.0015	0.0016	0.0027	0.0029	0.0038	0.0052	0.0022	0.0011	0.0009	0.0009	0.0013

Note: Samples = SUD-##-1994; SUD-1##-1995; SUD-2##-1997

Normalized whole-rock geochemical analyses and molar proportions for samples from drill core 70011.

sample	62	174	175	93	176	152	153	63	64	65	205	66	154	155	187
depth (m)	1799.8	1810.5	1812.0	1813.6	1816.6	1826.7	1831.8	1905.0	1920.2	2045.2	2164.1	2199.1	2249.4	2255.5	2257.3
SiO_2	59.76	59.74	59.80	58.90	60.26	54.46	58.95	59.42	59.21	58.10	59.53	59.93	58.58	51.61	53.16
TiO_2	0.59	0.60	0.59	0.68	0.57	0.58	0.65	0.68	0.51	0.49	0.64	0.44	0.59	0.53	0.55
Al_2O_3	16.00	15.77	15.88	16.83	15.85	15.12	16.18	16.66	16.25	17.58	16.75	17.05	15.76	15.55	15.19
FeOT	7.70	7.68	6.83	6.79	7.42	8.11	7.14	7.82	7.92	7.38	7.35	6.96	7.43	10.20	10.94
MnO	0.12	0.12	0.12	0.12	0.11	0.11	0.12	0.12	0.12	0.10	0.11	0.09	0.11	0.14	0.13
MgO	3.74	3.70	3.85	3.74	3.76	3.85	3.79	4.42	4.87	4.95	4.48	4.19	4.70	7.67	8.93
CaO	6.84	7.17	6.59	5.62	6.86	5.75	5.32	6.21	6.43	6.92	5.48	6.14	6.33	7.96	7.39
Na_2O	3.14	3.34	5.63	6.79	3.15	4.74	4.07	3.25	2.95	3.03	3.57	3.13	2.87	2.28	2.53
K_2O	2.00	1.73	0.55	0.38	1.90	0.77	1.37	1.25	1.60	1.34	1.95	1.94	1.72	1.57	1.08
P_2O_5	0.11	0.16	0.15	0.15	0.11	0.11	0.11	0.17	0.14	0.10	0.12	0.13	0.13	0.09	0.09
LoI	-	0.00	0.00	-	0.00	6.39	2.31	-	-	-	0.00	-	1.75	2.40	-
Total	100.00	100.00	100.00	100.00	100.00	100.00	100.00	100.00	100.00	100.00	100.00	100.00	100.00	100.00	100.00
SiO_2	0.9947	0.9943	0.9953	0.9803	1.0030	0.9064	0.9811	0.9890	0.9854	0.9670	0.9908	0.9974	0.9750	0.8590	0.8848
TiO_2	0.0074	0.0075	0.0074	0.0085	0.0071	0.0073	0.0081	0.0085	0.0064	0.0061	0.0081	0.0056	0.0074	0.0067	0.0068
Al_2O_3	0.1570	0.1547	0.1557	0.1651	0.1555	0.1483	0.1586	0.1634	0.1594	0.1724	0.1642	0.1672	0.1546	0.1525	0.1490
FeOT	0.0482	0.0481	0.0428	0.0425	0.0465	0.0508	0.0447	0.0490	0.0496	0.0462	0.0460	0.0436	0.0466	0.0639	0.0685
MnO	0.0017	0.0017	0.0017	0.0017	0.0016	0.0015	0.0017	0.0017	0.0017	0.0014	0.0016	0.0013	0.0015	0.0020	0.0019
MgO	0.0927	0.0918	0.0955	0.0928	0.0933	0.0956	0.0941	0.1096	0.1209	0.1229	0.1112	0.1039	0.1166	0.1903	0.2216
CaO	0.1219	0.1278	0.1176	0.1002	0.1223	0.1026	0.0948	0.1107	0.1146	0.1234	0.0978	0.1096	0.1130	0.1419	0.1318
Na_2O	0.0507	0.0538	0.0908	0.1096	0.0508	0.0766	0.0656	0.0524	0.0475	0.0489	0.0577	0.0505	0.0464	0.0368	0.0408
K_2O	0.0212	0.0183	0.0059	0.0040	0.0202	0.0082	0.0145	0.0133	0.0170	0.0143	0.0207	0.0206	0.0183	0.0166	0.0115
P_2O_5	0.0008	0.0011	0.0011	0.0011	0.0008	0.0008	0.0008	0.0012	0.001	0.0007	0.0009	0.0009	0.0009	0.0006	0.0006

Note: Samples = SUD-##-1994; SUD-1##-1995; SUD-2##-1997

Normalized whole-rock geochemical analyses and molar proportions for samples from drill core 70011.

sample	206	207	208	209	136	13	156	157	158	137	159	138	139	22	210	26
depth (m)	76.2	152.4	228.6	304.8	1085.1	1133.9	1170.4	1176.5	1182.6	1188.7	1210.1	1234.4	1240.5	1249.7	1310.6	1511.8
SiO_2	68.41	67.17	68.74	65.86	67.21	63.05	64.45	62.54	63.34	62.65	62.32	60.47	59.67	60.16	60.35	61.79
TiO_2	0.47	0.53	0.51	0.52	0.94	1.31	0.68	0.79	0.72	0.76	0.73	0.62	0.57	0.66	0.54	0.28
Al_2O_3	11.81	12.99	12.29	12.30	12.63	13.40	14.33	14.78	14.36	14.75	15.40	15.36	15.64	16.18	17.23	18.35
FeOT	6.46	4.67	5.99	7.01	6.66	9.27	7.32	7.79	7.74	7.83	7.50	7.24	7.52	7.99	6.35	4.08
MnO	0.10	0.08	0.07	0.12	0.08	0.12	0.10	0.10	0.11	0.11	0.11	0.11	0.12	0.13	0.10	0.05
MgO	4.40	4.07	3.80	4.10	0.85	1.57	2.43	2.54	2.46	2.61	3.34	3.22	3.43	3.88	3.61	4.04
CaO	2.84	3.30	3.06	3.92	2.45	4.80	4.60	5.59	5.18	5.32	4.63	5.62	5.80	6.08	6.40	4.34
Na_2O	4.04	5.07	3.55	3.35	3.28	3.42	3.71	3.34	3.36	3.36	5.17	3.07	2.97	2.93	3.73	5.51
K_2O	1.37	1.99	1.87	2.68	3.59	2.60	2.18	2.35	2.52	2.37	0.60	2.05	1.86	1.83	1.59	1.50
P_2O_5	0.11	0.13	0.12	0.13	0.20	0.45	0.21	0.18	0.20	0.24	0.20	0.11	0.15	0.16	0.10	0.06
LoI	0.00	0.00	0.00	0.00	2.12	0.00	0.00	0.00	0.00	0.00	0.00	2.12	2.27	0.00	0.00	0.00
Total	100.00	100.00	100.00	100.00	100.00	100.00	100.00	100.00	100.00	100.00	100.00	100.00	100.00	100.00	100.00	100.00
SiO_2	1.1385	1.1180	1.1441	1.0961	1.1186	1.0494	1.0726	1.0409	1.0542	1.0426	1.0371	1.0064	0.9932	1.0013	1.0045	1.0284
TiO_2	0.0059	0.0066	0.0064	0.0065	0.0118	0.0164	0.0085	0.0099	0.0090	0.0095	0.0091	0.0078	0.0072	0.0082	0.0068	0.0034
Al_2O_3	0.1158	0.1274	0.1205	0.1206	0.1238	0.1314	0.1406	0.1449	0.1408	0.1446	0.1511	0.1507	0.1534	0.1587	0.1690	0.1800
FeOT	0.0404	0.0292	0.0375	0.0439	0.0417	0.0580	0.0458	0.0488	0.0485	0.0490	0.0470	0.0453	0.0471	0.0500	0.0397	0.0255
MnO	0.0014	0.0011	0.0010	0.0017	0.0011	0.0017	0.0014	0.0014	0.0016	0.0016	0.0016	0.0015	0.0017	0.0019	0.0014	0.0007
MgO	0.1091	0.1010	0.0942	0.1016	0.0210	0.0390	0.0602	0.0630	0.0611	0.0648	0.0830	0.0799	0.0852	0.0963	0.0895	0.1002
CaO	0.0506	0.0588	0.0545	0.0700	0.0436	0.0857	0.0820	0.0996	0.0924	0.0948	0.0826	0.1002	0.1034	0.1084	0.1141	0.0775
Na_2O	0.0651	0.0819	0.0573	0.0541	0.0529	0.0553	0.0598	0.0539	0.0542	0.0541	0.0834	0.0496	0.0479	0.0473	0.0601	0.0888
K_2O	0.0146	0.0211	0.0198	0.0285	0.0381	0.0276	0.0231	0.0249	0.0267	0.0252	0.0063	0.0218	0.0198	0.0194	0.0169	0.0159
P_2O_5	0.0008	0.0009	0.0009	0.0009	0.0014	0.0032	0.0015	0.0013	0.0014	0.0017	0.0014	0.0008	0.0010	0.0011	0.0007	0.0004

Note: Samples = SUD-##-1994; SUD-1##-1995; SUD-2##-1997

Normalized whole-rock geochemical analyses and molar proportions for samples from drill core 70011.

sample	211	212	213	214	215	37	44	160	161	162	163	164	165	166g3
depth (m)	152.4	457.2	762.0	914.4	1066.8	1248.5	1333.5	1371.6	1394.5	1414.3	1416.1	1417.3	1421.3	1425.6
SiO_2	69.33	70.31	69.81	69.62	59.75	66.90	67.31	58.49	54.11	53.94	69.13	66.90	67.64	68.92
TiO_2	0.81	0.68	0.72	0.77	1.24	1.36	0.92	1.98	2.94	2.67	0.83	1.20	1.05	0.98
Al_2O_3	13.00	12.79	12.86	12.98	15.17	12.66	14.04	14.32	13.73	13.10	13.72	13.64	13.31	13.22
FeOT	5.54	6.04	6.23	6.34	10.32	6.73	6.02	11.10	12.41	13.20	4.94	6.52	6.45	4.44
MnO	0.08	0.09	0.08	0.08	0.19	0.10	0.08	0.13	0.15	0.18	0.06	0.07	0.06	0.05
MgO	0.65	0.51	0.59	0.41	0.98	1.38	1.19	2.80	3.28	3.89	1.23	1.12	1.12	1.35
CaO	3.17	1.69	2.10	2.11	2.49	2.94	2.75	7.09	6.95	6.15	2.61	2.71	3.36	4.29
Na_2O	3.33	3.42	3.52	3.62	5.98	4.32	4.11	3.23	3.15	3.96	3.83	4.41	5.54	5.05
K_2O	3.93	4.32	3.95	3.71	3.57	3.24	3.38	1.78	1.91	1.32	3.47	3.14	1.13	1.45
P_2O_5	0.16	0.13	0.14	0.15	0.32	0.37	0.19	1.09	1.37	1.58	0.16	0.28	0.34	0.27
LoI	0.00	0.00	0.00	0.00	0.00	0.00	0.00	0.00	0.00	0.00	0.00	0.00	0.00	0.00
Total	100.00	100.00	100.00	100.00	100.00	100.00	100.00	100.00	100.00	100.00	100.00	100.00	100.00	100.00
SiO_2	1.1538	1.1701	1.1619	1.1587	0.9944	1.1135	1.1202	0.9401	0.9006	0.8977	1.1505	1.1134	1.1258	1.1471
TiO_2	0.0101	0.0086	0.0091	0.0097	0.0155	0.0170	0.0116	0.0247	0.0368	0.0334	0.0104	0.0151	0.0131	0.0120
Al_2O_3	0.1275	0.1255	0.1261	0.1273	0.1488	0.1241	0.1377	0.1405	0.1347	0.1285	0.1346	0.1338	0.1305	0.1298
FeOT	0.0347	0.0378	0.0390	0.0397	0.0646	0.0421	0.0377	0.0695	0.0777	0.0827	0.0310	0.0408	0.0404	0.0278
MnO	0.0011	0.0013	0.0011	0.0011	0.0026	0.0014	0.0011	0.0018	0.0022	0.0026	0.0009	0.0010	0.0009	0.0007
MgO	0.0163	0.0127	0.0147	0.0102	0.0243	0.0341	0.0296	0.0696	0.0813	0.0965	0.0305	0.0279	0.0278	0.0335
CaO	0.0566	0.0302	0.0374	0.0377	0.0443	0.0525	0.0490	0.1264	0.1239	0.1096	0.0466	0.0483	0.0599	0.0765
Na_2O	0.0537	0.0553	0.0567	0.0617	0.0966	0.0697	0.0664	0.0521	0.0509	0.0639	0.0619	0.0712	0.0895	0.0814
K_2O	0.0417	0.0459	0.0419	0.0394	0.0379	0.0344	0.0359	0.0188	0.0203	0.0140	0.0369	0.0333	0.0120	0.0154
P_2O_5	0.0011	0.0009	0.0010	0.0011	0.0023	0.0026	0.0013	0.0077	0.0097	0.0112	0.0011	0.0020	0.0024	0.0019

Note: Samples = SUD-##-1994; SUD-1##-1995; SUD-2##-1997

Normalized whole-rock geochemical analyses and molar proportions for samples from drill core 70011.

sample	166g2	166g1	166q1	166q2	140	216	217	45	141	142	47	218	219	48
depth (m)	1425.6	1425.6	1425.7	1425.7	1432.6	1463.0	1493.5	1525.5	1569.7	1638.3	1679.4	1828.8	1981.2	2106.2
SiO_2	62.75	62.26	51.87	52.62	51.84	53.18	55.04	53.26	51.24	50.51	52.35	51.06	52.40	44.79
TiO_2	1.82	1.83	3.46	3.32	2.89	3.00	2.16	2.58	3.08	2.85	3.18	2.66	1.74	4.14
Al_2O_3	13.47	13.62	13.58	13.76	12.81	13.27	14.46	13.36	13.15	13.61	13.46	14.79	16.30	13.64
FeOT	7.64	7.97	14.18	13.66	13.11	13.27	11.65	13.57	13.15	13.31	13.56	13.29	12.00	16.92
MnO	0.11	0.10	0.21	0.21	0.16	0.18	0.15	0.16	0.18	0.16	0.17	0.15	0.13	0.18
MgO	2.34	2.38	3.67	3.59	3.49	3.80	3.72	4.03	3.65	3.79	3.85	4.14	4.29	5.43
CaO	4.94	4.93	6.89	6.68	7.19	7.83	7.12	7.57	7.46	8.02	7.87	8.61	8.89	10.21
Na_2O	5.03	4.84	3.24	3.24	2.93	2.92	3.11	2.81	2.82	2.84	2.89	2.90	2.80	2.49
K_2O	1.30	1.40	1.44	1.56	1.41	1.28	1.71	1.49	1.29	1.21	1.36	1.04	1.13	0.54
P_2O_5	0.60	0.66	1.46	1.36	1.11	1.29	0.88	1.18	1.15	1.16	1.32	1.36	0.32	1.66
LoI	0.00	0.00	0.00	0.00	3.07	0.00	0.00	0.00	2.83	2.55	0.00	0.00	0.00	0.00
Total	100.00	100.00	100.00	100.00	100.00	100.00	100.00	100.00	100.00	100.00	100.00	100.00	100.00	100.00
SiO_2	1.0443	1.0362	0.8633	0.8758	0.8628	0.8850	0.9160	0.8863	0.8528	0.8406	0.8712	0.8499	0.8721	0.7454
TiO_2	0.0228	0.0229	0.0434	0.0415	0.0361	0.0375	0.0270	0.0323	0.0385	0.0357	0.0398	0.0333	0.0218	0.0518
Al_2O_3	0.1321	0.1336	0.1331	0.1350	0.1257	0.1301	0.1418	0.1311	0.1290	0.1334	0.1320	0.1451	0.1599	0.1337
FeOT	0.0479	0.0499	0.0888	0.0855	0.0821	0.0831	0.0730	0.0849	0.0823	0.0834	0.0849	0.0832	0.0751	0.1060
MnO	0.0016	0.0014	0.0030	0.0030	0.0022	0.0026	0.0021	0.0023	0.0025	0.0022	0.0024	0.0021	0.0018	0.0025
MgO	0.0581	0.0591	0.0910	0.0891	0.0866	0.0943	0.0922	0.1000	0.0906	0.0940	0.0955	0.1026	0.1064	0.1348
CaO	0.0880	0.0880	0.1228	0.1191	0.1282	0.1396	0.1270	0.1349	0.1331	0.1430	0.1403	0.1536	0.1585	0.1821
Na_2O	0.0811	0.0781	0.0523	0.0522	0.0473	0.0470	0.0502	0.0454	0.0456	0.0458	0.0467	0.0468	0.0452	0.0401
K_2O	0.0138	0.0149	0.0153	0.0165	0.0150	0.0136	0.0181	0.0158	0.0137	0.0129	0.0144	0.0110	0.0120	0.0057
P_2O_5	0.0043	0.0046	0.0103	0.0096	0.0078	0.0091	0.0062	0.0083	0.0081	0.0082	0.0093	0.0096	0.0023	0.0117

Note: Samples = SUD-##-1994; SUD-1##-1995; SUD-2##-1997

Normalized whole-rock geochemical analyses and molar proportions for samples from drill core 70011.

sample	49	220	221	222	223
depth (m)	2220.5	2301.2	2362.2	2453.6	2545.1
SiO_2	55.87	57.34	57.24	56.92	56.66
TiO_2	0.78	0.47	0.44	0.43	0.38
Al_2O_3	6.12	17.67	17.70	17.94	18.42
FeOT	17.03	7.43	7.28	7.22	6.84
MnO	0.18	0.12	0.12	0.12	0.11
MgO	13.26	5.42	5.76	5.91	5.81
CaO	4.96	7.37	7.40	7.43	7.68
Na_2O	0.41	2.91	2.93	2.81	2.92
K_2O	1.26	1.16	1.07	1.14	1.12
P_2O_5	0.12	0.09	0.04	0.09	0.07
LoI	0.00	0.00	0.00	0.00	0.00
Total	100.00	100.00	100.00	100.00	100.00
SiO_2	0.9298	0.9543	0.9527	0.9473	0.9430
TiO_2	0.0098	0.0059	0.0056	0.0054	0.0048
Al_2O_3	0.0600	0.1733	0.1736	0.1759	0.1806
FeOT	0.1066	0.0465	0.0456	0.0452	0.0429
MnO	0.0026	0.0017	0.0017	0.0017	0.0016
MgO	0.3291	0.1345	0.1430	0.1467	0.1441
CaO	0.0885	0.1314	0.1320	0.1324	0.1369
Na_2O	0.0066	0.0470	0.0473	0.0453	0.0471
K_2O	0.0134	0.0124	0.0114	0.0121	0.0119
P_2O_5	0.0009	0.0006	0.0003	0.0006	0.0005

Note: Samples = SUD-##-1994; SUD-1##-1995; SUD-2##-1997

APPENDIX D: CIPW norms for SIC samples from drill core 70011.

depth (m)	15.2	45.7	76.2	79.2	82.3	83.9	83.9	89.9	93.0	121.9	152.4	182.9	243.8	304.8	456.6
SiO_2	65.30	67.60	70.80	73.20	72.10	68.90	68.30	77.40	74.60	70.00	69.90	68.60	69.30	69.40	68.56
TiO_2	0.53	0.46	0.31	0.31	0.18	0.27	0.30	0.15	0.51	0.80	0.81	0.83	0.80	0.85	0.96
Al_2O_3	12.40	13.20	14.00	13.80	14.80	15.60	15.40	12.40	11.60	12.30	12.40	12.40	12.50	12.40	13.07
Fe_2O_3	0.80	1.30	0.60	0.60	0.70	1.80	0.80	0.40	1.30	1.60	2.40	2.90	2.40	1.60	1.20
FeO	5.30	3.20	2.20	1.10	0.90	0.90	2.30	0.40	1.50	3.50	3.10	2.60	3.20	4.00	3.59
MnO	0.07	0.06	0.03	0.02	0.01	0.03	0.03	0.01	0.03	0.06	0.06	0.04	0.07	0.07	0.06
MgO	4.38	3.45	2.20	1.62	0.69	0.85	1.90	0.50	0.78	0.97	0.88	1.33	0.88	0.75	1.25
CaO	3.30	2.71	0.99	1.32	2.04	3.31	1.77	1.23	2.32	1.80	1.81	1.76	2.17	2.18	2.51
Na_2O	3.70	4.50	4.90	6.60	6.30	6.10	5.00	4.30	3.90	3.00	3.00	3.10	3.10	3.40	4.59
K_20	1.69	1.87	2.15	0.34	0.64	0.96	2.36	1.54	1.54	3.99	3.99	4.21	3.85	3.70	2.47
P_2O_5	0.13	0.13	0.09	0.11	0.06	0.12	0.13	0.02	0.08	0.17	0.17	0.17	0.18	0.19	0.27
Q	21.13	22.43	27.79	28.37	28.23	22.57	22.78	43.36	41.34	30.95	31.61	29.51	32.03	28.60	24.82
C	0.00	0.00	2.26	0.67	0.88	0.00	1.95	1.70	0.88	0.41	0.49	0.65	1.57	0.00	0.00
Or	9.99	11.05	12.71	2.01	3.78	5.67	13.95	9.10	9.10	23.58	23.58	24.88	22.76	21.87	14.60
Ab	31.31	38.07	41.46	55.84	53.30	51.61	42.30	36.38	33.00	25.38	25.38	26.23	26.23	28.77	38.84
An	12.24	10.30	3.69	5.20	7.83	12.36	7.30	5.34	7.19	7.19	7.24	5.72	4.53	7.65	7.77
Di	2.17	1.35	0.00	0.00	0.00	2.06	0.00	0.00	0.00	0.00	0.00	0.00	0.00	1.10	1.91
Hy	18.17	12.10	8.57	5.08	2.51	1.16	7.85	1.42	2.84	6.31	4.68	4.39	4.89	6.05	6.28
Mt	1.16	1.88	0.87	0.87	1.01	2.22	1.16	0.58	1.88	2.32	3.48	4.20	3.48	2.32	1.74
Hm	0.00	0.00	0.00	0.00	0.00	0.27	0.00	0.00	0.00	0.00	0.00	0.00	0.00	0.00	0.00
Il	1.01	0.87	0.59	0.59	0.34	0.51	0.57	0.28	0.97	1.52	1.54	1.58	1.52	1.61	1.82
Ap	0.31	0.31	0.21	0.26	0.14	0.28	0.31	0.05	0.19	0.40	0.40	0.40	0.43	0.45	0.64
Ce	0.23	0.23	0.23	0.23	0.68	0.23	0.23	0.23	1.36	0.23	0.23	0.68	1.82	0.23	0.23
Total	97.71	98.59	98.37	99.13	98.72	98.95	98.40	98.45	98.76	98.30	98.63	98.25	99.26	98.65	98.64
Or	23.04	25.24	28.76	5.65	9.49	13.97	31.68	15.74	15.79	38.20	37.77	41.39	38.37	37.63	30.94
Q	48.73	51.23	62.89	79.74	70.86	55.59	51.74	75.02	71.73	50.15	50.63	49.09	54.00	49.21	52.60
An	28.23	23.53	8.35	14.61	19.65	30.44	16.58	9.24	12.48	11.65	11.60	9.52	7.64	13.16	16.47
Q	41.00	50.03	69.39	73.40	73.19	62.54	60.06	86.51	80.47	69.63	72.62	74.48	77.27	67.61	63.85
An	23.75	22.98	9.21	13.45	20.30	34.25	19.25	10.65	14.00	16.18	16.63	14.44	10.93	18.09	19.99
Hy	35.25	26.99	21.40	13.14	6.51	3.21	20.70	2.83	5.53	14.20	10.75	11.08	11.80	14.30	16.16

CIPW norms for SIC samples from drill core 70011 (continued).

depth (m)	609.6	640.1	670.6	853.4	893.1	967.7	990.6	1066.8	1158.2	1219.2	1463.0	1493.5	1501.7	1502.4	1503.0
SiO_2	68.47	67.77	68.49	69.90	66.63	70.43	69.90	70.70	68.90	70.50	69.40	67.90	67.27	67.10	67.57
TiO_2	0.95	0.92	0.81	0.68	0.65	0.70	0.67	0.79	0.69	0.66	0.66	0.80	0.84	0.90	0.95
Al_2O_3	12.65	13.11	12.86	12.70	13.39	12.59	12.70	12.60	13.10	12.50	12.80	13.20	13.11	13.00	13.11
Fe_2O_3	1.61	1.90	1.89	1.40	2.20	1.30	1.20	1.20	1.50	1.30	1.70	1.90	1.70	1.80	2.00
FeO	4.22	4.10	3.59	4.40	4.60	3.70	4.60	3.70	4.10	3.80	3.30	4.10	4.80	5.00	4.40
MnO	0.08	0.05	0.07	0.07	0.08	0.06	0.07	0.06	0.08	0.08	0.07	0.08	0.09	0.10	0.10
MgO	0.90	1.72	0.91	1.05	0.96	0.85	0.85	0.94	0.65	0.52	0.39	0.54	0.67	0.73	0.64
CaO	2.49	1.16	2.52	1.37	2.71	1.64	1.13	2.20	2.15	2.11	2.36	2.48	2.68	2.79	3.02
Na_2O	3.61	3.30	3.19	3.50	3.50	3.30	3.50	3.50	3.50	3.50	3.30	3.80	4.20	3.50	4.10
K_2O	3.21	3.87	4.00	3.40	3.38	4.04	3.92	3.61	3.66	3.98	3.99	3.41	2.91	3.44	2.66
P_2O_5	0.23	0.24	0.18	0.13	0.12	0.13	0.13	0.13	0.13	0.13	0.15	0.17	0.18	0.19	0.21
Q	27.63	27.60	27.28	30.51	24.50	29.50	28.54	29.26	27.73	28.50	28.96	25.83	23.60	24.91	25.43
C	0.00	2.19	0.00	1.78	0.00	0.35	1.19	0.00	0.48	0.00	0.00	0.00	0.00	0.00	0.00
Or	18.97	22.87	23.64	20.10	19.98	23.88	23.17	21.34	21.63	23.52	23.58	20.15	17.20	20.33	15.72
Ab	30.54	27.92	26.99	29.61	29.61	27.92	29.61	29.61	29.61	29.61	27.92	32.15	35.54	29.61	34.69
An	8.84	3.55	8.96	4.05	10.85	6.66	4.12	8.01	7.92	6.65	8.33	8.89	8.33	9.61	9.52
Di	0.48	0.00	1.46	0.00	0.47	0.00	0.00	1.20	0.00	2.02	0.43	0.35	2.72	2.03	2.97
Hy	7.00	8.82	5.35	8.55	7.86	6.79	8.60	6.34	6.92	5.22	4.44	5.95	6.45	7.16	5.11
Mt	2.33	2.75	2.74	2.03	3.19	1.88	1.74	1.74	2.17	1.88	2.46	2.75	2.46	2.61	2.90
Hm	0.00	0.00	0.00	0.00	0.00	0.00	0.00	0.00	0.00	0.00	0.00	0.00	0.00	0.00	0.00
Il	1.80	1.75	1.54	1.29	1.23	1.33	1.27	1.50	1.31	1.25	1.25	1.52	1.60	1.71	1.80
Ap	0.54	0.57	0.43	0.31	0.28	0.31	0.31	0.31	0.31	0.31	0.36	0.40	0.43	0.45	0.50
Cc	0.52	0.23	0.23	0.68	0.45	0.23	0.23	0.23	0.68	0.23	0.68	0.68	0.23	0.23	0.23
Total	98.66	98.25	98.62	98.91	98.43	98.85	98.78	99.54	98.77	99.19	98.43	98.69	98.56	98.66	98.87
Or	34.22	42.34	39.48	36.77	36.11	39.77	41.50	36.41	37.76	40.09	38.74	36.72	35.01	37.06	31.02
Q	49.84	51.09	45.56	55.82	44.28	49.13	51.12	49.92	48.41	48.58	47.58	47.07	48.04	45.41	50.19
An	15.95	6.57	14.96	7.41	19.61	11.09	7.38	13.67	13.83	11.33	13.68	16.20	16.96	17.52	18.79
Q	63.56	69.05	65.59	70.77	56.70	68.68	69.17	67.09	65.14	70.60	69.40	63.51	61.49	59.76	63.48
An	20.34	8.88	21.54	9.39	25.11	15.51	9.99	18.37	18.60	16.47	19.96	21.86	21.70	23.06	23.76
Hy	16.10	22.07	12.86	19.83	18.19	15.81	20.84	14.54	16.26	12.93	10.64	14.63	16.81	17.18	12.76

CIPW norms for SIC samples from drill core 70011 (continued).

depth (m)	1503.6	1504.2	1524.0	1562.1	1566.7	1615.4	1646.0	1661.2	1676.4	1723.6	1726.7	1752.6	1799.8	1810.5	1812.0
SiO_2	67.00	66.63	65.70	62.20	61.40	56.79	53.90	53.80	55.40	56.32	56.85	58.40	59.00	59.22	59.32
TiO_2	0.89	0.94	1.06	1.38	1.46	1.82	1.85	1.85	1.38	1.15	0.99	0.54	0.58	0.59	0.59
Al_2O_3	13.12	12.76	13.50	13.60	13.60	13.37	13.20	13.70	14.70	14.73	15.28	15.90	15.80	15.63	15.75
Fe_2O_3	1.61	1.81	1.90	2.60	2.60	2.79	4.30	4.50	4.00	2.59	2.28	1.10	1.50	1.40	1.69
FeO	4.84	5.33	5.50	6.20	6.90	8.18	8.90	8.60	7.50	7.26	7.04	5.80	5.50	5.51	4.59
MnO	0.08	0.09	0.12	0.14	0.15	0.16	0.16	0.15	0.14	0.12	0.12	0.12	0.12	0.12	0.12
MgO	1.01	0.80	0.81	1.11	1.27	2.39	3.57	3.68	3.57	3.58	3.43	3.82	3.69	3.67	3.82
CaO	2.57	2.80	3.19	4.37	4.43	5.95	7.14	7.74	7.24	7.59	7.08	7.93	6.75	7.10	6.54
Na_2O	3.43	3.32	3.80	3.40	3.20	3.79	3.10	2.70	3.10	3.08	2.78	3.60	3.10	3.31	5.58
K_2O	3.46	3.57	2.82	2.45	2.46	2.13	1.64	1.63	1.68	1.46	2.07	1.21	1.97	1.71	0.55
P_2O_5	0.19	0.21	0.23	0.38	0.41	0.55	0.73	0.31	0.15	0.13	0.13	0.18	0.11	0.16	0.15
Q	24.91	24.72	23.11	21.35	20.96	10.16	9.49	10.00	9.64	10.57	11.00	9.92	12.65	12.05	5.89
C	0.00	0.00	0.00	0.00	0.00	0.00	0.00	0.00	0.00	0.00	0.00	0.00	0.00	0.00	0.00
Or	20.45	21.10	16.67	14.48	14.54	12.59	9.69	9.63	9.93	8.63	12.23	7.15	11.64	10.11	3.25
Ab	29.02	28.09	32.15	28.77	27.07	32.07	26.23	22.84	26.23	26.06	23.52	30.46	26.23	28.01	47.21
An	10.19	9.37	11.45	14.62	15.48	13.18	17.26	20.45	21.24	22.06	23.11	23.66	23.38	22.74	16.31
Di	0.59	2.16	1.38	1.75	0.02	10.20	10.60	12.66	11.32	11.70	8.76	10.94	5.65	8.91	12.37
Hy	8.45	7.79	8.31	9.09	11.54	10.82	13.65	12.19	11.74	12.62	13.82	13.17	14.53	12.95	9.75
Mt	2.33	2.62	2.75	3.77	3.77	4.04	6.23	6.52	5.80	3.76	3.31	1.59	2.17	2.03	2.45
Hm	0.00	0.00	0.00	0.00	0.00	0.00	0.00	0.00	0.00	0.00	0.00	0.00	0.00	0.00	0.00
Il	1.69	1.79	2.01	2.62	2.77	3.46	3.51	3.51	2.62	2.18	1.88	1.03	1.10	1.12	1.12
Ap	0.45	0.50	0.54	0.90	0.97	1.30	1.73	0.73	0.36	0.31	0.31	0.43	0.26	0.38	0.36
Cc	0.23	0.23	0.45	0.91	1.36	0.23	0.23	0.23	0.00	0.23	0.23	0.45	0.91	0.23	0.00
Total	98.31	98.37	98.84	98.25	98.50	98.05	98.63	98.78	98.87	98.12	98.16	98.81	98.53	98.53	98.71
Or	36.81	38.23	32.54	28.70	28.52	35.04	26.59	24.03	24.33	20.92	26.39	17.55	24.42	22.52	12.77
Q	44.84	44.79	45.11	42.32	41.11	28.28	26.04	24.95	23.62	25.62	23.74	24.36	26.54	26.84	23.14
An	18.34	16.98	22.35	28.98	30.36	36.68	47.37	51.02	52.05	53.47	49.87	58.09	49.05	50.65	64.09
Q	57.20	59.03	53.91	47.38	43.68	29.74	23.49	23.45	22.62	23.36	22.95	21.22	25.02	25.24	18.44
An	23.40	22.37	26.71	32.45	32.26	38.58	42.72	47.96	49.84	48.75	48.22	50.61	46.24	47.63	51.05
Hy	19.40	18.60	19.38	20.17	24.05	31.67	33.79	28.59	27.55	27.89	28.83	28.17	28.74	27.13	30.52

CIPW norms for SIC samples from drill core 70011 (continued).

depth (m)	1813.6	1816.6	1826.7	1831.8	1905.0	1920.2	2045.2	2164.1	2199.1	2249.4	2255.5	2257.3
SiO_2	58.10	59.54	54.94	59.34	58.50	58.30	57.50	58.30	59.40	59.04	52.15	52.50
TiO_2	0.67	0.56	0.59	0.65	0.67	0.50	0.48	0.63	0.44	0.60	0.54	0.54
Al_2O_3	16.60	15.55	15.25	16.28	16.40	16.00	17.40	16.40	16.90	15.88	15.72	15.00
Fe_2O_3	1.50	1.31	1.20	1.40	1.40	1.30	1.00	1.50	1.30	1.10	1.50	2.90
FeO	4.60	5.42	6.28	5.19	5.60	5.90	5.70	5.10	5.10	5.79	7.91	7.10
MnO	0.12	0.11	0.11	0.12	0.12	0.12	0.10	0.11	0.09	0.11	0.14	0.13
MgO	3.69	3.71	3.89	3.82	4.35	4.80	4.90	4.39	4.15	4.74	7.75	8.82
CaO	5.54	6.78	5.80	5.35	6.11	6.33	6.85	5.37	6.09	6.38	8.04	7.30
Na_2O	6.70	3.11	4.79	4.10	3.20	2.90	3.00	3.50	3.10	2.90	2.30	2.50
K_2O	0.37	1.88	0.78	1.38	1.23	1.58	1.33	1.91	1.92	1.74	1.58	1.07
P_2O_5	0.15	0.11	0.11	0.11	0.17	0.14	0.10	0.12	0.13	0.13	0.09	0.09
Q	1.10	13.09	10.98	11.18	13.42	13.07	10.25	10.26	12.51	12.42	1.17	3.01
C	0.00	0.00	4.10	0.00	0.03	0.20	0.00	0.00	0.00	0.00	0.00	0.00
Or	2.19	11.11	4.61	8.16	7.27	9.34	7.86	11.29	11.35	10.28	9.34	6.32
Ab	56.69	26.31	40.53	34.69	27.07	24.54	25.38	29.61	26.23	24.54	19.46	21.15
An	14.14	22.92	6.63	21.95	26.67	25.43	30.09	23.40	26.53	25.18	27.91	26.55
Di	8.04	7.72	0.00	1.63	0.00	0.00	1.10	1.49	1.28	4.09	8.27	6.31
Hy	11.58	13.58	19.46	16.24	19.08	21.11	20.70	17.49	17.44	18.73	27.92	28.91
Mt	2.17	1.90	1.74	2.03	2.03	1.88	1.45	2.17	1.88	1.59	2.17	4.20
Hm	0.00	0.00	0.00	0.00	0.00	0.00	0.00	0.00	0.00	0.00	0.00	0.00
Il	1.27	1.06	1.12	1.23	1.27	0.95	0.91	1.20	0.84	1.14	1.03	1.03
Ap	0.36	0.26	0.26	0.26	0.40	0.33	0.24	0.28	0.31	0.31	0.21	0.21
Cc	0.91	0.23	7.71	0.68	0.91	1.82	0.68	0.23	0.45	0.23	0.45	0.45
Total	98.45	98.19	97.14	98.05	98.16	98.68	98.67	97.44	98.83	98.52	97.92	98.15
Or	12.56	23.58	20.75	19.76	15.35	19.52	16.31	25.12	22.52	21.47	24.31	17.61
Q	6.31	27.78	49.41	27.08	28.34	27.32	21.27	22.83	24.83	25.94	3.05	8.39
An	81.12	48.64	29.84	53.16	56.31	53.16	62.43	52.06	52.65	52.59	72.64	74.00
Q	4.10	26.40	29.62	22.65	22.68	21.93	16.79	20.06	22.15	22.05	2.05	5.15
An	52.72	46.22	17.89	44.46	45.07	42.66	49.30	45.75	46.97	44.70	48.96	45.41
Hy	43.18	27.38	52.50	32.89	32.25	35.41	33.91	34.19	30.88	33.25	48.98	49.44

CIPW norms for SIC samples from drill core 70011 (continued).

depth (m)	76.2	152.4	228.6	304.8	1085.1	1133.9	1170.4	1176.5	1182.6	1188.7	1210.1	1234.4	1240.5	1249.7	1310.6	1511.8
SiO_2	67.80	66.20	67.70	64.80	67.74	62.60	63.79	61.99	62.70	61.79	61.44	60.88	60.12	59.50	59.90	60.60
TiO_2	0.47	0.52	0.50	0.51	0.95	1.30	0.67	0.78	0.72	0.75	0.72	0.63	0.58	0.65	0.54	0.27
Al_2O_3	11.70	12.80	12.10	12.10	12.73	13.30	14.19	14.64	14.21	14.54	15.18	15.47	15.75	16.00	17.10	18.00
Fe_2O_3	0.70	0.50	1.00	1.50	1.50	2.80	1.49	1.91	1.61	1.91	1.20	1.40	1.30	1.60	1.80	1.10
FeO	5.10	3.70	4.40	4.90	4.71	5.80	5.16	5.32	5.44	5.32	5.59	5.29	5.68	5.60	4.00	2.60
MnO	0.10	0.08	0.07	0.12	0.08	0.12	0.10	0.10	0.11	0.11	0.11	0.11	0.12	0.13	0.10	0.05
MgO	4.36	4.01	3.74	4.03	0.85	1.56	2.40	2.52	2.44	2.58	3.30	3.24	3.46	3.84	3.58	3.96
CaO	2.81	3.25	3.01	3.86	2.46	4.77	4.55	5.54	5.13	5.25	4.57	5.66	5.84	6.01	6.35	4.26
Na_2O	4.00	5.00	3.50	3.30	3.31	3.40	3.67	3.31	3.33	3.31	5.09	3.09	2.99	2.90	3.70	5.40
K_20	1.36	1.96	1.84	2.64	3.62	2.58	2.15	2.33	2.49	2.34	0.59	2.07	1.87	1.81	1.58	1.47
P_2O_5	0.11	0.13	0.12	0.13	0.20	0.45	0.21	0.18	0.20	0.24	0.20	0.11	0.15	0.16	0.10	0.06
Q	24.23	16.45	26.25	20.18	27.29	20.47	19.42	17.22	18.03	17.46	12.90	16.06	15.39	14.74	12.64	7.92
C	8.04	11.58	10.88	15.60	0.53	0.00	0.00	0.00	0.00	0.00	0.00	0.00	0.00	0.00	0.00	0.62
Or	33.84	42.30	29.61	27.92	21.40	15.25	12.71	13.77	14.72	13.83	3.49	12.23	11.05	10.70	9.34	8.69
Ab	9.96	6.70	11.88	10.41	28.01	28.77	31.05	28.01	28.17	28.01	43.07	26.14	25.30	24.54	31.31	45.69
An	2.16	6.46	1.34	5.94	7.74	13.41	15.90	18.21	16.48	17.91	16.84	22.23	24.04	25.30	25.39	18.85
Di	0.00	0.00	0.00	0.00	0.00	5.62	3.89	6.73	5.87	4.93	2.70	3.72	2.75	2.34	3.93	0.00
Hy	18.00	12.52	15.21	14.27	8.11	7.47	11.36	10.02	10.82	11.13	15.17	13.95	15.87	16.54	12.16	13.37
Mt	1.01	0.72	1.45	2.17	2.17	4.06	2.16	2.77	2.33	2.77	1.74	2.03	1.88	2.32	2.61	1.59
Hm	0.00	0.00	0.00	0.00	0.00	0.00	0.00	0.00	0.00	0.00	0.00	0.00	0.00	0.00	0.00	0.00
Il	0.89	0.99	0.95	0.97	1.80	2.47	1.27	1.48	1.37	1.42	1.37	1.20	1.10	1.23	1.03	0.51
Ap	0.26	0.31	0.28	0.31	0.47	1.07	0.50	0.43	0.47	0.57	0.47	0.26	0.36	0.38	0.24	0.14
Cc	0.23	0.23	0.23	0.23	1.14	0.23	0.23	0.00	0.23	0.23	0.45	0.23	0.23	0.23	0.23	0.68
Total	98.62	98.26	98.09	98.00	98.66	98.80	98.49	98.63	98.49	98.25	98.20	98.06	97.97	98.31	98.86	98.07
Or	56.18	64.87	51.77	51.67	37.92	31.04	26.46	27.99	29.90	28.11	10.50	24.21	21.89	21.09	19.72	24.51
Q	40.23	25.23	45.89	37.34	48.36	41.66	40.43	35.00	36.62	35.49	38.82	31.79	30.49	29.05	26.68	22.34
An	3.59	9.91	2.34	10.99	13.72	27.29	33.10	37.01	33.48	36.40	50.68	44.00	47.62	49.86	53.60	53.16
Q	54.58	46.43	61.33	49.96	63.26	49.50	41.60	37.89	39.77	37.55	28.72	30.74	27.83	26.05	25.18	19.73
An	4.87	18.23	3.13	14.71	17.94	32.43	34.06	40.07	36.36	38.52	37.50	42.55	43.47	44.72	50.59	46.96
Hy	40.55	35.34	35.54	35.33	18.80	18.07	24.34	22.05	23.87	23.94	33.78	26.70	28.70	29.23	24.23	33.31

CIPW norms for SIC samples from drill core 70011 (continued).

depth (m)	152.4	457.2	762.0	914.4	1066.8	1188.7	1217.7	1248.5	1280.2	1333.5	1348.7	1371.6	1394.5	1414.3	1416.1
SiO_2	68.80	69.80	69.50	69.20	57.90	59.57	61.92	66.60	59.32	67.10	57.20	56.00	53.58	53.21	68.64
TiO_2	0.80	0.68	0.72	0.77	1.20	2.20	1.85	1.35	2.32	0.92	2.43	1.96	2.91	2.64	0.82
Al_2O_3	12.90	12.70	12.80	12.90	14.70	12.28	12.97	12.60	13.16	14.00	13.23	14.20	13.60	12.93	13.63
Fe_2O_3	2.40	2.00	1.80	2.00	3.70	2.79	2.55	1.30	2.75	1.70	2.69	2.70	2.92	2.30	1.00
FeO	2.80	3.60	4.00	3.90	5.70	6.58	6.01	4.90	6.48	3.90	7.47	7.50	8.36	9.62	3.51
MnO	0.08	0.09	0.08	0.08	0.18	0.16	0.14	0.10	0.15	0.08	0.15	0.13	0.15	0.18	0.06
MgO	0.65	0.51	0.59	0.41	0.95	2.00	1.96	1.37	2.31	1.19	2.64	2.78	3.24	3.84	1.22
CaO	3.15	1.68	2.09	2.10	2.41	4.27	4.10	2.93	5.08	2.74	5.71	7.03	6.88	6.06	2.60
Na_2O	3.30	3.40	3.50	3.90	5.80	3.88	4.39	4.30	3.66	4.10	3.58	3.20	3.12	3.91	3.81
K_2O	3.90	4.29	3.93	3.69	3.46	2.19	2.14	3.23	2.66	3.37	2.03	1.76	1.89	1.30	3.45
P_2O_5	0.16	0.13	0.14	0.15	0.31	0.65	0.53	0.37	0.73	0.19	1.05	1.08	1.36	1.56	0.16
Q	27.74	28.09	27.48	26.41	5.87	16.97	16.81	20.96	14.71	22.06	13.47	13.01	10.30	7.40	24.90
C	0.00	0.00	0.00	0.00	0.56	0.00	0.00	0.00	0.00	0.00	0.00	0.00	0.00	0.00	0.00
Or	23.05	25.36	23.23	21.81	20.45	12.94	12.65	19.09	15.72	19.92	12.00	10.40	11.17	7.68	20.39
Ab	27.92	28.77	29.61	33.00	49.07	32.83	37.14	36.38	30.97	34.69	30.29	27.07	26.40	33.08	32.24
An	8.87	6.72	7.61	6.80	2.35	9.63	9.37	5.54	11.63	9.85	14.04	19.19	17.53	13.90	9.90
Di	4.76	0.11	1.04	1.74	0.00	6.10	6.26	4.48	7.30	1.04	6.18	5.09	6.40	3.93	1.10
Hy	1.23	5.22	5.75	4.51	8.13	8.37	7.89	7.03	8.21	6.83	11.26	12.93	13.31	19.34	6.86
Mt	3.48	2.90	2.61	2.90	5.36	4.04	3.70	1.88	3.99	2.46	3.90	3.91	4.23	3.33	1.45
Hm	0.00	0.00	0.00	0.00	0.00	0.00	0.00	0.00	0.00	0.00	0.00	0.00	0.00	0.00	0.00
Il	1.52	1.29	1.37	1.46	2.28	4.18	3.51	2.56	4.41	1.75	4.61	3.72	5.53	5.01	1.56
Ap	0.38	0.31	0.33	0.36	0.73	1.54	1.26	0.88	1.73	0.45	2.49	2.56	3.22	3.69	0.38
Cc	0.00	0.23	0.23	0.23	2.73	0.00	0.00	0.45	0.00	0.45	0.00	0.91	0.00	0.45	0.23
Total	98.95	98.99	99.26	99.21	97.53	96.60	98.59	99.27	98.66	99.50	98.23	98.80	98.08	97.83	99.01
Or	38.64	42.15	39.83	39.64	71.33	32.73	32.58	41.87	37.38	38.43	30.37	24.41	28.64	26.50	36.95
Q	46.50	46.68	47.12	48.00	20.47	42.92	43.29	45.97	34.97	42.56	34.09	30.54	26.41	25.53	45.12
An	14.87	11.17	13.05	12.36	8.20	24.36	24.13	12.15	27.65	19.00	35.54	45.05	44.95	47.96	17.94
Q	73.31	70.17	67.29	70.02	35.90	48.53	49.34	62.51	42.58	56.94	34.74	28.83	25.04	18.21	59.77
An	23.44	16.79	18.63	18.03	14.37	27.54	27.50	16.52	33.66	25.43	36.21	42.52	42.61	34.20	23.76
Hy	3.25	13.04	14.08	11.96	49.72	23.93	23.16	20.97	23.76	17.63	29.04	28.65	32.35	47.59	16.47

CIPW norms for SIC samples from drill core 70011 (continued).

depth (m)	1417.3	1421.3	1425.6	1425.6	1425.6	1425.7	1425.7	1432.6	1463.0	1493.5	1525.5	1569.7	1599.6	1638.3	1645.9
SiO_2	66.57	67.30	68.37	62.34	61.64	51.30	52.00	52.63	52.90	54.80	53.00	52.18	51.35	51.24	50.22
TiO_2	1.20	1.04	0.95	1.81	1.81	3.43	3.28	2.93	2.98	2.15	2.57	3.13	3.03	2.89	2.87
Al_2O_3	13.57	13.24	13.11	13.39	13.49	13.43	13.60	13.01	13.20	14.40	13.30	13.39	13.60	13.80	14.00
Fe_2O_3	1.60	2.51	1.40	1.80	2.00	3.71	3.40	9.24	3.00	3.00	3.70	5.46	5.55	10.03	3.36
FeO	4.39	3.51	2.70	5.19	5.29	9.32	9.10	3.67	8.60	7.70	8.80	7.14	7.25	3.18	8.74
MnO	0.07	0.06	0.05	0.11	0.10	0.21	0.21	0.16	0.18	0.15	0.16	0.18	0.17	0.16	0.16
MgO	1.12	1.11	1.34	2.33	2.36	3.63	3.55	3.55	3.78	3.70	4.01	3.72	4.73	3.84	3.86
CaO	2.69	3.34	4.25	4.91	4.89	6.81	6.60	7.30	7.79	7.09	7.53	7.60	6.97	8.13	9.32
Na_2O	4.39	5.52	5.01	5.00	4.80	3.21	3.20	2.98	2.90	3.10	2.80	2.88	3.70	2.88	3.40
K_20	3.12	1.12	1.44	1.29	1.39	1.42	1.54	1.43	1.27	1.70	1.48	1.31	0.62	1.23	1.28
P_2O_5	0.28	0.34	0.27	0.60	0.65	1.44	1.34	1.12	1.28	0.88	1.17	1.17	1.15	1.18	1.40
Q	21.09	23.29	25.08	15.95	15.89	8.76	9.18	14.70	11.00	10.31	10.44	12.40	8.69	12.59	3.62
C	0.00	0.00	0.00	0.00	0.00	0.00	0.00	0.00	0.00	0.00	0.00	0.00	0.00	0.00	0.00
Or	18.44	6.62	8.51	7.62	8.22	8.39	9.10	8.45	7.51	10.05	8.75	7.74	3.66	7.27	7.57
Ab	37.14	46.70	42.39	42.30	40.61	27.16	27.07	25.21	24.54	26.23	23.69	24.37	31.31	24.37	28.77
An	8.11	8.05	9.04	10.29	11.16	18.05	18.20	17.90	19.25	20.36	19.36	19.74	18.67	21.10	19.16
Di	2.34	4.69	6.34	7.85	6.77	4.71	4.27	7.58	8.58	6.96	8.02	8.31	6.73	8.48	14.79
Hy	6.50	3.21	2.56	7.19	7.79	15.48	15.60	5.33	13.90	14.17	15.18	9.03	12.59	5.63	11.14
Mt	2.32	3.64	2.03	2.61	2.90	5.38	4.93	3.86	4.35	4.35	5.36	7.92	8.05	2.39	4.87
Hm	0.00	0.00	0.00	0.00	0.00	0.00	0.00	6.58	0.00	0.00	0.00	0.00	0.00	8.38	0.00
Il	2.28	1.98	1.80	3.44	3.44	6.51	6.23	5.56	5.66	4.08	4.88	5.94	5.75	5.49	5.45
Ap	0.66	0.81	0.64	1.42	1.54	3.41	3.17	2.65	3.03	2.08	2.77	2.77	2.72	2.79	3.32
Cc	0.23	0.23	0.91	0.23	0.23	0.23	0.23	0.45	0.23	0.23	0.23	0.00	0.00	0.23	0.00
Total	99.11	99.21	99.30	98.90	98.55	98.08	97.99	98.28	98.05	98.82	98.68	98.22	98.18	98.72	98.68
Or	38.71	17.44	19.96	22.50	23.31	23.84	24.95	20.58	19.89	24.68	22.70	19.41	11.80	17.75	24.94
Q	44.27	61.35	58.83	47.11	45.05	24.89	25.16	35.81	29.13	25.32	27.08	31.09	28.01	30.74	11.93
An	17.02	21.21	21.21	30.39	31.64	51.28	49.89	43.61	50.98	50.00	50.22	49.50	60.19	51.51	63.13
Q	59.08	67.41	68.38	47.71	45.61	20.71	21.36	38.76	24.92	22.99	23.21	30.12	21.75	32.02	10.67
An	22.72	23.30	24.65	30.78	32.03	42.68	42.35	47.19	43.60	45.41	43.04	47.95	46.73	53.66	56.49
Hy	18.21	9.29	6.98	21.51	22.36	36.60	36.30	14.05	31.48	31.60	33.75	21.93	31.51	14.32	32.84

CIPW norms for SIC samples from drill core 70011 (continued).

depth (m)	1679.4	1722.1	1764.8	1828.8	1981.2	2072.6	2106.2	2220.5	2301.2	2362.2	2453.6	2545.1
SiO_2	52.50	47.80	51.94	51.50	52.40	46.55	45.00	54.80	57.10	56.60	56.80	56.30
TiO_2	3.19	3.97	2.76	2.66	1.74	3.36	4.16	0.77	0.47	0.44	0.43	0.38
Al_2O_3	13.50	11.60	14.82	14.80	16.30	14.20	13.70	6.00	17.60	17.50	17.90	18.30
Fe_2O_3	3.50	4.32	3.58	3.90	3.80	5.18	5.80	4.70	1.00	0.80	1.10	1.10
FeO	9.10	11.24	7.80	8.50	7.40	9.02	10.10	10.80	5.70	5.80	5.50	5.20
MnO	0.17	0.22	0.15	0.15	0.13	0.17	0.18	0.18	0.12	0.12	0.12	0.11
MgO	3.86	5.47	3.60	4.14	4.29	5.19	5.46	13.01	5.40	5.70	5.90	5.77
CaO	7.89	8.85	8.46	8.62	8.89	10.34	10.26	4.87	7.34	7.32	7.41	7.63
Na_2O	2.90	2.58	3.15	2.90	2.80	2.74	2.50	0.40	2.90	2.90	2.80	2.90
K_20	1.36	1.03	1.13	1.04	1.13	0.58	0.54	1.24	1.16	1.06	1.14	1.11
P_2O_5	1.32	1.61	1.35	1.36	0.32	1.53	1.67	0.12	0.09	0.04	0.09	0.07
Q	9.90	4.83	8.58	8.28	6.72	3.18	3.16	14.23	9.18	8.52	8.61	7.63
C	0.00	0.00	0.00	0.00	0.00	0.00	0.00	0.00	0.00	0.00	0.00	0.00
Or	8.04	6.09	6.68	6.15	6.68	3.43	3.19	7.33	6.86	6.27	6.74	6.56
Ab	24.54	21.83	26.65	24.54	23.69	23.18	21.15	3.38	24.54	24.54	23.69	24.54
An	19.81	17.03	22.97	24.30	28.58	24.74	24.57	10.91	31.59	31.61	32.91	33.64
Di	8.32	13.43	8.36	7.35	10.49	13.45	12.00	9.56	2.95	2.60	2.14	2.54
Hy	14.37	17.94	11.94	14.97	13.36	13.45	15.00	42.79	21.09	22.41	22.35	21.35
Mt	5.07	6.26	5.19	5.65	5.51	7.51	8.41	6.81	1.45	1.16	1.59	1.59
Hm	0.00	0.00	0.00	0.00	0.00	0.00	0.00	0.00	0.00	0.00	0.00	0.00
Il	6.06	7.54	5.24	5.05	3.30	6.38	7.90	1.46	0.89	0.84	0.82	0.72
Ap	3.13	3.81	3.20	3.22	0.76	3.62	3.98	0.28	0.21	0.09	0.21	0.17
Cc	0.23	0.00	0.00	0.23	0.23	0.00	0.23	0.23	0.23	0.45	0.23	0.23
Total	99.46	98.77	98.81	99.74	99.32	98.94	99.56	97.00	98.98	98.48	99.29	98.97
Or	21.30	21.79	17.47	15.88	15.91	10.94	10.32	22.57	14.40	13.51	13.97	13.72
Q	26.23	17.28	22.44	21.38	16.01	10.14	10.22	43.83	19.27	18.36	17.84	15.95
An	52.48	60.93	60.08	62.74	68.08	78.92	79.46	33.60	66.32	68.13	68.19	70.33
Q	22.46	12.14	19.73	17.41	13.81	7.69	7.40	20.95	14.84	13.62	13.48	12.18
An	44.94	42.79	52.82	51.10	58.73	59.80	57.50	16.06	51.07	50.54	51.53	53.72
Hy	32.60	45.08	27.45	31.48	27.46	32.51	35.10	62.99	34.09	35.83	34.99	34.09